CHAPTER ONE

1.0 INTRODUCTION

1.1 Drug discovery and development

The development of new drugs over the past century has transformed the practice of medicine, converting many fatal diseases into almost routine therapeutic exercises. It has changed and improved the quality of life by making it possible for almost all diseases affecting millions of people to be managed or reduced to minimal.

For many centuries, portions and herbs were the only sources of medicines. In the mid-nineteenth century, natural occurring drugs such as morphine from opium, cocaine from coca leaves, quinine from the bark of the cinchona tree, etc. have been the main source of disease treatment. Their active ingredients were isolated, purified and their structures determined (Firn, 2010).

Traditionally, the process of drug development has revolved around a screening approach in which several compounds are screened for drug-like activity without any previous knowledge on their drug-like potentials. The shortcomings of this approach such as incomplete cure and sometimes more toxicity in combating diseases lead to the concept of rational drug desig (Kuntz, 1992). However, many other approaches such as (i) chemical modification of known drug; (ii) random screening for biological activity of large number of compounds (natural or synthetic); (iii) rational drug design based on an understanding of the biological mechanisms and chemical structure and (iv) biotechnology and cloning using genes to produce larger

peptides and proteins have been introduced to enhance drug discovery and development (Berkowitz and Katzung, 2004).

1.1.1 Metals in drug development

Many metal containing compounds play a crucial role in living organism. This is due to their ability to readily form positively charged ion which tend to be soluble in biological fluids. While metal ions are electron deficient (positively charged) most biological molecules such as proteins are electron rich. In this way, metal ions bind and interact effectively with biological molecules such as protein, nucleic acid e.t.c. This interaction has resulted in wide variety of functions of metals such as carrying oxygen throughout the body, provision of the structural framework for the zinc fingers that regulate the function of genes in the nuclei cells, regulation of sugar metabolism e.t.c. In addition, most of the known enzymes perform their functions in the presence of transition metal cations such as Fe^{2+}, Fe^{3+}, Cu^{2+}, Co^{2+}, Mn^{2+} and Zn^{2+}. This has made the prospects for biological model better with the transition metals (Ming, 2003, Storr *et al*., 2006).

Medicinal application of transition metal complexes can be traced back to several centuries. Gold and copper have been used in local medicines for thousands of years by the Egyptians, Arabs, Chinese and Indians (Guo and Sadler, 1999). The beginning of the 20^{th} century saw metals making an impact on modern medicine with Paul Ehrlich's discovery of the arsenic organometallic drug "Salvarsan" or Ehrlich 606, for a successful treatment of *syphilis* (Gibaud and Metzler-Nolte, 2010).). Other metal-based compounds for the management of

infectious diseases include antimony for the treatment of the parasitic disease lesihmaniasis and gold complex, $K[Au(CN)_2]$ for the treatment of tuberculosis. Also, gold complexes such as auranofin have been used in the treatment of rheumatoid arthritis (Hambley, 2007).

An impetus to much current work on metal chemotherapy has come from the discovery of Barnett Rosenberg (Rosenberg, 1971) that some platinum complexes were effective against specific tumors. *Cisplatin*, a square planar Pt(II) complex [*cis*-dichlorodiamine platinum(II)] was approved for clinical use in 1978 against variety of cancers, especially testicular cancer (Jameison and Lippard, 1999). A diversity of metal-based drugs is now clinically available. Examples include, lithium carbonate as anti-depressant and sodium nitroprusside as anti-hypertensive (Dabrowiak, 2009).

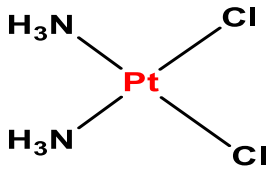

Cisplatin

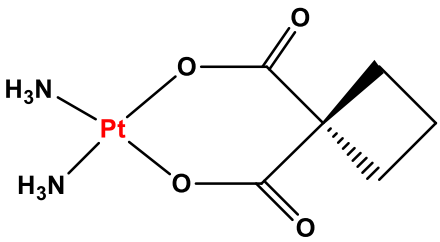

Carboplatin

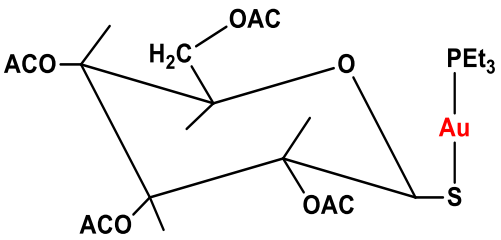

Auranofin

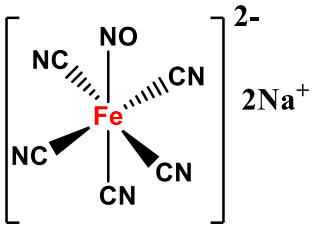

Sodium nitroprusside

Figure 1: Some metal-based drugs in clinical uses.

The outcome of these drugs in the treatment and management of diseases and infections stimulated the interest in developing more bioactive metal compounds for the treatment and management of several diseases such as tuberculosis.

1.2 Tuberculosis

Tuberculosis (TB) first identified by Robert Koch in 1882, is a chronic communicable disease caused by *Mycobacterium tuberculosis* (*M.TB*) (De Souza, 2006). Typically, *M.TB* attacks the lungs, although it can affect other organs such as bone tissue, the urinary tract, sexual organs, intestine and skin (Swamy, 2007). In 1993, the World Health Organization (WHO) declared TB a global health problem accounting for about two million deaths annually with mortality rate of four people every minute (WHO, 1994).

1.2.1 Anti-tuberculosis drug development

The first successful treatments for tuberculosis were all surgical. They were based on the observation that healed tuberculosis cavities were all closed. Surgical management was therefore directed at closing open cavities in order to encourage healing. These procedures were all used in the pre-antibiotic era. (Barris, 2000).

The advent of antibiotics in 1946 lead to the use of streptomycin. The tuberculosis therapy findings reveal that combined regmine of streptomycin and para aminosalicylic acid (PAS) reduced the emergence of bacterial resistance to either of the two drugs when given alone. The discovery of anti-TB property of INH in 1952 lead to further study which showed that a

combination of streptomycin , PAS and INH was more effective in preventing emergency of bacterial resistance. The high cost of PAS, which was used throughout the therapy, led to a search for affordable regimens for developing countries, with the substitution of PAS by thioacetazone .(Agrawal *et al*., 2001, Pillay *et al*., 2006).

1.2.3 Current anti-tuberculosis drugs

Antituberculosis drugs can be divided into the following categories:

- **First-line drugs (FLDs)**

The present day short-course chemotherapy (SCC) regimens consist of four first-line anti-TB drugs: isoniazid (INH), rifampicin (RMF), pyrazinamide (PYZ) and ethambutol (EMB). For latent tuberculosis, the standard treatment is six to nine months of isoniazid alone. If the organism is known to be fully sensitive, then treatment is with isoniazid, rifampicin, and pyrazinamide for two months, followed by isoniazid and rifampicin for four months. (Mehta *et al.,* 2003). The reason for the combination therapy is due to the different mode of action of the drugs used in the regimen. INH is bacteriocidal against replicating bacteria. EMB is bacteriostatic at low doses, but at higher doses used in TB treatment it is bacteriocidal. RMP is bacteriocidal and has a sterilizing effect. PYZ is only weakly bacteriocidal, but is very effective against bacteria located in acidic environments, inside macrophages, or in areas of acute inflammation (Keshavjee and Farmer, 2012).

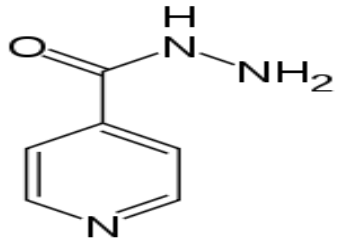

Isoniazid

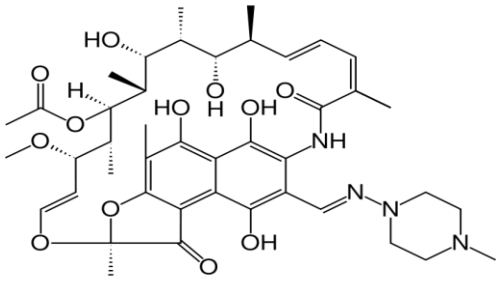

Rifampicin

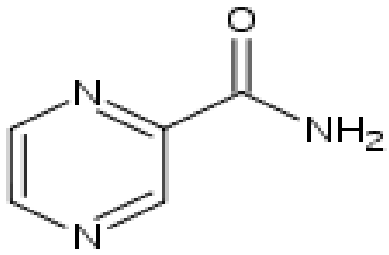

Pyrazinamide

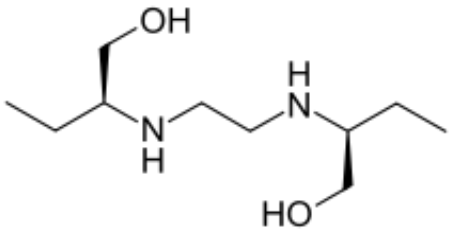

Ethambutol

Figure 2: Structures of WHO approved anti-tuberculosis FLDs (Mehta *et al.*, 2003).

- **Second-line drugs (SLDs)**

A drug may be classed as second-line instead of first-line for one of three possible reasons: it may be less effective (e.g. p-aminosalicylic acid); or, it may have toxic side-effects (e.g. cycloserine); or it may be unavailable in many developing countries (e.g. fluoroquinolones) compared to the first line drugs.

The second line drugs are considered as the reserved therapy utilized for treatment of tuberculosis. These drugs are often used in special conditions like resistance to first line therapy, extensively drug-resistant tuberculosis (XDR-TB) or multidrug-resistant tuberculosis (MDR-TB) arise. There are six classes of second-line drugs (SLDs) used for the

treatment of TB. (a) aminoglycosides: e.g. amikacin (AMK), kanamycin (KM), (b) polypeptides: e.g. capreomycin, viomycin, enviomycin; (c) Fluoroquinolones: e.g. ciprofloxacin (CIP), levofloxacin, moxifloxacin (MXF); (d) thioamides: e.g. ethionamide, prothionamide (e) cycloserine: e.g. closerin and (f) Terizidone (Blumberg *et al*., 2003).

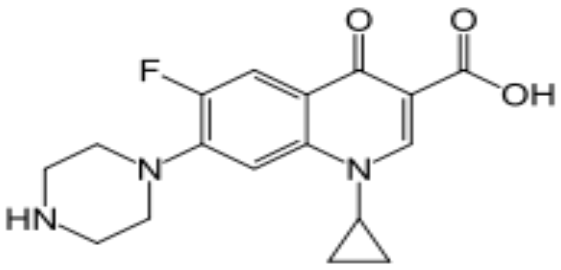

Ciprofloxacin

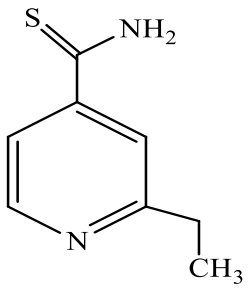

Ethionamide

Figure 3: Structures of some WHO approved anti-tuberculosis SLDs (Blumberg *et al*., 2003).

- **Third line drugs (TLDs)**

Other drugs that may be useful, but are not on the WHO list of SLDs are: rifabutin, macrolides e.g. clarithromycin (CLR), linezolid (LZD), thioacetazone (T), thioridazine, arginine and vitamin D. These drugs may be considered "third-line drugs" either because they are not very effective (e.g. clarithromycin) or because their efficacy has not been proven (e.g. linezolid, R207910). Rifabutin is effective, but is not included on the WHO list because for most developing countries, it is impractically expensive (Grange and Zumla, 2002).

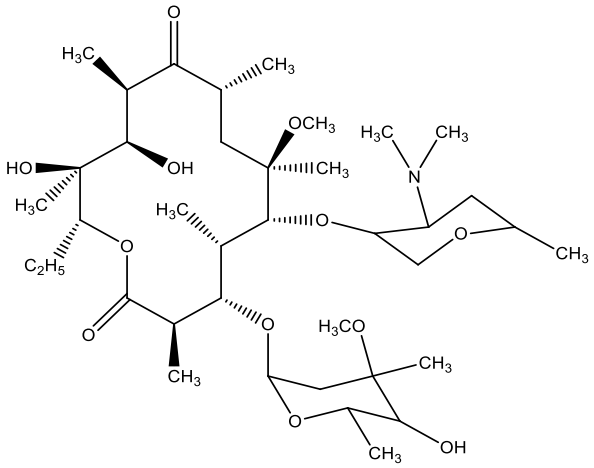

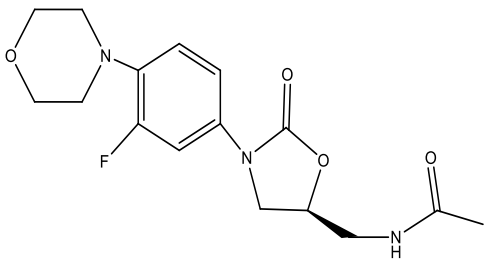

Clarithromycin Linezolid

Figure 4: Structures of some anti-tuberculosis TLDs (Grange and Zumla, 2002).

In spite of these major advances made in the anti-tuberculosis drug development, tuberculosis still remains a global health challenge. An alarming increase in the number of TB cases has been further fueled by the HIV pandemic which account for about 25% of the total TB burden (Corbett *et al*.; 2002, Sharma *et al*., 2005, Kwan and Ernst, 2011). New drugs that can offer improvements over current therapies are desperately needed. This includes the need to accelerate investigations to identify new types of metal-based bioactive drugs. Basically, research in this area is focused on molecular modifications of the existing drugs which have been shown to improve their therapeutic properties (Sriram *et al*., 2009, Hearn *et al*., 2009) and the search of new classes of compounds active against the pathogen using the metal-based approach (Tarallo *et al*., 2010, Joseph *et al*., 2012).

The metal-based approach involves the use of bioactive metal compounds. The property of a ligand surrounding the metal ion has great influence on the property of the metal complex.

Ligand modifies the physical and chemical properties of the metal ion, can also modify the oral or systemic bioavailability of the metal ion and assist in targeting specific tissues or enzymes (Thompson and Orvig, 2003, Thompson and Orvig, 2006).

1.3 Statement of Problem

Tuberculosis has killed millions of people since it was identified, making it one of the most pandemic diseases in recorded history (WHO, 2012). Based on the trend over the past few years a total of 225 million new cases and 79 million deaths are expected from tuberculosis between 1998 and 2030 if effective treatment measures are not taken globally to redress the trend (Rakesh *et al*., 2009). Although**,** significant scientific and therapeutic progresses have been made since the first clinical identification of tuberculosis, the more common treatment involve the Directly Observed Therapy (DOT) which requires six to twelve months with INH and rifampicin or pyrazinamide or ethambutol followed by a continuation phase of treatment with INH and rifampicin (Blumberg *et al*., 2003). However, hopes that tuberculosis could be completely eliminated using these drugs have been dashed with the emergence of drug resistant strain of *M.TB* and co-morbidity of TB with HIV/AIDS. Over 300,000 new cases of resistant TB are diagnosed around the world each year and 79% of the cases show resistance to three or more of the commonly used drugs (Szekely *et al*., 2008). Resistance of *M.TB* is a consequence of the lengthy regimes which most times create poor patients' adherence. This accelerates the conditions for acquired drug resistance to virtually all the available first line drugs. Furthermore, the potency of INH can be lost by the action of *N*-acetyltransferase (NATs) at the hydrazine unit.

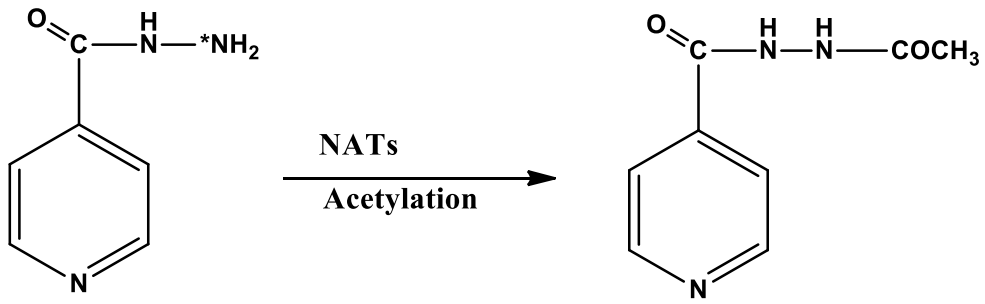

Isoniazid (Active) **Acetyl isoniazid (Inactive)**

Scheme 1: Acetylation of INH by NATs

This poses a challenge in the chemotherapy and treatment of tuberculosis because INH is the mainstay for the treatment of tuberculosis. Thus, the development of new anti-TB agents to combat the resistance to the known drugs is highly desirable and urgent.

1.4 Aim of study

The study aims to synthesize and investigate the *in-vitro* anti-tuberculosis activity of novel heterocyclic Schiff bases derived from aminopyridines and isonicotinic acid hydrazide (INH) and their copper(II), nickel(II) and cobalt(II) complexes against *Mycobacterium tuberculosis* .

1.5 Specific objectives of the study include:

1. Synthesis and characterization of 2- and 4-aminopyridine based Schiff bases.
2. Synthesis and characterization of Schiff bases derived from INH.
3. Synthesis and characterization of cobalt(II), nickel(II) and copper(II) complexes of the synthesized Schiff bases.
4. Evaluation of the *in-vitro* anti-tuberculosis activity of the synthesized Schiff bases and the metal complexes on *Mycobacterium tuberculosis.*

1.6 Significance of study

New metal complexes with potential application in tuberculosis therapy will be synthesized and evaluated. The mode of action of these new compounds are expected to be different from those of the existing anti-TB agents due to the presence of metal ion introduced. Thus, the bacterial resistance may not be readily observed. This will be done through modification of a compound with anti-tuberculosis effect and synthesis of new compounds.

1.7 Definition of terms

Heterocyclic compounds: Organic compounds in which one or more of the ring carbon atoms have been replaced by another element such as nitrogen, oxygen, sulfur, phosphorus etc.

Synthesis: Any process or reaction used for the building up a complex compound by union of simpler compounds or elements.

Schiff base: A neutral molecule that contains a carbon-nitrogen double bond (C=N).

Metal complex: A compound that consists of a central metal ion surrounded by ligands.

Tuberculosis: a bacterial infection caused by *Mycobacterium tuberculosis*.

Anti-tuberculosis agents: drugs used to treat tuberculosis.

Ligand: An ion or molecule that binds to a central metal atom to form a coordination complex.

1.8 List of abbreviations

AAS Atomic Absorption Spectroscopy

AIDS Acquired immunodeficiency syndrome

AMK Amikacin

CFU	Colony Forming Unit
CIP	Ciprofloxacin
CLR	Clarithromycin
DMF	Dimethylformamide
DMSO	Dimethylsulphoxide
DOT	Direct observed therapy
EMB	Ethambutol
EtOH	Ethanol
FASII	Fatty Acid Synthase II
FLDs	First line drugs
HIV	Human immunodeficiency virus
INH	Isonicotinic Acid Hydrazide
IR	Infrared spectroscopy
KM	Kanamycin
LZD	Linezolid
MDR-TB	Multidrug-resistant tuberculosis
MIC	Minimum inhibitory concentration
mp	Melting point
M.TB	*Mycobacterium tuberculosis*
M.wt	Molecular weight
MXF	Moxifloxacin
NATs	N-arylaminoacetyl transferase
NMR	Nuclear Magnetic Resonance spectroscopy

PAS Para amino salicylic acid

PYZ Pyrazinamide

Rf Retardation factor

RMF Rifampicin

SB Schiff base

SCC Short-course chemotherapy

SD Standard deviation

SLDs Second line drugs

TB Tuberculosis

TLDs Third line drugs

UV Ultraviolet visible spectroscopy

WHO World Health Organization

CHAPTER TWO

2.0 LITERATURE REVIEW

Heterocycles are organic compounds that contain a non carbon atom such as nitrogen, oxygen, sulphur, phosphorous etc within the ring structure. The ring may either be aromatic or alicylic. About half of the known organic compounds are heterocyclic in nature (Joule and Mills, 2013). Some examples are pyridine (C_5H_5N), thiophene (C_4H_4S), furan (C_4H_4O) etc.

Heterocyclic compounds have a wide range of applications. They are used as optical brightening agents, as antioxidants, as corrosion inhibitors, and as additives with a variety of other functions. Many dyestuffs and pigments have heterocyclic structures. Heterocyclic compounds are also widely distributed in nature. They include adenine, guanine, pyrimidine and purine bases of the genetic material, as well as the essential amino acids such as proline, histidine and tryptophan. The vitamins and coenzyme precursors thiamine, riboflavin, folic acid, the photosynthesizing pigment, chlorophyll and the oxygen transporting pigment, hemoglobin are all heterocycles. Essential diet ingredients such as thiamin (Vitamin B1), riboflavin (Vitamin B2), Pyridoxol (Vitamin B6), nicotinamide (Vitamin B3), and ascorbic acid (Vitamin C) are heterocyclic compounds (Eicher *et al*., 2013).

The pyridine nucleus is an important hetero aromatic class of compounds with a wide range of activities. Their synthesis has been the focus of much interest for chemists and medicinal researchers. Many synthetic pyridine derivatives are important therapeutic agents, for example isoniazid a major anti-tuberculosis agent, sulphapyridine one of the sulfonamide anti-bacterial, prialdoxime an antihypertensive and 4-Substituted 1,4-dihydropyridines (1,4-

DHPs), an important class of drugs for the treatment of cardiovascular diseases, Alzheimer's disease and used as chemo sensitizer in tumor therapy. Some herbicides (Paraquat) and fungicides (Davicil) are also pyridine derivatives (Joule and Mill, 2013). One of the reasons for widespread use of heterocyclic compounds is that their structures can be subtly manipulated to achieve the required functional modifications (Joule *et al*., 1995). In view of this, they have been found very useful as starting materials in the synthesis of Schiff bases (Mittal *et al*., 2009, Surati, 2011).

2.1 Schiff Bases

Schiff bases (SB) are compounds which contain an imine or azomethine group (C=N). They are obtained by the condensation reaction of a primary amine and an aldehyde or ketone according to the reaction scheme shown below:

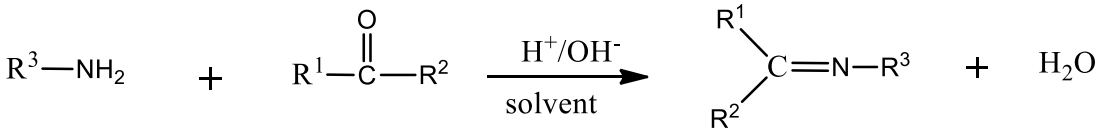

Primary amine Aldehyde or Ketone Schiff base

Scheme 2: Synthetic route to Schiff base formation.

Where R^1 is a hydrogen atom or any organic side chain and R^2, R^3 are any organic side chains which may be variously substituted. Schiff bases that contain aryl substituent are substantially more stable and more readily synthesized than those which contain alkyl substituent which can polymerise (Hine and Yeh, 1967). In general, aldehydes react faster than ketones in condensation reactions leading to the formation of Schiff bases, as the reaction centre in the aldehyde is sterically less hindered. Furthermore, the extra carbon of

ketone donates electron density to the azomethine (C=N) carbon which makes the ketone less electrophilic compared to aldehyde hence ketones form mannich bases (Fessenden and Fessenden, 1998).

2.2 Synthetic approaches to Schiff bases

The first preparation of imines was reported in the 19th century by Schiff (Schiff, 1864). Since then a variety of methods for the synthesis of imines have been described. These include the following

2.2.1 Classical Method

The synthetic route reported by Schiff in 1864 involved the condensation of a carbonyl compound with an amine under azeotropic distillation (Moffett, 1963). This method is refered to as the classical method and is still widely used in Schiff base synthesis (Azzouz, 2010, Fasina and Dada, 2013, Li *et al*., 2013). Mild acids such as glacial acetic acid or formic acid are usually employed as catalyst in the synthesis of Schiff bases (SBs). However, Chakraborty *et al*.,(1994) proposed as an alternative, the use of substances that function as Bronsted-Lowry or Lewis acids to activate the carbonyl group of aldehydes, catalyse the nucleophilic attack by amine, and dehydrate the system, eliminating water as the final step.

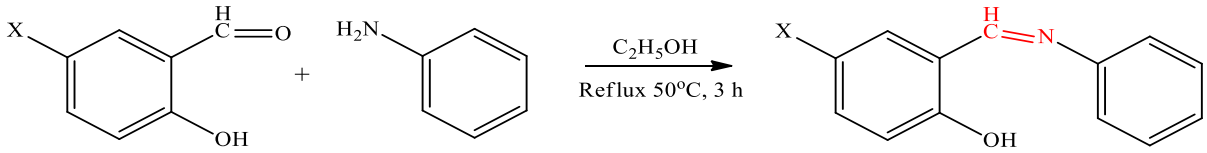

X = H (L1), OCH_3 (L2), NO_2 (L3), naphtyl(L4)

Scheme 3: Synthesis of Schiff base by classical method (Fasina and Dada, 2013).

Since then, many Bronsted-Lowry or Lewis acids have been used for the synthesis of Schiff bases. They include, $ZnCl_2$, $TiCl_4$, $MgSO_4$, alumina, H_2SO_4, HCl, P_2O_5/Al_2O_3, CH_3COOH, $NaHCO_3$ (Baricordi *et al*., 2004, Naeimi *et al*., 2006, Kulkarni *et al*., 2009, Zheng *et al*., 2009).

2.2.2: Non-Classical Method

Recent years have witnessed a major drive to increase the efficiency of organic transformations while lowering the amount of waste materials. Many organic solvents are volatile and pose an environmental threat by polluting the atmosphere. The replacement of volatile organic solvents in organic reaction processes is an important green chemistry goal. The use of environmental benign, facile and low costing method for the synthesis of Schiff bases is currently of interest. These include: microwave irradiationin absence of solvent when a reactant is liquid (Yang *et al*., 2002, Gopalakrishnan *et al*., 2007, Chakraborty, *et al*., 2012) and in the presence of minium solvent when both reactants are solids microwave irradiation/solvent (Jain and Mishra, 2012, Bhagat *et al*., 2013), ultrasound irradiation (Guzen *et al*., 2007), grindstone method (Yang and Sun, 2006, Vibhute *et al*., 2009) and water based reaction (Arshi *et al*., 2009, Khadsan *et al*., 2010).

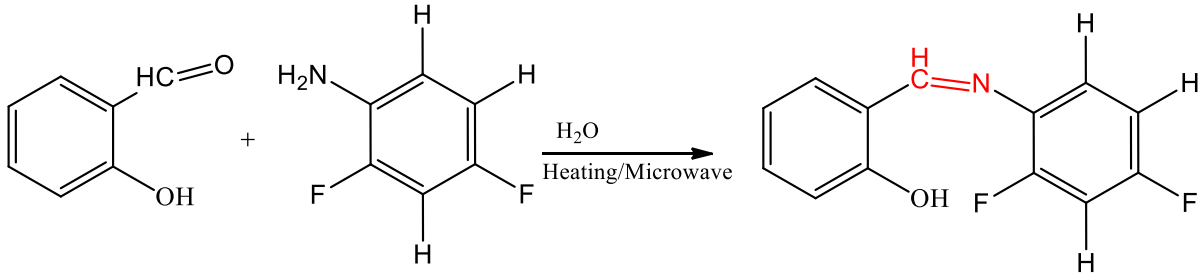

Scheme 4: Synthesis of Schiff base by non classical method (Bhagat *et al*., 2012).

.

2.3: Mechanism of Schiff base formation

The mechanism of Schiff base formation involves a nucleophilic addition of a primary amine to the carbonyl group. Synthesis of Schiff base can either be acid or base catalyzed. The acid catalyzed reaction is preferred as base catalyzed reaction usually results in the formation of various side products such as benzoin or the base itself may acts as a nucleophile. However, use of acid may reduce the nucleophilicity of the amine, therefore an optimum condition of (pH 4.5) is highly desirable. At this pH, the carbonyl oxygen atom is protonated to give a carbocation that is more susceptible to nucleophilic attack by the amine.

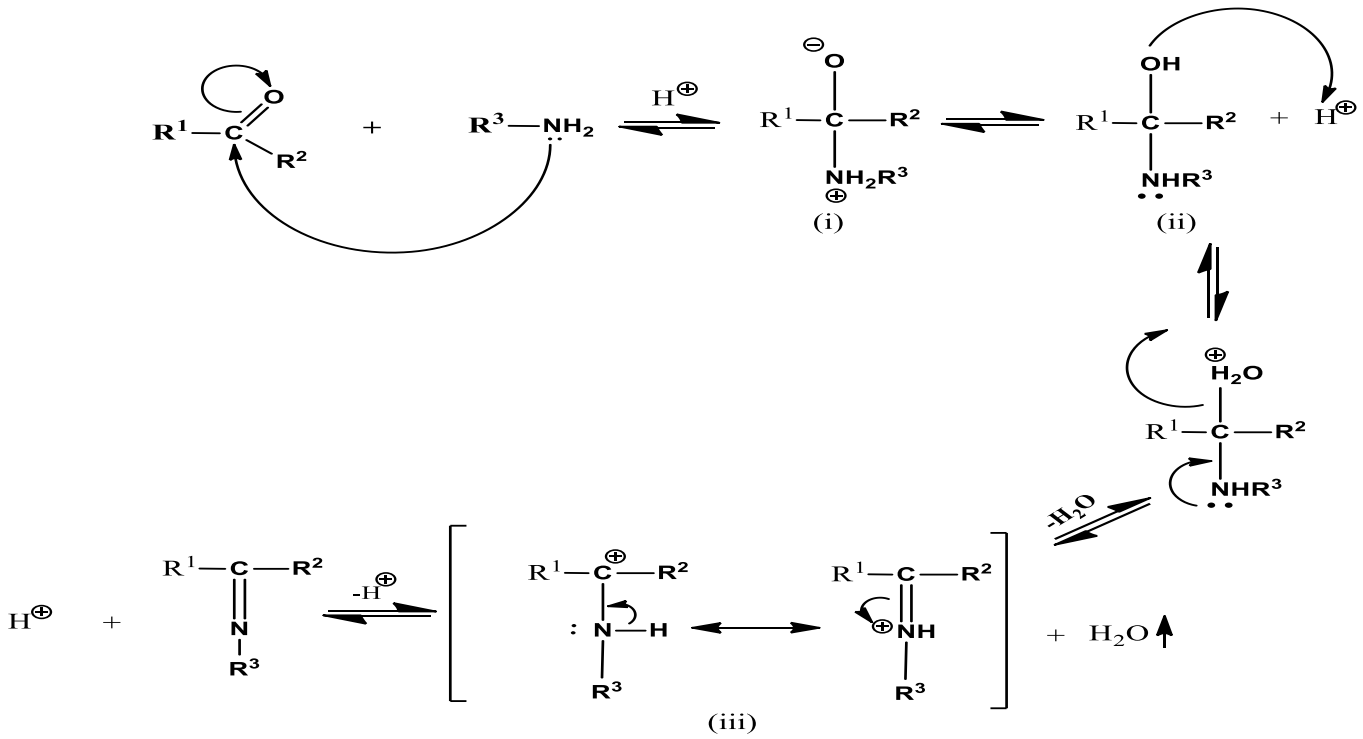

Scheme 5: Acid-catalyzed Schiff base formation

Reaction of an amine with the carbonyl gives a protonated amino alcohol (i). The net effect of abstraction of a proton from (i) gives an unstable intermediate called carbinolamine (ii). Protonation of the carbinolamine and loss of a molecule of water gives the resonance-stabilized carbocation (iii). Loss of a proton from (iii) gives a Schiff base.

2.4 Applications of Schiff bases

Schiff bases derived from aromatic amines and aldehydes have a wide variety of applications. Several studies (Kabak *et al*. 1999 and Patel *et al*. 1999), have shown that the presence of a lone pair of electrons in the sp^2 hybridized orbital of nitrogen atom of the azomethine group is of considerable chemical and biological importance.

2.4.1 Chemical applications

Schiff bases derived from aminopyridines have been used as spectrofluorimetric analytical reagents for monitoring of small pH changes as well as for sensitive metal ion determinations (Cimerman *et al*., 2000, Ibrahim and Sharif, 2007). Notable among the recent use of Schiff bases as analytical reagents are : indicator electrode in the potentiometric titration of mercury ions (Ganjali *et al*. 2007), zirconium ion (Shamspur *et al*., 2012) and trace determination of Dy(III) ions in some binary mixtures, mouth washing solution, soil and sedimemt samples (Pourjavid *et a*l., 2012).

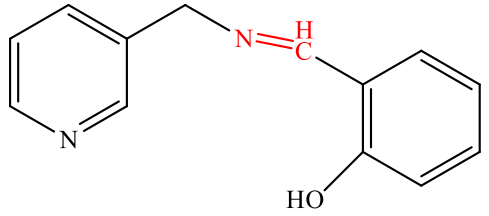

(*E*)-2-(((pyridin-3-ylmethyl)imino)methyl)phenol

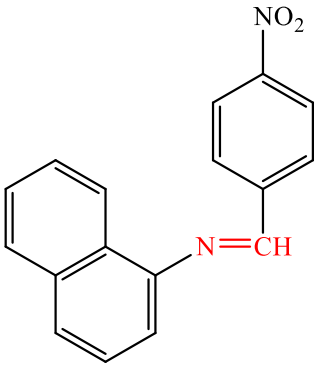

(*E*)-*N*-(4-nitrobenzylidene)naphthalen-1-amine

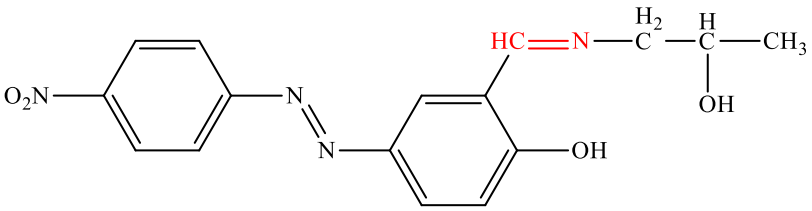

2-(((2-hydroxypropyl)imino)methyl)-4-((*E*)-(4-nitrophenyl)diazenyl)phenol

Figure 5: Some Schiff bases used as analytical reagent

Schiff bases are used as dyes for dyeing acetate and synthetic fibers (Marwani *et al*., 2012). These dyes have high photostability against photobleaching which makes them useful in colour photography to reduce the photosensitivity of photographic emulsions.

Schiff bases have been reported to exhibit excellent catalytic property in the hydrogenation of olefins (Olie and Olive, 1984) and in biomimetic catalytic reactions (Hernandes *et al*., 2002).

N-benzylidene pyridine-4-amines, Schiff bases prepared by condensation of 4-aminopyridine with aromatic aldehydes were used as precursor in the synthesis of aminobarbituric derivatives with hypnotic property (Al-Douh *et al*., 2003).

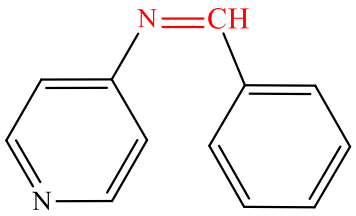

(*Z*)-*N*-benzylidenepyridin-4-amine

Figure 6 4-aminopyridine based Schiff base a precursor in the synthesis of aminobarbituric derivatives

The Schiff bases which are able to form protective layers on the surface have been utilized for the preparation of anticorrosive materials and can serve as effective corrosion inhibitors. The commercially employed corrosion inhibitors include many aldehydes or amines. The presence of C=N functionality in Schiff bases makes them more efficient for this purpose. In the use of Schiff base as corrosion inhibitor , chemisorptions is the major interaction. They

have the capability to make bonds with the metal surface due to the electron rich centers available in Schiff bases . (Li *et al*., 1999, Talati *et al*., 2005, Behpour *et al*., 2010).

A number of substituted Schiff bases have been synthesized by Aggarwal *et al*. (2009). The compounds were characterized by NMR and mass spectrometry and screened for antifungal activity against pathogenic fungi, namely, Sclerotium rolfsii and Rhizoctonia bataticola, and for their effect on nitrification inhibition under laboratory conditions. Maximum antifungal activity was exhibited by (2,4-dichlorobenzylidene)-(2,4,5-trichlorophenyl)-amine and (3-nitrobenzylidene)-(2,4,5-trichlorophenyl)-amine against both fungi. Maximum nitrification inhibition (IN) in the range 91-96% was exhibited by (2,4-dichlorobenzylidene)-(2-fluoro phenyl)-amine, (3-nitrobenzylidene)-(4-fluorophenyl)-amine, (2,6-dichlorobenzylidene)-(4-fluorophenyl)-amine and (2,6-dichlorobenzylidene)-(3-fluorophenyl)-amine.

2.4.2 Biological applications

The presence of C=N in many organic compound is responsible for their biological property. Some examples are thiacetazone and nitrofyrazone

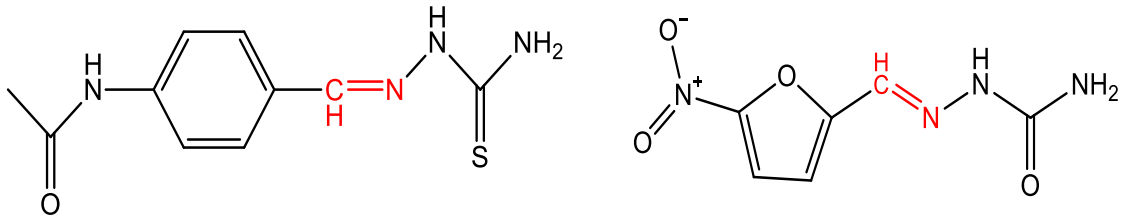

Thiacetazone Nitrofyrazone

Figure 7: Structure of some drugs containing imine bond.

Schiff bases appear to be important intermediates in a number of enzymatic reactions involving interaction of an enzyme with an amino or a carbonyl group of the substrate. One example involves the Chemistry of vision which makes use of an imine linkage between the aldehyde derived from vitamin A and the opsin protein situated in the retina eye. The chemical changes in the cell take place with the help of proteins which catalyze the changes and vitamins play their role as coenzymes i.e., they are assisting the functioning of many enzymes. The most important is the active form of the vitamin B6 which is pyridoxal phosphate. The most important feature is that the amino acid groups in the enzymes make an imine with the aldehydic groups in vitamin B6. The transfer of the amino group from one amino acid to another i. e., transamination is actually catalyzed by the coenzymes which are bound to enzymes and possesses significant importyance in the biosynthesis of amino acids. The imine to the pyridoxal and the modified amino acid linkage is cleaved by the enzyme-catalyzed hydrolysis in the last step (Arulmurugan *et al*., 2010).

Several synthetic Schiff bases have been found to exhibit biological activity as a result of which they have been investigated for use as antimalarial (Rathelot et al., 1995, Gemma *et al*., 2010), antibacterial (Bayrak *et al*., 2009, Fasina and Dada, 2013), antifungal (Karthikeyan *et al*., 2006, Guo *et al*., 2007), anticonvulsant (Ragavendran *et al*., 2007, Pandey and Srivastava, 2009), antitumor (Vicini *et al*., 2006), antiviral (Sriram *et al*., 2006) and antituberculosis (Lourenco *et al*., 2008, Pandey *et al*., 2011, Utku *et al*.,2011) agents.

The significant antimicrobial role of Schiff bases and hydrazide-hydrazone derivatives towards the development of new drugs was recently reviewed by Rollas and Kucukguzel, (2007) and Da Silva *et al*. (2011), respectively.

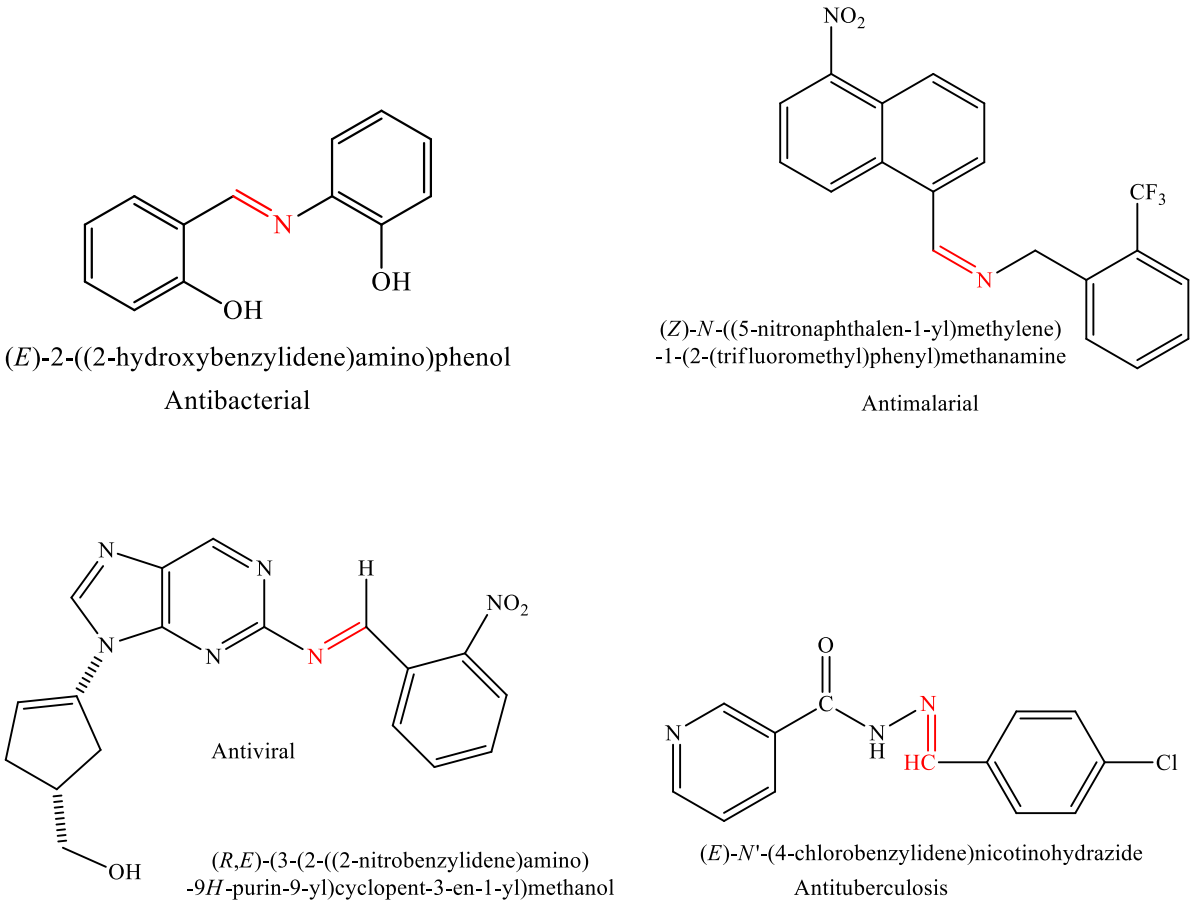

Figure 8: Examples of some bioactive Schiff bases

Schiff bases are generally excellent chelating agents especially when a functional group like –OH or –SH is present close to the azomethine group so as to form a five or six membered ring with the metal ion. They have been used in coordination Chemistry to form stable transition metal complexes (Behpour *et al*., 2010, Abd El-Halim *et al*., 2011, Sakthilatha and Rajavel,. 2013).

2.5 Schiff base Transition Metal complexes

In broad definition, transition metals are elements of atomic numbers 21-31, 39-49 and 71-81. A more restricted classification of the transitions element preferred by many chemists is limited to elements with atomic numbers 22-28, 40-46, and 72-78, inclusive. All of the elements in this classification have one or more electrons present in an unfilled *d*-subshell in at least one well-known oxidation state. Transition metals have a distinct tendency to form complexes because of the presence of empty *d* orbitals to accept lone pairs of electrons from a ligand.

Schiff base transition metal complexes are molecules that consist of central transition metal ion surrounded by Schiff base ligand. They have been known from as early as 1840, even before the general preparation of the Schiff bases ligands themselves when a dark green crystalline solid, bis(salicylaldimino)Cu(II) was isolated from the reaction of cupric acetate, salicyladehyde and aqueous ammonia (Holm and Solomon, 1966).

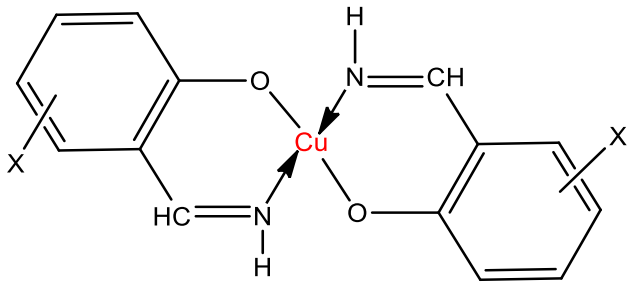

Figure 9: Structure of bis(salicylaldimino)Cu(II) complex

2.6 Synthetic routes to Schiff base transition metal complexes

Several methods are known for synthesizing Schiff base transition metal complexes such as the direct and template method.

2.6.1 Direct Method: The most effective and used method is the direct method. In this method, the isolation and purification of Schiff bases are carried out before complexation. The complexes are then prepared by treating the metal salt and Schiff bases. One of the advantages of this method is that it is possible to perform spectral characterization of complexes by comparing with the spectral data of the ligands. (Aboul-Melha, 2008, Singh and Dhakarey, 2009, Fugu *et al*., 2013, Alias *et al*., 2014).

2.6.2 Template Method: In this method, synthesis of the complexes are carried out without the isolation of Schiff bases. It is a one step or pot synthesis with the aldehyde, amine and metal salt present in the reaction medium. Several researches have used this method in the synthesis of Schiff base metal complexes (Ulucam and Reynek, 2007, Ababei *et al* ., 2011, Sakthilatha and Rajavel, 2013, Singh, *et al*., 2014).

2.7 Transition metal complexes as therapeutic agents

Transition metal compolexes with their versatile coordination numbers, geometries, oxidation states, ligand binding affinities, redox and spectroscopic properties are suitable for designing metal based therapeutic agents (Hambley, 2007, Haas and Franz, 2009). The unique properties of these transition metals is important to understand its interaction with the biology molecule.

2.7.1: Copper complexes as therapeutic agents

Copper (Cu) is a transition metal with the symbol Cu (from latin cuprum) and atomic number 29. It can exist in oxidized (Cu^{2+}) and reduced (Cu^{+}) states within the body. Copper complexes are most extensively studied for therapeutic and diagnostic applications because Cu is a suitable cofactor for a variety of enzymes involved in many biological processes; such as energy metabolism (cytochrome c oxidase) and antioxidative activity (copper zinc superoxide dismutase, SOD1) (McCord and Fridovic, 2003).

Cu complexes of bis(thiosemicarbazones) (Cu^{II}(btsc)s) have been investigated as metallodrugs and diagnostic agents (Dearling *et al*., 2002). More recently, these complexes have also been investigated as potential agents to treat neurodegeneration with glyoxalbis(N (4)-methyl-3-thiosemicarbazonato)copper(II) (Cu^{II}(gtsm)) reported to have neuroprotective action in cell culture and animal models of Alzheimer's disease (Donnelly *et al*., 2008, Crouch *et al*., 2009 and Paterson and Donnelly, 2011).

A Cu(II) complex (Cu(II) gamma-polyglutamic acid) has been shown to have insulin-mimetic activity (Karmaker *et al*., 2007). Also, treatment of diabetic mice with Cu sulfate resulted in decreased blood glucose levels and improved pancreas morphology (Sitasawad *et al*., 2001).

Cu complexes have been used in the treatment of inflammatory diseases. Commonly used anti-inflammatory agents include non-steroidal anti-inflammatory drugs (NSAIDs), which is a large group of compounds including ibuprofen, aspirin and naproxen. Cu-NSAIDs

exhibited increased anti-inflammatory activity and reduced gastrointestinal toxicity compared to their parent drugs (Agotegaray *et al*., 2010).

Topical application of Cu-complexes have been useful in the treatment of various skin conditions such as wounds, ultraviolet (UV) induced damage and skin cancers. Administration of Cu-aspirinate to mice following UV exposure resulted in a suppression of reactive oxygen species (ROS) generation and increase of SOD activity (Fujimori *et al.*, 2007). Various studies on wound healing have focused on Cu complexed to the tri-peptide glycyl-histidyl-L-lysine (GHK). Treatment of rats with Cu-GHK resulted in an up-regulation of matrix metalloproteinases, which are required to degrade the extracellular matrix and remove damaged tissue (Simeon *et al*., 1999). Topical application of Cu-GHK to open wounds in rabbits resulted in significantly faster neovascularization and formation of new tissue (Gul *et al*., 2008).

Copper(II) complexes with strong abilities of binding and cleaving DNA have been reported , many of which exhibited excellent apoptosis-regulating and anticancer activity (Li *et al*., 2013, Liang *et al*., 2014).

2.7.2 Nickel complexes as therapeutic agents

Nickel (Ni) is a transition metal with atomic number 28. Both Ni(I) and Ni(II) species are being studied increasingly because of the possible involvement of these oxidation states in nickel containing metalloenzymes (Nestle *et al*., 2002).

Nickel is an essential component in different types of enzymes such as urease, carbon monoxidedehydrogenase, and hydrogenase (Abu-Surrah and Kettunen, 2006). Recently, some results showing also apparent potential of thisplatinum group element in antitumor studies have been reported. For example the cytotoxicityof the nickel (II) complexes containing 1,2-naphtoquinone-based thiosemicarbazone ligands (NQTS) was tested on MCF7 human breast cancer cell line and compared tofree ligand and another naphthoquinone, commercial antitumor drug etoposide. According to the reported data, Ni-NQTS complex has the highest antitumor activity with an IC50 of 2.2 μM. The mechanistic study of action showed inhibition of topoisomerase II Recent studies showed that the corresponding nickel of semicarbazones (Fig 12) have even greater inhibitory effect on MCF7 cell growth. They display IC50 values in 2-5 μM range and also in general they produce lower side effect than thiosemicarbazones.

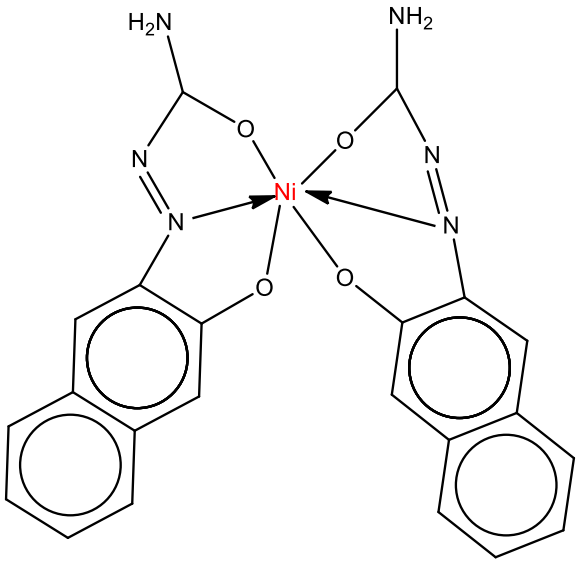

Figure 10: Structure of a Ni(II)-semicarbazonebased antitumor complex (Abu-Surrah and Kettunen, 2006)

In 2010, new methoxy-substituted nickel(II)(salophene) derivatives are synthesized and their anticancer properties were investigated (Lee *et al.*, 2010). [Ni(II)(3-methoxy-salophene)] inhibited proliferation and induced apoptosis in a concentration dependent manner, giving evidence for the involvement of CD95 receptor-mediated, extrinsic pathway. Furthermore, [Ni(II)(3-methoxy-salophene)] overcame vincristine drug resistance in Burkitt-like lymphoma cells (BJAB)and human B-cell precursor cells (Nalm-6)

2.7.3 Cobalt complexes as therapeutic agents

Cobalt is a versatile transition metal for drug development with the symbol Co and atomic number 27. It possesses a diverse array of properties that can be manipulated to yield promising drug candidates. Common oxidation states of cobalt include +2 and +3, although compounds with oxidation state +1 are also well developed. Cobalt is located between iron and nickel and shares many physical and chemical properties with these two elements.

The most important biological compound of cobalt is vitamin B_{12}. It is the only vitamin having tightly bound cobalt ion. Cobamide, a B_{12} derivative is important in the synthesis of amino acids in the body which are used to make proteins (Hamza *et al*., 2000).

It has been discovered that attaching a cobalt complex to aspirin significantly changes the molecule's anticancer properties. Further investigation by Otta's team revealed that Co-aspirin could inhibit cell growth and the formation of small blood vessels-two factors crucial for tumor growth (Ott *et al*., 2009). These studies stimulated the potential for the discovery of new anti-tumor therapies by adding cobalt complex fragment to established drugs.(Dimiza, *et al*., 2012).

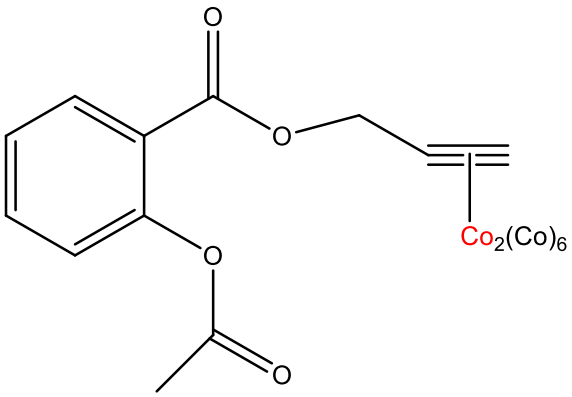

Figure 11: Hexacarbonyldicobalt-aspirin complex (Ott *et al.*, 2009)

Cobalt complexes have also been reported by Heffern *et al*. 2013, as redox-responsive drug carriers. They observed that coordination to cobalt ion can deactivate antitumor cytotoxins such as nitrogen mustards, DNA intercalators , and the MMP-inhibitor marimastat.

Some hexacarbonyl dicobalt complexes exhibited promising activity against several human cancer cell lines. They displayed antiproliferative activities with IC_{50} values in the range of 5–50 µM in human breast cancer cell lines (Sousa-Pedrares *et al*., 2008).

The incorporation of a more physiologically relevant metal like copper, nickel and cobalt is particularly pertinent for future development of metal based therapeutics as these compounds could have important beneficial outcomes in many diseases.

2.8. Applications of Schiff base transition metal complexes

Interest in the applications of transition metal complexes of Schiff bases stems from the fact that Schiff bases offer opportunities for inducing substrate chirality and tuning the metal centered electronic factor to yield a more desired property. The data available for Schiff bases transition metal complexes in literature embraces very wide and diversified application, comprising vast areas of industrial, analytical and multiple aspects of biological application. Among all the Schiff base complexes, those derived from salicylaldiimines and those containing the pyridine core are important compounds in medicine and pharmaceutical chemistry due to their ability to inhibit enzymes (Savchenko *et al*., 2010).

Schiff base metal complexes have been known to act as highly efficient catalysts in various synthesis and other useful reactions (Rao *et al*., 2007; Jammi *et al*., 2008).

Some series of Schiff base copper(II) complexes derived from amino acids have been employed as catalyst in the kinetic hydrolytic reactions of amino acid esters. These compounds exhibited enhanced (10-50 times) hydrolytic rate more than simple copper(II) ion (Chakrabroty *et al*.,1994).

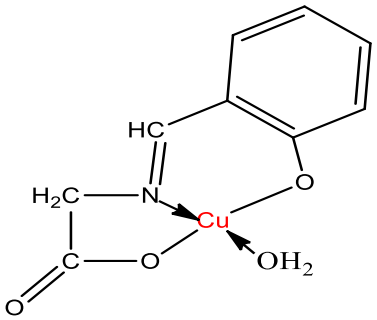

Figure 12: Structure of Schiff base copper(II) complex as catalytic agent (Chakrabroty *et al*.,1994).

The interactions of various materials with applied electromagnetic fields are dealt by non-linear optics(NLO) for introducing new electromagnetic fields with different physical properties like frequency and phase. The dynamic image processing, optical communication and optical computing utilizes such type of materialsin manuplating photonic signals in an efficient manner which enhances their significance. The ability of Schiff transition metal complexes to tailor metal-organic interactions and various oxidation states of metals present in such systems makes these complexes potential building blocks for non-linear optical materials. Di Bella and co-workers reported the NLO properties exhibited by bis(salicylaldiminato)metal Schiff base complexes. Several researches have invesugated on NLO properties of Schiff base transition metal complexes (Trujillo *et al*., 2010, Ananthi *et al*., 2012, An *et al*., 2014).

A series of VO(II), Co(II), Ni(II), Cu(II) and Zn(II) complexes have been synthesized from azo Schiff base ligand derived from 5-(4-chloro-phenyl)diazenyl)-2-hydroxybenzaldehyde and 2-hydroxybenzohydrazide. The compounds were characterized on the basis of spectral and analytical analysis. The results reveal a distorted square planar for the Cu(II), square pyramidal geometry for oxovanadium and tetrahedral for other complexes. All the synthesized complexes can serve as potential photoactive materials as indicated from the characteristics fluorescence properties (Anitha *et al*., 2011).

Transition metal [Co(II), Ni(II), Cu(II) and Zn(II)] complexes of substituted 2-aminopyridine Schiff bases were prepared and characterized by physical, analytical and spectral data. Based on these data, an octahedral geometry was proposed for the complexes The compounds were

evaluated for their *in-vitro* antibacterial activity against *Staphylococcus aureus*, *Escherichia coli* and *Pseudomonas aeruginosa.* The complexed Schiff bases showed more antibacterial activity against one or more bacterial species as compared to the uncomplexed compound (Chohan *et al*., 2001).

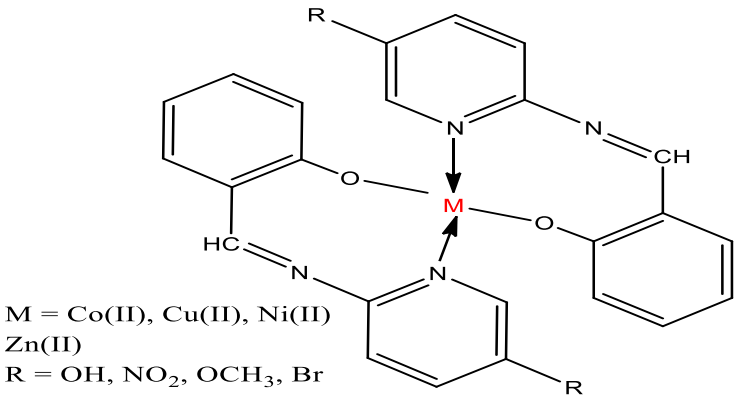

Figure 13: Proposed structure of substituted 2-aminopyridine based Schiff base metal(II) complex (Chohan *et al*., 2001).

Pandey and Srivastava (2009), have reporetd a series of new Schiff bases of 2-aminopyridine synthesized through the condensation reaction between 2-aminopyridine with different aldehydes / ketones and cyclic ketones. The compounds were evaluated for anticonvulsant properties against seizures induced by maximal electroshock (MES), and chemically induced seizures in mice. The acute adverse effects profiles were assessed with respect to impairments of motor co-ordination by rotorod test in mice. These Schiff bases showed better anticonvulsant potency against MES and Sc.-PTZ induced seizures while found moderately active against Sc.-STY induced seizure screen than that of reference drugs Phenytoin and Phenobarbital.

Spinu *et al*. (2008), have synthesized new Schiff base complexes of Fe(II), Co(II), Ni(II), Cu(II), Zn(II) and Cd(II) derived from 2-thiophenecarboxaldehyde with 2-aminopyridine. The compounds were screened for their *in-vitro* activity against *Staphylococcus aureus*, *Escherichia coli* and *Pseudomonas aeruginosa.* The metal complexes showed enhanced activity than the uncomplexed Schiff base.

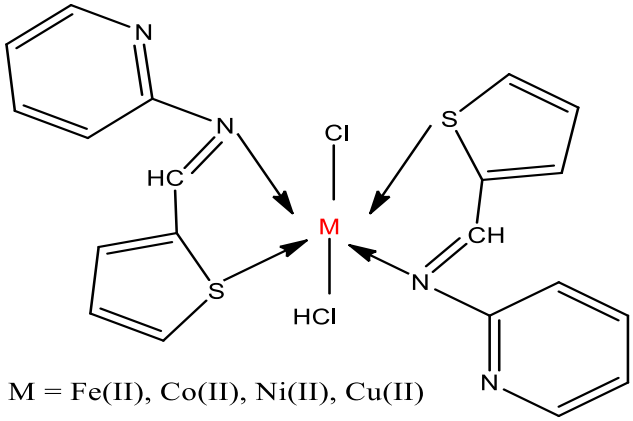

Figure 14: Proposed structure of 2-aminopyridine based Schiff base metal(II) complex (Spinu *et al*., 2008).

A series of new metal chelates of Co(II), Ni(II) and Cu(II) with a Schiff base ligands derived from condensation of 2-thienyl glyoxal and 2-aminopyridine derivatives were characterized *via* elemental analysis, IR, Mass, NMR, magnetic and electronic spectral data. The antibacterial and antifungal activity of the Schiff bases and their complexes against *Escherichia coli*, *Proteus vulgaris*, *Aspergillus niger* and *Aspergillus flavus* have shown that the complexes were more active than the free ligands (Singh and Dhakarey, 2009).

The Schiff base complexes of Co(II), Ni(II) Cu(II) and Zn(II) were synthesized from 4-pyridine carboxaldehyde with 3-aminopyridine. The complexes were characterized by

elemental analysis, molar conductance, molecular weight determination, infrared spectroscopy, x-ray diffraction and scanning electron microscope. Octahedral arrangement of ligand around the metal ions was suggested. The antimicrobial and cleavage activity have also been studied for the synthesized compounds. The antimicrobial results indicate that the metal complexes are better antimicrobial agents as compared to the Schiff base. against the bacteria namely, *Staphylococcus aureus, Escherichia coli, Klebsiella Pneumonia* and fungi like *Candida albicans, Aspergillus niger* and *Pencillium* sp (Sheeja-Lovely and Chridtudhas, 2013).

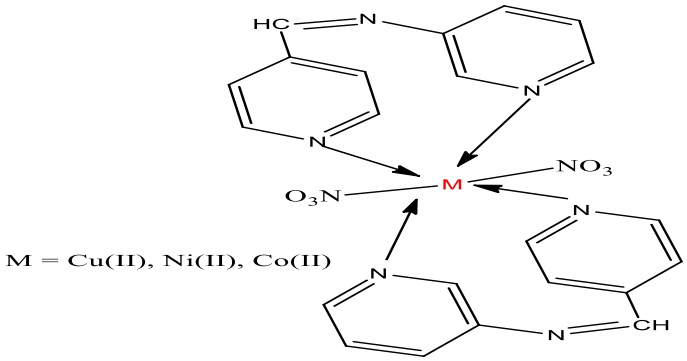

Figure 15: Proposed structure of 3-aminopyridine based Schiff base metal(II) complex (Sheeja-Lovely and Chridtudhas, 2013).

Nazir *et al*. (2013), reported the synthesis, characterization and biological evaluation of Zn(II), Cu(II), Ni(II), Co(II), Mn(II), Cr(II) and Cd(II) transition metal complexes of Schiff bases salicylidene gemifloxacin derived from gemifloxacin and salicylaldehyde. The prepared compounds exhibited antibacterial activity against some selected bacteria such as *Staphylococcus aureus*, *Escherichia coli*, in the order: metal complexes > Schiff base ligands > Parent drugs.

Complexes having formular type $[ML_2].2H_2O$ (where M = Cu(II), n = 0.5; M = Co(II), n = 2; M = Ni(II), n = 3 and M = Zn(II), n = 2) and $[Cu(L)_2]$ were synthesized with Schiff base formed by the condensation of isonicotinic acid hydrazide and 2,3-dione 1H-indole. The ligand and the complexes were characterized by elemental analysis, IR, UV-Vis-NIR, ^{I}HNMR and ^{13}NMR spectroscopy, thermal analysis, magnetic susceptibility and molar conductivity measurements. The antibacterial activity of the ligand and its complexes was tested on *Staphylococcus aureus*, *Escherichia coli* and *Salmonella typhinurium*. In the *Staphylococcus aureus* only the Co(II) complex enhanced the activity of the ligand. Generally, the ligand and its complexes exhibited less activity than ampicillin drug. The test against *Escherichia coli* indicates that the new compounds have a much intense activity than gentamicin drug. All the complexes have a greater inhibitory capacity than the ligand but less than ciprofloxacin drug (Kriza *et al*., 2010).

Copper(II) complexes of some aroyl hydrazone of α-pyridine have been synthesized and characterized using analytical and spectral analysis. The compounds were screened for antimicrobial activities on *Staphylococcus aureus, Escherichia coli, Pseudomonas aeruginosa, Salmonella typhi and Bacillus subtilis*. The metal complexes were more active compared to their corresponding ligand (Karbouj *et al*., 2010).

The antifungal behavior of a tridentate ONO donor ligand, -bromo-acetoacetanilide isonicotinylhydrazone toward Mn(II), Co(II), Ni(II), Cu(II) and Zn(II) was studied. Based on elemental analysis, conductivity measurements, electronic, infrared and nuclear magnetic resonance spectral studies, the ligand acted as tridentate monoanion forming octahedral

complexes with Mn(II), Co(II), Ni(II) and Zn(II). In the case of Cu(II) complex, a square planar complex was formed. The metal complexes were found to be more active than the ligand against the selected pathogenic fungal strains (Deepa and Aravindakshan, 2004).

Copper (II), nickel(II) and cobalt(II) complexes of Schiff's base derived from *o*-phenylenediamine and 5-bromosalicylaldehyde were characterized by elemental analysis, IR and electronic absorption spectra. They possess growth inhibitory activity against *Escherichia coli* and *staphylococcus aureus* (Fasina *et al*., 2012).

Schiff base synthesized from 5-bromo-3-fluorosalicylaldehyde and benzidine and its complexes with Cu (II) and Ni (II) has been tested against four pathogenic bacteria namely *Staphylococcus aureus* and *Bacillus subtilis*) as Gram-positive bacteria and *Escherichia coli* and *K. pneumoniae*) as Gram-negative bacteria. Copper complex showed higher activity than Ni complex (Vedanayaki *et al*., 2010).

A tridentate Schiff base derived from 2-aminothiazole and fufural-, thiophene- and pyrrole-2-carboxyaldehyde coordinated to Co(II), Ni(II), Cu(II) and Zn(II) through the azomethine and thiazole nitrogens, fufuraal oxygen, thiophene sulphur and pyrrole nitrogen respectively were identified on the basis of their physical, analytical and spectral data. All the Schiff bases were found to be biologically active and their complexes showed more significant antibacterial activity against *Escherchia coli, Pseudomomas aeruginosa, Staphylococcus aureus* and *Klebsiella pneumoniae* in comparison to the uncomplexed Schiff bases (Chohan and Kausar, 2000).

Rosu *et al*. (2011), synthesized six new copper(II) complexes from the Schiff base derived from 1-phenyl-2,3-dimethyl-4-amino-3-pyrazolin-5-one and 4-methoxysalicyaldehyde. The compounds were characterized by spectroscopic analysis. The crystal structure of the Schiff base ligand as well as one of its copper(II) complex [$Cu(L_2)$] was determined by X-ray diffraction studies. The *in-vitro* antibacterial activity against *Staphylococcus aureus var. Oxford* 6538, *Pseudomomas aeruginoas ATCC* 9027, *Klebsiella pneumonia ATCC* 100131 and *Escherchia coli ATCC* 10536. Some of the complexes showed enhanced activity more than streptomycin and activity was dependent on the metal salt anion used.

Transition metal complexes with Schiff base ligands have shown promising nucleolytic activity. The interaction of transition metal complexes with DNA have been studied extensively for their use as probes for DNA structure and their potential application in chemotherapy (Liu *et al*., 2011).

Halli *et al*. (2011), synthesized a series of Co(II), Ni(II), Cu(II), Zn(II), Cd(II), and Hg(II) with Schiff base derived from the condensation of benzofuran-2-carbohydrazide and thiophene-2-aldehyde. The structures of the complexes were proposed in the light of their IR, UV-vis, ^{1}HNMR, ESR spectral data and magnetic studies. On the basis of these studies, 6 coordinated octahedral polymeric structures were assigned to the Co(II), Ni(II), and Cu(II) complexes, and 4 coordinated tetrahedral geometries to the Zn(II), Cd(II), and Hg(II) complexes. The complexes had higher antibacterial and antifungal activity than their corresponding ligands. The DNA cleavage studies revealed that the complete cleavage of

DNA was observed for Zn(II) and partial cleavage of DNA was observed for the Ni(II) and Hg(II) complexes.

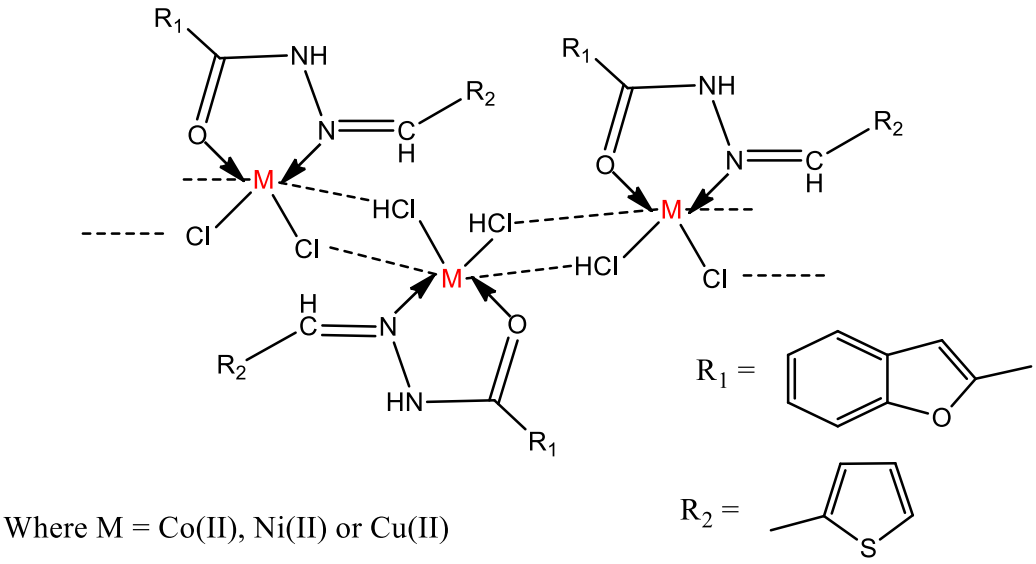

Figure 16: Proposed structure of Co(II), Ni(II), or Cu(II) complexes as DNA cleaving agent (Halli *et al*., 2011).

Novel oxovanadium (IV) complexes with 2-methyl-3-(pyridine-2-ylmethylene)quinazolin-4(3H)one or 3-(2-hydroxy-3-methoxybenzylidene amino)-2-methyl quinoli-4(3H)one were synthesized . Based, on the spectral and analytical results, a square planar geometry was assigned to all the complexes. The DNA binding and nuclease activity revealed that the complexes can act as effective DNA cleaving agents (Prasad *et al*., 2011).

A rapid, efficient, clean and environmentally benign exclusive synthesis of Schiff bases as new ligands was developed using condensation of 2-aminonicotinic acid with salicyldehyde, 5- nitrosalicyldehyde, 5-bromosalicyldehyde and 5-methoxysalicyldehyde efficiently in a

water suspension medium using acid catalyst with excellent yields under microwaves. The synthesized Schiff bases and their transition metal complexes were evaluated for their *in vitro* antibacterial activity against four gram-negative namely *Escherichia coli, Pseudomonas aeruginosa, Salmonella typhi, Shigella flexneri* and two gram-positive bacterial stains by the agar-well diffusion method. Schiff bases were found to exhibit either no or low to moderate activity but all the complexes exhibited varied vigorous activity against different bacteria. Schiff bases which were inactive before complexation became active and less active became more active upon coordination with mentioned bivalent transition metal ions. The compound L3H was found to be active against all the Grampositive and Gram-negative bacteria. The compound L4H was found to be inactive against the Gram-negative species, *Escherichia coli*, *Pseudomonas aeruginosa* and *Salmonella typhi* and the Gram-positive species, *Bacillus subtilis*. The compound L1H showed no inhibitory action against the Gram-negative species, *Salmonella typhi* and *Shigella flexneri*, and the Gram-positive species, *Bacillus subtilis*. The Schiff base, L2H was found to be inactive against the Gram-negative species, *Pseudomonas aeruginosa* and *Shigella flexneri*. In contrast, the growth of all the Gram-negative and Gram-positive species was inhibited by all the metal complexes under investigation (Srivastava *et al*., 2011).

Notable among synthesis, characterization and biological studies of heterocyclic Schiff bases and their complexes are the works of Chohan *et al*., (2000), Mashaly *et al*,. (2004), Raman *et al*., (2004),. Osowole *et al*., (2005), Mittal *et al*., (2009), Mohammed *et al*., (2009), Gwaram *et al*., (2012). They all directed their efforts looking at changes in the stretching frequencies of C=N, OH and C-O of Schiff bases and the metal complexes. The information obtained has

been used to predict the geometry and propose a structure for the complexes. The biological activity of these compounds suggest that the metal complexes exhibited enhanced activity than the uncomplexed Schiff bases.

2.9 Anti-tuberculosis drug related to the present study

Isonicotinic acid hydrazine (INH) also known as isoniazid (Laniazid, Nydrazid) is an organic compound with a simple structure containing a pyridine ring and a hydrazide group and both molecules are essential for its high activity against *M. TB.* The compound was first synthesized in 1912 but its activity against tuberculosis was first discovered by Gerhard Domagk's team in 1952 (Fox 1999). It has a very high *in-vivo* inhibitory activity on *Mycobacterium tuberculosis*. INH is very significant in the current recommended standard TB therapy and is the mainstay for the treatment of TB (Bernstein *et al*., 1952, Wang *et al*., 1998, Timmns and Deretics, 2006).

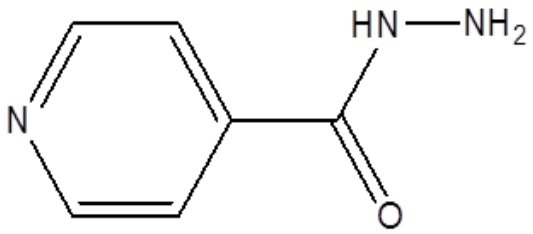

Figure 17: Structure of Isonicotinic acid hydrazide (INH)

2.9.1 Mechanism of action of INH

INH penetrates the host cells readily and diffuses across the *M. tuberculosis* memebrane. It is a pro-drug, requiring the oxidative activation by the *M. tuberculosis* catalase-peroxide

enzyme KatG. The killing activity of the active metabolites of INH is by the inhibition of mycolic acid synthesis, a long fatty acid found in the cell wall of the bacterium. The activated INH binds tightly to the NADH-dependent enoyl acyl carrier protein (ACP) reductanse InhA, a component of the fatty acid synthase II system of the bacterium forming a covalent adduct, isonicotinic InhA acyl NADH (Takayama *et al*., 1972, Banerjee *et al*., 1994, Vilcheze *et al*., 2000).

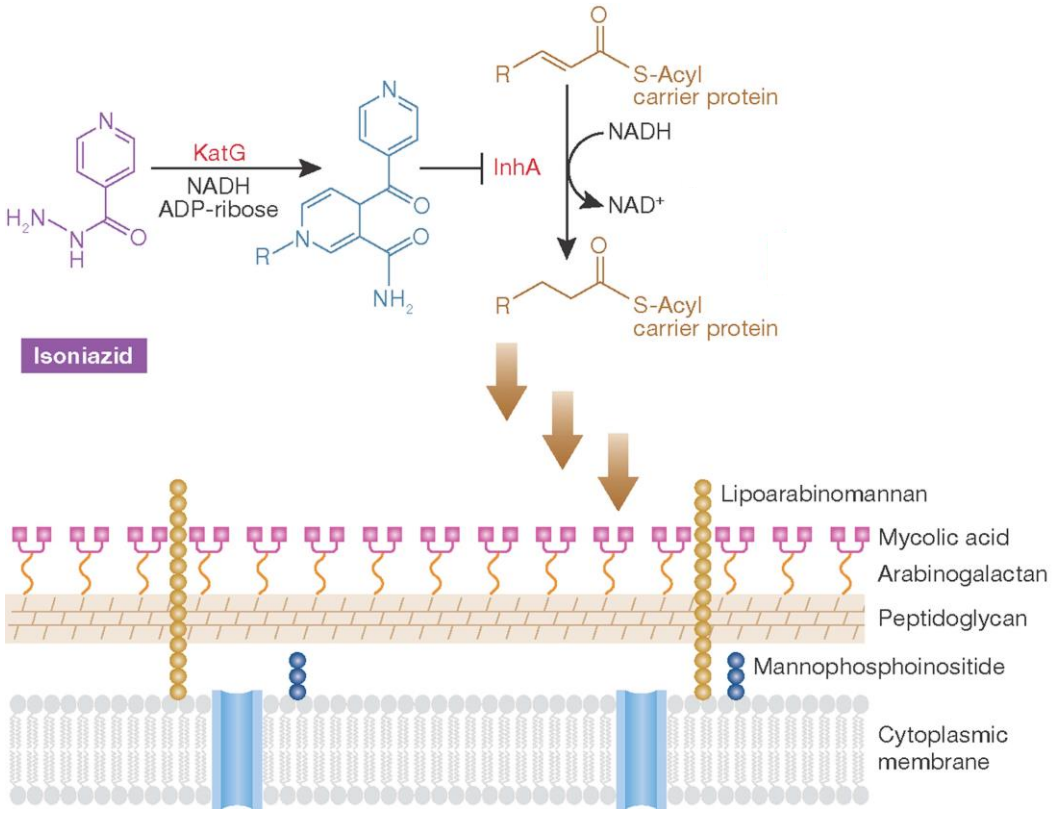

Scheme 6: Schematic diagram showing the mechanism of actionof isoniazid

2.9.2 Factors associated with INH resistance

Resistance against INH is associated mostly with mutations or deletions in KatG that block the activation step of the drug (Lee *et al*., 2001, Zhang *et a*l., 2005, Vilcheze *et al*., 2006).

Acetylation of INH by N-arylaminoacetyl transferase (NATs) is another factor that causes resistance against INH. These enzymes are found in both *Mycobacteria* and mammalian hosts, and they deactivate INH by means of reaction at the hydrazine unit as shown in **scheme 1**. Therefore, structurally blocking INH toward the actions of NATs at the hydrazine unit may combat the onset and increase of resistance.

2.10 Approaches to the development of new anti-tuberculosis agents

Development of new anti-tuberculosis agents can be biologically or non-biologically inspired. The two approaches are in use concurrently.

2.10.1 Biological inspired approach:

Molecular modification by nature has been going on since the beginning of life. Chemists had learned well from nature the significance of small changes in chemical structure of drugs of the biological activity in living organism. This is evident in natural modification of the alkolids: morphine, codeine and thebaine. In addition, are the sex hormones and sulfanilamide development. By further alteration of these structures more potent and more useful hormonal drugs have been prepared by chemists (Schueler, 1964).

Development of new drugs from already known molecules that have been in use for several years and have proven safe and efficient is an attractive strategy for pharmaceutical and clinical progress (Cocco *et al*., 1999, Costi *et al*., 1999, Falzari *et al*., 2005, Chen *et al*., 2006).

Special attention is given to INH, an important drug in the therapeutic arsenal for TB treatment. Molecular modification of INH has resulted in the development of new INH derivatives .with possible greater activity (no resistant), lower toxicity and fewer side effect (Protopopova *et al*., 2005). Recently, the INH molecule incorporated on a pyrazoline nucleus, showed activity against strains of *M. tuberculosis* which are resistant to INH.

Structural modification of INH carried out by reacting INH and various aldehydes and ketones gave the desired Schiff bases. The Schiff base containing cyclohexone moiety was active against *M.tuberculosis* $H37R_V$, exhibiting an MIC value of 0.03 mg/l. which is more potent than INH. Additionally, the Schiff base was not toxic against cell line VERO (epithelial cells from healthy monkey kidney). The therapeutic safety and effectiveness of this compound is higher than 40,000, making it an excellent lead for the development of anti-tuberculosis agents (Hearn and Cyammon, 2004). This finding stimulated the synthesis of forty-six Schiff bases by this group. The compounds were screened against *M.tuberculosis* strain $H_{37}RV$. All the compounds were active and displayed MICs necessary to inhibit growth of the organism by 90%. Compounds displaying MICs value of 0.06 μg/mL or less were derived from cyclohexanones and benzaldehyde (Hearn *et al*., 2009).

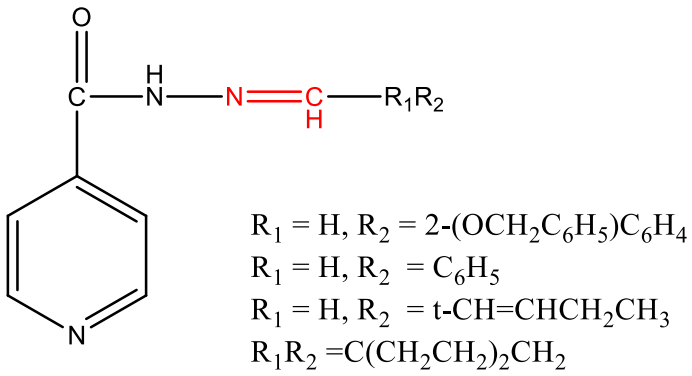

Figure 18: Antitubercular Schiff bases derived from cyclohexanones and benzaldehyde (Hearn *et al*., 2009).

Various INH derivatives were prepared by introducing INH pharmacophore into ortho-hydroxy acetophenone to form acid hydrazones. The compounds were screened against *M. tuberculosis* H_{37}RV using the Alamar blue susceptibility test The compounds inhibited the growth of *M. tuberculosis* with MIC ranging from 0.56-4.61μM. The Schiff base containing -OH was found to be the most active with an MIC of 0.56 μM when compared to INH (MIC of 2.04 μM). The *in-vivo* assay show that this compound decreased the bacterial load in murine lung tissue by 3.7-log10 as compared to controls, which was equipotent to INH (Sriram *et al*., 2005).

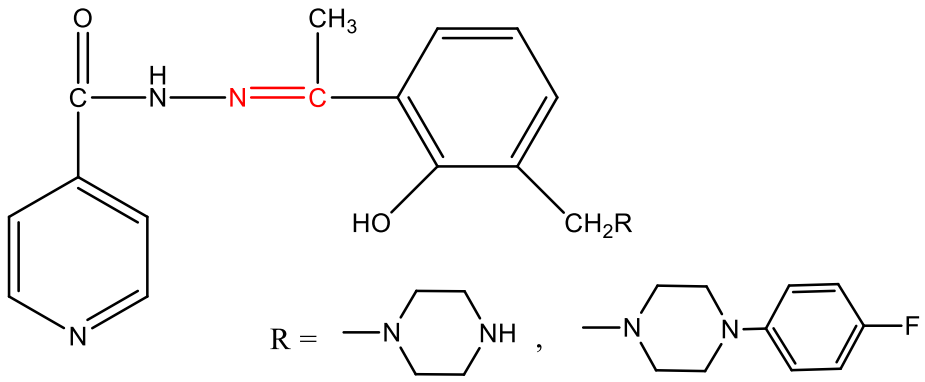

Figure 19: Antitubercular Schiff bases derived from Isoniazid (Sriram *et al*., 2005).

As part of the ongoing search for new INH derivative. Schiff bases, 2'-monosubstituted isonicotinohydrazides and cyanoboranes were evaluated for their *in-vitro* antimycobacterial activity. Some of the tested compounds displayed excellent MICs (0.025 μg/mL - 0.2 μg/mL) to moderate MICs (6.25 - 12.5 μg/mL) against ethambutol and rifampicin resistant strains (Maccari *et al*., 2005).

Sriram *et al.* (2009), synthesized new series of INH based Schiff bases as potential antimycobacterial agents. The fluoro containing Schiff base was found to be most potent with MIC of 0.49 μM against *M. tuberculosis* H_{37}RV and INH-resistant *M. tuberculosis.*

Utku *et al*., (2011), studied the *in-vitro* antimycobacterial activities of 6-substituted -3(2H)-pyridazinone-2-acetyl-2-(substituted/non-substituted acetophenone) hydrazone derivatives by the agar proportion method against *Mycobacterium tuberculosis* H_{37}RV. The bromo substituted Schiff base exhibited the best antimycobacterial activity with MIC value of 5 μg/ml.

Six novel Schiff bases derived from D-mannitol were synthesized and evaluated for their *in-vitro* anti-tuberculosis activity against *Mycobacterium tuberculosis* H_{37}RV using the Almar Blue susceptibility test. All the nitro (*o*-NO_2, *m*-NO_2 and *p*-NO_2) derivatives exhibited significant activities at 12.5, 25.0 and 25.0 μg/ml respectively when compared to first line drug such as ethambutol (Ferreira *et al*., 2009).

Two series of N´-(E)-heteroaromatic-isonicotinohydrazide derivatives and 1-(7-chloroquinolin-4-yl)-2-[(heteroaromatic)methylene]hydrazone derivatives were synthesized

and evaluated for their *in-vitro* antibacterial activity against Mycobacterium tuberculosis H37Rv. Several compounds were non-cytotoxic and exhibited significant minimum inhibitory concentration (MIC) activity (3.12, 2.50, 1.25, or 0.60 µg/ml), which can be compared to that of the first-line drugs ethambutol (3.12 µg/ml) and rifampicin (2.0 µg/ml) (Ferreira *et al*., 2010).

3-Isonicotinyl hydrazones of 1-alkyl Isatin derivatives were synthesized and investigated against bovine, human sensitive and human resistant strain of *M. tuberculosis* using the proportion method. The unsubstituted, 1-propyl, 1-propynyl and 1-benzyl groups exhibited the same level of potent inhibitory activity with INH. However, the later has no activity against human resistant strain (Aboul-Fadi *et al*., 2003).

Lourenco *et al*. (2007), reported the *in-vitro* evaluation of nitro containing isoniazid Schiff base derivatives against *Mycobacterium tuberculosis* $H_{37}R_V$. The para substituted ligand showed enhanced activity with MIC value of 1.2 µg/mL. This demonstrates the importance of nitro group in the modification of anti-tubercular activity of isoniazid.

Eighteen variety of *N*-(4-(substituted phenyl amino)-6-(pyridin-2-ylamino)-1,3, 5,-trizin-2-yl)isonicotinohydrazide were synthesized using 2-aminopyridine, isonicotinic acid hydrazide and cyanuric chloride. Their structures were confirmed by IR and NMR spectral analyses. They were tested for their *in-vitro* anti-tuberculosis activity against *M. tuberculosis* using the BACTEC 460 radiometric system. Electron-rich groups at para position produced significant inhibition activity at MIC value ranging from 0.0614-0.0211µM (Raval *et al*., 2010).

A series of twenty two Schiff bases derived from INH and benzaldehyde derivatives were evaluated for their *in-vitro* antibacterial activity against *M. tuberculosius* $H_{37}R_V$ using Alamar Blue susceptibility test. The halogen and methoxy containing Schiff bases exhibited significant activity at 0.31-0.62g/ml when compared with first line drugs such as INH and rifampicin (Lourenco *et al*., 2008).

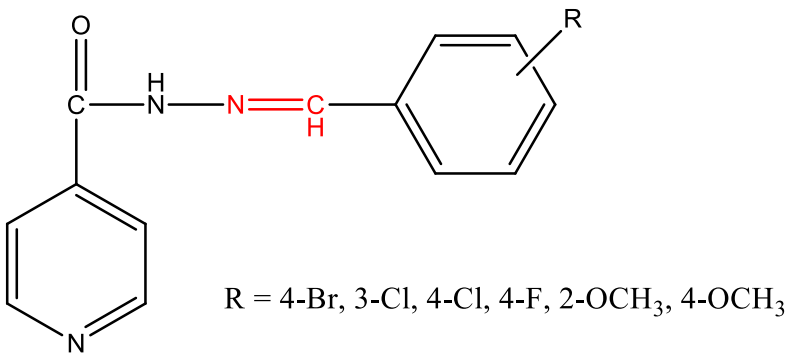

Figure 20: Antitubercular Schiff bases derived from monosubstituted benzaldehyde and isoniazid (Lourenco *et al*., 2008).

Schiff base derivatives of isoniazid, pyrazinamide, *p*-aminosalicylic acid, ethambutol and ciprofloxacin have been synthesized. The lipophilicity and antituberculosis activity results reveal that the new compounds with respect to the parent drugs have a more effective transport through cellular membranes and compounds containing isoniazid or pyrazinamide moiety were more active against *M. TB* $H_{37}RV$ 2-hydroxy-4-{[(isonicotinoylhydrazone)methyl]amino}benzoic acid showed the highest inhibition (99%) of *M.tuberculosis* $H_{37}RV$ at 0.39 µg/ml (Imramovsky *et al*., 2007).

Schiff base conjugate of *p*-aminosalicylic acid have been synthesized. Compounds containing hydroxyl-rich side chains show enhanced activity against *Mycobacterium smegmatis* and *bovis* BCG (Patole *et al*., 2006).

An isonicotinoyldithiocarbazic acid complexes with Ni, Co and Zn evaluated for anti mycobacterium activity against MDR-strain and *M. tuberculosis* $H_{37}Rv$ exhibited enhanced *in vitro* activity at MIC 10, 100, 50 μg/mL and 2, 2, and 50 μg/ml (Kanwar *et al*,.2008).

N-isonicotinamido-2-furanketimine (INH-F^1) and N-isonicotinamido-5-methyl-2-furanket imine(INH-F^2) complexes of Pd(II) and Pt(II) have also been prepared and characterized by analytical, spectral and X-ray powder diffraction studies. The *in-vitro* antimycobacterial activity of the ligands and their metal complexes evaluated against *Mycobacterial smegmatis*, showed that the activity of the ligands increased in the presence of metal ions (Sharma *et al*., 2010).

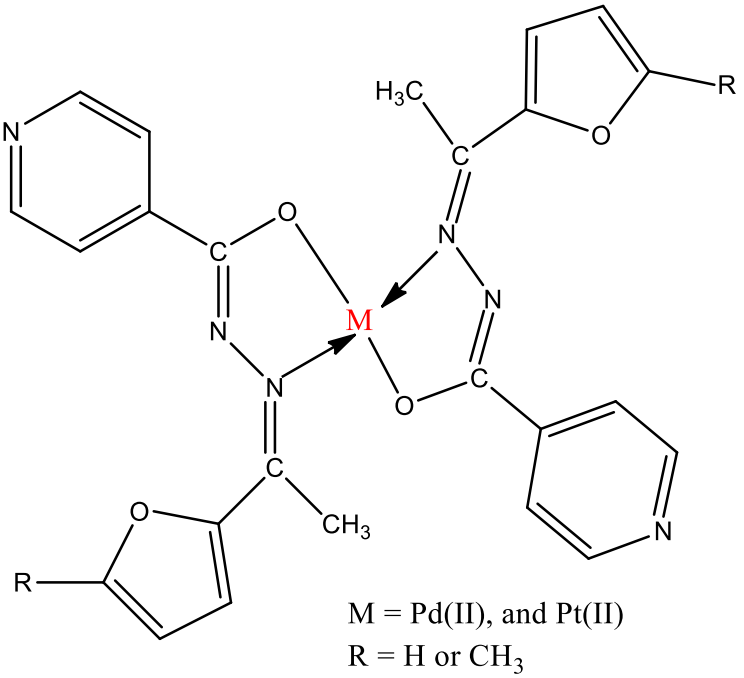

Figure 21: Schiff base Pd(II) and Pt(II) complexes as antitubercular agent (Sharma *et al*., 2010).

.

Schiff base complexes of pyrazinamide, an antitubercular drug have been synthesized and characterized. The pure drug and its metal complexes were screened against Mycobacterium tuberculosis *in vitro* in order to compare the antitubercular activity of the parent drug with various metal complexes. The results indicate that the complexes of pyrazinamide inhibit the growth of the bacteria to a greater extent than the pyrazinamide alone (Budhani *et al*., 2010)

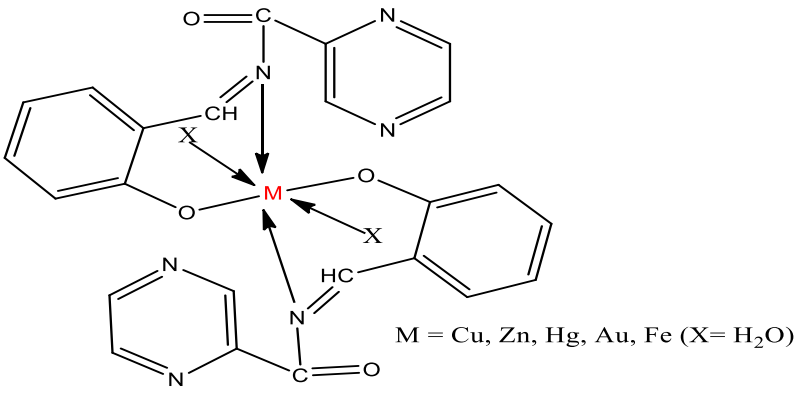

Figure 22: Schiff base complexes of pyrazinamide, an antitubercular drug (Budhani *et al*., 2010).

2.10.2 Non-biologically inspired approach

This involves searching for new compounds/agents that can be active against *Mycobacterium tuberculosis*. The main stay of this approach is based on Paul Ehrlich pioneering methods. The application is to screen a library of compounds in order to obtain evidence of activity without any information about what structure can show activity. In this context, several compounds have been synthesized and evaluated for their anti-tuberculosis potency

Twenty Schiff bases of 2-amino-5-aryl-1,3-4-oxadiazoles were synthesized for their antituberculosis activity using Microplate Alamar Blue Assay (MABA) against *M. tuberculosis* strain $H37R_V$. All the compounds showed appreciable activity at the single concentration of 6.25 μg/mL. Compounds having nitro– NO_2 group in either one or both of the aromatic rings showed increased activity compared to the halogenated compounds. The presence of the nitro group might be responsible for imparting considerably toxicity to the compounds resulting in the increased anti-tubercular activity (Harish and Kumar, 2009).

Nandi and Sankar (2012), synthesised Schiff bases from the 4-aminopyridine and toluene or acetic acid by using Dean Stark apparatus. After synthesis, the docking studies were done to estimate their antitubercular effect in comparision with standard drug isoniazid. From the docking studies result the compounds formed in this process were effective as anti-tubercular agent.

The *in-vitro* antimycobacterial activity of nine potential anti-tuberculosis metal complexes of *N*-benzylidene-pyridine carboxamidrazones on *M.TB* $H37R_V$ have been investigated. The result showed 32-64 fold enhancement in the anti-tuberculosis activity of the ligands upon copper complexation with MIC values in the range of 2 to 4 μM which are comparable with those observed for isoniazid (Sandbhor *et al*., 2002).

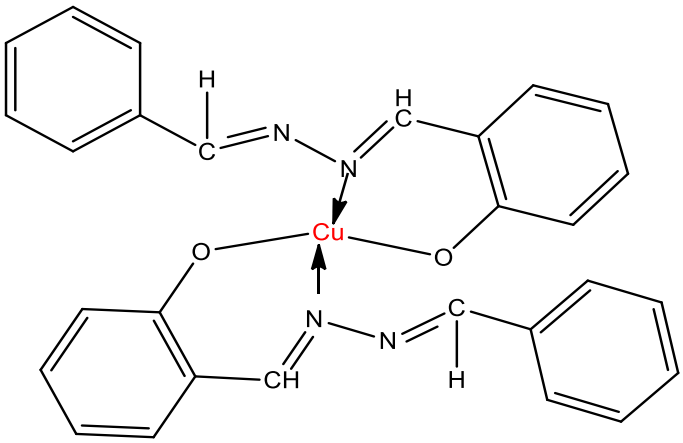

Figure 23: Proposed structure of INH copper complex as potential antitubercular agent (Sandbhor *et al*., 2002).

Novel transition metal complexes (Zn (II)) of bidentate Schiff base ligands were synthesized and characterized. The metal complexes showed increased *in-vitro* activity against *M.tuberculosis* when compared to pyrazinamide and streptomycin (Sawant *et al*., 2013).

Siddappa and Sunilkumar, (2013) reported the *in-vitro* antituberculosis activity of Cu(II), Co(II) and Ni(II), Mn(II) and Zn(II) complexes of heterocyclic based Schiff base. The results revealed that the activities of Cu(II), Co(II) and Ni(II), with MIC 6.25 µg/mL were similar to that of Streptomycin but less than that of Pyrazinamide drug, whereas Mn(II) and Zn(II) complexes showed moderate activity with MIC at 12.5 µg/ml.

New oxomolybdenum(V) and dioxomolybdenum(VI) complexes of 2-hydroxy-5-bromobenzylidene isonicotinoyl hydrazide as potential antituberculosis agents against *M.tuberculosis H*37R_V have been reported (Nair and Thankamani, 2010).

Joseph *et al*. (2012), prepared copper(II) complexes of 3-hydroxyflavonone based Schiff bases and evaluated their *in-vitro* anti-tuberculosis activity. The Cu(II) complex of 4-((2-mercaptophenyl)imino)-2-phenylchroman-3-ol with MIC value of 4 µM x 10^{-3} was found to be more active than ethambutol with MIC value of 9 µM x 10^{-3}.

Novel Fe(II) complexes were designed as potential therapeutic agents against tuberculosis by Tarallo, *et al*., (2010). The complexes showed *in-vitro* inhibitory activity on *M.TB* H_{37}Rv at 0.78 µg/mL than some second line drugs in clinical use as streptomycin (1.00 µg/ml), ciprofloxacin (2.00 µg/ml), ethambutol (0.94-1.88 µg/ml).

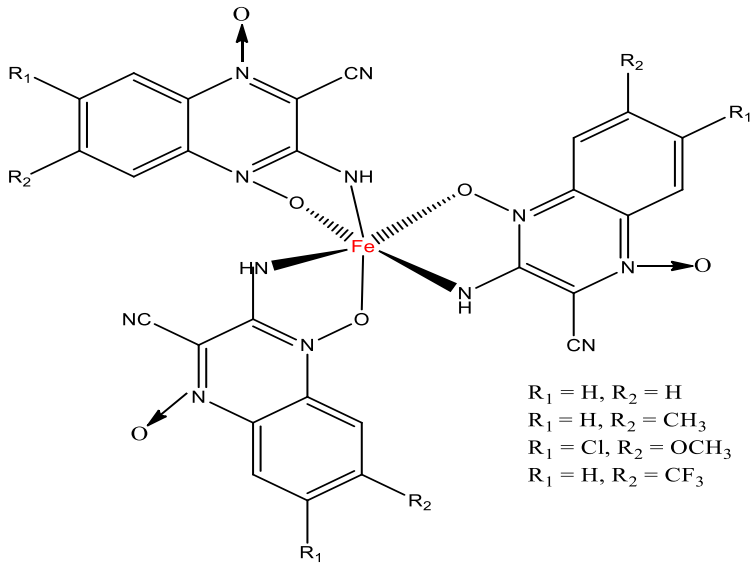

Figure 24: Iron(III) complexes as potential antitubercular agent (Tarallo, *et al*., 2010).

A series of novel transition metal complexes of Co(II), Ni(II), Cu(II) and Mn(II) were synthesized from the Schiff base derived from isatin monohydrazone and *P*-dimethylammino benzaldehyde. The Schiff base and its metal complexes were screened for anti-tuberculosis activity. The complexes showed increased activity against *Mycobacterium tuberculosis* strain H37Rv compared with standard drug streptomycin (Sangamesh *et al*., 2011).

The available drugs for treating mycobacteria infection are losing the battle against the disease as the bacillus continues to build up resistance. The desired characteristics for new drug candidates include different mechanism of action to avoid or reduce resistance, favourable biopharmaceutical and pharmacokinetic properties, and low incidences of side effects. Schiff base transition metal complexes have been shown to possess these properties.

To the best of our knowledge and as far as open literature is concerned, information on the anti-tuberculosis activity of heterocyclic Schiff base transition metal complexes is very sparse. The current research will therefore provide additional baseline data on the synthesis and anti-tuberculosis activity of some INH and pyridine based Schiff base transition metal complexes.

CHAPTER THREE

3.0 EXPERIMENTAL

3.1 Reagents

The chemicals 2-aminopyridine, 4-aminopyridine, Isonicotinic acid hyadrazide (INH), 2-hydroxybenzaldehyde (salicyladehyde), 5-bromo-2-hydroxybenzaldehyde, 5-nitro-2-hydroxybenzaldehyde, 5-methoxy-2-hydroxybenzaldehyde, 2-pyrrole carboxaldehyde, 2-thiophene carboxaldehyde, *p*-toluene sulfonic acid monohydrate, copper(II) chloride dihydrate, nickel(II) chloride hexahydrate, cobalt(II) chloride hexahydrate were obtained commercially from Aldrich Chemicals Co Ltd.

Solvents: ethanol, N, N-dimethylformamide (DMF), dimethylsulfoxide (DMSO), hexane, toluene, ammonia, pet-ether, formic acid and glacial acetic acid of analytical or spectroscopic grade were also obtained commercially from Aldrich Chemicals Co Ltd and used without further purification.

3.1.1 Instruments

Thin layer chromatography (TLC) was run on a pre-coated Merck TLC silica gel 60 F_{254} plates viewed under UV light (254/365nm). Melting points were determined on a Stuart SMP3 melting point apparatus. The results were uncorrected. Infrared spectra were recorded on an FTS 7000 series Digilab Win-IR Pro spectrometer equipped with the ATR- (attenuated total reflectance) Diamond Selenium accessory using the thin-film method as described in the manufacturer's manual. The spectra were recorded in the region 4000-400 cm^{-1}. The ^{1}H and ^{13}C NMR spectra were recorded on a Varian 300 MHz spectrometer using deuterated chloroform ($CDCl_3$) or dimethyl sulfoxide (DMSO-d_6) as solvent with tetramethylsilane

(TMS) as the internal reference. All spectra were recorded at ambient temperature and the chemical shifts are referenced relative to the solvent peaks. Elemental analyses were performed with a Perkin -Elmer 2400 CHNS/O analyzer. The electronic spectra of the compounds were recorded in DMF solution on a Cecil Super Aquarius 9000 series UV-Vis spectrophotometer using 1 cm quartz cell at room temperature immediately after preparing the solutions. The metal analysis was carried out on Perkin-Elmer Atomic Absorption spectrometer AAnalyst 200. The molar conductance measurements were carried out on a Syntronics digital direct reading conductivity meter using conductivity cell having a cell constant 1.0.

Antituberculosis screening was done at the tuberculosis unit, Nigeria Institute of Medical Research, Yaba, Lagos State, Nigeria.

Sample Digestion

1.0±0.5 g of the Schiff base metal complex was weighed, transferred into a kjeldahl flask and 25 ml of aqua regia was added. The mixture was digested on a hot plate at 120 ^{o}C in a fume cupboard until a clear solution of less than 5 ml was obtained. The digest was poured into a 25-ml standard flask and made up to the mark with deionized water. The solution was filtered into a clean plastic bottle and stored in the refrigerator prior to analysis. This digestion was carried out in duplicate for each sample. A blank digest was also obtained (Mendham *et al.*, 2004).

$$\%\, M = \frac{result\ of\ AAS \times 25}{mass\ of\ sample} \times 100$$

Where M = Cu, Ni or Co

Mass of sample is in grams (g).

3.2 Synthesis of Schiff bases

3.2.1. Synthesis of *N*-(2-hydroxybenzylidene)pyridine-2-amine (L1)

A mixture of 2-hydroxybenzaldehyde (24.50 mg, 0.20 mmol.) and 2-aminopyridine (18.80 mg , 0.20 mmol.) in hot absolute ethanol (30 ml) was stirred in a round bottom flask for 10 minutes. 0.3 ml of formic acid was added and the reaction mixture refluxed for 6 h at 60^{o}C. The solvent was evaporated using rotavap to one-quarter the volume of the mixture and then allowed to cool to room temperature. The resulting precipitate was filtered and recrystallized to obtain compound **L1** as a yellow-orange solid. Yield: 26.12 mg (66%); mp: 62–64^{o}C; R_f : 0.52. IR (cm^{-1}): 3058, 2365, 1603, 1586, 1554, 1496, 1465, 1450, 1428, 1350, 1276, 1184, 1142, 1110, 1044, 1030, 993, 958, 913, 787, 623, 562; ^{1}H NMR (300 MHz, $CDCl_3$) δ_H: 6.91–8.49 (m, 8H), 9.41 (s, 1H), 13.40 (s, 1H); ^{13}C NMR (75 MHz, $CDCl_3$) δ_C: 117.21, 118.93, 119.19, 120.44, 122.54, 133.44, 133.81, 138.45, 148.92, 151.51, 161.82, 164.70.

Anal.calcd. for $C_{12}H_{10}N_2O$: C, 72.71, H, 5.08, N, 14.10. Found, C, 72.33, H, 5.03, N, 14.00

3.2.2: Synthesis of *N*-(5-nitro-2-hydroxybenzylidene)pyridine-2-amine (L2)

A solution of 5-nitro-2-hydroxybenzaldehyde (33.40 mg, 0.20 mmol.) in hot absolute ethanol (10 ml) was added dropwise to a solution of 2-aminopyridine (18.80 mg , 0.20 mmol.) in hot absolute ethanol (10 ml) with stirring. The mixture was heated to reflux at 65^{o}C for 8 h in a round bottom flask. The yellow solid obtained was filtered, washed severally with cold distilled water and ethanol and then recrystallized from ethanol:hexane (1:1) mixture. The desired yellow solid product **L2** was dried over silica gel in a dessicator. Yield: 22.10 mg

(46%); mp: 182–184^{0}C; R_f: 0.68. IR (cm^{-1}): 3331, 1595, 1556, 1526, 1426, 1373, 1285, 1195, 1147, 1099, 1023, 930, 863, 728, 646, 552; ^{1}H NMR (300 MHz, $CDCl_3$) δ_H: 7.10–8.54 (m, 7H), 9.53 (s, 1H), 14.56 (s, 1H); ^{13}C NMR (75 MHz, $CDCl_3$) δ_C: 117.79, 118.49, 120.51, 123.60, 128.90, 129.52, 131.63, 138.76, 149.25, 155.78, 162.89, 167.63.

Anal. calcd. for $C_{12}H_9N_3O_3$: C, 59.26, H, 3.73, N, 17.28. Found: C, 59.14, H, 3.56, N, 16.96.

3.2.3: Synthesis of *N*-(5-bromo-2-hydroxybenzylidene)pyridine-2-amine (L3)

A solution of 5-bromo-2-hydroxybenzaldehyde (40.20 mg, 0.20 mmol.) in hot absolute ethanol (20 ml) was added to a solution of 2-aminopyridine (18.80 mg , 0.20 mmol.) in hot absolute ethanol (10 ml) in a round bottom flask. The reaction mixture was refluxed at 60^{o}C for 6 h. The mixture was allowed to cool to room temperature and the light-orange crystals formed were collected by filtration. Recrystallized from ethanol:hexane (1:1) mixture afforded pure samples of **L3**. Yield: 45.40 mg (81%); mp: 138–140^{0}C; R_f: 0.50. IR (cm^{-1}): 1608, 1586, 1550, 1461, 1428, 1381, 1341, 1276, 1184, 1144, 1100, 990, 918, 870, 814, 782, 700, 628, 607; ^{1}H NMR (300 MHz, $CDCl_3$) δ_H: 6.89–8.49 (m, 7H), 9.34 (s, 1H), 13.42 (s, 1H); ^{13}C NMR (75 MHz, $CDCl_3$) δ_C: 110.60, 119.28, 120.35, 120.65, 122.99, 135.26, 136.36, 138.56, 149.05, 156.98, 160.86, 163.40.

Anal. calcd. for $C_{12}H_9N_2OBr$: C, 52.01, H, 3.27, N, 10.10. Found: C, 51.96, H, 3.21, N, 9.88

3.2.4: Synthesis of *N*-(5-methoxy-2-hydroxybenzylidene)pyridine-2-amine (L4)

A mixture of 5-methoxy-2-hydroxybenzaldehyde (30.40 mg, 0.20 mmol.) and 2-aminopyridine (18.80 mg , 0.20 mmol.) in hot absolute ethanol (40 ml) was stirred in a 100 ml round bottom flask for 2 h at room temperature and then refluxed at 60^{o}C for 6 h. The mixture was allowed to cool to room temperature and the dark-orange crystals formed were collected by filtration, recrystallized from ethylacetate: hexane (3:7) mixture and dried over silica gel in a desiccator. Yield: 34.20 mg (75%); mp: 82–84^{0}C; R_f: 0.45. IR (cm^{-1}): 3021, 1598, 1580, 1557, 1519, 1454, 1394, 1356, 1334, 1316, 1271, 1169, 1137, 1061, 1029, 915, 875, 701, 641, 610; ^{1}H NMR (300 MHz, $CDCl_3$) δ_H: 3.39 (s, 3H), 6.93–8.48 (m, 7H), 9.37 (s, 1H), 12.93 (s, 1H); ^{13}C NMR (75 MHz, $CDCl_3$) δ_C: 55.78, 115.79, 118.05, 118.44, 120.46, 121.50, 122.52, 138.42, 148.88, 152.20, 156.16, 157.49, 164.41.

Anal.calcd for $C_{13}H_{12}N_2O_2$:C, 68.42, H, 5.26, N, 12.28. Found:C, 68.32, H, 5.28, N, 12.14.

3.2.5: Synthesis of *N*-(2-hydroxybenzylidene)pyridine-4-amine (L5)

A degassed mixture of 4-aminopyridine (75.00 mg, 0.80 mmol.), 2-hydroxybenzaldehyde (98.00 mg, 0.80 mmol.), and *p*-toluene sulfonic acid monohydrate (10 mg) in dry toluene (100 ml) was refluxed in nitrogen atmosphere under Dean-Stark condition for 24 h. The solvent was removed under reduced pressure and the residue recrystallized from toluene to afford **L5** as a deep yellow solid. Yield: 12.80 mg (81%); mp: 77–78^{0}C; R_f : 0.55. IR (cm^{-1}): 3324, 1587, 1557, 1398, 1339, 1271, 1214, 1148, 1121, 1056, 930, 845, 801, 730, 679; ^{1}H NMR (300 MHz, $CDCl_3$) δ_H: 6.95–7.05 (m, 2H), 7.14 (d, *J* 6.6 Hz, 2H), 7.46 (t, *J* 15.6 Hz, 2H), 8.61 (s, 1H), 8.65 (d, *J* 5.4 Hz, 2H), 12.57 (s, 1H). ^{13}C NMR (75 MHz, $CDCl_3$) δ_C: 116.10, 151.15, 155.46, 117.50, 118.64, 119.45, 132.92, 134.37, 161.29, 165.68.

Anal. calcd. for $C_{12}H_{10}N_2O$: C, 72.71, H, 5.08, N, 14.10. Found: C, 72.62, H, 5.02, N, 13.96.

3.2.6: Synthesis of *N*-(5-nitro-2-hydroxybenzylidene)pyridine-4-amine (L6)

A degassed mixture of 4-aminopyridine (56.00 mg, 0.60 mmol.), 5-nitro-2-hydroxybenzaldehyde (73.00 mg, 0.60 mmol.), and *p*-toluene sulfonic acid monohydrate (10 mg) in dry toluene (100 ml) was refluxed under Dean-Stark condition for 24 h under nitrogen atmosphere. The solvent was removed under reduced pressure and the residue recrystallized from toluene to afford **L6** as a yellow solid. Yield: 14.60 mg (75%); mp: 193–194^{0}C; R_f : 0.32. IR (cm^{-1}): 1652, 1584, 1524, 1471, 1354, 1280, 1228, 1173, 1081, 947, 888, 820, 751, 718, 639; ^{1}HNMR (300 MHz, $CDCl_3$) δ_H: 7.09–7.22 (m, 3H), 8.30–8.44 (m, 2H), 8.56 (s, 1H), 8.717 (t, *J* 8.4Hz, 2H), 10.01; ^{13}CNMR (75 MHz, $CDCl_3$) δ_C: 115.94, 118.58, 119.04, 128.95, 129.30, 129.67, 131.63, 151.44, 164.14, 166.39.

Anal. calcd. for $C_{12}H_9N_3O_3$: C, 59.26, H, 3.77, N, 17.28. Found: C, 58.96, H, 3.63, N, 17.06.

3.2.7: Synthesis of *N*-(5-bromo-2-hydroxybenzylidene)pyridine-4-amine (L7)

A degassed mixture of 4-aminopyridine (63.00 mg, 0.67mmol.), 5-bromo-2--hydroxybenzaldehyde (135.00 mg, 0.67 mmol.), and *p*-toluene sulfonic acid monohydrate (10 mg) in dry toluene (100 ml) was refluxed in nitrogen under Dean-Stark conditions for 24 h. The solvent was removed under reduced pressure and the residue recrystallized from hexane:ethylacetate:ethanol (1:1:0.1) to afford **L7** as orange crystals. Yield: 18.60 mg (84%); mp: 139–141^{0}C; R_f : 0.42. IR (cm^{-1}): 1615, 1582, 1550, 1472, 1411, 1354, 1328, 274, 1183, 1078, 985, 916, 867, 804, 781, 738, 689; ^{1}H NMR (300 MHz, $CDCl_3$) δ_H: 6.96 (d, *J* 8.7 Hz, 2H), 7.13 (d, *J* 5.4Hz, 2H), 7.48–7.54 (m, 2H), 8.54 (s, 1H), 8.66 (s, 2H), 12.57 (s, 1H); ^{13}C

NMR (75 MHz, $CDCl_3$) δ_C: 110.88, 116.05, 119.53, 119.97, 134.80, 136.93, 151.26, 154.93, 160.27, 164.38.

Anal. calcd. for $C_{12}H_9BrN_2O$: C, 52.01, H, 3.27, N, 10.11. Found: C, 52.16, H, 3.18, N, 9.82.

3.2.8: Attempted Synthesis of *N*-(5-methoxy-2-hydroxylbenzylidene)pyridine-4-amine

A mixture of 4-aminopyridine (57.00 mg, 0.60 mmol.), 5-methoxy-2--hydroxybenzaldehyde (91.00 mg, 0.60 mmol.) and *p*-toluene sulfonic acid monohydrate (10 mg) in dry toluene (100 ml) was refluxed in nitrogen under Dean-Stark conditions for 24 h. The solvent was removed under reduced pressure and the residue was recrystallized from hexane:ethylacetate (7:3). Attempts to isolate the desired product were unsuccessful.

3.2.9 Synthesis of *N*-(2-hydroxybenzylidene)isonicotinohydrazide(L8)

A solution of 2--hydroxybenzaldehyde (12.20 mg, 0.10 mmol.) in absolute ethanol (10ml) was added to a solution of isonicotinic acid hydrazide (13.70 mg, 0.10 mmol.) in hot absolute ethanol (20 ml) in a round bottom flask. 0.3 ml glacial acetic acid was added and reaction stirred at room temperature for 1 h. The mixture was further refluxed at 60 ^oC for 6 h and allowed to cool to room temperature. The light yellow precipitate obtained was collected by filtration, recrystallized from ethanol:hexane (1:1) mixture and the dried over silica gel in a desiccator. Yield: 22.20 mg (92%) mp: 256–257^{0}C, R_f : 0.75. IR (cm^{-1}): 3308, 3002, 1675, 1611, 1567, 1489, 1407, 1353, 1289, 1272, 1159, 1067, 1034, 971, 949, 929, 891, 871, 850; ^{1}H NMR (300 MHz, DMSO-d_6) δ_H: 6.65 (m, 2H), 7.34 (t, *J* 15.3Hz, 1H), 7.65 (dd, *J* 18Hz, 1H), 7.87 (d, *J* 6Hz, 2H), 8.69 (s, 1H), 8.81 (d, *J* 4.5Hz, 2H),), 11.11 (s, 1H); 12.31 (s, 1H);

^{13}C NMR (75 MHz, DMSO-d_6) δ_C: 116.97, 119.22, 119.96, 122.05, 129.72, 132.28, 140.50, 149.46, 150.92, 158.01, 161.87.

Anal. calcd. for $C_{13}H_{11}N_3O_2$: C, 64.72, H, 4.60, N, 17.42. Found: C, 64.89, H, 4.49, N, 17.83.

3.2.10 Synthesis of *N*-(5-nitro-2-hydroxybenzylidene)isonicotinohydrazide (L9)

A mixture of 5-nitro-2-hydroxybenzaldehyde (30.00 mg, 0.18 mmol) and isonicotinic acid hydrazide (24.60 mg, 0.18 mmol.) in boiling DMSO (70 ml) was heated to reflux for 8 h. The mixture was allowed to cool to room temperature and the solvent removed under reduced pressure. The yellow precipitate obtained was recrystallized from DMSO. Yield: 45.81 mg (89%); mp: 310–312^{0}C; R_f : 0.35. IR (cm^{-1}): 3305, 3065, 1738, 1664, 1608, 1580, 1545, 1495, 1437, 1413, 1373, 1325, 1296, 1064, 994, 960, 841, 741, 684, 640; ^{1}H NMR (300 MHz, DMSO-d_6) δ_H: 7.13 (d, *J* 9.3Hz, 1H), 7.86 (d, *J* 6.3Hz, 2H), 8.20 (d, *J* 9.0Hz, 1H), 8.61 (d, *J* 3.0Hz, 1H), 8.76 (s, 1H), 8.81 (d, *J* 4.8Hz, 2H), 12.20 (s, 1H); 12.42 (s, 1H); ^{13}C NMR (75 MHz, DMSO-d_6) δ_C: 117.68, 120.59, 122.07, 123.85, 127.44, 140.40, 145.41, 150.94, 162.17, 163.22

Anal. calcd. for $C_{13}H_{10}N_4O_4$: C, 54.24, H, 3.80, N, 19.37. Found: C, 54.55 H, 3.52, N, 19.57.

3.2.11 Synthesis of *N*-(5-bromo-2-hydroxybenzylidene)isonicotinohydrazide (L10)

A stirred solution of isonicotinic acid hydrazide (4.11mg, 0.30 mmol.) in hot absolute ethanol (50 mL) was added a solution of 5-bromo-2-hydroxybenzaldehyde (6.03 mg, 0.30 mmol.) in hot absolute ethanol (30 ml). 0.5 ml glacial acetic acid was added and the mixture refluxed for 8 h. Slow evaporation of the reaction mixture gave a white solid collected by filtration. Recrystallized from ethanol afforded pure samples of **L10**. Yield: 9.13 mg (95%); mp: 261–

264^0C; R_f: 0.78. IR (cm^{-1}): 3252, 3068, 2957, 1669, 1616, 1550, 1473, 1407, 1376, 1339, 1286, 1264, 1194, 1158, 1062, 997, 926, 853, 833, 795; ^{1}H NMR (300 MHz, DMSO-d_6) δ_H: 6.93 (d, *J* 8.7Hz, 1H), 7.45 (dd, *J* 11.7Hz, 1H), 7.85 (m, 3H), 8.65 (s, 1H), 8.81 (d, *J* 5.4Hz, 2H), 11.14 (s, 1H); 12.36 (s, 1H); ^{13}C NMR (75 MHz, DMSO-d_6) δ_C: 111.09, 119.23, 121.84, 122.07, 130.60, 134.44, 140.41, 146.81, 150.91, 156.98, 162.02.

Anal. calcd. for $C_{13}H_{10}BrN_3O_2$: C, 48.77, H, 3.15, N, 13.13. Found: C, 48.75 H, 2.79, N, 13.15.

3.2.12 Synthesis of *N*-(5-methoxy-2-hydroxybenzylidene)isonicotinohydrazide (L11)

A mixture of isonicotinic acid hydrazide (5.00 mg, 0.04 mmol.) and 5-methoxy-2-hydroxybenzaldehyde (5.60 mg, 0.04 mmol.) in hot absolute ethanol (50 ml) was heated to reflux at 60^oC for 12 h. An orange solid compound that separated out was collected by filtration, recrystallized from hexane:ethylacetate:ethanol (7:3:0.1) mixture and dried over silica gel in a desiccator. Yield: 9.62 mg (86%); mp: 205–207 ^{o}C; R_f : 0.45. IR (cm^{-1}): 3188, 3053, 2835, 1649, 1613, 1580, 1543, 1490, 1366, 1332, 1299, 1268, 1206, 1177, 1116, 1085, 1035, 991, 842, 823, 782, 753, 727; ^{1}H NMR (300 MHz, DMSO-d_6) δ_H: 3.72 (s, 3H), 6.95 (m, 2H), 7.18 (d, *J* 3.3Hz, 1H), 7.86 (d, *J* 5.7Hz, 2H), 8.68 (s, 1H), 8.81 (d, *J* 4.2Hz, 2H), 10.53 (s, 1H); 12.29 (s, 1H); ^{13}C NMR (75 MHz, DMSO-d_6) δ_C: 56.00, 112.22, 117.89, 119.21, 119.50, 122.08, 140.59, 148.77, 150.91, 152.09, 152.71, 161.93.

Anal. calcd. for $C_{14}H_{13}N_3O_3$: C, 61.99, H, 4.83, N, 15.49. Found: C, 61.82, H, 4.87, N, 15.67.

3.2.13 Synthesis of (E)-N^1 ((1H-pyrrol-2-yl)methylene)isonicotinohydrazide (L12)

A stirred solution of isonicotinic acid hydrazide (13.70 mg, 0.10 mmol.) in hot absolute ethanol (10 ml) was added a solution (10 ml) of 2-pyrrolecarboxaldehyde (9.50 mg, 0.10 mmol.) in hot absolute ethanol (10 ml). 0.3 ml glacial acetic acid was added and the mixture refluxed at 65^{o}C for 4 h. Slow evaporation of the reaction mixture gave a yellow solid. The solid was collected by filtration and recrystallized from ethanol. Yield: 18.60 mg (87%); mp: 234–237 ^{o}C; R_f : 0.32. IR (cm^{-1}): 3056, 2968, 1645, 1594, 1570, 1436, 1411, 1291, 1220, 1131, 1095, 1061, 1035, 999, 951, 882, 777, 733, 682; ^{1}H NMR (300 MHz, DMSO-d_6) δ_H: 6.17 (q, *J* 7.8Hz, 1H), 6.53 (s, 1H), 6.94 (d, *J* 1.8Hz, 1H), 7.82 (d, *J* 6.6Hz, 2H), 8.29 (s, 1H); 8.78 (d, *J* 5.7Hz, 1H), 11.60 (s, 1H), 11.73 (s, 1H); ^{13}C NMR (75 MHz, DMSO-d_6) δ_C: 110.10, 114.66, 122.18, 123.65, 127.44, 141.48, 142.63, 150.95, 161.66.

Anal. calcd. for $C_{11}H_{10}N_4O$: C, 61.67, H, 4.71, N, 26.15. Found: C, 62.16, H, 4.64, N, 26.27

3.2.14 Synthesis of (E)-N^1 ((thiophen-2-yl)methylene)isonicotinohydrazide (L13)

A mixture of isonicotinic acid hydrazide (13.70 mg, 0.10 mmol.) and 2-thiophene carboxaldehyde (11.22mg, 0.10 mmol.) in hot absolute ethanol (50 ml) bottom flask was stirred for 30 mins. To this mixture, 0.4 ml glacial acetic acid was added and the mixture refluxed at 65 ^{o}C for 8 h. A light yellow solid obtained was collected by filtration, recrystallized from ethanol and dried over silica gel in a desiccator. Yield: 18.70 mg (81%); mp: 241–242 ^{o}C; R_f : 0.20. IR (cm^{-1}): 3204, 3028, 1661, 1593, 1576, 1550, 1412, 1365, 1321, 1294, 1221, 1156, 1060, 1044, 997, 933, 908, 848, 746; ^{1}H NMR (300 MHz, DMSO-d_6) δ_H: 7.17 (q, *J* 8.4Hz, 1H), 7.52 (d, *J* 4.2Hz, 1H), 7.71 (d, *J* 5.1Hz, 2H), 7.81 (t, *J* 5.7Hz, 1H), 8.68

(s, 1H), 8.79 (d, *J* 5.7Hz, 2H), 12.03 (s, 1H); ^{13}C NMR (75 MHz, DMSO-d_6) δ_C: 122.01, 128.49, 130.00, 132.13, 139.27, 140.94, 144.58, 150.86, 161.96.

Anal. calcd. for $C_{11}H_9N_3OS$: C, 57.13, H, 3.92, N, 18.17, S, 13.86 Found: C, 57.64, H, 3.85, N, 18.93, S, 13.44.

3.3 Synthesis of Schiff base metal complexes.

3.3.1: Synthesis of copper(II) complex of L1 (L1A)

A solution of copper(II) chloride dehydrate (1.88 mg, 1.10 mmol.) in hot ethanol: water (1:1, 5 ml) was added to a solution of (*N*-(2-hydroxybenzylidene)pyridin-2-amine) (1.98 mg, 1.00 mmol) in hot absolute ethanol (15 ml). The mixture was stirred at room temperature for 1 h and was refluxed at 50 ^{o}C for 3 h. The green solution obtained was reduced to half the volume using rotavap and left at room temperature. A dark green solid separated on cooling and was collected by filtration, washed severally with cold ethanol:water (1:1) mixture and dried over silica gel in a dessicator. Yield: 2.07 mg (54%); mp: 164–166 ^{o}C. IR (cm^{-1}): 1595, 1558, 1459, 1424, 1373, 1286, 1195, 1147, 1034, 1022, 930, 863, 807, 749, 714, 680, 605, 516, 451.

Anal. calcd. for $C_{12}H_{15}ClCuN_2O_4$: C, 41.15, H, 4.32, N, 8.00, Cu, 18.14. Found: C, 41.66, H, 3.94, N, 8.12, Cu, 20.55.

3.3.2: Synthesis of nickel(II) complex of L1 (L1B)

A solution of nickel(II) chloride hexahydrate (1.19 mg, 0.50 mmol.) in ethanol:water mixture (1:1, 5 ml) was added to a solution of (*N*-(2-hydroxybenzylidene)pyridin-2-amine) (1.98 mg, 1.00 mmol.) in hot absolute ethanol (15 ml). The reaction mixture was stirred at room

temperature for 1 h and refluxed at 60 ^{o}C for 4 h. The yellowish green solid obtained after cooling at room temperature was collected by filtration, washed severally with cold absolute ethanol and dried over silica gel in a desiccator. Yield: 1.49 mg (61%); mp: 241–245 ^{o}C. IR (cm^{-1}): 1635, 1595, 1561, 1056, 1435, 1397, 1287, 1180, 1147, 1033, 997, 918, 862, 811, 782, 726, 662, 628, 570, 521, 492.

Anal. calcd. for $C_{24}H_{22}N_4NiO_4$: C, 58.93, H, 4.53, N, 11.45, Ni, 12.00. Found: C, 59.13, H, 4.07, N, 11.87, Ni, 12.74.

3.3.3. Synthesis of cobalt(II) complex of L1 (L1C)

An aqueous solution (10 ml)of cobalt(II) chloride hexahydrate (2.97 mg, 1.25 mmol.) was added to a solution of *N*-(2-hydroxybenzylidene)pyridin-2-amine (4.95 mg, 2.50 mmol.) in hot absolute ethanol (20 ml). The mixture was refluxed at 60 ^{o}C for 6 h and allowed to cool at room temperature. The golden yellow precipitate formed upon addition of pet-ether (10 ml) to reaction mixture was collected by filtration, washed severally with pet-ether and dried over silica gel in a dessicator. Yield: 3.9 mg (63 %); mp: 310-313 ^{o}C. IR (cm^{-1}): 3016, 1734, 1600, 1562, 1523, 1458, 1425, 1390, 1288, 1216, 1179, 1057, 1032, 988, 925, 856, 755, 645, 625, 597, 483, 445.

Anal. calcd. for $C_{24}H_{22}CoN_4O_4$: C, 58.90, H, 4.53, N, 11.45, Co, 12.04. Found: C, 58.26, H,4.19, N, 11.65, Co, 12.44.

3.3.4 Synthesis of copper(II) complex of L2 (L2A)

To a stirred solution of *N*-(5-nitro-2-hydroxybenzylidene)pyridine-2-amine (12.15 mg, 5.00 mmol) in hot absolute ethanol (25 ml) was added a solution of copper(II) chloride dihydrate

(9.40 mg, 5.50 mmol) in ethanol:water (1:1, 15 ml). The mixture was stirred at room temperature for 1 h and heated to reflux at 50 ^{o}C for 4 h. The green solid obtained after cooling at room temperature was collected by filtration, washed repeatedly with cold ethanol:water mixture (1:1) and kept to dry over silica gel in a desiccator. Yield: 11.66 mg, (57%); mp: 249–256 ^{o}C. IR (cm^{-1}): 3311, 1605, 1560, 1519, 1424, 1373, 1247, 1101, 1059, 1003, 850, 793, 753, 620, 507, 482, 444.

Anal. calcd. for $C_{14}H_{16}ClCuN_3O_5$: C, 41.49, H, 3.98, N, 10.37, Cu, 15.68. Found: C, 42.18, H, 3.32, N, 11.06, Cu, 15.54.

3.3.5 Synthesis of nickel(II) complex of L2 (L2B)

A solution of nickel(II) chloride hexahydrate (1.55 mg, 1.30 mmol.) in ethanol:water (1:1, 5 ml) mixture was added to a solution of *N*-(5-nitro-2-hydroxybenzylidene)pyridine-2-amine (6.32 mg, 2.60 mmol.) in hot absolute ethanol (15 ml). The mixture was stirred at room temperature until solid formed. This was then refluxed at 60 ^{o}C for 6 h. The yellowish-green solid obtained after cooling at room temperature was collected by filtration, washed repeatedly with cold ethanol-water (1:1) and kept dry over silica in a desiccator. Yield: 3.79 mg(46%); mp: >349 ^{o}C. IR (cm^{-1}): 3290, 3078, 1602, 1549, 1485, 1336, 1291, 1101, 1081, 1061, 994, 961, 884, 842, 748, 685, 641, 544, 515, 451.

Anal. calcd. for $C_{24}H_{24}NiN_6O_{10}$: C, 46.86, H, 3.93, N, 13.66, Ni, 9.50. Found: C, 46.07, H, 2.91, N, 13.01, Ni, 9.54.

3.3.6 Synthesis of cobalt(II) complex of L2 (L2C)

To hot ethanolic solution (15 ml) of *N*-(5-nitro-2-hydroxybenzylidene)pyridine-2-amine (6.08 mg, 2.50 mmol) in a 100 ml round bottom flask was added an aqueous solution (10 ml) of cobalt(II) chloride hexahydrate (2.97 mg, 1.25 mmol). The mixture was stirred at room temperature for 1 h and refluxed at 60 ^{o}C for 6 h. A brown solid was obtained on cooling to room temperature. This was collected by filtration, washed with cold ethanol and dried over silica gel in a desiccator. Yield: 3.92 mg (51 %); mp: 266-269 ^{o}C. . IR (cm^{-1}): 3260, 2556, 1687, 1600, 1549, 1501, 1474, 1449, 1346, 1269, 1225, 1179, 1151, 1105, 1021, 981, 846, 824, 745, 703, 679, 648, 512, 471.

Anal. calcd. for $C_{24}H_{26}CoN_6O_{11}$: C, 45.51, H, 4.14, N, 13.27, Co, 9.30. Found: C, 44.98, H, 4.09, N, 12.67, Co, 9.49.

3.3.7 Synthesis of copper(II) complex of L3 (L3A)

To a stirred solution of *N*-(5-bromo-2-hydroxybenzylidene)pyridine-2-amine (5.50 mg, 2.00 mmol) in hot absolute ethanol (10 ml) was added a solution of copper(II) chloride dihydrate (3.76 mg, 2.20 mmol) in hot absolute ethanol (10 ml). The mixture was stirred under reflux at 50 ^{o}C for 4 h. The green solid obtained was collected by filtration, washed severally with cold absolute ethanol and dried over silica gel in a dessicator. Yield: 4.80 mg (62 %); mp: 289-295^{o}C. IR (cm^{-1}): 1678, 1587, 1524, 1471, 1322, 1281, 1096, 944, 905, 888, 825, 717, 639, 511, 477.

Anal. calcd. for $C_{12}H_{10}BrClCuN_2O_2$: C, 36.66 , H, 2.56, N, 7.13, Cu, 16.16. Found: C, 38.41, H, 2.50, N, 7.25, Cu, 16.67.

3.3.8 Synthesis of nickel(II) complex of L3 (L3B)

A solution (10 ml) of *N*-(5-bromo-2-hydroxybenzylidene)pyridine-2-amine (5.50 mg, 2.00 mmol) in hot ethanol was added a solution of nickel(II) chloride hexahydrate (2.38 mg, 1.00 mmol) in ethanol-water (1:1, 5 ml). The mixture formed a precipitate instantly. This was stirred at room temperature for 1 h and refluxed at 60 ^{o}C for 3 h. The greenish-yellow solid obtained after cooling at room temperature was collected by filtration, washed severally with cold ethanol-water (1:1) mixture and dried over silica gel in a desiccator. Yield: 4.5 mg (67 %); mp: >349 ^{o}C. IR (cm^{-1}): 3269, 1734, 1637, 1610. 1595, 1568, 1520, 1437, 1374, 1306, 1280, 1163, 1106, 1079, 995, 879, 828, 778, 697, 565, 451, 427.

Anal. calcd. for $C_{24}H_{24}Br_2N_4NiO_6$: C, 42.21, H, 3.54, N, 8.20, Ni, 8.59. Found: C, 41.94, H, 3.59, N, 8.61, Ni, 9.23.

3.3.9 Synthesis of cobalt(II) complex of L3 (L3C)

An aqueous solution (10 ml)of cobalt(II) chloride hexahydrate (2.97 mg, 1.25 mmol) was added to a hot ethanolic solution (10 ml) of *N*-(5-bromo-2-hydroxybenzylidene)pyridin-2-amine (6.90 mg, 2.50 mmol). The mixture was refluxed at 60 ^{o}C for 6 h. The solid product obtained was collected by filtration after cooling at room temperature, washed three times with 5 ml ethanol-water (1:1) mixture and dried over silica gel in a desiccator. Yield: 4.07 mg (59 %); mp: 234-237 ^{o}C. IR (cm^{-1}): 3059, 1593, 1566, 1516, 1452, 1373, 1285, 1161, 1100, 979, 927, 872, 831, 805, 772, 743, 698, 565, 472, 467.

Anal. calcd. for $C_{24}H_{20}Br_2CoN_4O_4$: C, 44.54, H, 3.11, N, 8.66, Co, 9.11. Found: C, 44.10, H, 3.60, N, 8.17, Co, 9.83.

3.3.10 Synthesis of copper(II) complex of L4 (L4A)

A mixture of *N*-(5-methoxy-2-hydroxybenzylidene)pyridine-2-amine (4.56 mg, 2.00 mmol) and copper(II) chloride dihydrate (1.88 mg, 1.10 mmol) in hot absolute ethanol (25 ml) was stirred at room temperature for 1 h and refluxed at 50 ^{o}C for 4 h. A brown solid obtained on cooling at room temperature was collected by filtration, washed severally with cold absolute ethanol and dried over silica gel in a desiccator. Yield: 2.06 mg (53 %); mp: 208-209 ^{o}C. IR (cm^{-1}): 1607, 1538, 1435, 1339, 1285, 1149, 1054, 930, 843, 800, 728, 681, 649, 587, 560, 549. 534.

Anal. calcd. for $C_{15}H_{19}ClCuN_2O4$: C, 46.16, H, 4.91, N, 7.18, Cu, 16.28. Found: C, 47.01, H, 4.55, N, 7.98, Cu, 16.91.

3.3.11 Synthesis of nickel(II) complex of L4 (L4B)

A solution of nickel(II) chloride hexahydrate (2.61 mg, 1.10 mmol) in ethanol:water solution (1:1, 5 ml) was added to a solution of *N*-(5-methoxy-2-hydroxylbenzylidene)pyridine-2-amine (4.56 mg, 2.0 mmol) in hot absolute ethanol (20 ml). The mixture was stirred at room temperature for 1 h and refluxed at 60 ^{o}C for 4 h. The brown solid obtained after cooling at room temperature was collected by filtration, washed with cold ethanol-water (1:1) mixture and allowed to dry in a dessicator over silica gel. Yield: 3.32 mg (55 %); mp: >349 ^{o}C. IR (cm^{-1}): 1617, 1531, 1474, 1405, 1349, m1292, 1217, 1163, 1056, 948, 878, 767, 682, 487, 426.

Anal. calcd. for $C_{26}H_{26}N_4NiO_6$: C, 56.86, H, 4.77, N, 10.69, Ni, 10.20. Found: C, 57.21, H, 5.07, N, 11.02, Ni, 10.54.

3.3.12 Synthesis of cobalt(II) complex of L4 (L4C)

A solution (10 ml) of *N*-(5-methoxy-2-hydroxybenzylidene)pyridine-2-amine (5.70 mg, 2.50 mmol) in ethanol was added an aqueous solution (10 ml) of cobalt(II) chloride hexahydrate (2.97 mg, 1.25 mmol). The reaction mixture was refluxed at 60 ^{o}C for 4 h and left to stir at room temperature for 2 h upon which a golden-yellow solid was obtained. The solid product was collected by filtration, washed with diethyl ether, and cold ethanol and dried over silica gel in a desiccator. Yield: 3.36 mg (49 %); mp: >349 ^{o}C. IR (cm^{-1}): 2983, 1616, 1506, 1362, 1269, 1152, 1059, 969, 848, 801, 708, 627, 571.

Anal. calcd. for $C_{26}H_{26}CoN_4O_6$: C, 56.84, H, 4.77, N, 10.20, Co, 10.73. Found: C, 55.96, H, 3.90, N, 10.15, Co, 11.08.

3.3.13 Synthesis of copper(II) complex of L5 (L5A)

A solution of *N*-(2-hydroxybenzylidene)pyridine-4-amine (3.96 mg, 2.00 mmol) in hot absolute ethanol (10 ml) was added a hot solution of copper(II) chloride dihydrate (1.88 mg, 1.10 mmol) in hot absolute ethanol (5 ml). The mixture was heated to reflux at 50 ^{o}C for 4 h. The green solid obtained was collected by filtration, washed severally with absolute ethanol and dried over silica gel in a desiccator. Yield: 2.07 mg (60 %); mp: 244 ^{o}C (dec.). IR (cm^{-1}): 3464, 1594, 1581, 1527, 1438, 1372, 1147, 1058, 1027, 902, 869, 748, 655, 528, 489.

Anal. calcd. for $C_{12}H_{11}ClCuN_2O_2$: C, 45.87, H, 3.53, N, 8.92, Cu, 20.22. Found: C, 46.32, H, 3.00, N, 8.40, Cu, 20.74.

3.3.14 Synthesis of nickel(II) complex of L5 (L5B)

A solution of nickel(II) chloride hexahydrate (2.38 mg, 1.00 mmol) in ethanolic:water (1:1, 5 ml) was added a solution of (*N*-(2-hydroxybenzylidene)pyridin-4-amine) (3.96 mg, 2.00 mmol) in hot absolute ethanol (10 ml) in a 100 ml round bottom flask. The mixture was stirred at room temperature for 1 h heated to reflux at 60 ^{o}C for 3 h. The light green solution was allowed to cool and precipitated by the drop-wise addition of ammonia solution. The solid was collected by filtration, washed severally with cold ethanol:water (1:1) mixture and dried in a desiccator over silica gel. Yield: 2.39 mg (49%); mp: 265 ^{o}C (dec.). IR (cm^{-1}): 1591, 1521, 1490, 1448, 1390, 1357, 1319, 1173, 1143, 1054, 1014, 982, 926, 867, 836, 752, 734, 541, 529, 485.

Anal. calcd. for $C_{24}H_{22}N_4NiO_4$: C, 58.93, H, 4.53, N, 11.45, Ni, 12.00. Found: C, 59.31, H, 3.88, N, 11.11, Ni, 13.54.

3.3.15 Synthesis of cobalt(II) complex of L5 (L5C)

An aqueous solution (10 ml)of cobalt(II) chloride hexahydrate (2.97 mg, 1.25 mmol) was added to hot ethanolic solution (10 ml) of *N*-(2-hydroxybenzylidene)pyridin-4-amine (4.95 mg, 2.50 mmol). The mixture was heated to reflux at 60 ^{o}C for 6 h and stirred at room temperature for another 1 h upon which solid was formed. The golden-yellow solid was collected by filtration, washed with ethanol:water (1:1) and dried over silica gel in a desiccator. Yield: 3.33 mg (54 %); mp: 298-303 ^{o}C. IR (cm^{-1}): 1590, 1524, 1491, 1462, 1444, 1387, 1351, 1319, 1174, 1124, 1056, 1027, 980, 866, 834, 753, 735, 445, 414.

Anal. calcd. for $C_{24}H_{22}CoN_4O_4$: C, 58.90, H, 4.53, N, 11.45, Co, 12.04. Found: C, 60.64, H, 4.02, N, 10.81, Co, 13.17.

3.3.16 Synthesis of copper(II) complex of L6 (L6A)

An ethanolic solution (10 ml) of copper(II) chloride dihydrate (3.76 mg, 2.20 mmol) was added to hot ethanolic solution (25 ml) of *N*-(5-nitro-2-hydroxybenzylidene)pyridine-4-amine (9.72 mg, 4.00 mmol) in a 100 ml round bottom flask. The mixture was stirred for 1 h and further refluxed at 50 ^{o}C for 6 h. The mixture was allowed to cool at room temperature and the green solid formed was collected by filtration, washed repeatedly with ethanol:water mixture (1:1) and dried over silica gel in a desiccator. Yield: 1.67 mg (39%); mp: >349 ^{o}C. IR (cm^{-1}): 3212, 1597, 1508, 1424, 1373, 1246, 1101, 1087, 1003, 850, 826, 720, 622, 508, 482, 444.

Anal. calcd. for $C_{12}H_{10}ClCuN_3O_4$: C, 40.12, H, 2.81, N, 11.70, Cu, 17.69. Found: C, 40.07, H, 2.61, N, 10.78, Cu, 18.19.

.

3.3.17 Synthesis of nickel(II) complex of L6 (L6B)

A solution of nickel(II) chloride hexahydrate (2.38 mg, 1.00 mmol) in ethanol:water (1:1, 5 ml) was added to hot ethanolic solution (10 ml) of *N*-(5-nitro-2-hydroxybenzylidene) pyridine-4-amine (4.86 mg, 2.00 mmol). The mixture was stirred for 1 h and further refluxed at 60 ^{o}C for 4 h. The greenish solution was reduced to half of the volume using a rotavap. The light-green solid obtained was collected by filtration, washed repeatedly with ethanol:water (1:1) mixture and dried over silica gel in a desiccator. Yield: 3.15 mg (52%); mp: 296-299 ^{o}C. IR (cm^{-1}): 1735, 1651, 1542, 1415, 1397, 1367, 1291, 1202, 1137, 1082, 923, 833, 799, 753, 728, 693, 667, 507, 461.

Anal. calcd. for $C_{24}H_{26}N_6NiO_8$: C, 53.07, H, 2.97, N, 15.47, Ni, 10.81. Found: C, 54.93, H, 3.02, N, 14.76, Ni, 10.23.

3.3.18 Synthesis of cobalt(II) complex of L6 (L6C)

An aqueous solution (10 ml) of cobalt(II) chloride hexahydrate (2.97 mg, 1.25 mmol) was added to hot ethanolic solution (10 ml) of *N*-(5-nitro-2-hydroxybenzylidene)pyridine-4-amine (6.08 mg, 2.50 mmol). The mixture was stirred at room temperature for 1 h and heated to reflux at 60 ^{o}C for 4 h. The resulting mixture was cooled, reduced to half its volume using rotavap and was left at room temperature. A reddish brown solid obtained was collected by filtration, washed severally with ethanol:water (1:1) mixture and dried over silica gel in a dessicator. Yield: 4.93 mg (58%); mp: 248-251 ^{o}C. IR (cm^{-1}): 3421, 1597, 1574, 1507, 1456, 1395, 1369, 1335, 1216, 1196, 1160, 1084, 1055, 922, 855, 804, 696, 490, 428.

Anal. calcd. for $C_{24}H_{20}CoN_6O_8$: C, 49.75, H, 3.48, N, 14.51, Co, 10.17. Found: C, 50.26, H, 3.02, N, 15.8,5 Co, 9.71.

3.3.19 Synthesis of copper(II) complex of L7 (L7A)

An ethanolic solution (5 ml) of copper(II) chloride dihydrate (1.88 mg, 1.10 mmol) was added to hot ethanolic solution (15 ml) of *N*-(5-bromo-2-hydroxybenzylidene)pyridine-4-amine (4.86 mg, 2.00 mmol). The precipitate formed instantly was heated to reflux at 50 ^{o}C for 4 h. The mixture was allowed to cool at room temperature and the light green solid formed was collected by filtration, washed repeatedly with absolute ethanol and kept to dry in a desiccator containing silica gel. Yield: 2.33 mg (59%); mp: 248 ^{o}C (dec.). IR (cm^{-1}): 2359, 1739, 1598, 1517, 1452, 1391, 1333, 1316, 1279, 1168, 1028, 933, 874, 700, 642, 626, 563, 464, 439.

Anal. calcd. for $C_{12}H_{10}BrClCuN_2O_2$: C, 36.66, H, 2.56, N, 7.13, Cu, 16.16. Found: C, 38.49, H, 2.17, N, 6.63, Cu, 16.00.

3.3.20 Synthesis of nickel(II) complex of L7 (L7B)

A solution of nickel(II) chloride dihydrate (2.38 mg, 1.00 mmol) in ethanol:water (1:1, 5 ml) was added to hot ethanolic solution (15 ml) of *N*-(5-bromo-2-hydroxybenzylidene)pyridin-4-amine (5.54 mg, 2.00 mmol). The mixture was stirred at room temperature for 1 h upon which a solid was formed. This was further refluxed at 60 ^{o}C for 4 h. A light green solid obtained on cooling at room temperature was collected by filtration, washed severally with cold ethanol:water (1:1) mixture and dried over silica gel in a desiccator. Yield: 3.43 mg (63%); mp: 300-303 ^{o}C. IR (cm^{-1}): 1596, 1511, 1490, 1459, 1416, 1387, 1319, 1205, 1132, 1079, 1060, 981, 841, 820, 695, 453, 428.

Anal. calcd. for $C_{24}H_{16}Br_2N_4NiO_2$: C, 47.18, H, 2.64, N, 9.17, Ni, 9.61. Found: C, 46.49, H, 2.67, N, 8.48, Ni, 9.80.

3.3.21 Synthesis of cobalt(II) complex of L7 (L7C)

An aqueous solution (10 ml) of cobalt(II) chloride hexahydrate (2.97 mg, 1.25 mmol) was added to hot ethanolic solution (10 ml) of *N*-(5-bromo-2-hydroxybenzylidene)pyridin-4-amine (6.90 mg, 2.50 mmol). The mixture was heated to reflux at 60 ^{o}C for 4 h and further stirred at room temperature for 3 h. A reddish brown precipitate was obtained on addition of pet-ether (15 ml). The solid was collected by filtration, washed severally with pet-ether and dried over silica gel in a desiccator. Yield: 4.78 mg (66 %); mp: >349 ^{o}C. IR (cm^{-1}): 3060, 1597, 1554, 1470, 1353, 1334, 1279, 1211, 1170, 1081, 987, 913, 870, 848, 818, 781, 628, 529, 523, 429.

Anal. calcd. for $C_{24}H_{24}Br_2CoN_4O_6$: C, 42.19, H, 3.54, N, 8.20, Co, 8.63. Found: C, 41.54, H, 2.79, N, 7.56, Co, 8.51.

3.3.22 Synthesis of copper(II) complex of L8 (L8A)

An aqueous solution (10 ml) of copper(II) chloride dihydrate (1.71 mg, 1.00 mmol) was added to hot ethanolic solution (25 ml) of *N*-(2-hydroxybenzylidene)isonicotinohydrazide (2.41 mg, 1.00 mmol). The mixture was heated to reflux at 60 ^{o}C for 6 h and allowed to cool. The green solid obtained was collected by filtration, washed repeatedly with cold absolute ethanol and dried over silica gel in a dessicator. Yield = 3.42mg (54%); m.p: >349 ^{o}C. IR (cm^{-1}): 3000, 1602, 1544, 1506, 1437, 1300, 1200, 1152, 1061, 892, 846, 498, 466.

Anal. calcd. for $C_{26}H_{2O}CuN_6O_9$: C, 49.25, H, 4.77, N, 13.25, Cu, 10.02. Found: C, 49.79, H, 4.74, N, 13.08, Cu, 10.85.

3.3.23 Synthesis of nickel(II) complex of L8 (L8B)

A hot aqueous solution (10 ml) of nickel(II) chloride hexahydrate (2.38 mg, 1.00 mmol) was added to hot ethanolic solution (25 ml) of *N*(2-hydroxybenzylidene)isonicotinohydrazide (2.41 mg, 1.00 mmol). The resulting mixture was stirred under reflux for 6 h and allowed to cool to room temperature. The brown solid obtained was collected by filtration, washed severally with ethanol:water (1:1) mixture and dried over silica gel in a desiccator. Yield: 2.58 mg (61%); mp: >349 ^{o}C. IR (cm^{-1}): 3366, 1595, 1544, 1441, 1277, 1197, 1151, 1068, 889, 846, 750, 674, 495. 463.

Anal. calcd. for $C_{13}H_{20}ClN_3NiO_7$: C, 36.79, H, 4.75, N, 9.90, Ni, 13.88. Found: C, 37.21, H, 4.15, N, 10.07, Ni, 11.57.

3.3.24 Synthesis of cobalt(II) complex of L8 (L8C)

An aqueous solution (10 ml)of cobalt(II) chloride hexahydrate (2.38 mg, 1.00 mmol) was added to hot ethanolic solution (25 ml) of *N*-(2-hydroxybenzylidene)isonicotinohydrazide (2.41 mg, 1.00 mmol). The mixture was heated to reflux at 60 ^{o}C for 6 h and stirred at room temperature for 1 h to obtain a reddish-brown solid. The solid product was collected by filtration, washed severally with ethanol:water (1:1) mixture and dried over silica gel in a desiccator. Yield:2.56 mg (63%); mp: >349.1 ^{o}C. IR (cm^{-1}): 3013, 1738, 1592, 1539, 1285, 1200, 1154, 1063, 585, 508, 464.

Anal. calcd. for $C_{13}H_{18}ClCoN_3O_6$: C, 38.39, H, 4.46, N, 10.33, Co, 14.49. Found: C, 38.11, H, 3.71, N, 10.28, Co, 14.09.

3.3.25 Synthesis of copper(II) complex of L9 (L9A)

An aqueous solution (10 ml) of copper(II) chloride dehydrate (1.71 mg, 1.00 mmol) was added to a stirred solution of *N*-(5-nitro-2-hydroxybenzylidene)isonicotinohydrazide (2.86mg, 1.00 mmol) in hot absolute ethanol (25 ml) in a round bottom flask. The mixture was refluxed at 60 ^{o}C for 6 h and allowed to cool to room temperature. The dark green solid obtained was collected by filtration , washed repeatedly with absolute ethanol and dried over silica gel in a desiccator. Yield = 4.65 mg (66%); mp: >349 ^{o}C. IR (cm^{-1}): 3066, 1602, 1496, 1365, 1321, 1242, 1191, 1129, 1100, 946, 896, 795, 731, 692, 597, 518, 467, 446.

Anal. calcd. for $C_{26}H_{26}CuN_8O_{12}$: C, 44.23, H, 3.70, N, 15.87, Cu, 9.00. Found: C, 44.16, H, 2.40, N, 15.23, Cu, 9.91.

3.3.26 Synthesis of nickel(II) complex of L9 (L9B)

A hot solution (10 ml) of nickel(II) chloride hexahydrate (2.38 mg, 1.00 mmol) in aqueous medium was added to a hot solution of *N*-(5-nitro-2-hydroxybenzylidene)isonicotinohydra zide (2.86 mg, 1.00 mmol) in hot absolute ethanol (25 ml) in a round bottom flask. The mixture was stirred under reflux at 65 ^{o}C for 4 h. The brown solid obtained was collected by filtration, washed severally with ethanol:water (1:1) mixture and dried over silica gel in the desiccator. Yield: 2.52 mg (56%); mp: >349 ^{o}C. IR (cm^{-1}):3358, 3050, 1595, 1541, 1418, 1384, 1269, 1086, 951, 907, 834, 754, 720, 631, 587, 517.

Anal. calcd. for $C_{13}H_{17}ClN_4NiO_8$: C, 34.59, H, 3.80, N, 12.41, Ni, 13.00. Found: C, 34.86, H, 3.40, N, 12.38, Ni, 12.85

3.3.27 Synthesis of cobalt(II) complex of L9 (L9C)

An aqueous solution (10 ml) of cobalt(II) chloride hexahydrate (2.38 mg, 1.00 mmol) was added to a solution (25 ml) of *N*-(5-nitro-2-hydroxybenzylidene)isonicotinohydrazide (2.86 mg, 1.00 mmol) in hot ethanol. The mixture was stirred under reflux at 60 ^{o}C for 6 h and allowed to cool to room temperature. The brownish solid product obtained was collected by filtration, washed severally with ethanol:water (1:1) mixture and dried over silica gel in a dessicator. Yield: 4.30 mg (65 %); mp: >349 ^{o}C. IR (cm^{-1}): 3294, 3067, 1595, 1545, 1492, 1458, 1437, 1296, 1242, 1099, 961, 922, 832, 750, 686, 579, 511, 456.

Anal. calcd. for $C_{26}H_{24}CoN_8O_{11}$: C, 45.69, H, 3.54, N, 16.40, Co, 8.62. Found: C, 45.70, H, 3.12, N, 16.00, Co, 8.72.

3.3.28 Synthesis of copper(II) complex of L10 (L10A)

To a stirred solution of *N*-(5-bromo-2-hydroxybenzylidene)isonicotinohydrazide (3.20 mg, 1.00 mmol) in hot absolute ethanol (25 ml) was added an aqueous solution (10 ml) of copper(II) chloride dihydrate (1.71 mg, 1.00 mmol). The mixture was heated to reflux at 60 ^{o}C for 4 h and allowed to cool to room temperature. The brown solid obtained was collected by filtration, washed severally with absolute ethanol and allowed to dry in a dessicator over silica gel. Yield: 4.49 mg (58%); mp: 313-317 ^{o}C. IR (cm^{-1}): 3049, 1597, 1499, 1448, 1415, 1379, 1352, 1285, 1176, 1030, 856, 816, 727, 690, 663, 645, 591, 541, 483.

Anal. calcd. for $C_{26}H_{26}Br_2CuN_6O_8$: C, 40.35, H, 3.39, N, 10.86, Cu, 8.21. Found: C, 40.00, H, 2.43, N, 10.57, Cu, 8.81.

3.3.29 Synthesis of nickel(II) complex of L10 (L10B)

To a stirred solution of *N*-(5-bromo-2-hydroxybenzylidene)isonicotinohydrazide (3.20 mg, 1.00 mmol) in hot absolute ethanol (25 ml) was added a hot aqueous solution (10 ml) of nickel(II) chloride hexahydrate (2.38 mg, 1.00 mmol).The mixture was heated to reflux at 65 ^{o}C for 4 h and allowed to cool to room temperature. The brown solid product obtained was collected by filtration, washed severally with ethanol:water (1:1) and dried over silica gel in the desiccator. Yield: 2.29 mg (51%); mp: 307-309 ^{o}C. IR (cm^{-1}):3320, 2359, 1592, 1543, 1499, 1442, 1420, 1381, 1316, 1272, 1152, 889, 761, 726, 622, 495.

Anal. calcd. for $C_{13}H_{13}BrClN_3NiO_4$: C, 34.75, H, 2.92, N, 9.35, Ni, 13.06. Found: C, 35.95, H, 3.29, N, 9.45, Ni, 13.27

3.3.30 Synthesis of cobalt(II) complex of L10 (L10C)

To a stirred solution of *N*-(5-bromo-2-hydroxybenzylidene)isonicotinohydrazide (3.20 mg, 1.00 mmol) in hot absolute ethanol (25 ml) in a round bottom flask was added an aqueous solution (10 ml) of cobalt(II) chloride hexahydrate (2.38 mg, 1.00 mmol). The mixture was heated to reflux at 60 ^{o}C for 6 h and stirred at room temperature for 1 h. The reddish-brown precipitate obtained was collected by filtration, washed severally with cold absolute ethanol and dried over silica gel in a dessicator. Yield: 4.16 mg (60 %); mp: 254-257 ^{o}C. IR (cm^{-1}): 3015, 1598, 1539, 1436, 1419, 1288, 1201, 1153, 1066, 713, 688, 585, 508, 464.
Anal. calcd. for $C_{26}H_{18}Br_2CoN_6O_4$: C, 45.69, H, 3.54, N, 16.40, Co, 8.62. Found: C, 45.70, H, 3.12, N, 16.00, Co, 8.72.

3.3.31 Synthesis of copper(II) complex of L11 (L11A)

To a stirred solution of *N*-(5-methoxy-2-hydroxybenzylidene)isonicotinohydrazide (2.71 mg, 1.00 mmol) in hot absolute ethanol (25 ml) in a round bottom flask was added an aqueous solution (10 ml) of copper(II) chloride dihydrate (1.71 mg, 1.00 mmol.). The mixture was stirred under reflux for 4 h and allowed to cool to room temperature. The brown solid obtained was collected by filtration, washed severally with absolute ethanol and dried over silica gel in a desiccator. Yield: 2.22 mg (33%); mp: >349.1 ^{o}C. IR (cm^{-1}): 3246, 3054, 2834, 1677, 1616, 1539, 1489, 1419, 1344, 1287, 1259, 1145, 1030, 967, 762, 705, 601, 488.
Anal. calcd. for $C_{28}H_{32}CuN_6O_{10}$: C, 49.74, H, 4.77, N, 12.43, Cu, 9.40. Found: C, 49.68, H, 3.96, N, 12.20, Cu, 8.89.

3.3.32 Synthesis of nickel(II) complex of L11 (L11B)

An aqueous solution (10 ml) of nickel(II) chloride hexahydrate (2.38 mg, 1.00 mmol) was added to hot ethanolic solution (25 ml) of *N*-(5-methoxy-2-hydroxybenzylidene)isonicotino hydrazide (2.71 mg, 1.00 mmol) in a round bottom flask. The mixture was heated to reflux at 65 ^{o}C for 6 h and allowed to cool to room temperature. The brown solid obtained was collected by filtration, washed severally with ethanol:water (1:1) and dried over silica gel in the desiccator. Yield: 3.20 mg (71%); mp: >349 ^{o}C. IR (cm^{-1}):3334, 2833, 1601, 1539, 1500, 1465, 1418, 1373, 1316, 1272, 1165, 1067, 962, 905, 750, 700, 650, 510, 479.

Anal. calcd. for $C_{14}H_{22}ClN_3NiO_8$: C, 37.00, H, 4.88, N, 9.25, Ni, 12.91. Found: C, 37.79, H, 4.54, N, 9.19, Ni, 13.40.

3.3.33 Synthesis of cobalt(II) complex of L11 (L11C)

An aqueous solution (10 ml) of cobalt(II) chloride hexahydrate (2.38 mg, 1.00 mmol) was added to a solution of *N*-(5-methoxy-2-hydroxybenzylidene)isonicotinohydrazide (2.71 mg, 1.00 mmol) in hot absolute ethanol. The mixture was heated to reflux at 60 ^{o}C for 6 h and stirred at room temperature for 2 h. The reddish-brown precipitate obtained was collected by filtration, washed severally with ethanol:water (1:1) mixture and dried over silica gel in a desiccator. Yield: 2.81 mg (68 %); mp: 268.8 ^{o}C (dec.). IR (cm^{-1}): 3247, 1677, 1615, 1574, 1538, 1489, 1373, 1278, 1257, 1029, 966, 929,895,879, 763, 680, 597, 498.

Anal. calcd. for $C_{14}H_{14}ClCoN_3O_4$: C, 43.94, H, 3.69, N, 10.98, Co, 15.40. Found: C, 43.88, H, 3.88, N, 10.91, Co, 15.12.

3.3.34 Synthesis of copper(II) complex of L12 (L12A)

To a stirred solution of (E)-N^1((1H-pyrrol-2-yl)methylene)isonicotinohydrazide (4.28 mg, 2.00 mmol.) in hot absolute ethanol (25 ml) in a round bottom flask was added an aqueous solution (10 ml) of copper(II) chloride dehydrate (1.71 mg, 1.00 mmol.). The mixture was heated to reflux at 60 ^{o}C for 4 h and allowed to cool to room temperature. The dark green solid obtained on addition of ammonia solution was collected by filtration, washed severally with cold ethanol:water mixture and dried over silica gel in a dessicator. Yield: 2.28 mg (81%); mp: >349 ^{o}C. IR (cm^{-1}): 3312, 3195, 2968, 1643, 1588, 1518, 1364, 1305, 1243, 1188, 1068, 922, 884, 854, 829, 790, 707, 689, 596.

Anal. calcd. for $C_{11}H_{12}CuN_4O_{2.5}$: C, 38.95, H, 3.57, N, 16.52, Cu, 18.73. Found: C, 39.28, H, 3.32, N, 15.94, Cu, 18.29.

3.3.35 Synthesis of nickel(II) complex of L12 (L12B)

To a stirred solution of (E)-N^1((1H-pyrrol-2-yl)methylene)isonicotinohydrazide (4.28 mg, 2.00 mmol) in hot absolute ethanol (25 ml) in a round bottom flask was added an aqueous solution (10 ml) of nickel(II) chloride hexahydrate (2.38 mg, 1.00 mmol). The mixture was stirred under reflux at 65 ^{o}C for 4 h and allowed to cool to room temperature. The light green solid obtained was collected by filtration, washed severally with cold absolute ethanol:water (1:1) and dried over silica gel in a desiccator. Yield: 2.42 mg (49%); mp: 265 ^{o}C (dec.). IR (cm^{-1}):3108, 2955, 2861, 1603, 1569, 1533, 1413, 1361, 1152, 1060, 996, 953, 882, 785, 697, 610, 492, 428.

Anal. calcd. for $C_{22}H_{19}N_8NiO_{2.5}$: C, 53.47, H, 3.88, N, 22.68, Ni, 11.88. Found: C, 53.22, H, 3.86, N, 22.19, Ni, 10.97.

3.3.36 Synthesis of cobalt(II) complex of L12 (L12C)

To a stirred solution of (E)-N^1((1H-pyrrol-2-yl)methylene)isonicotinohydrazide (4.28 mg, 2.00 mmol) in hot absolute ethanol (25 ml) in a round bottom flask was added an aqueous solution (10 ml) of cobalt(II) chloride hexahydrate (2.38 mg, 1.00 mmol). The mixture was heated to reflux at 65 ^{o}C for 6 h and allowed to cool to room temperature. The reddish-brown solid obtained was filtered, washed severally with absolute ethanol and dried over silica gel in a desiccator over silica gel. Yield: 2.716mg (54%); mp: 298-303 ^{o}C. IR (cm^{-1}): 3108, 2968, 2866, 1738, 1602, 1569, 1528, 1412, 1323, 1215, 1097, 1014, 966, 952, 881, 838, 777, 695, 609, 497, 420.

Anal. calcd. for $C_{22}H_{20}CoN_8O_3$: C, 52.49, H, 4.00, N, 22.26, Co, 11.71. Found: C, 52.48, H, 3.95, N, 21.70, Co, 11.32.

3.3.37 Synthesis of copper(II) complex of L13 (L13A)

To a stirred solution of (E)-N^1((thiophen-2-yl)methylene)isonicotinohydrazide (4.62 mg, 2.00 mmol) in hot absolute ethanol (25 ml) in a round bottom flask was added an aqueous solution (10 ml) of copper(II) chloride dihydrate (1.71 mg, 1.00 mmol). The mixture was refluxed at 60 ^{o}C for 4 h and allowed to cool to room temperature. The dark green solid obtained was collected by filtration, washed severally with cold absolute ethanol and allowed to dry in a desiccator over silica gel. Yield: .1.80 mg 5(9%); mp: >349 ^{o}C. IR (cm^{-1}): 3066, 1584, 1569, 1516, 1507, 1413, 1362, 1212, 1057, 1055, 842, 781, 692, 548, 470.

Anal. calcd. for $C_{11}H_{12}ClCuN_3O_3S$: C, 36.17, H, 3.31, N, 11.50, Cu, 17.40. Found: C, 35.95, H, 3.01, N, 11.14, Cu, 17.01.

3.3.38 Synthesis of nickel(II) complex of L13 (L13B)

To a stirred solution of (E)-*N*^{1}((thiophen-2-yl)methylene)isonicotinohydrazide (4.62 mg, 2.00 mmol) in hot absolute ethanol (25 ml) in a round bottom flask was added an aqueous solution (10 ml) of nickel(II) chloride hexahydrate (2.38 mg, 1.00 mmol). The mixture was stirred under reflux at 65 ^{o}C for 6 h. The brown solid product obtained was collected by filtration, washed severally with absolute ethanol:water (1:1) and dried over silica gel in a dessicator. Yield: 3.63 mg (63%); mp: 300-305 ^{o}C. IR (cm^{-1}):3065, 2969, 1584, 1507, 1516, 1354, 1211, 1058, 996, 848, 757, 716, 652, 597, 494, 432.

Anal. calcd. for $C_{22}H_{22}N_6NiO_5S_2$: C, 46.09, H, 3.87, N, 14.66, Ni, 10.24. Found: C, 46.57, H, 3.57, N, 14.55, Ni, 10.72.

3.3.39 Synthesis of cobalt(II) complex of L13 (L13C)

To a stirred solution of (E)-*N*^{1}((thiophen-2-yl)methylene)isonicotinohydrazide (4.62 mg, 2.00 mmol) in hot absolute ethanol (25 ml) in a round bottom flask was added an aqueous solution (10 ml) of cobalt(II) chloride hexahydrate (2.38 mg, 1.00 mmol). The mixture was stirred under reflux at 65 ^{o}C for 6 h and allowed to cool to room temperature. The brown solid obtained was collected by filtration, washed severally with cold ethanol:water (1:1) mixture and dried over silica gel in a desiccator. Yield: 3.70 mg (66%); mp: >349 ^{o}C. IR (cm^{-1}): 3066, 1582, 1518, 1418, 1373, 1349, 1314, 1261, 1166, 1059, 1015, 990, 947, 846, 755, 698, 554, 516.

Anal. calcd. for $C_{22}H_{18}CoN_6O_3S_2$: C, 49.16, H, 3.38, N, 15.64, Co, 10.96. Found: C, 49.37, H, 3.10, N, 15.41, Co, 10.38.

3.4 Anti-tuberculosis activity study

The antituberculosis test was performed according to the modified proportion method reported by Adeleye *et al*., (2005).

Preparation of Culture Medium: Twelve freshly laid chicken eggs were washed with detergents and sterilized with commercially obtained methylated spirit. The eggs were cracked aspectically into a sterile blender followed by the addition of 300 ml of mineral salt solution and 100 ml of 2% malachite green. The whole mixture was blended intermittently at 10 secs interval to give the Lowenstein-Jensen (LJ) medium. Stock solutions of the test and reference compounds in DMF (0.04 mg/ml) were prepared, filtered through a 0.22 μg pore size membrane and diluted to give solutions with concentrations 0.4, 0.2 and 0.1 μg/ml. A control experiment were set up using a growth medium (LJ medium without sample) and the solvent only. 7-10 ml of the LJ medium was poured into a sterile universal container and inspissated at 85 ^{o}C for 45 mins (LJ slope). Three LJ slopes were prepared for each concentration of samole screened.Prior to loading of the samples sterility check was carried out by allowing the solid medium to stand at room temperature for 24 hrs.

Innoculation of LJ slopes containing the compounds with bacterial culture: 1.0 mg of the organism (*Mycobacterial tuberculosis* H37R_V) was introduced into MC-Cartney bottles, containing 2.0 ml of distilled water together with 5 glass beads. The MC-Cartney bottles were shaken for 20-30 secs using a vortex mixer. 5.0 ml of distilled water was added slowly while continuously mixing. The opacity of the bacterial dilution was adjusted by the addition

of distilled water to get a standard suspension using MaC-Farland No. 1 as a comparative standard.

1.0 ml of the bacterial suspension was taken from the MC-Cartney bottle and discharged into 9.0 ml of distilled water in a test tube to produce the first dilution of 10^{-1} CFU (colony forming unit). In the same way, 1.0 ml of the 10^{-1} CFU/ml bacterial suspension was discharged into the next test tube containing 9.0 ml of distilled water to produce the second dilution of 10^{-2} CFU/ml. Further serial dilutions were done until the 4-fold dilution steps were achieved. The bacterial dilutions of 10^{-2} CFU/ml and 10^{-4} CFU/ml of the *M.TB H*37R_V and a well characterized clinical isolate (coded isolate from NIMR stock culture) were inoculated on each slope with the test compound, the reference compound and control. The inoculated slopes were loosely closed with a cap to allow for evaporation and then incubated at 37 ^{o}C. After the liquid part of the inoculums had evaporated in 24 h, the cap of the universal container was firmly closed and left to incubate at 37 ^{o}C for a period of 28 days. The active compounds were further incubated for 14 days. INH was used as reference compound. The results are based on % critical proportion calculated as

$$\%\ critical\ proportion = \frac{number\ of\ colonies\ on\ LJ\ slope\ with\ test\ compound}{number\ of\ colonies\ on\ LJ\ slope\ without\ test\ compound} \times 100$$

CHAPTER FOUR

4.0 RESULTS

4.1 Synthesis of Schiff bases

Thirteen Schiff bases were synthesized using condensation reaction between 2-aminopyridine, 4-aminopyridine, INH with 2-hydroxybebzaldehyde derivatives and heteroaromatic aldehydes.

4.2 Synthesis and Characterization of 2-aminopyridine Schiff bases

Four Schiff bases namely *N*(2-hydroxybenzylidene)pyridin-2-amine (**L1**), *N*(5-nitro-2-hydroxybenzylidene)pyridin-2-amine (**L2**), *N*(5-bromo-2-hydroxybenzylidene)pyridin-2-amine (**L3**) and *N*(5-methoxy-2-hydroxybenzylidene)pyridin-2-amine (**L4**) derived from 2-hydroxybenzaldehyde, 5-nitro-2-hydroxybenzaldehye, 5-bromo-2-hydroxybenzaldehyde and 5-methoxy-2-hydroxybenzaldehyde with 2-aminopyridine respectively were synthesized.

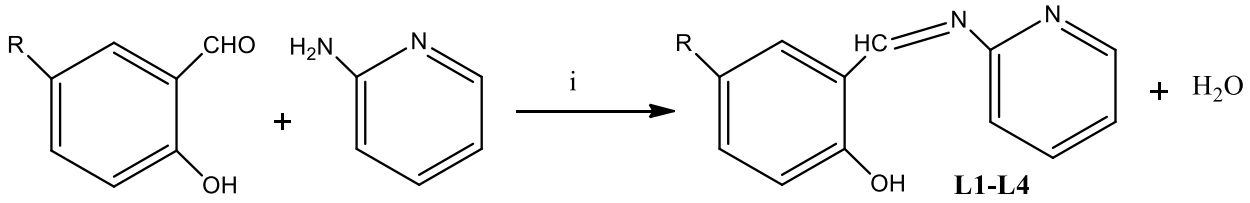

Reagents and conditions: (i) Formic acid, ethanol, heat (60-65^{o}C), 6-8 h

R = H, NO_2, Br, OCH_3

Scheme 7 : Synthesis of 2-aminopyridine-based Schiff bases.

4.2.1 Physical and analytical data of 2-aminopyridine Schiff bases

The physical and analytical data of the compounds are presented in Table 1.

The melting points in the range 62-184 ^{o}C. The yields obtained after purification with suitable solvents were in the range 46-81%. The elemental analysis calculated for each compound was in agreement with the experimental values

Table 1: Physical and analytical data of 2-aminopyridine Schiff bases

Ligand code	Molecular formular (M.wt(g/mol))	Color	mp (^{o}C)	Yield(%)	Microanalysis: % Calculated (Found)		
					C	H	N
L1	$C_{12}H_{10}N_2O$ (198)	Yellow-orange	62-64	66	72.71 (72.33)	5.08 (5.03)	14.10 (14.00)
L2	$C_{12}H_9N_3O_3$ (243)	Yellow	182-184	46	59.26 (59.14)	3.73 (3. 56)	17.28 (16.96)
L3	$C_{12}H_9BrN_2O$ (277)	Light orange	138-140	81	52.01 (51.96)	3.27 (3.21)	10.10 (9.88)
L4	$C_{13}H_{12}N_2O_2$ (228)	Dark-orange	82-84	75	68.42 (68.32)	5.26 (5.28)	12.28 (12.14)

M.wt = molecular weight; mp = Melting point.

4.2.2 IR spectra of the 2-aminopyridine Schiff bases

The IR spectra of the Schiff bases show bands in the range 3058-3331 cm^{-1}. In addition, all the compounds displayed bands at 1595-1608 cm^{-1}, 1271-1285 cm^{-1} and 1030-1100 cm^{-1}.

Table 2: Characteristic IR (cm^{-1}) bands of 2-aminopyridine-based Schiff bases

Ligand code	Structure	IR bands (cm^{-1})			
		ν_{OH}	$\nu_{C=N}$	ν_{C-O}	$\delta_{C=N}$ (py)
L1	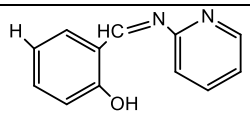	3058	1603	1276	1030
L2	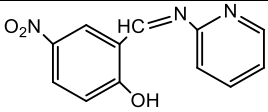	3331	1595	1285	1099
L3	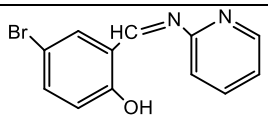	--	1608	1276	1100
L4	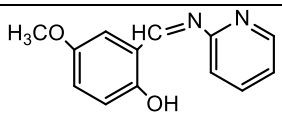	3021	1598	1271	1061

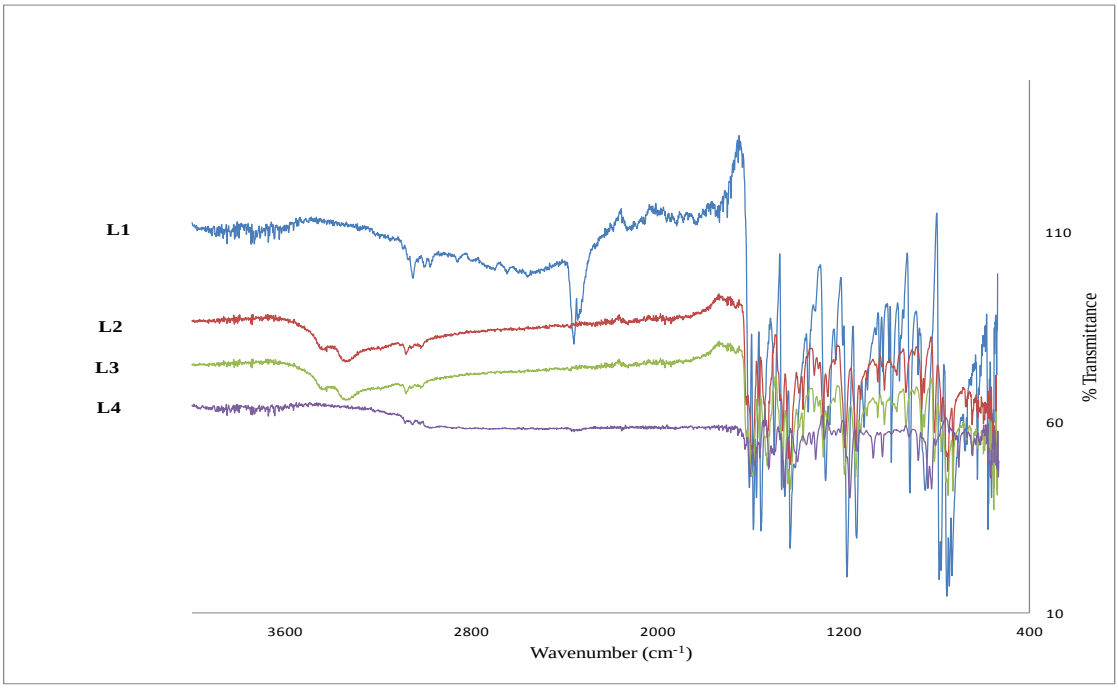

Figure 25 : Infrared spectra of 2-aminopyridine-based Schiff bases **L1-L4**

4.2.3 NMR spectra of 2-aminopyridine Schiff bases

Both proton (^{1}H-NMR) and carbon (^{13}C-NMR) spectra of the 2-aminopyridine Schiff bases were obtained in deuterated chloroform ($CDCl_3$) using tetra methyl silane (TMS) as internal standard. The ^{1}H-NMR spectra showed sharp singlet at 9.41 and 13.40 ppm for compound **L1**, 9.53 and 14.56 ppm for compound **L2,** 9.34 and 13.42 ppm for compound **L3.**and 9.37 and 12.93 ppm for compound **L4.** The ^{13}C-NMR displayed a signal at 161.82 and 164.70 ppm, 162.89 and 167.63 ppm, 160.86 and 163.40 and 157.49 and 164.41 ppm for compounds **L1**, **L2**, **L3** and **L4** respectively.. All the carbons present in each Schiff base were identified. The spectra are shown in Figures 26a-29b.

Table 3: Characteristic ^{1}H and ^{13}C NMR bands of 2-aminopyridine-Schiff bases

Ligand code	Structure	Chemical shift (ppm)					
		HC=N		C-OH		OCH_3	
		δ_H	δ_C	δ_H	δ_C	δ_H	δ_C
L1	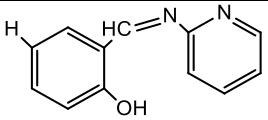	9.41	161.82	13.40	164.70	-	-
L2	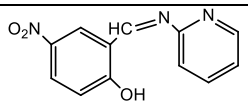	9.53	162.89	14.56	167.63	-	-
L3	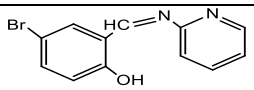	9.34	160.86	13.42	163.40	-	-
L4	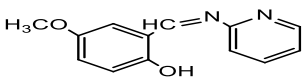	9.37	157.49	12.93	164.41	3.79	55.78

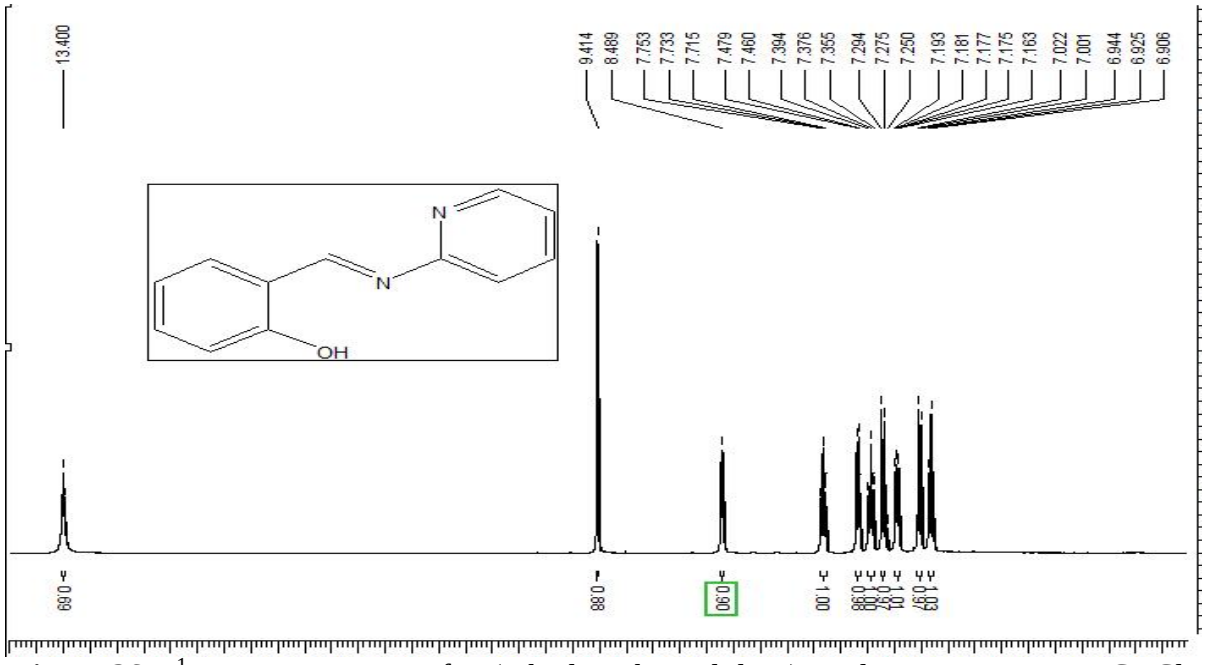

Figure 26a: ^{1}H NMR spectrum of *N*-(2-hydroxybenzylidene)pyridine-2-amine **L1** in $CDCl_3$

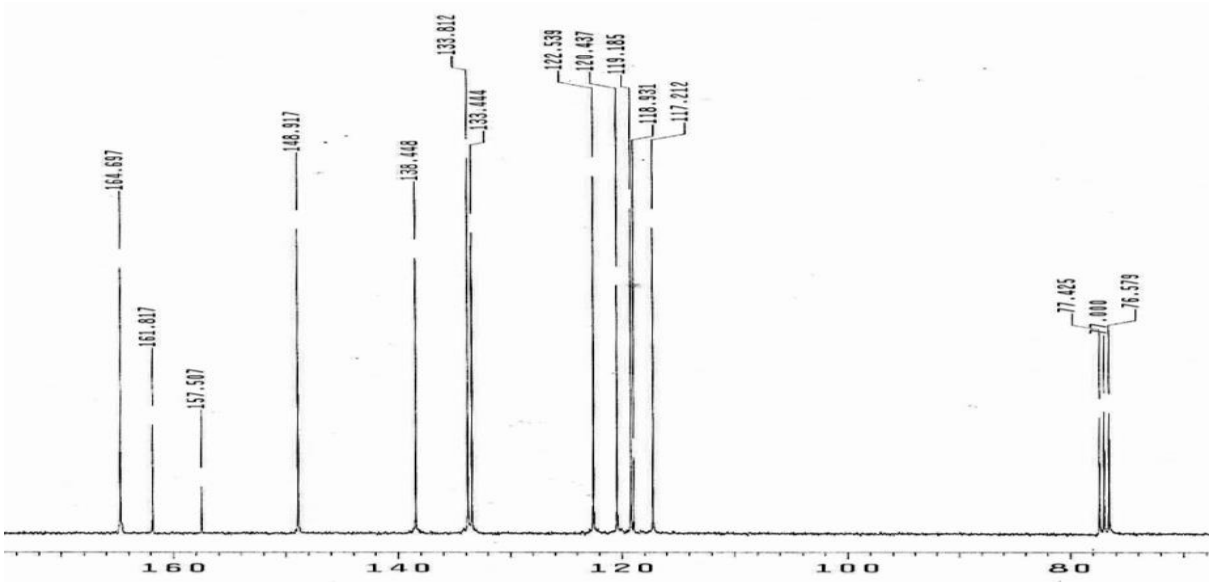

Figure 26b: ^{13}C NMR spectrum of *N*-(2-hydroxybenzylidene)pyridine-2-amine **L1** in $CDCl_3$

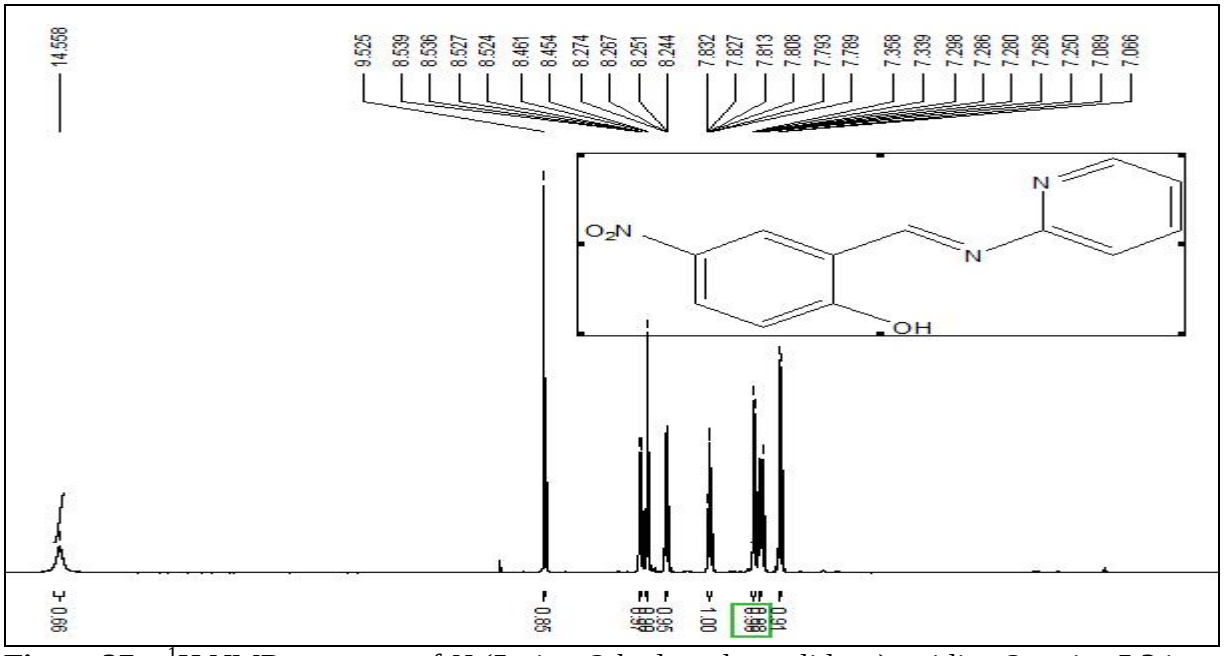

Figure 27a: ^{1}H NMR spectrum of *N*-(5-nitro-2-hydroxybenzylidene)pyridine-2-amine **L2** in $CDCl_3$

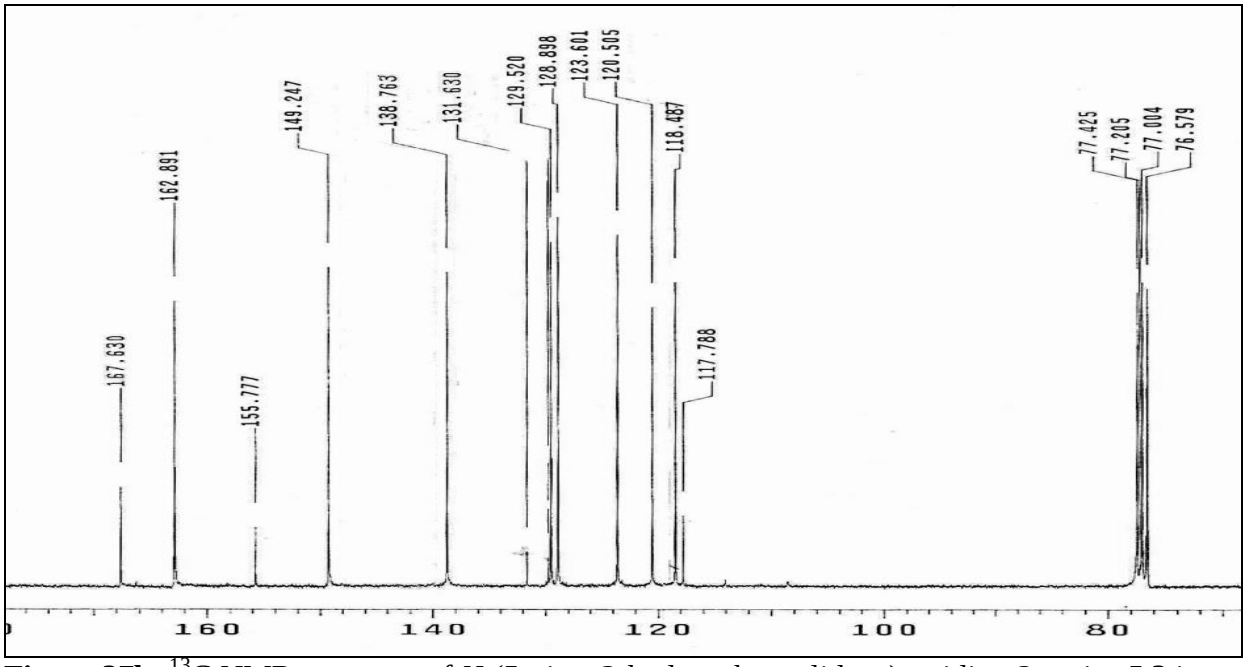

Figure 27b: ^{13}C NMR spectrum of *N*-(5-nitro-2-hydroxybenzylidene)pyridine-2-amine **L2** in $CDCl_3$

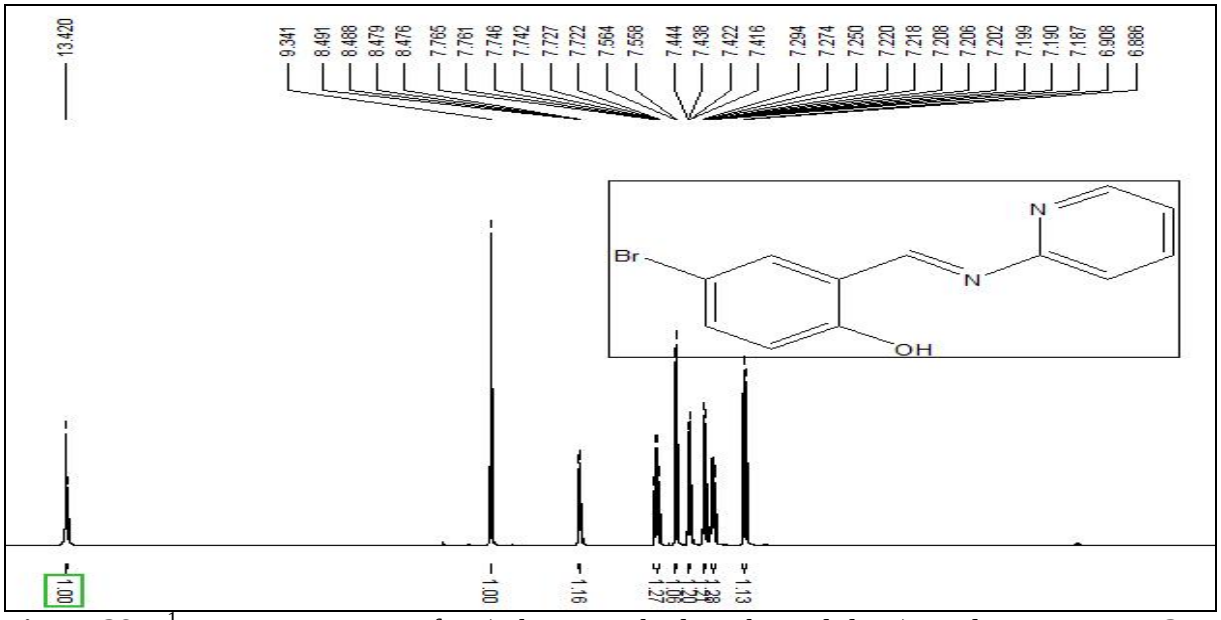

Figure 28a: ^{1}H NMR spectrum of *N*-(5-bromo-2-hydroxybenzylidene)pyridine-2-amine **L3** in $CDCl_3$

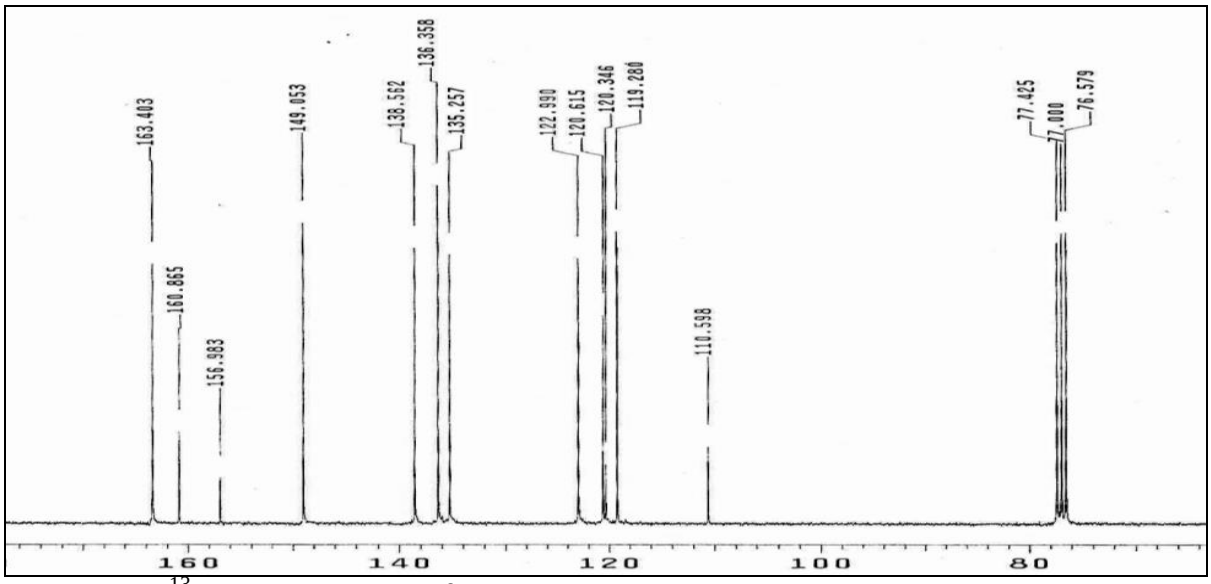

Figure 28b: ^{13}C NMR spectrum of *N*-(5-bromo-2-hydroxybenzylidene)pyridine-2-amine **L3** in $CDCl_3$

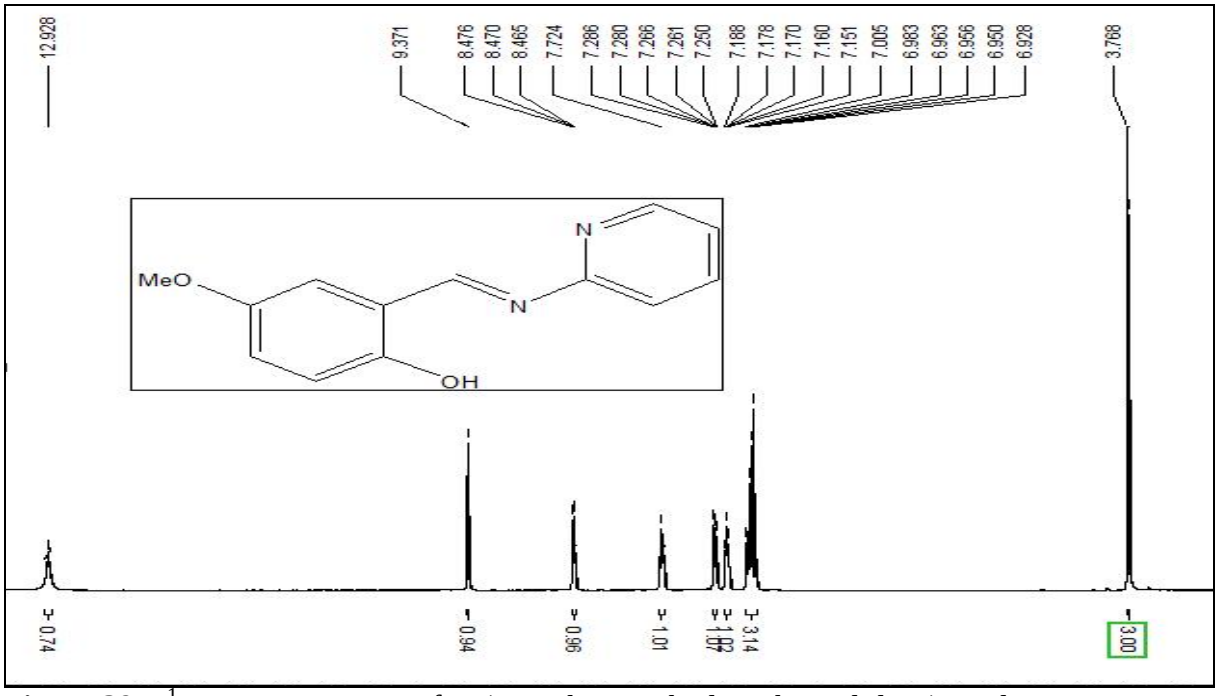

Figure 29a: ^{1}H NMR spectrum of *N*-(5-methoxy-2-hydroxybenzylidene)pyridine-2-amine **L4** in $CDCl_3$

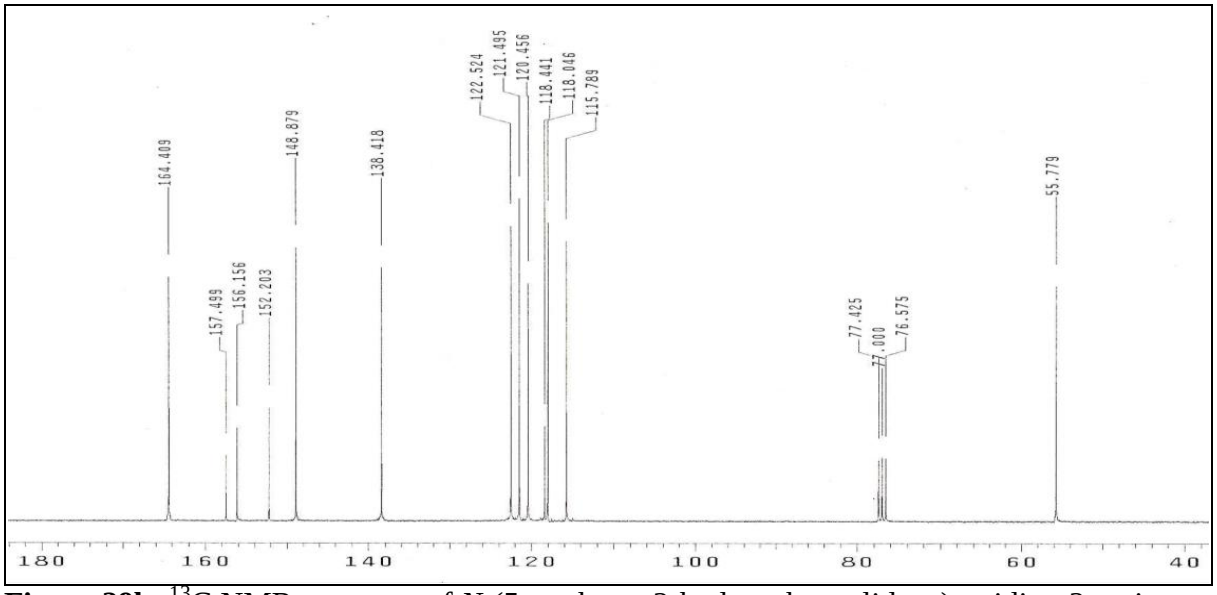

Figure 29b: ^{13}C NMR spectrum of *N*-(5-methoxy-2-hydroxybenzylidene)pyridine-2-amine **L4** in $CDCl_3$

4.2.4: Electronic absorption spectra of 2-aminopyridine Schiff bases

The electronic spectra of 10^{-5} M solution of the 2-aminopyridine Schiff bases in DMF consist of various bands in the 200-500 nm region. Compounds **L1** and **L2** show three absorption bands at 268, 303 and 358 nm and 273 nm, 373 and 431 nm respectively. Two bands appeared at 305 and 358 nm and 305 and 365 nm in the spectra of compounds **L3** and **L4** respectively.

Table 4: Electronic absorption bands for 2-aminopyridine- Schiff bases **L1-L4**

Ligand Code	Band A λmax(nm)	Log∈	Band B λmax(nm)	Log∈	Band C λmax (nm)	Log∈	Band D λmax (nm)	Log∈
L1	268	3.77	303	3.86	358	3.42	-	-
L2	273	4.23	-	-	373	3.93	431	4.57
L3	-	-	305	3.35	358	3.42	-	-
L4	-	-	305	3.28	365	3.57	-	-

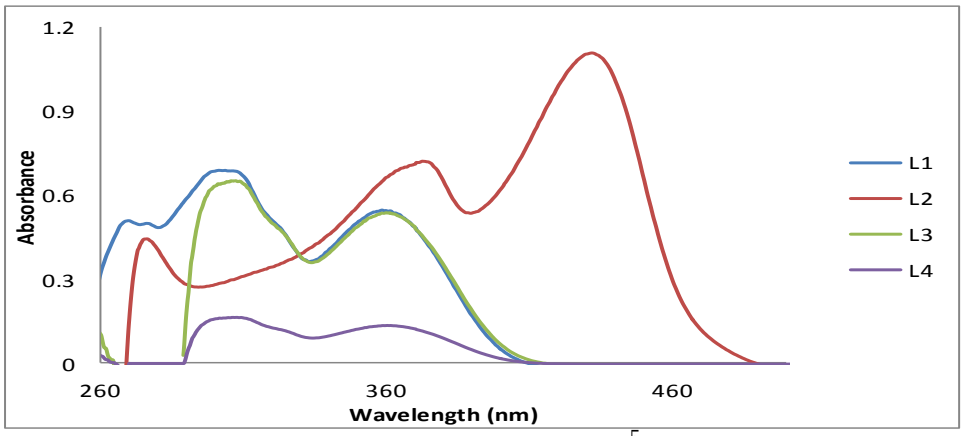

Figure 30: Electronic absorption spectrum of **L1-L4** in 10^{-5} M DMF solution

4.3 Synthesis and Characterization of 4-aminopyridine Schiff bases

Schiff bases namely *N*(2-hydroxybenzylidene)pyridin-4-amine (**L5**), *N*(5-nitro-2-hydroxybenzylidene)pyridin-4-amine (**L6**), *N*(5-bromo-2-hydroxybenzylidene)pyridin-4-amine (**L7**) derived from 2-hydroxybenzaldehyde, 5-nitro-2-hydroxybenzaldehyde and 5-bromo-2-hydroxybenzaldehyde with 4-aminopyridine were synthesized

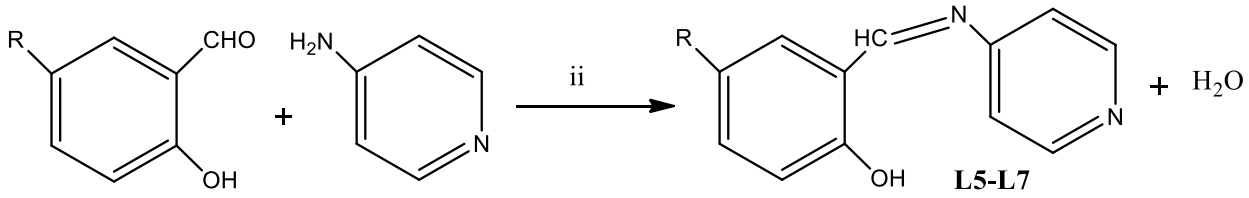

Reagents and conditions: (ii) $C_6H_8O_4S$, toluene, $N_{2(g)}$, heat , 24 h

R = H, NO_2, Br

Scheme 8 : Synthesis of 4-aminopyridine-based Schiff bases.

4.3.1 Physical and analytical data of 4-aminopyridine Schiff bases

The physical and analytical data of the compounds are presented in Table 5. The compounds were obtained in good yield after purification from suitable solvents in the range 75-84%. The melting points of the pure isolated compounds were in the range 77-78^{o}C, 193-194^{o}C and 139-141 ^{o}C for the unsubstituted **L5**, nitro substituted **L6** and bromo substituted **L7** respectively. The elemental analysis support the molecular formular suggested for the Schiff bases.

Table 5: Physical and analytical data of 4-aminopyridine-Schiff bases

Ligand code	Molecular formular (M.wt. (g/mol))	Colour	mp:(^{o}C)	Yield(%)	Microanalysis: %Calculated (Found)		
					C	H	N
L5	$C_{12}H_{10}N_2O$ (198)	Yellow-orange	77-78	81	72.71 (72.62)	5.08 (5.02)	14.10 (13.96)
L6	$C_{12}H_9N_3O_3$ (243)	Yellow	193-194	75	59.26 (58.96)	3.77 (3.63)	17.28 (17.06)
L7	$C_{12}H_9BrN_2O$ (277)	Orange	139-141	84	52.01 (52.16)	3.27 (3.18)	10.11 (9.82)

M.wt = Molecular weight; mp = Melting point

4.3.2: IR spectra of 4-aminopyridine Schiff bases

All the Schiff bases (**L5-L7**) displayed significant bands at 1587-1650 cm^{-1}, 1271-1280 cm^{-1} and 1056-1081 cm^{-1}. In addition, the IR spectrum of the unsubstituted Schiff base (**L5**) show a band at 3324 cm^{-1}.

Table 6.: Characteristic IR (cm^{-1}) bands of 4-aminopyridine-based Schiff bases

Ligand code	Structure	IR bands (cm^{-1})			
		ν_{OH}	$\nu_{C=N}$	ν_{C-O}	$\delta_{C=N}$ (py)
L5	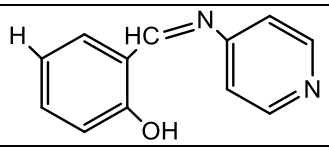	3324	1587	1271	1056
L6	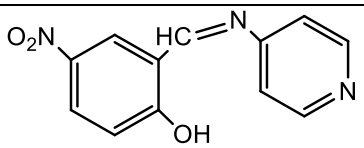	-	1650	1280	1081
L7	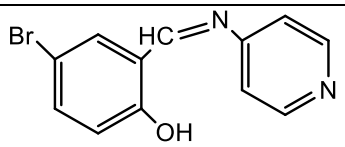	-	1615	1274	1078

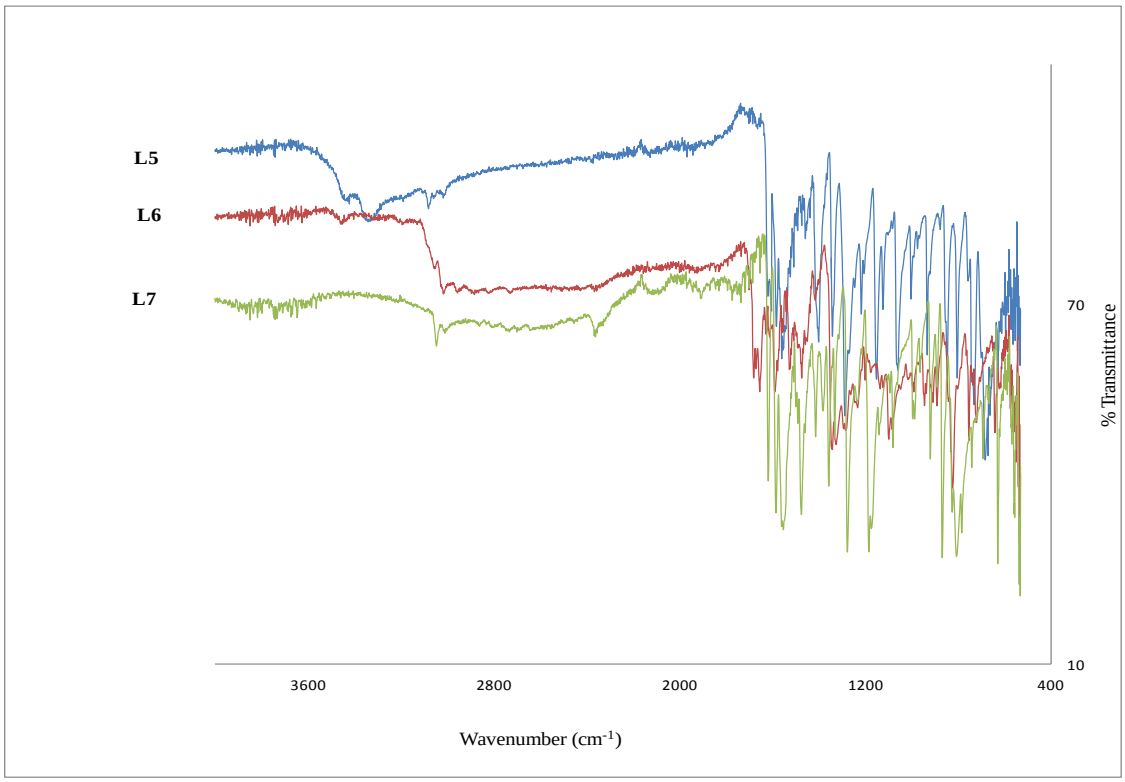

Figure 31 : Infrared spectra of 4-aminopyridine-based Schiff bases **L5-L7**

4.3.3 NMR spectra of 4-aminopyridine Schiff bases

Both proton (^{1}H-NMR) and carbon (^{13}C-NMR) spectra were obtained for each of the compounds. The ^{1}H-NMR spectra showed a sharp singlet at 8.61 and 12.75 ppm, 8.56 and 10.01 ppm and 8.66 and 12.57 ppm for compounds **L5, L6** and **L7** respectively in deuterated chloroform using tetra methyl silane (TMS) as internal standard. The ^{13}C NMR displayed a signal at 161.29 and 165.68 ppm, 164.14 and 166.39 ppm and 160.27 and 164.38 ppm for compounds **L5**, **L6** and **L7** respectively. All the carbons present in each Schiff base were identified. The spectra are shown in Figures 32a-34b.

Table 7: Characteristic ^{1}H and ^{13}C NMR bands of 4-aminopyridine-based Schiff bases

Ligand code	Structures	Chemical shift (ppm)			
		HC=N		C-OH	
		δ_H	δ_C	δ_H	δ_C
L5	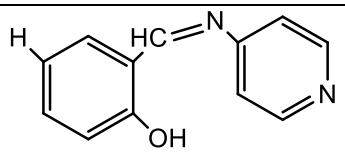	8.61	161.29	12.57	165.68
L6	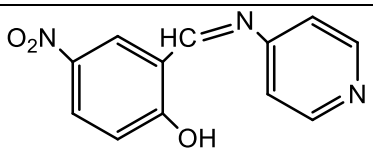	8.56	164.14	10.01	166.39
L7	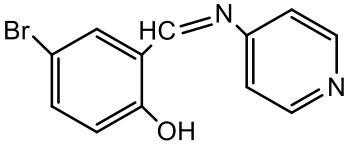	8.66	160.27	12.57	164.38

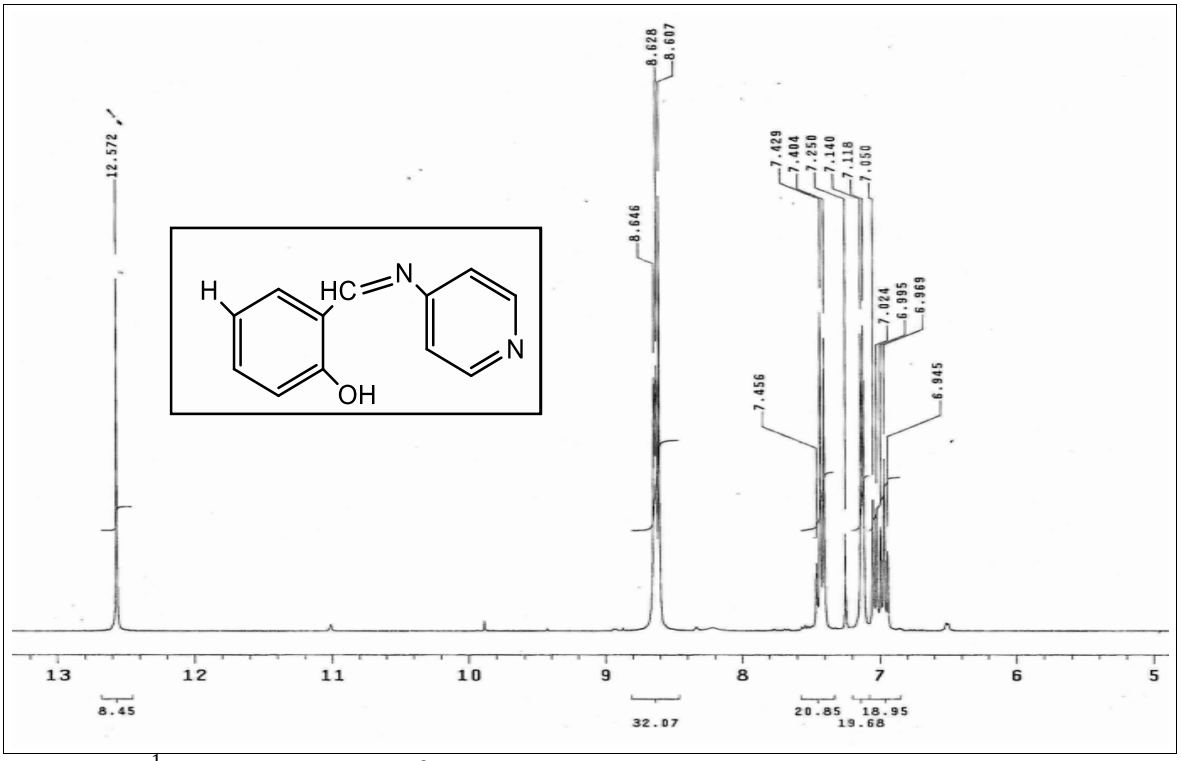

Figure 32a: ^{1}H NMR spectrum of *N*-(2-hydroxybenzylidene)pyridine-4-amine **L5** in $CDCl_3$

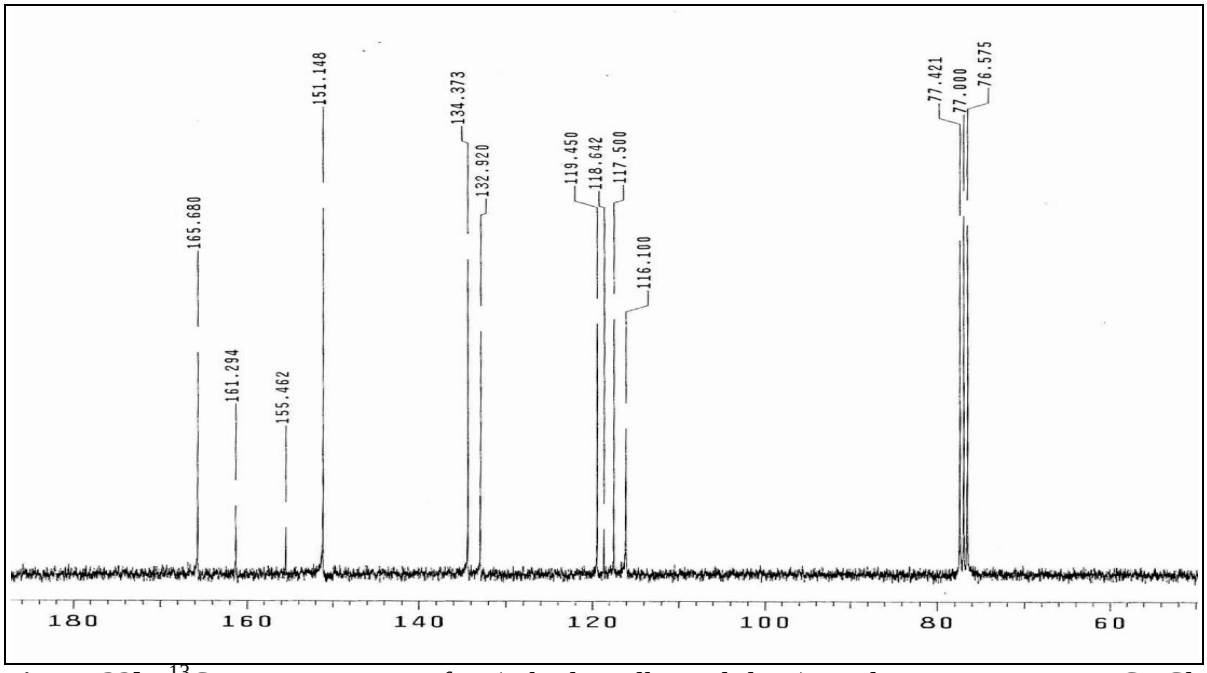

Figure 32b: ^{13}C NMR spectrum of *N*-(2-hydroxylbenzylidene)pyridine-4-amine **L5** in $CDCl_3$

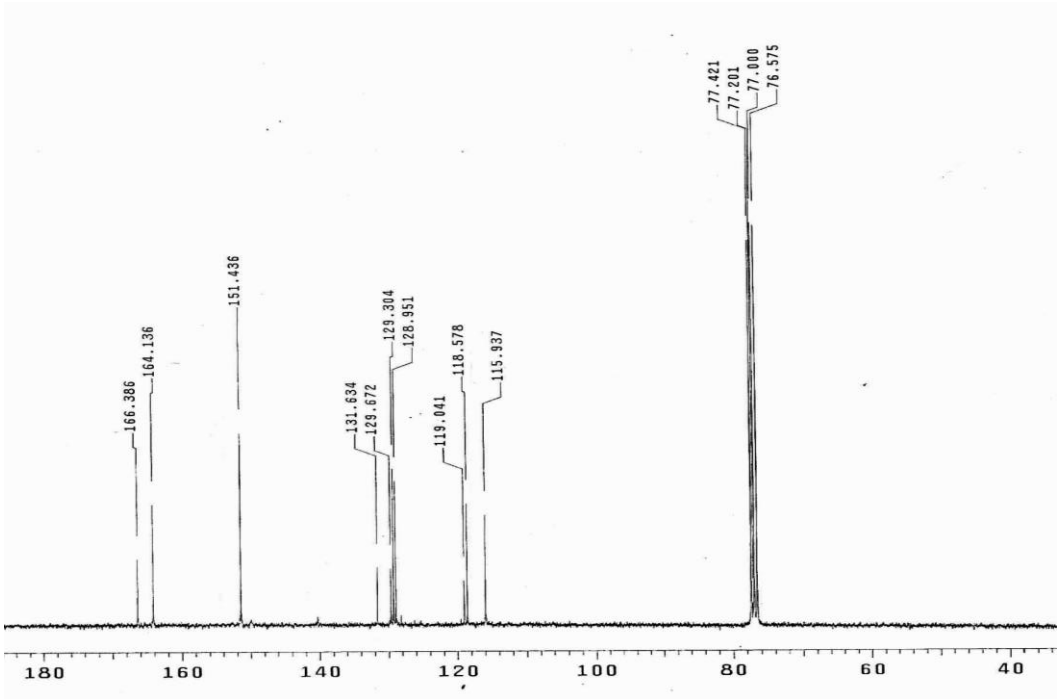

33b: ^{13}C NMR spectrum of *N*-(5-nitro-2-hydroxybenzylidene)pyridine-4-amine **L6** in $CDCl_3$

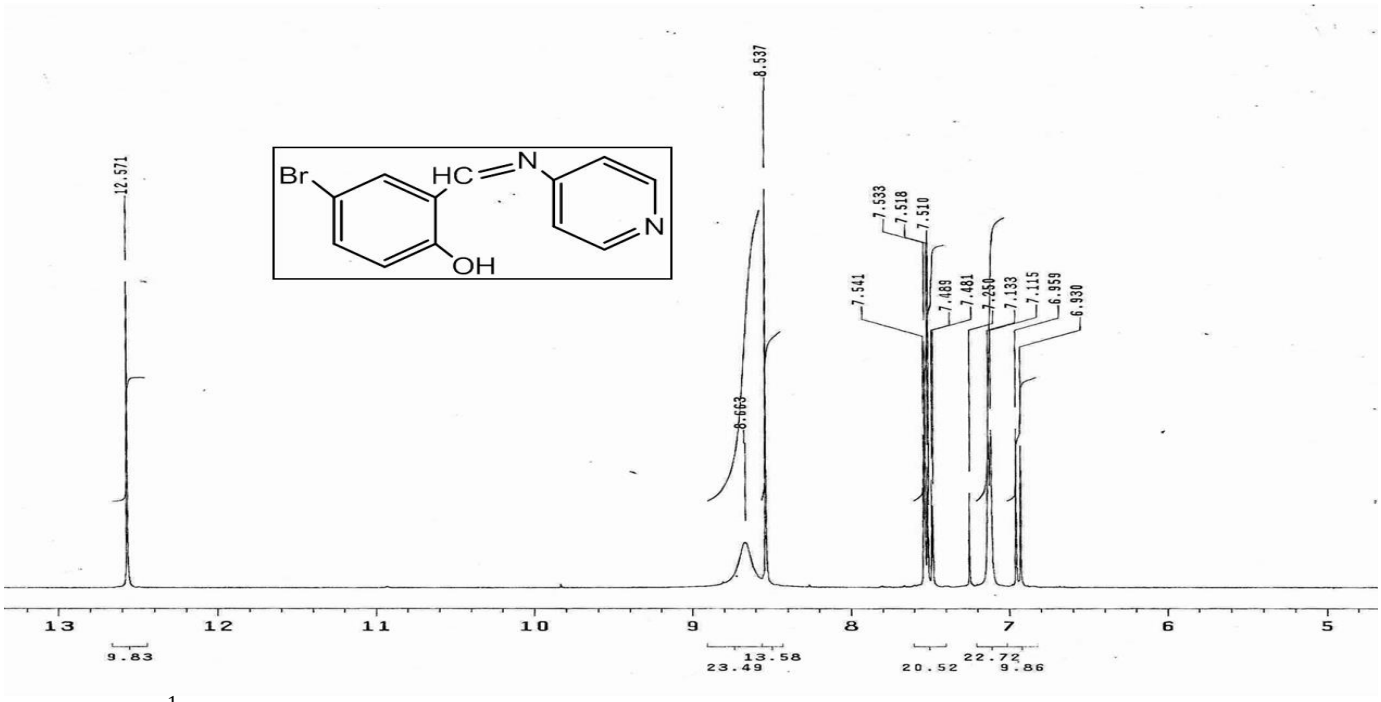

Figure 34a: ^{1}H NMR spectrum of *N*-(5-bromo-2-hydroxybenzylidene)pyridine-4-amine **L7** in $CDCl_3$

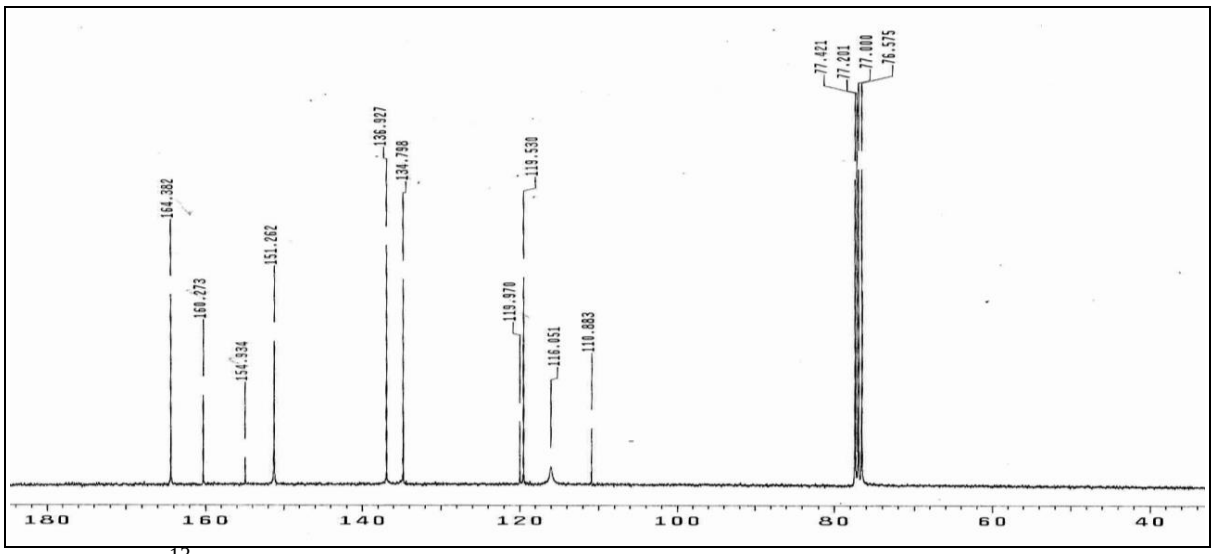

Figure 34b: ^{13}C NMR spectrum of *N*-(5-bromo-2-hydroxybenzylidene)pyridine-4-amine **L7** in $CDCl_3$

4.3.4: Electronic absorption spectra of 4-aminopyridine Schiff bases

The electronic spectra of 10^{-5} M solution of the 4-aminopyridine Schiff bases in DMF consist of various bands in the 200-500 nm region. Compound **L6** displayed three absorption bands at 275, 369 and 430 nm. Two bands appeared at 277 and 333 nm and 278 and 349 nm in the spectra of compounds **L5** and **L7** respectively.

Table 8: Electronic absorption bands for4-aminopyridine- Schiff bases

Ligand Code	Band A λmax(nm)	Log∈	Band C λmax(nm)	Log∈	Band D λmax (nm)	Log∈
L5	277	4.46	333	4.26	-	
L6	275	4.03	369	4.24	430	4.43
L7	278	4.28	349	3.81	-	

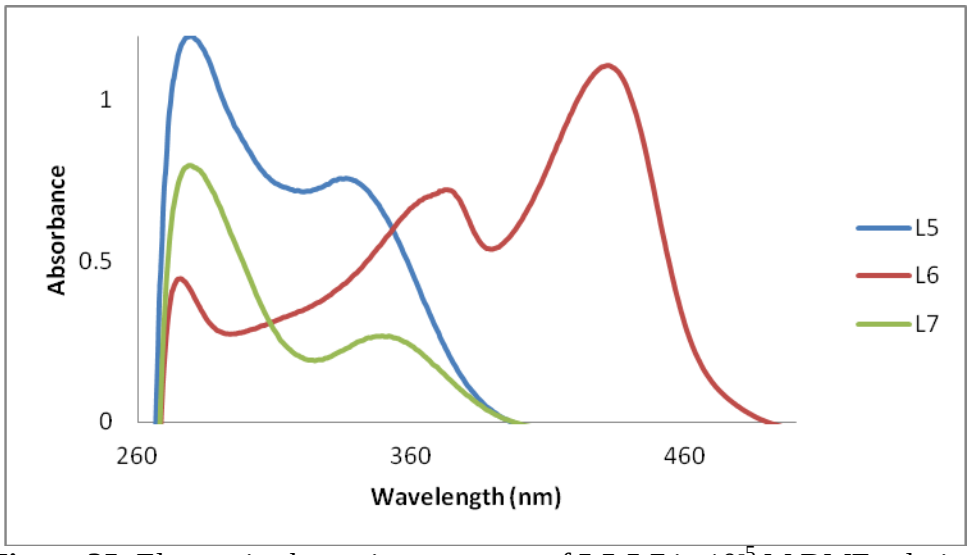

Figure 35: Electronic absorption spectrum of **L5-L7** in 10^{-5} M DMF solution

4.4 Synthesis and Characterization of INH Schiff bases

Two classes of INH based Schiff bases were synthesized in this study. These are Schiff bases derived using 2-hydroxybenzaldehyde derivatives and heteroaromatic aldehydes. Four Schiff bases were derived using 2-hydroxybenzaldehyde derivatives, they are: N-(2-hydroxybenzylidene)isonicotinohydrazide(**L8**), N-(5-nitro-2-hydroxybenzylidene)isonicotino hydrazide(**L9**), N-(5-bromo-2-hydroxybenzylidene)isonicotinohydrazide (**L10**), N-(5-methoxy-2-hydroxybenzylidene)isonicotinohydrazide (**L11**) and two Schiff bases namely (E)-N^1 ((1H-pyrrol-2-yl)methylene)isonicotinohydrazide (**L12**), (E)-N^1 ((thiophen-2-yl)methylene)isonicotinohydrazide (**L13**) were derived using heteroaromatic aldehydes.

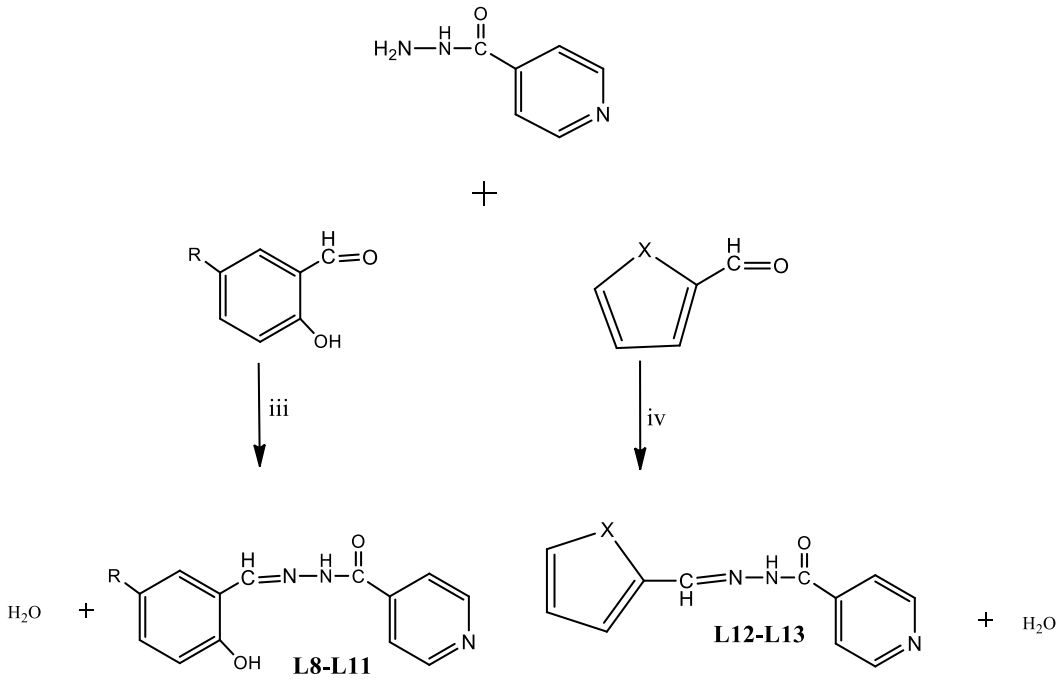

Reagnts and condition (iii): Glacial acetic acid, Ethanol, 65-70^{o}C, 6-12 h
(iv): Glacial acetic acid, Ethanol, 65^{o}C, 4-12 h
R = H, NO_2, (boiling DMSO, 8 h), Br, OCH_3
X = NH, S

Scheme 9 : Synthesis of INH Schiff bases.

4.4.1. Physical and analytical data of INH Schiff bases

The physical and analytical data are presented in Table 3. The compounds were obtained in excellent yields between 81-95% after recrystallization from suitable solvents. The melting points of the pure isolated compounds were in the range 77-312^{o}C. The elemental analysis calculated for each compound was in agreement with the experimental values.

Table 9: Physical and analytical data of INH-Schiff bases

Ligand code	Molecular formular (M.wt. (g/mol))	Colour	mp: (^{o}C)	Yield(%)	Microanalysis : % Calculated (Found)		
					C	H	N
L8	$C_{13}H_{11}N_3O_2$ (241)	Yellow	256-257	92	64.72 (64.89)	4.60 (4.49)	17.42 (17.83)
L9	$C_{13}H_{10}N_4O_4$ (286)	Yellow	310-312	89	54.24 (54.55)	3.80 (3.52)	19.37 (19.57)
L10	$C_{13}H_{10}BrN_3O_2$ (320)	White	261-264	95	48.77 (48.75)	3.15 (2.79)	13.13 (13.15)
L11	$C_{14}H_{13}N_3O_3$ (271)	Orange	205-207	86	61.99 (61.82)	4.83 (4.87)	15.49 (15.67)
L12	$C_{11}H_{10}N_4O$ (214)	Yellow	234-237	87	61.67 (62.16)	4.71 (4.64)	26.15 (26.27)
L13	$C_{11}H_9N_3OS$ (320)	Light-yellow	241-242	81	57.13 (57.64)	3.92 (3.85)	18.17 (18.93)

M.wt = molecular weight; mp = melting point

4.4.2 IR spectra of the INH Schiff bases

The IR spectra of the all the INH Schiff bases derived using 2-hydroxybenzaldehyde derivatives aldehydes show bands in the range 3188-3308 cm^{-1}, 3002-3069 cm^{-1}, 1649-1675 cm^{-1}, 1608-1616 cm^{-1} and 1286-1299 cm^{-1}.

Table 10a: Characteristic IR (cm^{-1}) bands of INH Schiff bases bearing 2-hydroxybenzaldehyde derivative aldehydes

Ligand code	Structure	IR bands (cm^{-1})				
		ν_{OH}	ν_{NH}	$\nu_{C=O}$	$\nu_{C=N}$	ν_{C-O}
L8	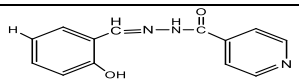	3308	3002	1675	1611	1289
L9	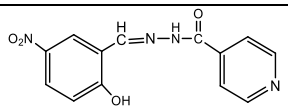	3305	3069	1664	1608	1296
L10	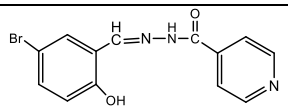	3252	3068	1669	1616	1286
L11	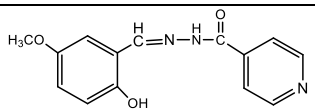	3188	3053	1649	1613	1299

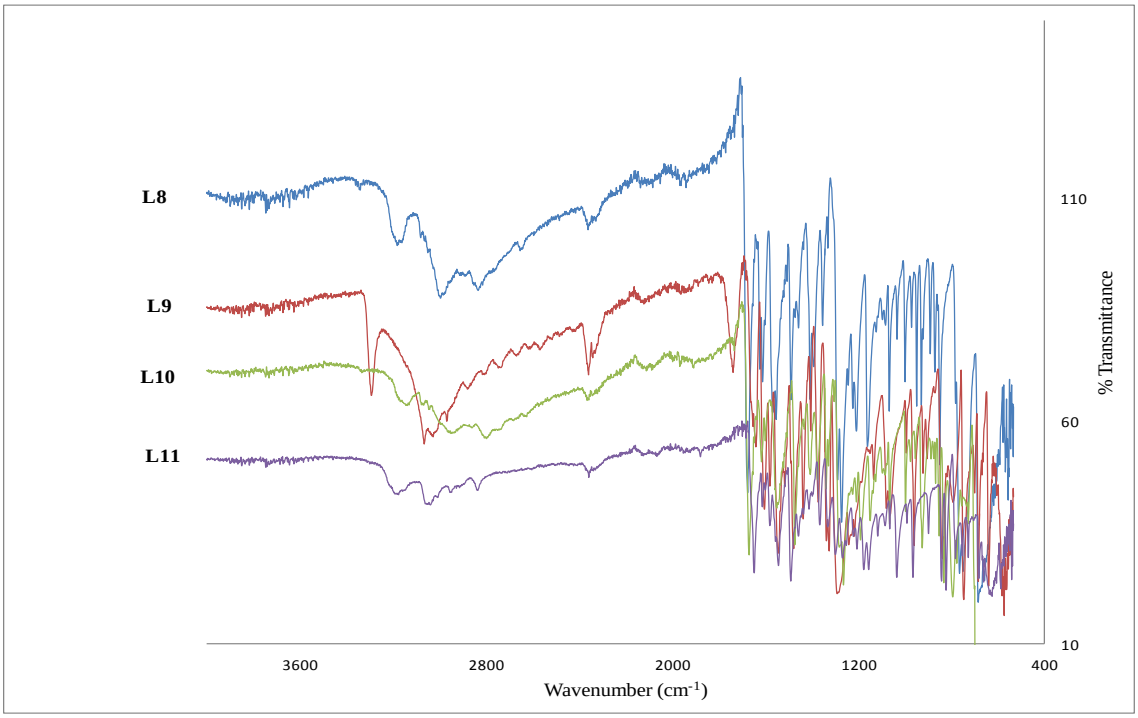

Figure 36: Infrared spectra of 2-hydroxybenzaldehyde derivatives INH-based Schiff bases **L8-L11**

In addition, INH Schiff bases bearing heteroaromatic aldehydes displayed bands in the range 3026-3118 cm^{-1}, 1644-1661 cm^{-1} and 1593-1617 cm^{-1}.

Table 10b: Characteristic IR (cm^{-1}) bands of INH Schiff bases bearing heteroaromatic aldehydes

Ligand code	IR bands (cm^{-1})				
		ν_{NH}	$\nu_{C=O}$	$\nu_{C=N}$	$\nu_{C=N(py)}$
L12	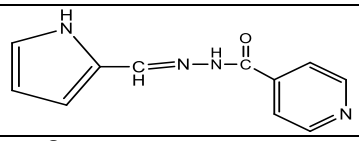	3056	1645	1594	1411
L13	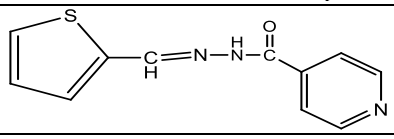	3028	1661	1593	-

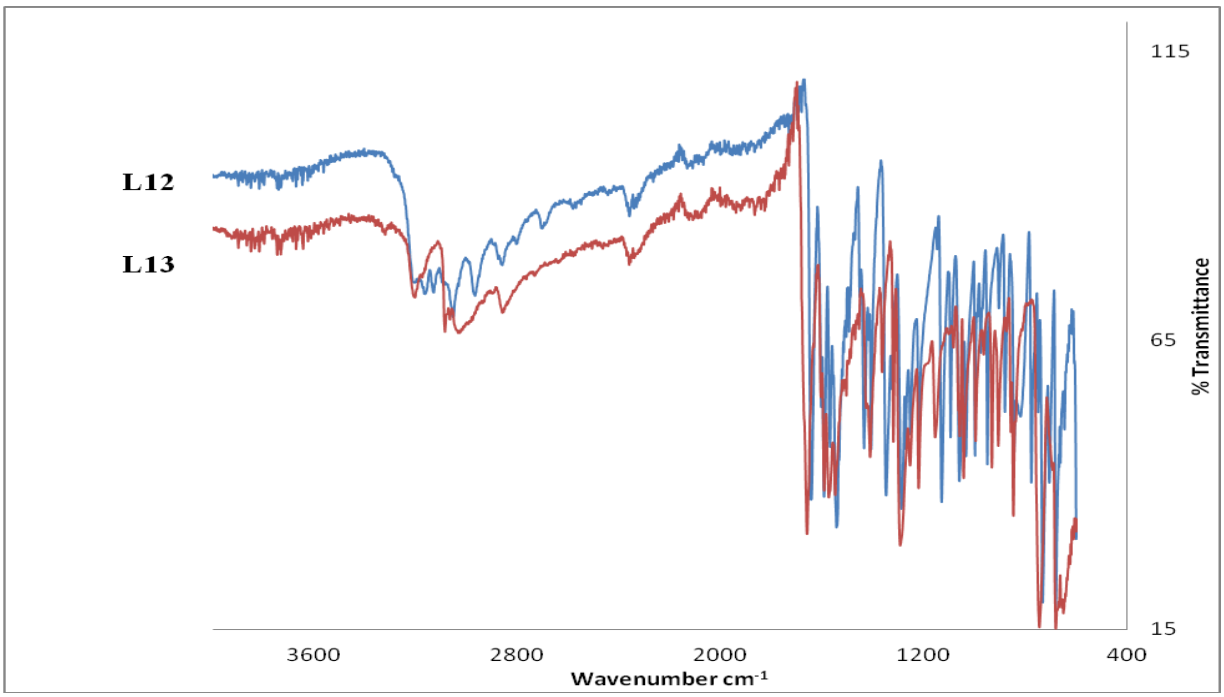

Figure 37 : Infrared spectra of INH-based Schiff bases bearing heteroaromatic aldehydes **L12-L13**

4.4.3: NMR spectra of INH Schiff bases

Both proton (^{1}H-NMR) and carbon (^{13}C-NMR) spectra were obtained for each of compounds **L8-L11**. The ^{1}H-NMR spectra displayed a sharp singlet at 8.69 and 12.31 ppm, 8.76 and 12.43 ppm, 8.65 and 12.36 and 8.68 and 12.29 ppm for compounds **L8, L9, L10** and **L11** respectively in deuterated DMSO using tetra methyl silane (TMS) as internal standard. The ^{13}C NMR displayed a signal at 140.46 and 158.01 ppm, 140.40 and 162.17 ppm, 140.41 and 156.98 ppm and 140.59 and 152.71 ppm for compounds **L8**, **L9**, **L10** and **L11** respectively. In addition, signals were observer at 161.87, 163.22, 162.02 and 161.93 respectively. Compound **L11** displayed a significant signal at δ_H 3.72 and δ_C 56.00. All the carbons present in each Schiff base were identified.The spectra are shown in Figures 38a-41b.

Table 11a: Characteristic ^{1}H and ^{13}C NMR bands of INH Schiff bases

Ligand code	Structure	Chemical shift (ppm)							
		HC=N		C-OH		NH	C=O	OCH_3	
		δ_H	δ_C	δ_H	δ_C	δ_H	δ_C	δ_H	δ_C
L8	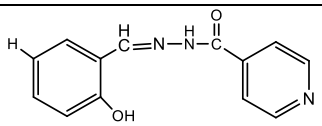	8.69	140.46	12.31	158.01	11.11	161.87	-	-
L9	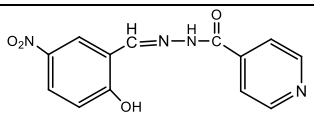	8.76	140.40	12.43	162.17	12.20	163.22	-	-
L10	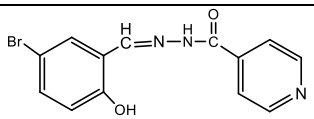	8.65	140.41	12.36	156.98	11.14	162.02	-	-
L11	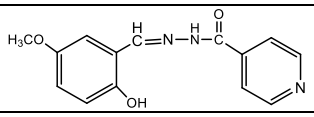	8.68	140.59	12.29	152.71	10.53	161.93	3.72	56.00

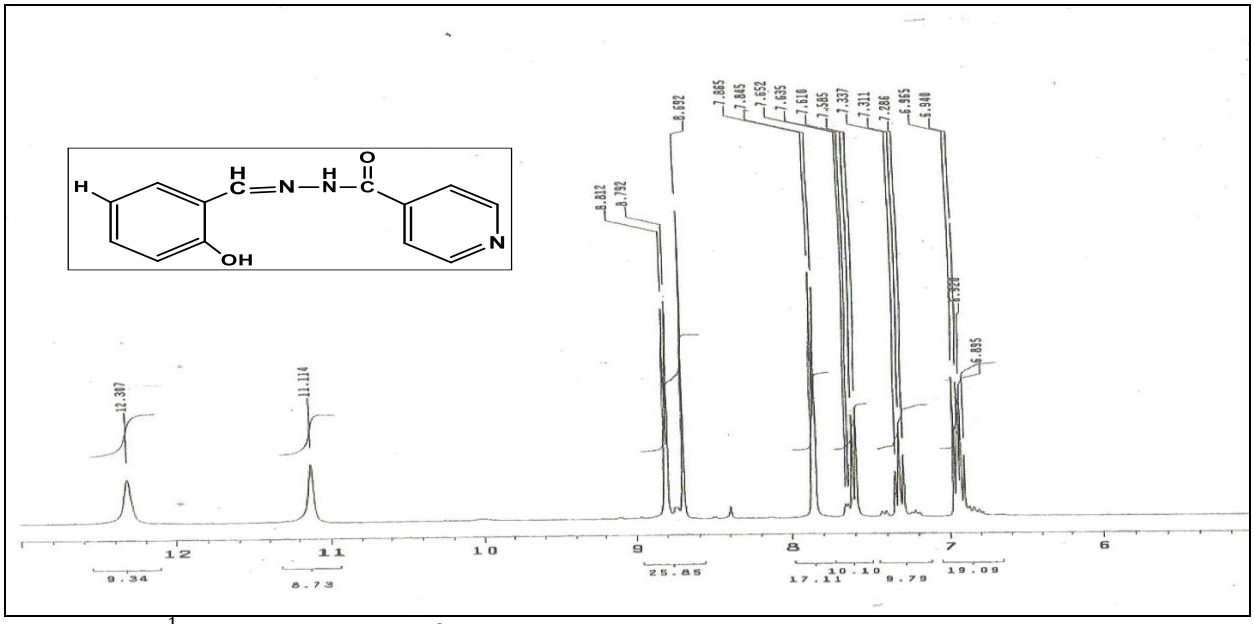

Figure 38a: ^{1}H NMR spectrum of *N*-(2-hydroxybenzylidene)isonicotino hydrazide **L8** in DMSO-d_6

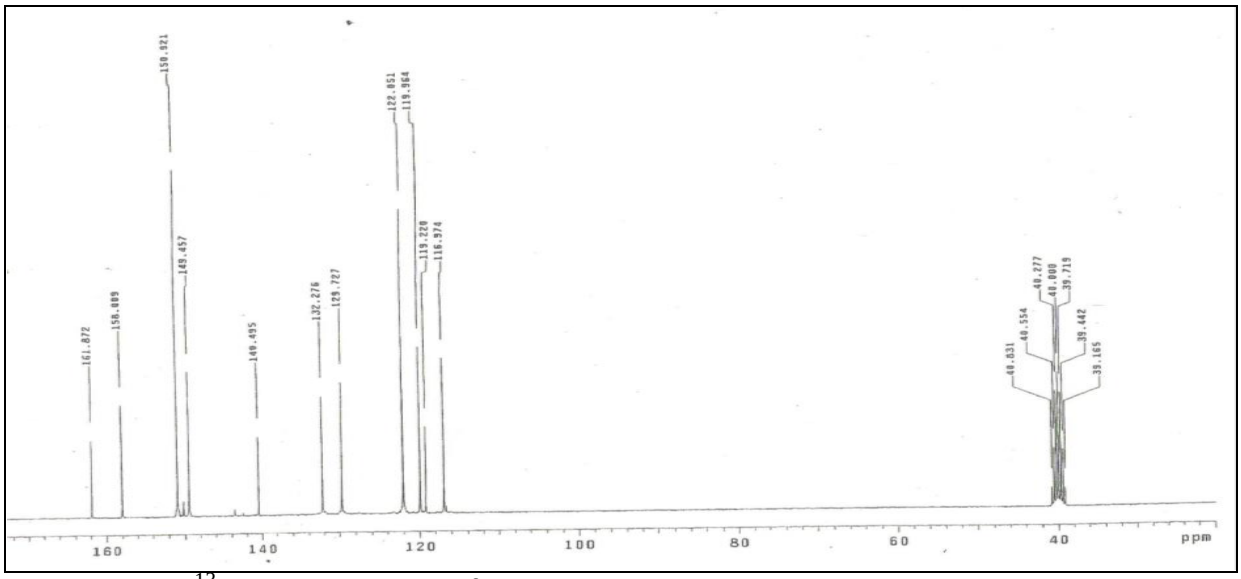

Figure 38b: ^{13}C NMR spectrum of *N*-(2-hydroxybenzylidene)isonicotino hydrazide **L8** in DMSO-d_6

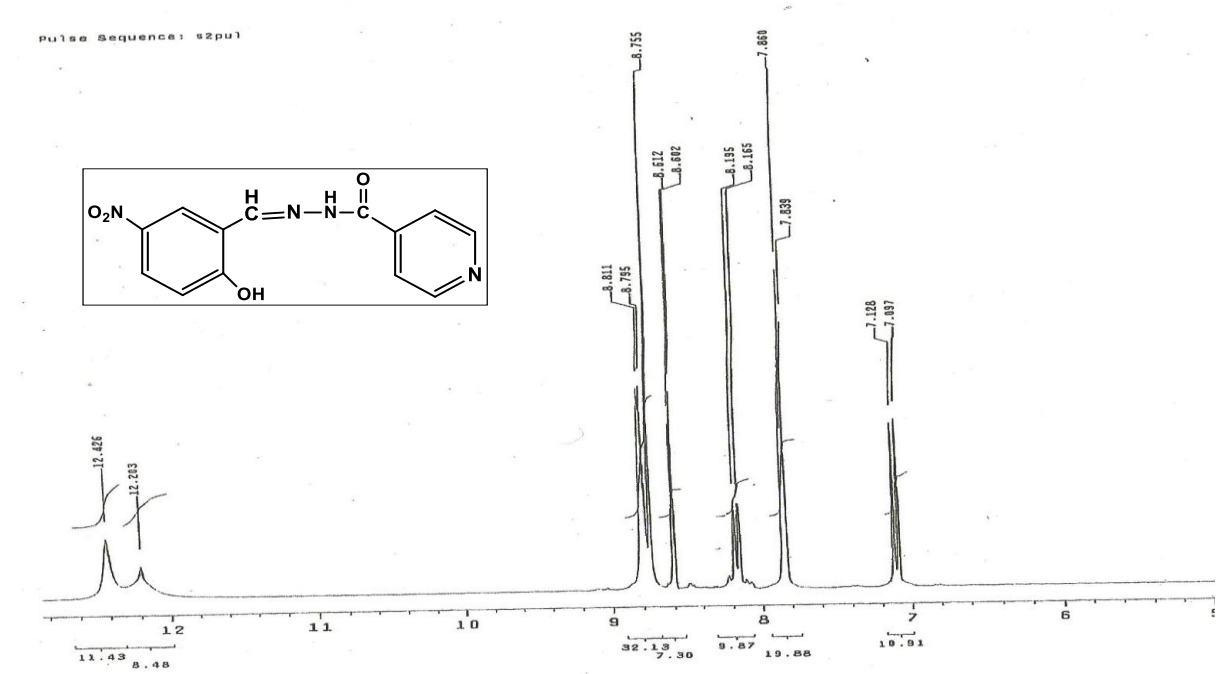

Figure 39a: ^{1}H NMR spectrum of *N*-(5-nitro-2-hydroxybenzylidene)isonicotino hydrazide **L9** in DMSO-d_6

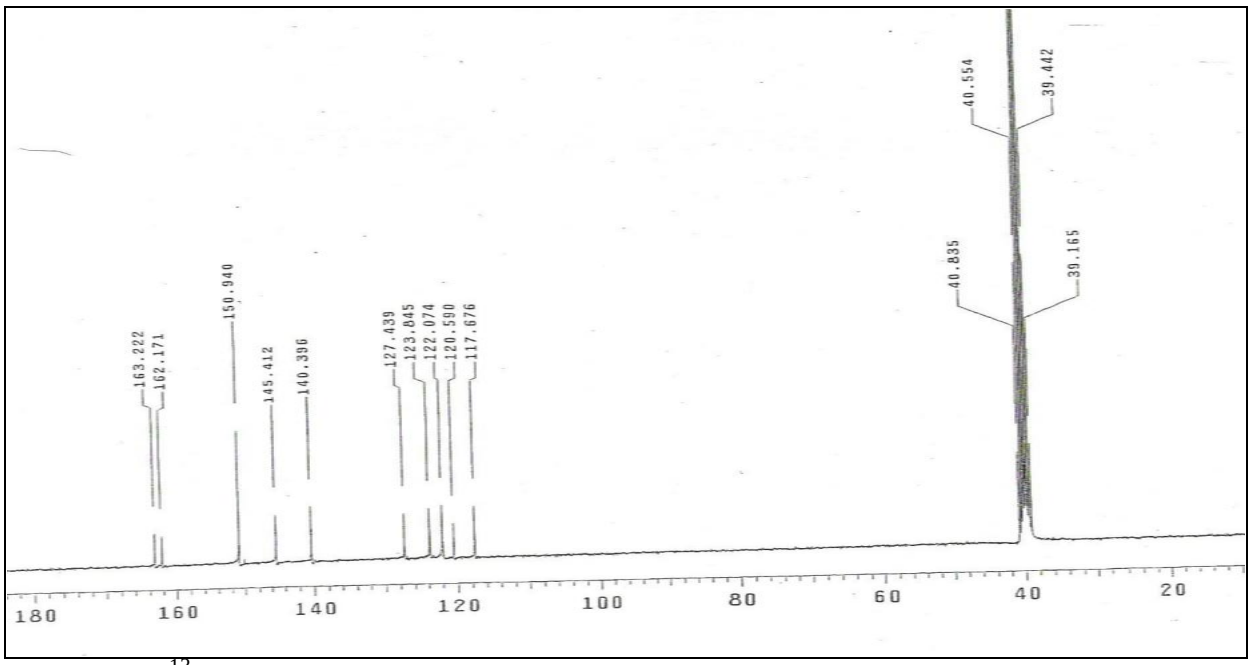

Figure 39b: ^{13}C NMR spectrum of *N*-(5-nitro-2-hydroxybenzylidene)isonicotino hydrazide **L9** in DMSO-d_6

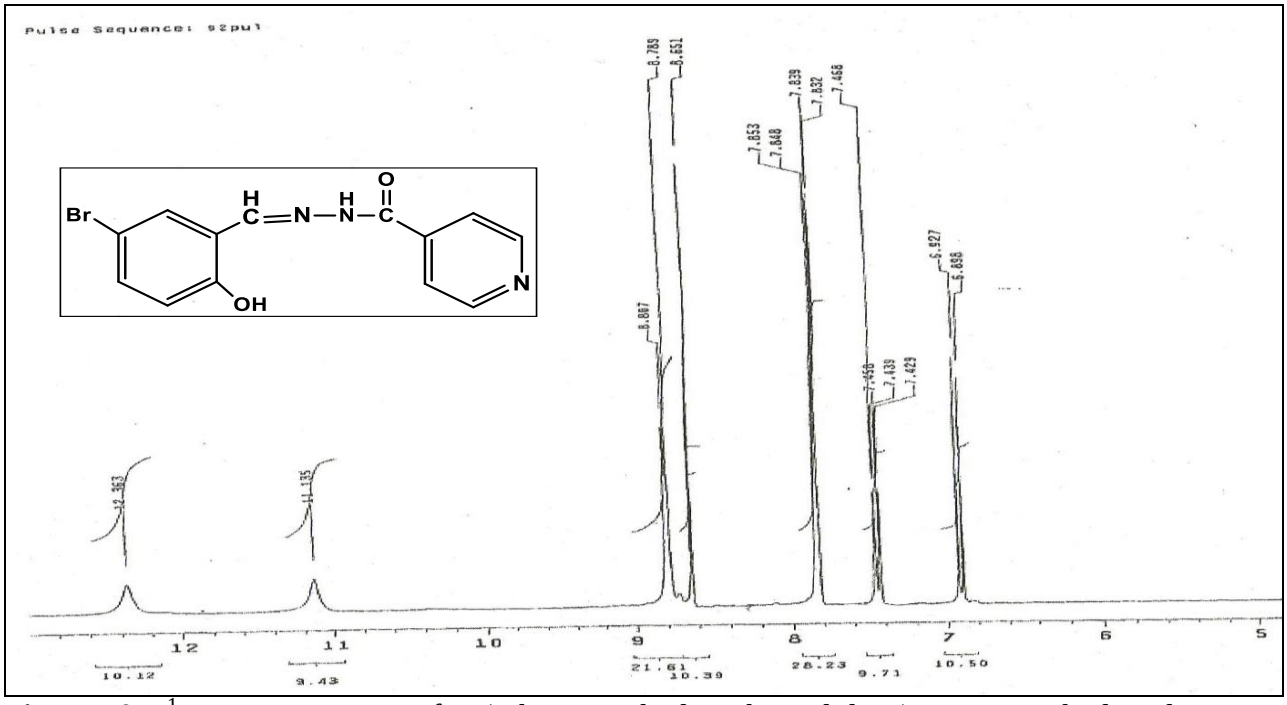

Figure 40a: [1]H NMR spectrum of *N*-(5-bromo-2-hydroxybenzylidene)isonicotino hydrazide

L10 in DMSO-d_6

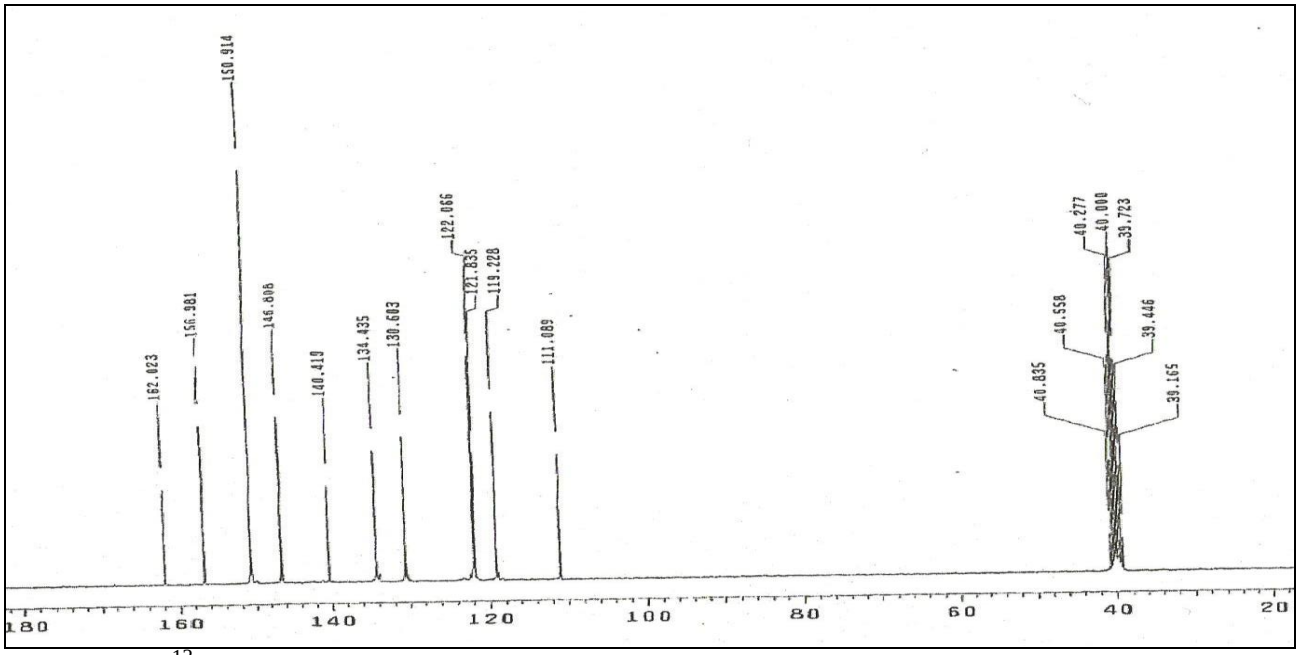

Figure 40b: [13]C NMR spectrum of *N*-(5-bromo-2-hydroxybenzylidene)isonicotino hydrazide

L10 in DMSO-d_6

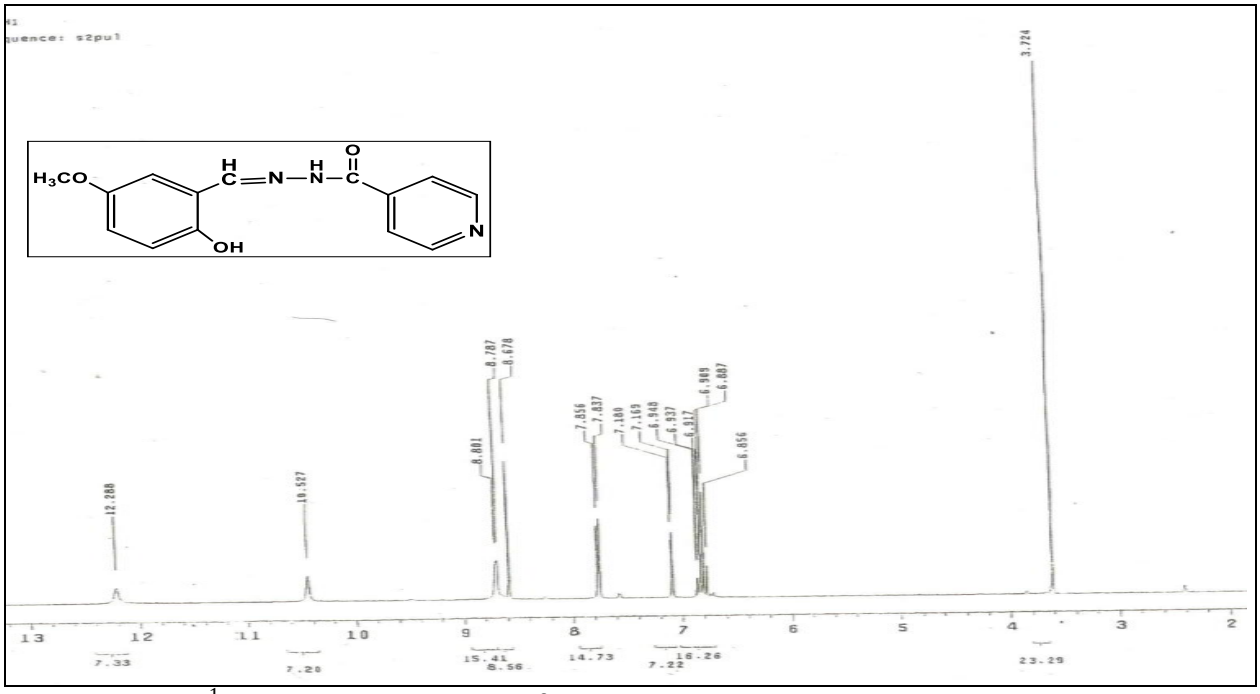

Figure 41a: ^{1}H NMR spectrum of *N*-(5-methoxy-2-hydroxybenzylidene)isonicotino hydrazide **L11** in DMSO-d_6

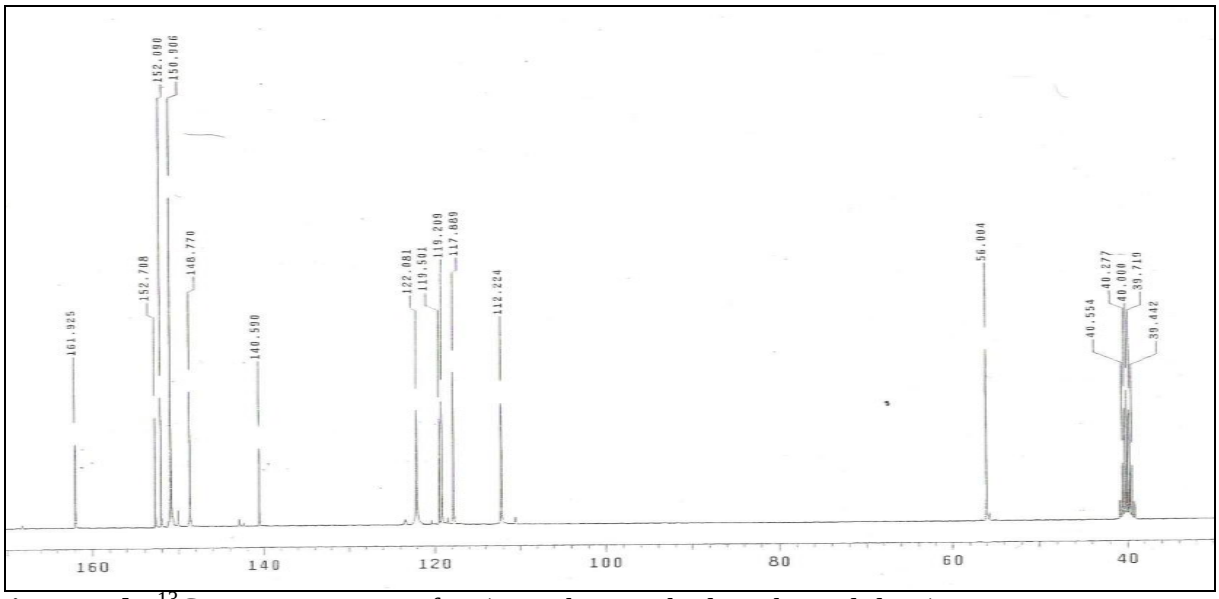

Figure 41b: ^{13}C NMR spectrum of *N*-(5-methoxy-2-hydroxybenzylidene)isonicotino hydrazide **L11** in DMSO-d_6

The proton (^{1}H) and carbon (^{13}C) NMR spectra of INH Schiff bases with hetero atom moiety (**L12** and **L13**) were obtained in a deuterated DMSO. A sharp singlet was observed at 8.29 and 8.68 ppm and 11.73 and12.03 ppm in the ^{1}H NMR spectra of all the Schiff bases (**L12** and **L13**). In addition compound **L12** displayed a sharp singlet at 11.60 ppm. The ^{13}C NMR spectra showed signals at 141.48 and140.94 ppm and 161.66 and161.96 ppm. All the protons and carbons present in the each ligand were identified. The spectra are presented in Figures 42a-43b.

Table 11b: Characteristic ^{1}H and ^{13}C NMR bands of INH Schiff bases

Ligand code	Chemical shift δ_{TMS} (ppm)					
	Structures	HC=N		C=O	NH	NH (pyrrole)
		δ_H	δ_C	δ_C	δ_H	δ_H
L12	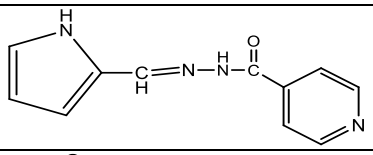	8.29	141.48	161.66	11.73	11.60
L13	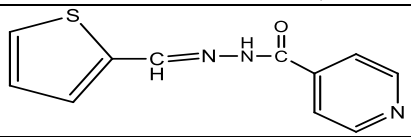	8.68	140.94	161.96	12.03	-

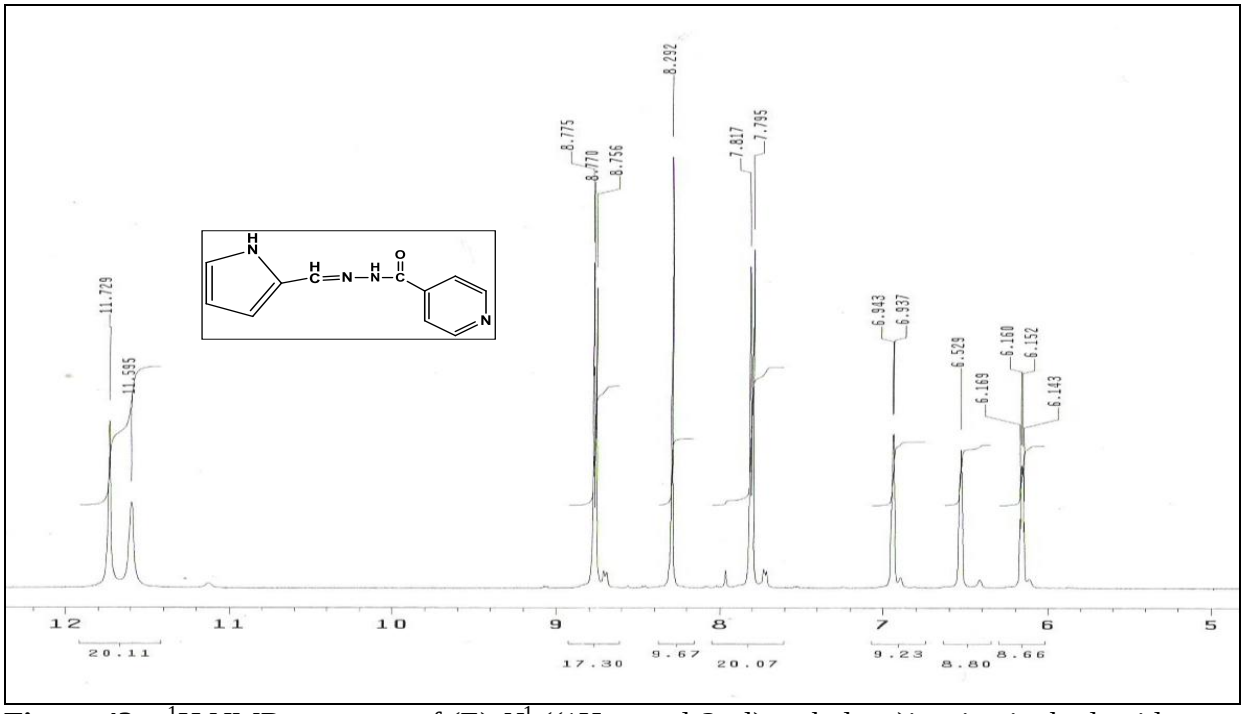

Figure 42a: ^{1}H NMR spectrum of (E)-N^{1} ((1H-pyrrol-2-yl)methylene)isonicotinohydrazide **L12** in DMSO-d_6

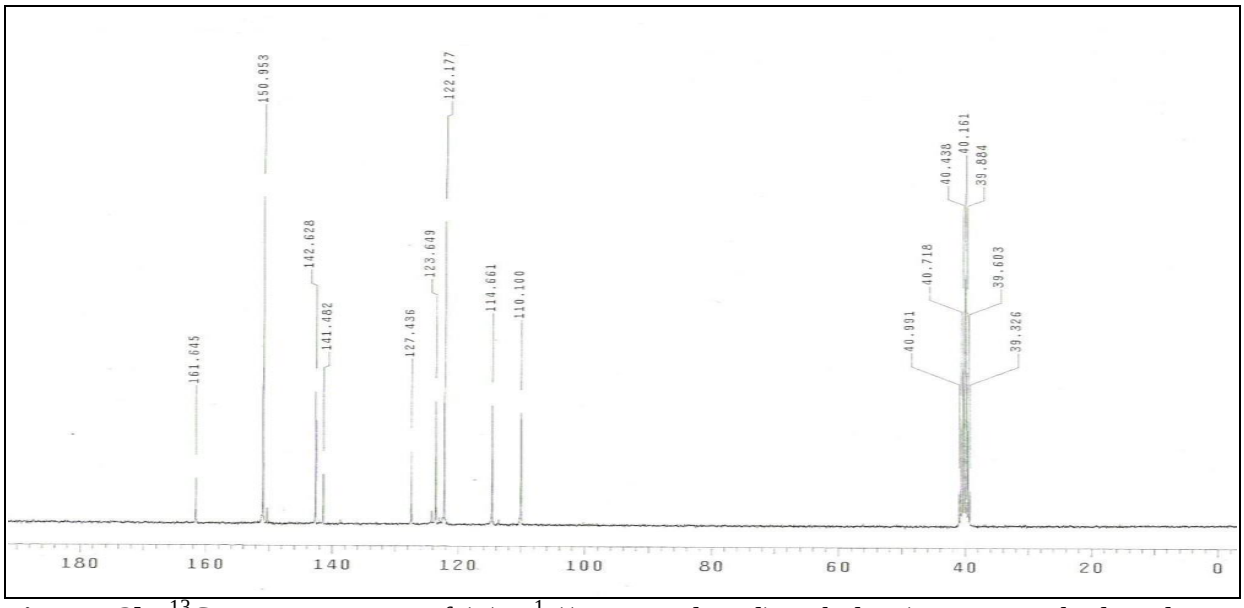

Figure 42b: ^{13}C NMR spectrum of (E)-N^{1} ((1H-pyrrol-2-yl)methylene)isonicotinohydrazide **L12** in DMSO-d_6

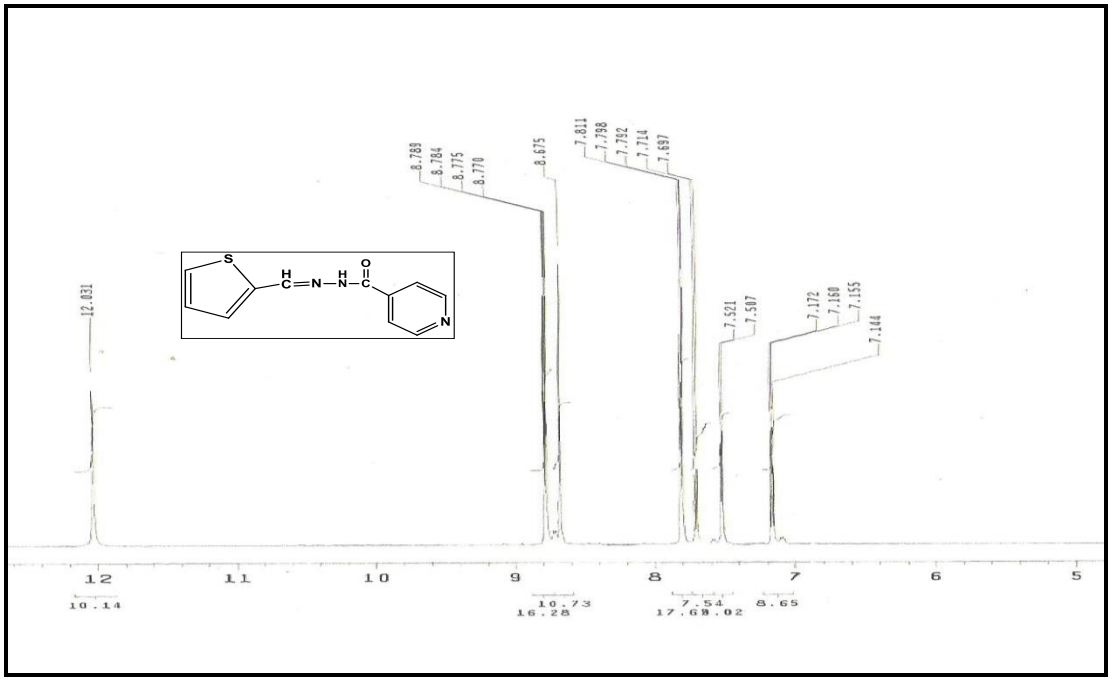

Figure 43a: ^{1}H NMR spectrum of (E)-N^{1} ((thiophene-2-yl)methylene)isonicotinohydrazide **L13** in DMSO-d_6

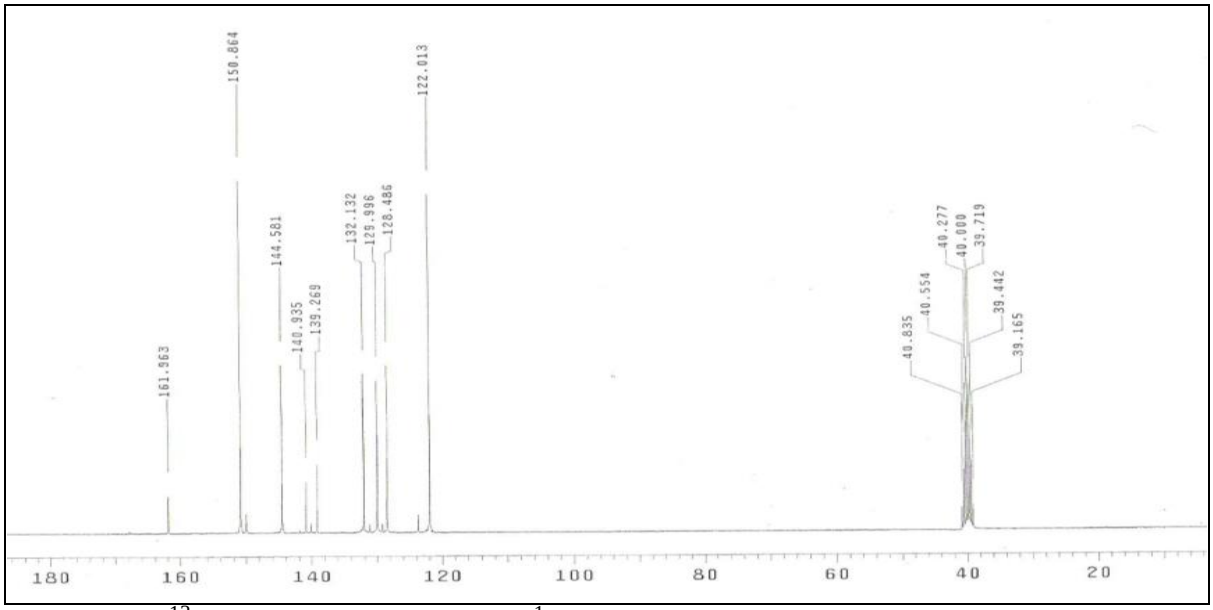

Figure 43b: ^{13}C NMR spectrum of (E)-N^{1} ((thiophene-2-yl)methylene)isonicotinohydrazide **L13** in DMSO- d_6

4.4.4: Electronic absorption spectra of INH Schiff bases

The electronic spectra of 10^{-5} M solution of the INH Schiff bases in DMF consist of various bands in the 200-500 nm region. The spectra of compounds **L8, L10,** and **L11** consist of three absorption bands in the range 288-340 nm. Two bands were observed in the spectra of compounds **L9** within the 296-363 nm region.

Table 12a: Electronic absorption bands for INH-Schiff bases (L8-L11)

Ligand Code	Band A λmax(nm)	Log∈	Band B λmax(nm)	Log∈	Band C λmax (nm)	Log∈
L8	289	4.56	303	4.90	331	4.95
L9	-	-	296	5.04	363	4.96
L10	288	4.79	304	4.94	340	4.92
L11	288	5.14	304	5.09	337	5.06

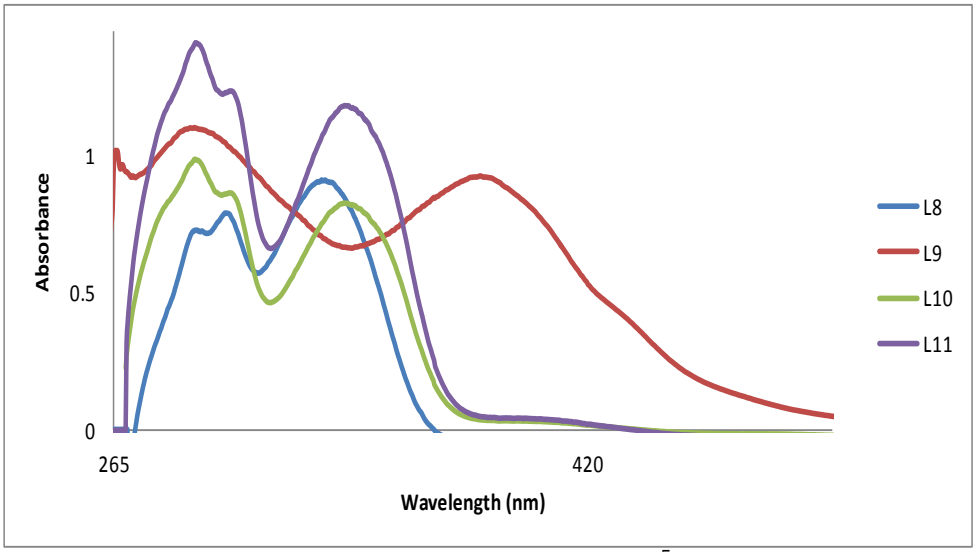

Figure 44: Electronic absorption spectrum of **L8-L11** in 10^{-5} M DMF solution

The spectra of Compounds **L12** and **L3** consist of only one absorption band in the range 335-318 nm respectively. Two bands were observed in the spectrum of compound **L14** at 274 and 326 nm region.

Table 12b: Electronic absorption bands for INH-Schiff bases (**L12-L13**)

Ligand Code	Band A λmax(nm)	Log∈	Band B λmax(nm)	Log∈
L12	-	-	335	5.13
L13	274	4.91	326	5.08

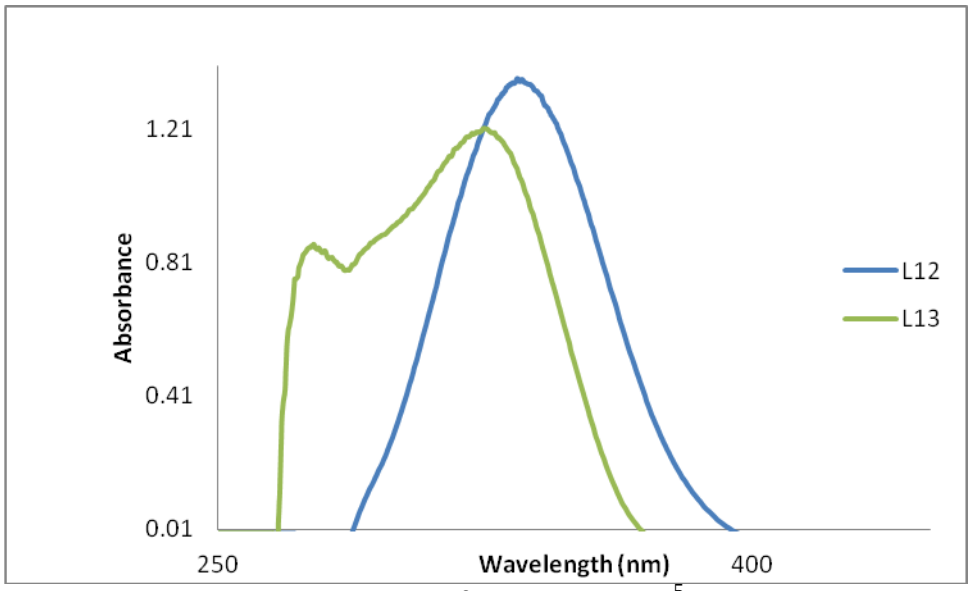

Figure 45: Electronic absorption spectrum of **L12-L13** in 10^{-5} M DMF solution

4.5 Synthesis and characterization of Schiff bases metal complexes.

Three groups of Schiff base metal complexes were synthesized using in this stydy. Each group consists of Cu(II) designated "**A**", Ni(II) "**B**" and Co(II) "**C**" complexes. They are 2-aminopyridine Schiff base metal complexes (**L1A-L4C**), 4-aminopyridine Schiff base metal complexes (**L5A-L7C**), and INH Schiff base metal complexes (**L8A-L13C**).

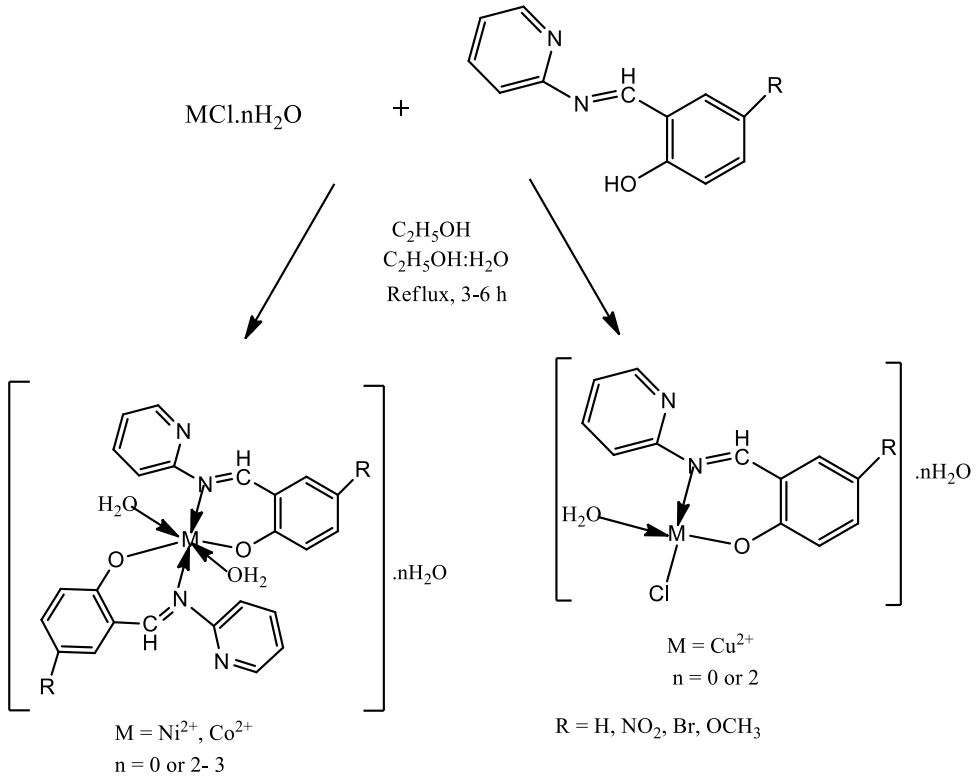

Scheme 10: Representative scheme for the synthesis of **L1A-L4C**

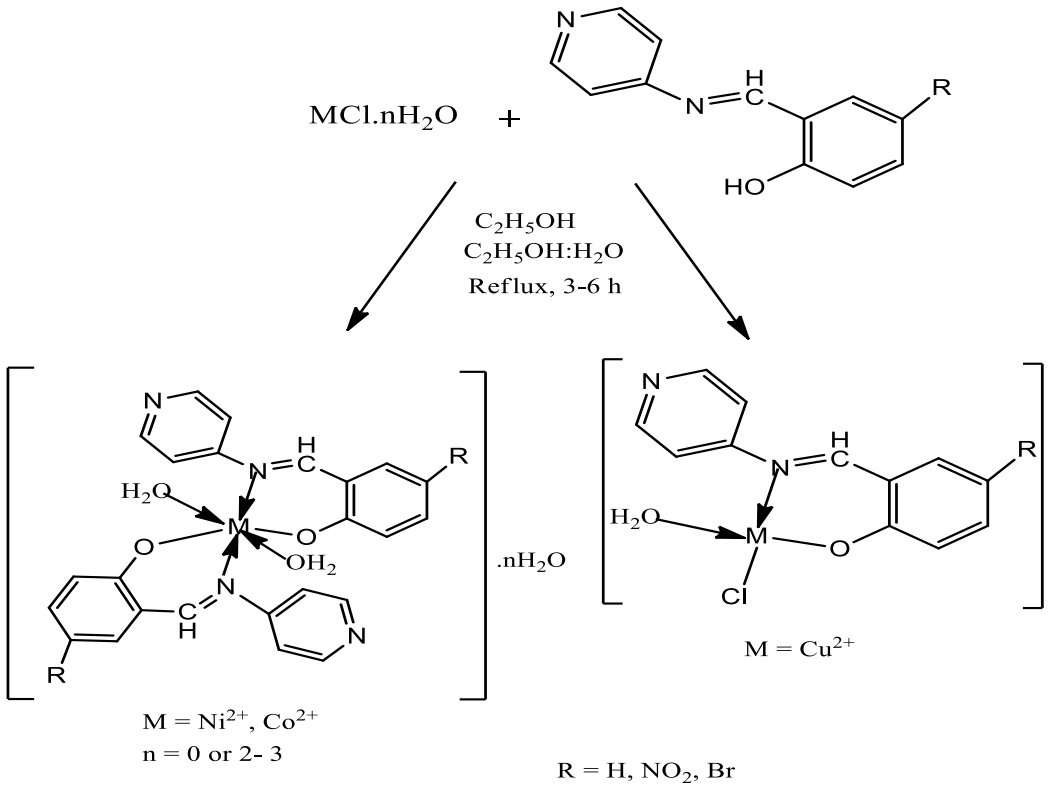

Scheme 11: Representative scheme for the synthesis of **L5A-L7C**

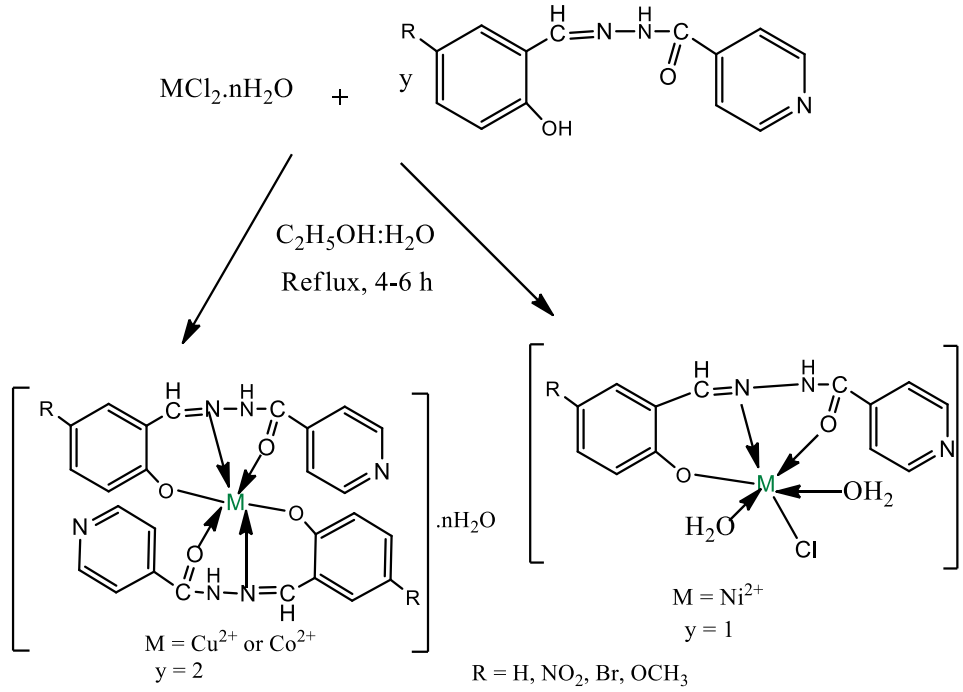

Scheme 12: Representative scheme for the synthesis of **L8A-L13C**

4.5.1 Physical and analytical data of *N*(2-hydroxybenzylidene)pyridin-2-amine complexes.

The physical and analytical data of the metal complexes of pure isolated *N*(2-hydroxybenzylidene)pyridin-2-amine are presented in Table 13. The complexes were all obtained in moderate to good yields in the range 54-63%. The melting points were determined to be in the range 164-313 ^{o}C. The elemental analysis data are within the acceptable range.

Table 13: Physical and analytical data for the complexes of *N*(2-hydroxybenzylidene)Pyridin -2-amine SBs

Complex code	Molecular formular (M.wt, (g/mol))	mp: (^{o}C)	Yield (%)	Microanalysis % Calculated (Found)			
				C	H	N	M
L1A	$C_{12}H_{15}ClCuN_2O_4$ (349)	164-166	54	41.15 (41.66)	4.32 (3.94)	8.00 (8.12)	18.14 (20.55)
L1B	$C_{24}H_{22}N_4NiO_4$ (488)	241-245	61	58.93 (59.13)	4.53 (4.07)	11.45 (11.87)	12.00 (12.74)
L1C	$C_{24}H_{22}CoN_4O_4$ (489)	310-313	63	58.90 (58.26)	4.53 (4.19)	11.45 (11.65)	12.04 (12.44)

M.wt = molecular weight; mp = Melting point

4.5.2. Infrared spectra of *N*(2-hydroxybenzylidene)pyridin-2-amine metal complexes

The Cu(II), Ni(II) and Co(II) complexes of *N*(2-hydroxybenzylidene)pyridin-2-amine were characterized using IR spectroscopy. The results are presented in Table 14 and IR spectrum shown in Figure 46.

Table 14: Characteristic IR bands (cm^{-1}) for the complexes of *N*(2-hydroxybenzylidene)pyridin-2-amine

Complex code	Complexes	*v*C=N	*v*C-O	*v*C=N (pyridine)	*v*(H_2O)	*v*(M-O)	*v*(M-N)
L1A	[CuL1 Cl.H_2O].2H_2O	1595	1286	1034	863	516	451
L1B	[Ni$(L1)_2$].2H_2O	1595	1287	1033	-	521	492
L1C	[Co$(L1)_2$ .2H_2O]	1734	1288	1032	856	483	445

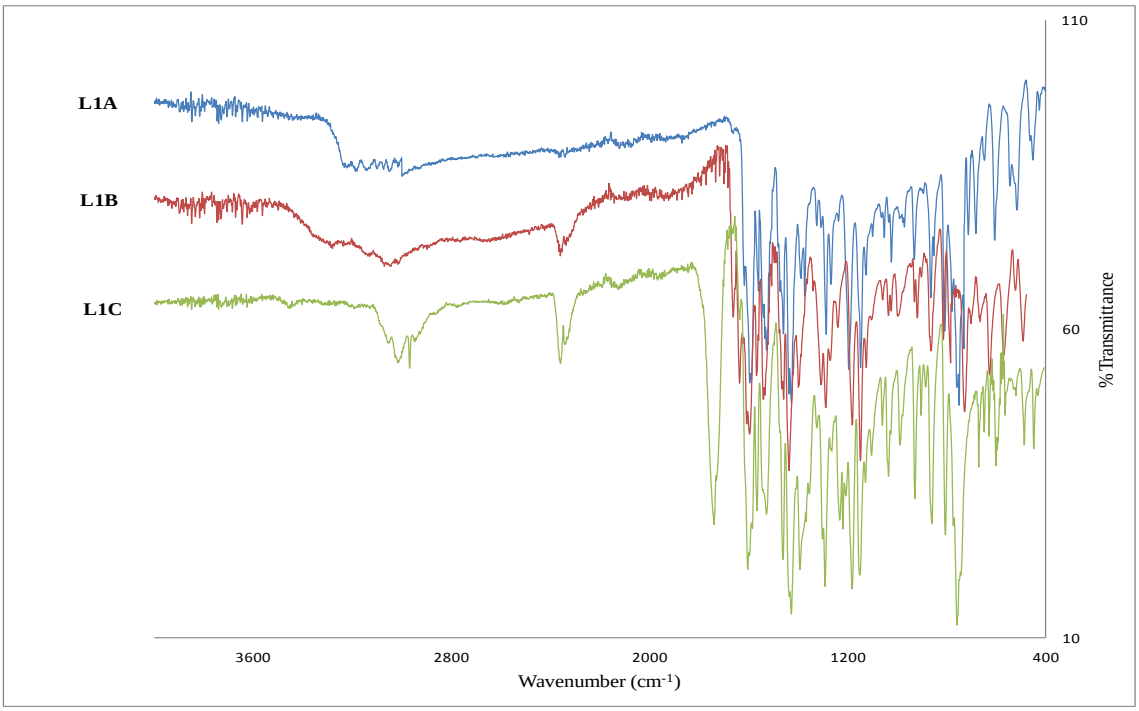

Figure 46: IR spectrum of *N*(2-hydroxybenzylidene)pyridin-2-amine complexes

4.5.6: Electronic absorption spectra of *N*(2-hydroxybenzylidene)pyridin-2-amine metal complexes

The electronic spectra recorded in 10^{-3} M solution *N*(2-hydroxybenzylidene)pyridin-2-amine metal complexes (**L1A-L1C**) in DMF are listed in Tables 15. The spectrum is shown in Figure 47.

Table 15: Electronic absorption bands and molar conductance for the complexes of *N*(2-hydroxybenzylidene)pyridin-2-amine

Complex code	Complex	λ_{max}(nm)	Assignment	Molar conductance ($ohm^{-1}cm^2mol^{-1}$)	Proposed Geometry
L1A	$[CuL1\ Cl.H_2O].2H_2O$	292, 356, 410	π-π* n-π* d-d	5.20	Square planar
L1B	$[Ni(L1)_2].2H_2O$	351, 496	n-π* d-d	2.16	Square planar
L1C	$[Co(L1)_2\ 2H_2O]$	311, 430, 503	n-π* d-d d-d	2.42	Octahedral

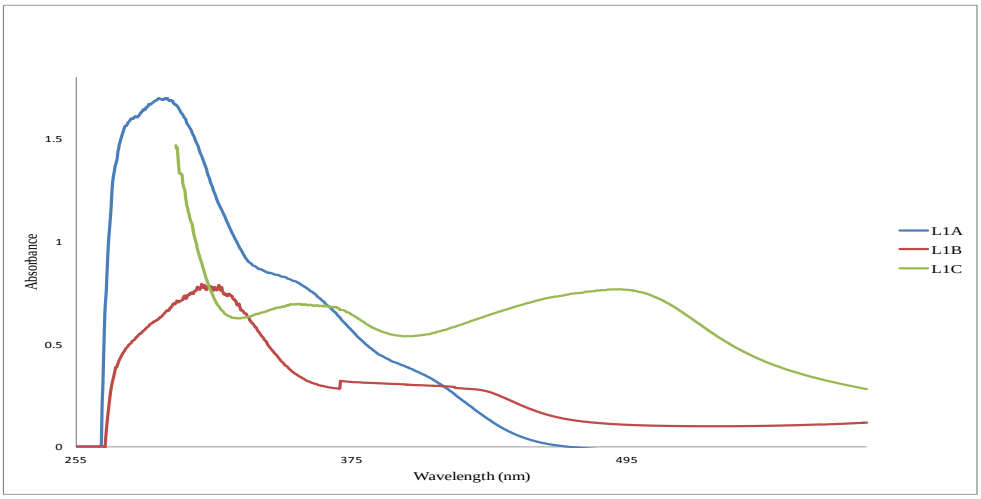

Figure 47: : Electronic absorption spectrum of *N*(2-hydroxybenzylidene)pyridin-2-amine metal complexes in DMF.

4.5.7 Physical and analytical data of *N*(5-nitro-2-hydroxybenzylidene)pyridin-2-amine complexes.

The physical and analytical data of the metal complexes of pure isolated *N*(5-nitro-2-hydroxybenzylidene)pyridin-2-amine are presented in Table 16. The complexes were all obtained in moderate to good yields in the range 46-57%. The melting points were determined to be in the range 249- >349 ^{o}C. The elemental analysis data are within the acceptable range.

Table 16: Physical and analytical data forthe complexes of *N*-(5-nitro-2-hyroxybenzylidene) pyridin-2-amine

Complex code	Molecular formular (M.wt, (g/mol))	mp: (^{o}C)	Yield (%)	Microanalysis % Calculated (Found)			
				C	H	N	M
L2A	$C_{14}H_{16}ClCuN_3O_5$ (405)	249 -256	57	41.49 (42.18)	3.98 (3.32)	10.37 (11.06)	15.68 (15.54)
L2B	$C_{24}H_{24}NiN_6O_{10}$ (614)	>349	46	46.86 (46.07)	3.93 (2.91)	13.66 (13.01)	9.54 (9.50)
L2C	$C_{24}H_{26}CoN_6O_{11}$ (633)	266 -269	51	45.51 (44.98)	4.14 (4.09)	13.27 (12.67)	9.30 (9.49)

M.wt = molecular weight; mp = Melting point

4.5.8. Infrared spectra of *N*(5-nitro-2-hydroxybenzylidene)pyridin-2-amine metal complexes

The Cu(II), Ni(II) and Co(II) complexes of *N*(5-nitro-2-hydroxybenzylidene)pyridin-2-amine were characterized using IR spectroscopy. The results are presented in Table 17 and IR spectrum shown in Figure 48.

Table 17: Characteristic IR bands (cm^{-1}) for the complexes of *N*(5-nitro-2-hydroxybenzylidene)pyridin-2-amine

Complex code	Complex	*v*C=N	*v*C-O	*v*C=N (pyridine)	*v*(H_2O)	*v*(M-O)	*v*(M-N)
L2A	[CuL2.Cl.H_2O].C_2H_5OH	1605	1247	1101	3311/850	482	444
L2B	[Ni$(L2)_2$.2H2O].2H_2O	1602	1291	1101	842	515	451
L2C	[Co$(L2)_2$ 2H_2O].3H_2O	1600	1269	1105	846	512	471

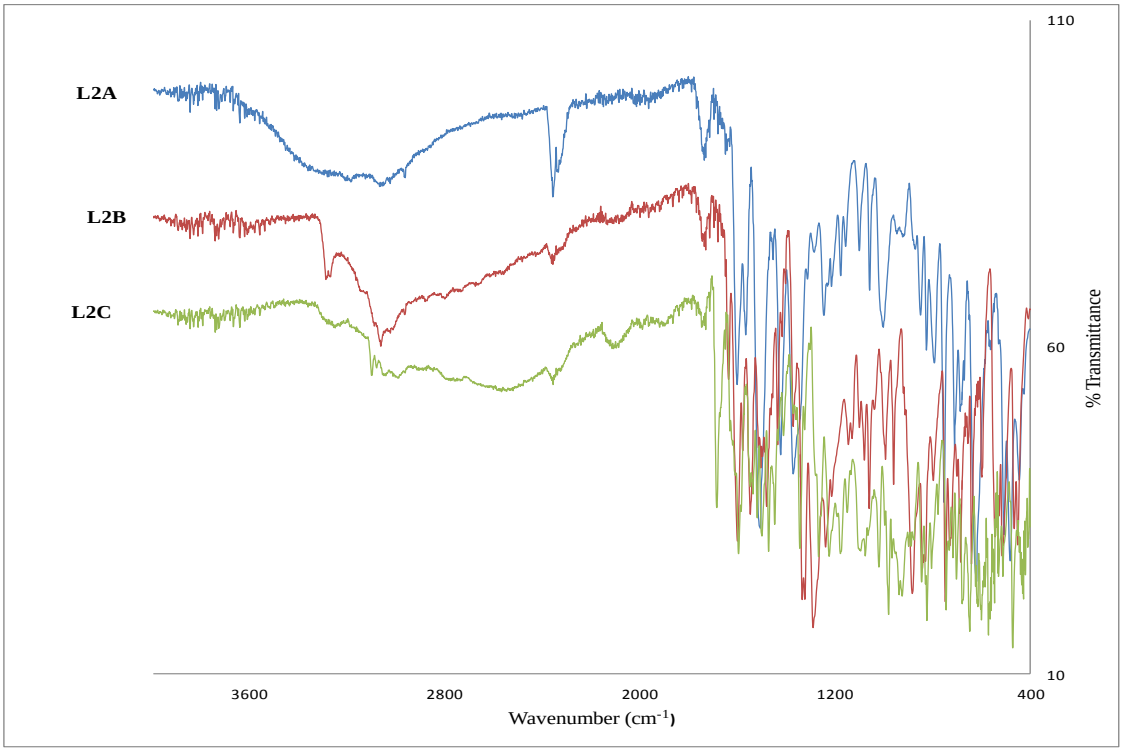

Figure 48: IR spectrum of *N*(5-nitro-2-hydroxybenzylidene)pyridin-2-amine complexes

4.5.9 Electronic absorption spectra of *N*(5-nitro-2-hydroxybenzylidene)pyridin-2-amine metal complexes

The electronic spectra recorded in 10^{-3} M solution *N*(5-nitro-2-hydroxybenzylidene)pyridin-2-amine metal complexes (**L2A-L2C**) in DMF are listed in Tables 18. The spectrum is shown in Figure 49.

Table 18: Electronic absorption bands and molar conductance for the *N*(5-nitro-2-hydroxybenzylidene)pyridin-2-amine complexes

Complex code	Complex	λ_{max}(nm)	Assignment	Molar conductance ($ohm^{-1}cm^2mol^{-1}$)	Proposed Geometry
L2A	[CuL2 Cl H_2O].C_2H_5OH	296 359	π-π* CT	3.20	Square planar
L2B	[Ni$(L2)_2$.2H2O].2H_2O	587 652	d-d d-d	2.85	Octahedral
L2C	[Co$(L2)_2$ 2H_2O].3H_2O	603 629(sh) 674	d-d d-d d-d	3.63	Octahedral

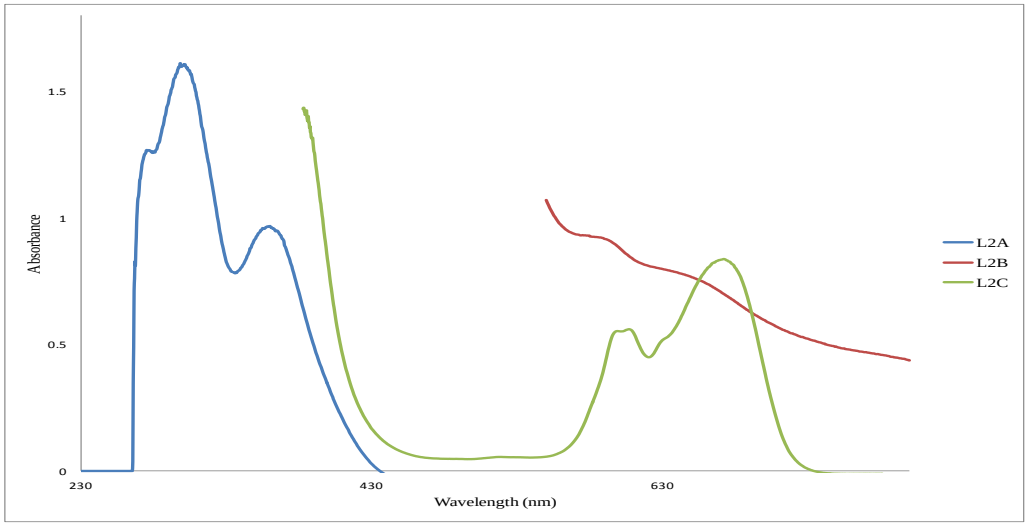

Figure 49: Electronic absorption spectrum spectrum of *N*(5-nitro-2-hydroxybenzylidene)pyridin-2-amine metal complexes in DMF.

4.5.10 Physical and analytical data of *N*(5-bromo-2-hydroxybenzylidene)pyridin-2-amine complexes.

The physical and analytical data of the metal complexes of pure isolated *N*(5-bromo-2-hydroxybenzylidene)pyridin-2-amine are presented in Table 19. The complexes were all obtained in moderate to good yields in the range 59-62%. The melting points were determined to be in the range 234- >349 ^{o}C. The elemental analysis data are within the acceptable range.

Table 19: Physical and analytical data for the complexes of *N*(5-bromo-2-hydroxy benzylidene)pyridin-2-amine

Complex code	Molecular formular (M.wt. (g/mol))	mp: (^{o}C)	Yield (%)	Microanalysis % Calculated (Found)			
				C	H	N	M
L3A	$C_{12}H_{10}BrClCuN_2O_2$ (390)	289 -295	62	36.66 (38.41)	2.56 (2.50)	7.13 (7.25)	16.16 (16.67)
L3B	$C_{24}H_{24}Br_2N_4NiO_6$ (680)	>349	67	42.21 (41.94)	3.54 (3.59)	8.20 (8.61)	8.59 (9.23)
L3C	$C_{24}H_{20}Br_2CoN_4O_4$ (645)	234-237	59	44.54 (44.10)	3.11 (3.60)	8.66 (8.17)	9.11 (9.83)

M.wt. = molecular weight; mp = Melting point

4.5.11 Infrared spectra of *N*(5-bromo-2-hydroxybenzylidene)pyridin-2-amine metal complexes

The Cu(II), Ni(II) and Co(II) complexes of *N*(5-bromo-2-hydroxybenzylidene)pyridin-2-amine were characterized using IR spectroscopy. The results are presented in Table 20 and IR spectrum shown in Figure 50.

Table 20: Characteristic IR bands (cm^{-1}) for the complexes of *N*(5-bromo-2-hydroxybenzylidene)pyridin-2-amine

Complex code	Complex	*v*C=N	*v*C-O	*v*C=N (pyridine)	*v*(H_2O)	*v*(M-O)	*v*(M-N)
L3A	[CuL3.Cl.H_2O]	1587	1281	1098	888	511	477
L3B	[Ni(L3)$_2$.2H2O].2H_2O	1637	1280	1106	3269/879	451	427
L3C	[Co(L3)$_2$.2H2O]	1593	1285	1100	872	472	467

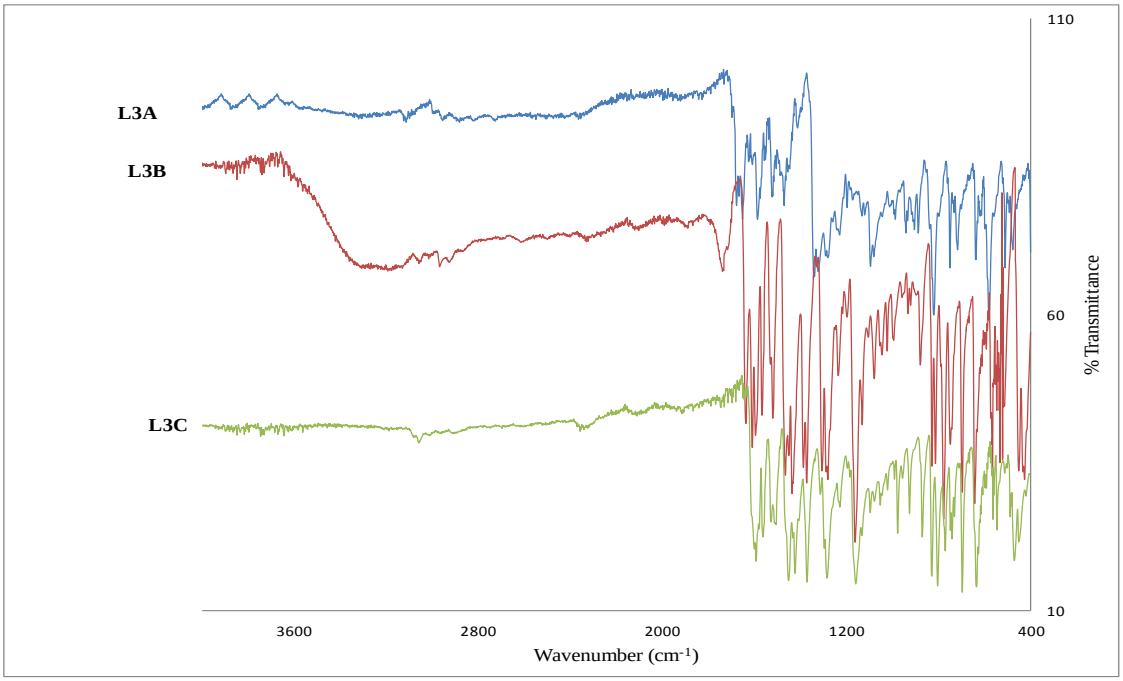

Figure 50: IR spectrum of *N*(5-bromo-2-hydroxybenzylidene)pyridin-2-amine complexes

4.5.12 Electronic absorption spectra of *N*(5-bromo-2-hydroxybenzylidene)pyridin-2-amine metal complexes

The electronic spectra recorded in 10^{-3} M solution *N*(5-bromo-2-hydroxybenzylidene)pyridin-2-amine metal complexes (**L3A-L3C**) in DMF are listed in Tables 21. The spectrum is shown in Figure 51.

Table 21: Electronic absorption bands and molar conductance for the complexes of *N*(5-bromo-2-hydroxybenzylidene)pyridin-2-amine

Complex code	Complex	λ_{max}(nm)	Assignment	Molar conductance ($ohm^{-1}cm^2mol^{-1}$)	Proposed Geometry
L3A	[CuL3 Cl H_2O]	283 349 425	π-π* n-π* d-d	6.80	Square planar
L3B	[Ni(L3)$_2$ 2H_2O].2H_2O	402 677	CT d-d	3.26	Octahedral
L3C	[Co(L3)$_2$ 2H_2O]	593 648	d-d d-d	3.71	Octahedral

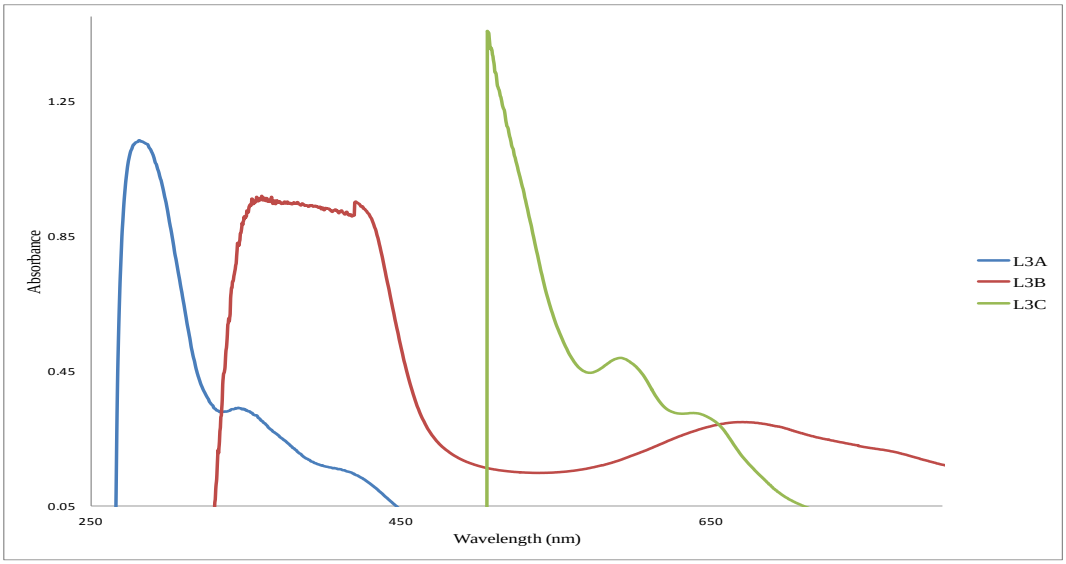

Figure 51: Electronic absorption spectrum of *N*(5-bromo-2-hydroxybenzylidene)pyridin-2-amine metal complexes in DMF.

4.5.13 Physical and analytical data of *N*(5-methoxy-2-hydroxybenzylidene)pyridin-2-amine complexes.

The physical and analytical data of the metal complexes of pure isolated *N*(5-methoxy-2-hydroxybenzylidene)pyridin-2-amine are presented in Table 22. The complexes were all obtained in moderate yield in the range 49-55%. The melting points were determined to be in the range 208- >349 ^{o}C. The elemental analysis data are within the acceptable range.

Table 22: Physical and analytical data for the complexes of *N*(5-methoxy-2-hydroxy benzylidene)pyridin-2-amine

Complex code	Molecular formular (M.wt. (g/mol))	mp: (^{o}C)	Yield (%)	Microanalysis % Calculated (Found)			
				C	H	N	M
L4A	$C_{15}H_{19}ClCuN_2O4$ (389)	208-209	53	46.16 (47.01)	4.91 (4.55)	7.18 (7.98)	16.28 (16.91)
L4B	$C_{26}H_{26}N_4NiO_6$ (549)	>349	55	56.86 (57.21)	4.77 (5.07)	10.69 (11.02)	10.20 (10.54)
L4C	$C_{26}H_{26}CoN_4O_6$ (549)	>349	49	56.84 (55.96)	4.77 (3.90)	10.20 (10.15)	10.73 (11.08)

M.wt. = molecular weight; mp = Melting point

4.5.14. Infrared spectra of *N*(5-methoxy-2-hydroxybenzylidene)pyridin-2-amine metal complexes

The Cu(II), Ni(II) and Co(II) complexes of *N*(5-methoxy-2-hydroxybenzylidene)pyridin-2-amine were characterized using IR spectroscopy. The results are presented in Table 23 and IR spectrum shown in Figure 52.

Table 23: Characteristic IR bands (cm^{-1}) for the complexes of *N*(5-methoxy-2-hydroxybenzylidene)pyridin-2-amine

Complex code	Complex	*v*C=N	*v*C-O	*v*C=N (pyridine)	*v*(H_2O)	*v*(M-O)	*v*(M-N)
L4A	[CuL4 Cl.H_2O].C_2H_5OH	1607	1285	1054	843	549	534
L4B	[Ni$(L4)_2$].2H_2O	1617	1292	1056	-	487	426
L4C	[Co$(L4)_2$ .2H_2O]	1616	1269	1059	848	627	571

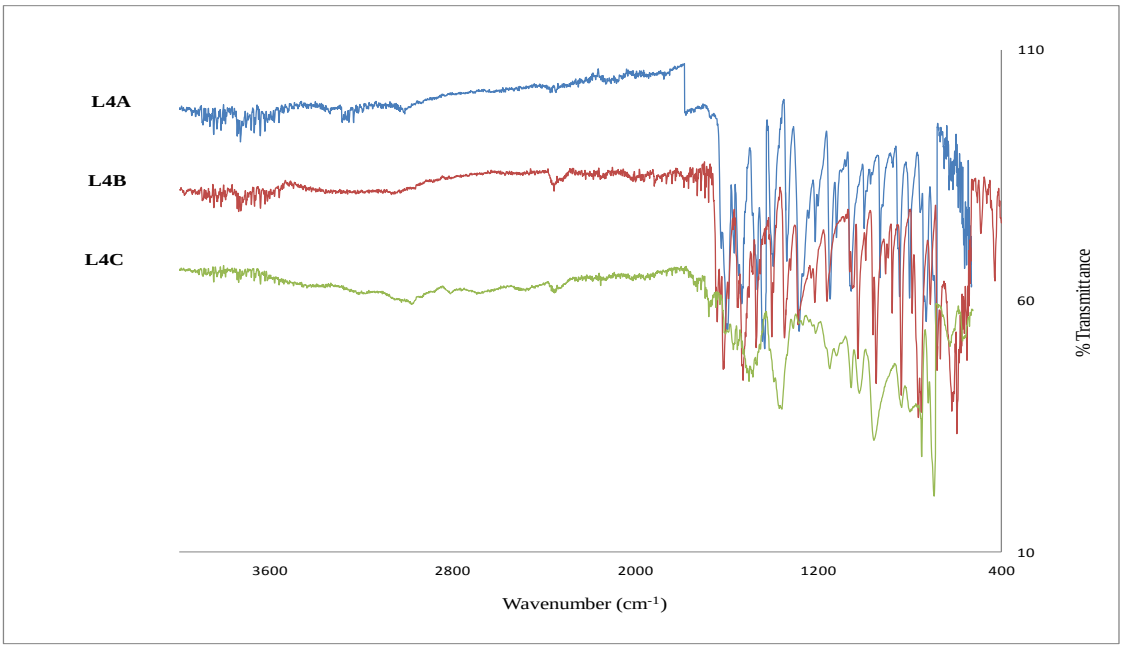

Figure 52: IR spectrum of *N*(5-methoxy-2-hydroxybenzylidene)pyridin-2-amine complexes

4.5.15 Electronic absorption spectra of *N*(5-methoxy-2-hydroxybenzylidene)pyridin-2-amine metal complexes

The electronic spectra recorded in 10^{-3} M solution *N*(5-methoxy-2-hydroxybenzylidene) pyridin-2-amine metal complexes (**L4A-L4C**) in DMF are listed in Tables 24. The spectrum is shown in Figure 53. .

Table 24: Electronic absorption bands and molar conductance for the complexes of *N*(5-methoxy-2-hydroxybenzylidene)pyridin-2-amine

Complex code	Complex	λ_{max}(nm)	Assignment	Molar conductance ($ohm^{-1}cm^2mol^{-1}$)	Proposed Geometry
L4A	[CuL4 Cl.H_2O].C_2H_5OH	280 311 430	π-π* n-π* d-d	8.4	Square Planar
L4B	[Ni(L4)$_2$].2H_2O	300 385 454	n-π* CT d-d	3.9	Square planar
L4C	[Co(L4)$_2$ .2H_2O]	606 673	d-d d-d	3.3	Octahedral

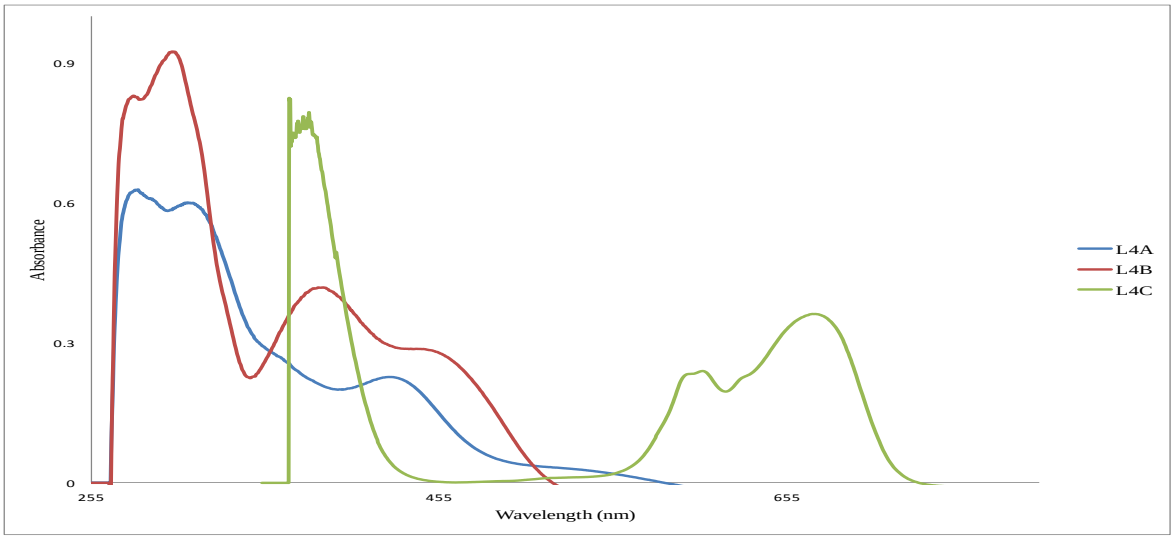

Figure 53: Electronic absorption spectrum of *N*(5-methoxy-2-hydroxybenzylidene)pyridin-2-amine metal complexes in DMF.

4.5.16 Physical and analytical data of *N*(2-hydroxybenzylidene)pyridin-4-amine complexes.

The physical and analytical data of the metal complexes of pure isolated *N*(2-hydroxybenzylidene)pyridin-4-amine are presented in Table 25. The complexes were all obtained in moderate to good yields in the range 49-60%. The melting points were determined to be in the range 244-303 ^{o}C. The elemental analysis support the structural formula deduce for each complex.

Table 25: Physical and analytical data for the complexes of *N*(2-hydroxybenzylidene) pyridin-4-amine

Complex code	Complex (M.wt. (g/mol))	mp (^{o}C)	Yield (%)	Microanalysis % Calculated (Found)			
				C	H	N	M
L5A	$C_{12}H_{11}ClCuN_2O_2$ (314)	244 (dec.)	60	45.87 (46.32)	3.53 (3.00)	8.92 (8.40)	20.22 (20.74)
L5B	$C_{24}H_{22}N_4NiO_4$ (488)	265 (dec.)	49	58.93 (59.31)	4.53 (3.88)	11.45 (11.11)	12.00 (13.54)
L5C	$C_{24}H_{22}CoN_4O_4$ (489)	298-303	54	58.90 (60.64)	4.53 (4.02)	11.45 (10.81)	12.04 (13.17)

M.wt. = molecular weight; mp = Melting point

4.5.17 Infrared spectra of *N*(2-hydroxybenzylidene)pyridin-4-amine complexes

The Cu(II), Ni(II) and Co(II) complexes of *N*(2-hydroxybenzylidene)pyridin-4-amine were characterized using IR spectroscopy. The results are presented in Table 26 and IR spectrum shown in Figure 54.

Table 26: Characteristic IR bands (cm^{-1}) for the complexes of *N*(2-hydroxybenzylidene) pyridin-4-amine

Complex code	Complex	*v*C=N	*v*C-O	*v*C=N (pyridine)	*v*(H_2O)	*v*(M-O)	*v*(M-N)
L5A	[CuL5.Cl.H_2O]	1581	1372	1058	869	528	489
L5B	[Ni(L5)$_2$.2H2O]	1591	1319	1054	867	529	485
L5C	[Co(L5)$_2$.2H2O]	1590	1319	1056	866	445	414

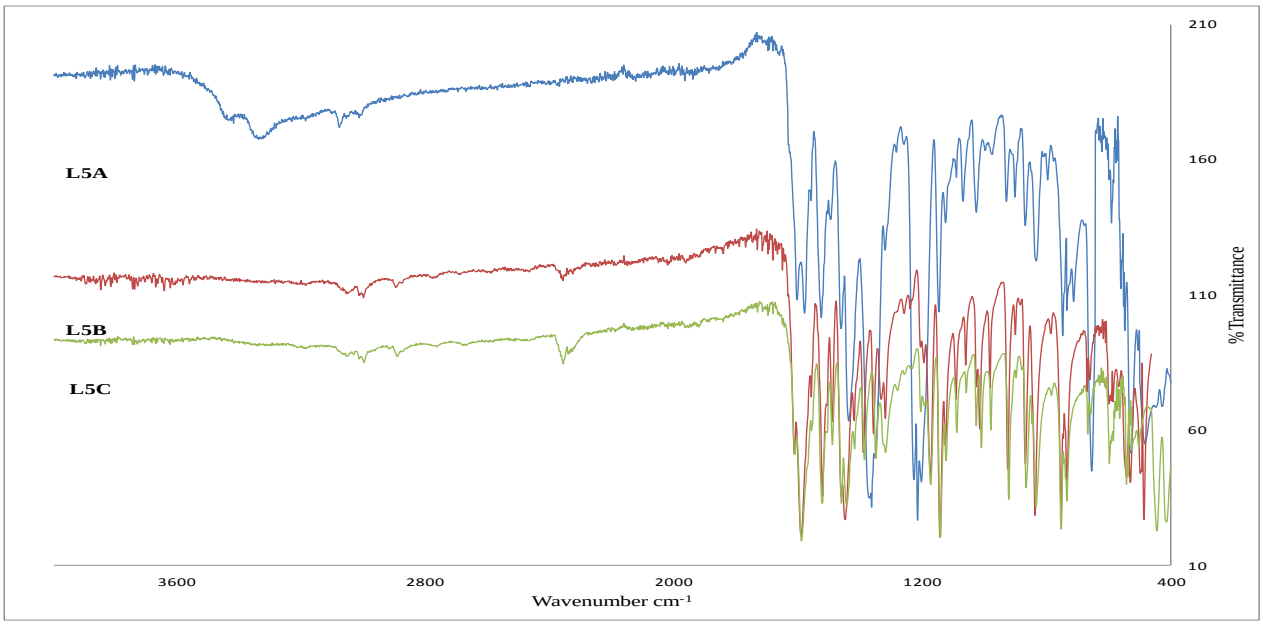

Figure 54: IR spectrum of *N*(2-hydroxybenzylidene)pyridin-4-amine complexes

4.5.18 Electronic absorption spectra of *N*(2-hydroxybenzylidene)pyridin-4-amine metal complexes

The electronic spectra recorded in 10^{-3} M solution *N*(2-hydroxybenzylidene)pyridin-4-amine metal complexes (**L5A-L5C**) in DMF are listed in Table 27. The spectrum is shown in Figure 55. .

Table 27: Electronic absorption bands and molar conductance for the complexes of *N*(2-hydroxybenzylidene)pyridin-4-amine

Complex code	Complex	λ_{max}(nm)	Assignment	Molar conductance ($ohm^{-1}cm^2mol^{-1}$)	Proposed Geometry
L5A	[CuL5.Cl.H_2O]	272 329 401	π-π* n-π* d-d	4.24	Square planar
L5B	[Ni(L5)$_2$.2H2O]	561 677	d-d	1.94	Octahedral
L5C	[Co(L5)$_2$.2H2O]	656	d-d	2.20	Octahedral

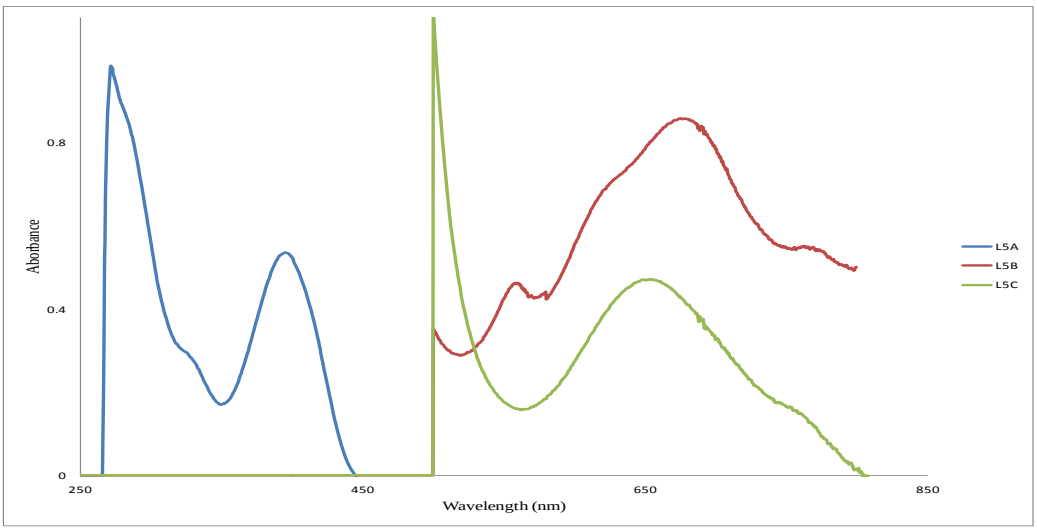

Figure 55: Electronic absorption spectrum of *N*(2-hydroxybenzylidene)pyridin-4-amine metal complexes in DMF.

4.5.19 Physical and analytical data of *N*(5-nitro-2-hydroxybenzylidene)pyridin-4-amine complexes.

The physical and analytical data of the metal complexes of pure isolated *N*(5-nitro-2-hydroxybenzylidene)pyridin-4-amine are presented in Table 28. The complexes were all obtained in moderate yield in the range 39-58%. The melting points were determined to be in the range 248- >349 ^{o}C. The elemental analysis support the structural formula deduce for each complex.

Table 28: Physical and analytical data for the complexes of *N*(5-nitro-2-hydroxy benzylidene)pyridin-4-amine

Complex code	Complex (M.wt. (g/mol))	mp (^{o}C)	Yield (%)	Microanalysis % Calculated (Found)			
				C	H	N	M
L6A	$C_{12}H_{10}ClCuN_3O_4$ (359)	>349	39	40.12 (40.07)	2.81 (2.61)	11.70 (10.78)	17.69 (18.19)
L6B	$C_{24}H_{26}N_6NiO_8$ (542)	296-299	52	53.07 (54.93)	2.97 (3.02)	15.47 (14.76)	10.81 (10.23)
L6C	$C_{24}H_{20}CoN_6O_8$ (579)	248-251	58	49.75 (50.26)	3.48 (3.02)	14.51 (15.15)	10.17 (9.71)

M.wt. = molecular weight; mp = Melting point

4.5.20 Infrared spectra of *N*(5-nitro-2-hydroxybenzylidene)pyridin-4-amine complexes

The Cu(II), Ni(II) and Co(II) complexes of *N*(5-nitro-2-hydroxybenzylidene)pyridin-4-amine were characterized using IR spectroscopy. The results are presented in Table 29 and IR spectrum shown in Figure 56.

Table 29: Characteristic IR bands (cm^{-1}) for the complexes of *N*(5-nitro-2-hydroxybenzylide

ne)pyridin-4-amine

Complex code	Complex	*v*C=N	*v*C-O	*v*C=N (pyridine)	*v*(H_2O)	*v*(M-O)	*v*(M-N)
L6A	[CuL6.Cl.H_2O]	1597	1373	1087	850	482	444
L6B	[Ni($L6)_2$]	1651	1291	1082	-	507	461
L6C	[Co($L6)_2$.2H_2O]	1597	1335	1084	855	490	428

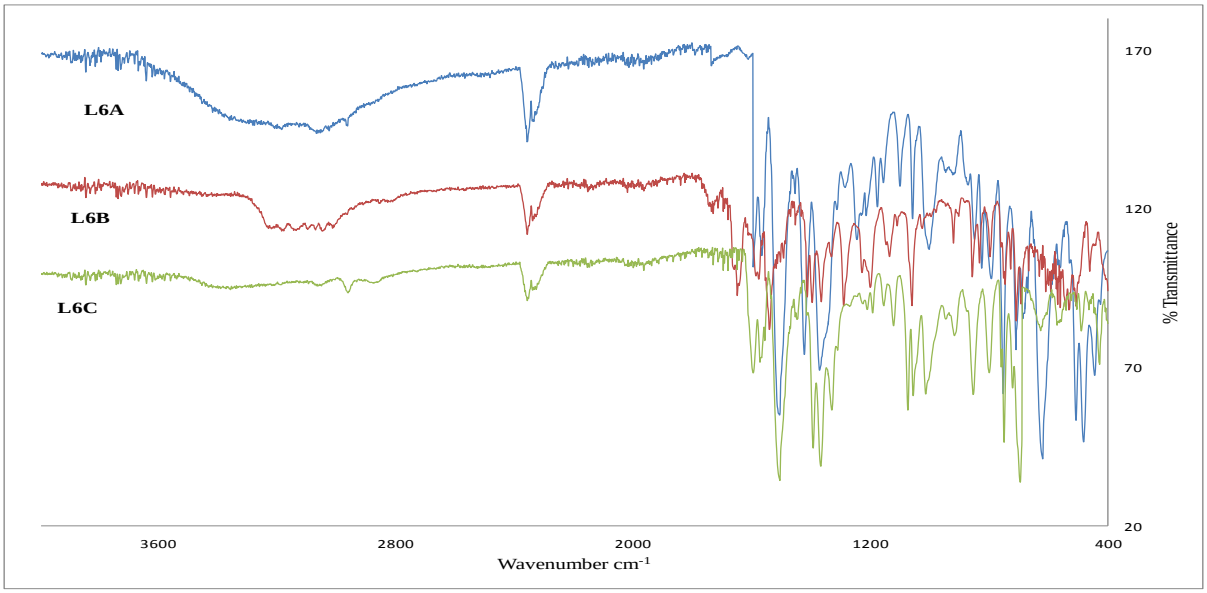

Figure 56: IR spectrum of *N*(5-nitro-2-hydroxybenzylidene)pyridin-4-amine complexes

4.5.21 Electronic absorption spectra of *N*(5-nitro-2-hydroxybenzylidene)pyridin-4-amine metal complexes

The electronic spectra recorded in 10^{-3} M solution *N*(5-nitro-2-hydroxybenzylidene)pyridin -4-amine metal complexes (**L6A-L6C**) in DMF are listed in Tables 30. The spectrum is shown in Figure 57. .

Table 30: Electronic absorption bands and molar conductance for the complexes of *N*(5-nitro-2-hydroxybenzylidene)pyridin-4-amine

Complex code	Complex	λ_{max}(nm)	Assignment	Molar conductance ($ohm^{-1}cm^2mol^{-1}$)	Proposed Geometry
L6A	[CuL6.Cl.H_2O]	286, 331, 412	π-π* n-π* d-d	3.60	Square planar
L6B	[Ni(L6)$_2$]	402	d-d	3.83	Square planar
L6C	[Co(L6)$_2$.2H_2O]	558	d-d	2.10	Octahedral

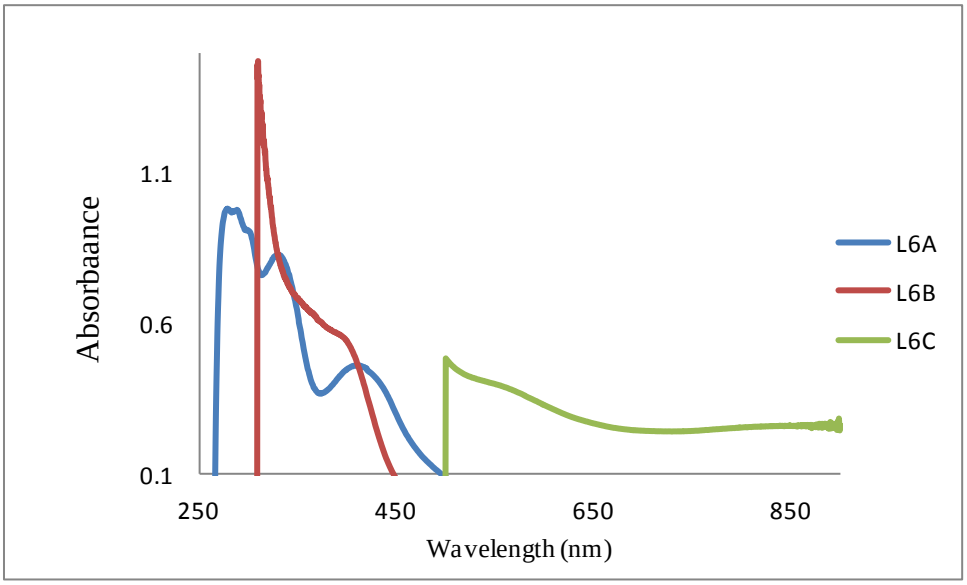

Figure 57: Electronic absorption spectrum of *N*(5-nitro-2-hydroxybenzylidene)pyridin-4-amine metal complexes in DMF.

4.5.22 Physical and analytical data of *N*(5-bromo-2-hydroxybenzylidene)pyridin-4-amine complexes.

The physical and analytical data of the metal complexes of pure isolated *N*(5-bromo-2-hydroxybenzylidene)pyridin-4-amine are presented in Table 31. The complexes were all obtained in moderate yield in the range 59-66%. The melting points were determined to be in

the range 248- >349 ^{o}C. The elemental analysis support the structural formula deduce for each complex.

Table 31: Physical and analytical data for the complexes of *N*(5-bromo-2-hydroxy benzylidene)pyridin-4-amine

Complex code	Complex (M.wt (g/mol))	mp(^{o}C)	Yield (%)	Microanalysis % Calculated (Found)			
				C	H	N	M
L7A	$C_{12}H_{10}BrClCuN_2O_2$ (393)	248 (dec)	59	36.66 (38.49)	2.56 (2.17)	7.13 (6.63)	16.16 (16.00)
L7B	$C_{24}H_{16}Br_2N_4NiO_2$ (607)	300-303	63	47.18 (46.49)	2.64 (2.67)	9.17 (8.48)	9.61 (9.80)
L7C	$C_{24}H_{24}Br_2CoN_4O_6$ (683)	>349	66	42.19 (41.54)	3.54 (2.79)	8.20 (7.56)	8.63 (8.51)

M.wt = molecular weight; mp = Melting point

4.5.23 Infrared spectra of *N*(5-bromo-2-hydroxybenzylidene)pyridin-4-amine complexes

The Cu(II), Ni(II) and Co(II) complexes of *N*(5-bromo-2-hydroxybenzylidene)pyridin-4-amine were characterized using IR spectroscopy. The results are presented in Table 32 and IR spectrum shown in Figure 58.

Table 32: Characteristic IR bands (cm^{-1}) for the complexes of *N*(5-bromo-2-hydroxybenzylidene)pyridin-4-amine

Complex code	Complex	*v*C=N	*v*C-O	*v*C=N (pyridine)	*v*(H_2O)	*v*(M-O)	*v*(M-N)
L7A	[CuL7.Cl.H_2O]	1598	1279	1080	874	464	439
L7B	[Ni($L7)_2$]	1596	1319	1079	-	453	428
L7C	[Co($L7)_2$.2H2O].2H_2O	1597	1279	1081	870	523	429

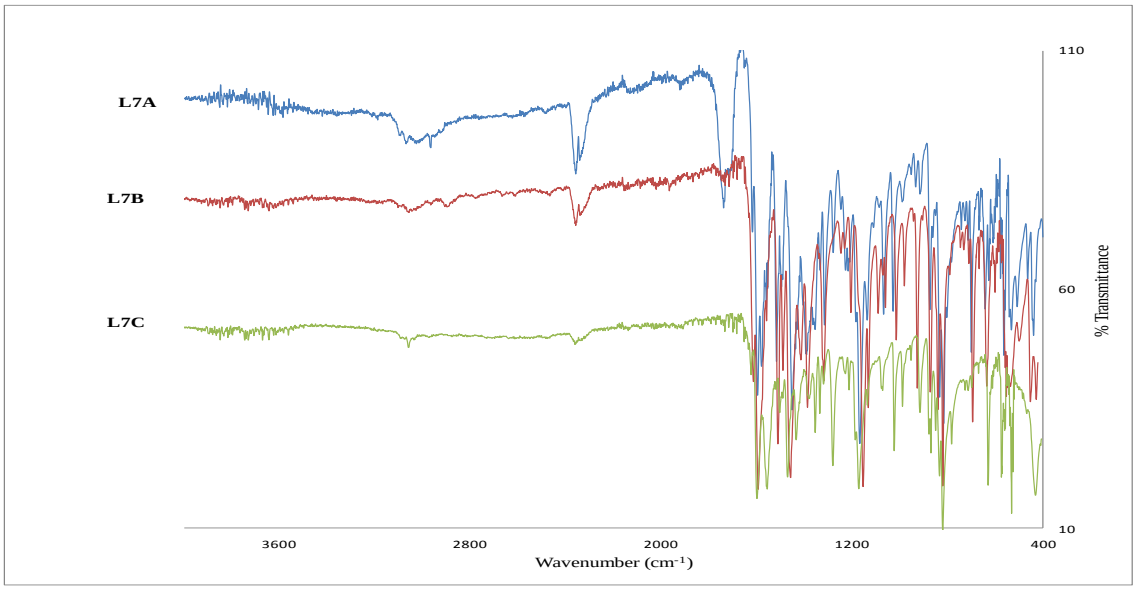

Figure 58: IR spectrum of *N*(5-bromo-2-hydroxybenzylidene)pyridin-4-amine complexes

4.5.24 Electronic absorption spectra of *N*(5-bromo-2-hydroxybenzylidene)pyridin-4-amine metal complexes

The electronic spectra recorded in 10^{-3} M solution *N*(5-bromo-2-hydroxybenzylidene)pyridin-4-amine metal complexes (**L7A-L7C**) in DMF are listed in Tables 33. The spectrum is shown in Figure 59.

Table 33: Electronic absorption bands and molar conductance for the complexes of *N*(5-bromo-2-hydroxybenzylidene)pyridin-4-amine

Complex code	Complex	λ_{max}(nm)	Assignment	Molar conductance ($ohm^{-1}cm^{2}mol^{-1}$)	Proposed Geometry
L7A	[CuL7.Cl.H_2O]	280 334 424	π-π* n-π* d-d	3.92	Square planar
L7B	[Ni$(L7)_2$]	274 424	π-π* d-d	1.75	Square planar
L7C	[Co$(L7)_2$ $2H_2O$].$2H_2O$	742	d-d	2.18	Octahedral

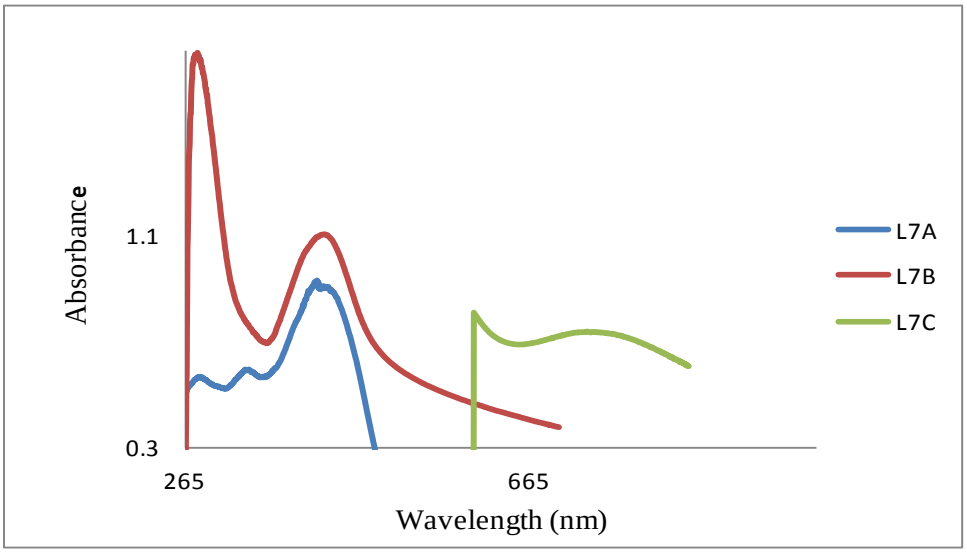

Figure 59: Electronic absorption spectrum of *N*(5-bromo-2-hydroxybenzylidene)pyridin-4-amine metal complexes in DMF.

4.5.25 Physical and analytical data of *N*-(2-hydroxybenzylidene)isonicotinohydrazide metal complexes.

The physical and analytical data of the metal complexes of *N*-(2-hydroxybenzylidene) isonicotinohydrazide are presented in Table 34. The complexes were all obtained in moderate to good yield in the range 54-63%. The melting points were determined to be >349 ^{o}C. The elemental analysis data is in agreement with the molecular formula suggested for each metal complex.

Table 34: Physical and analytical data for the complexes of *N*-(2-hydroxybenzylidene) isonicotinohydrazide

Complex code	Complex (M.wt. (g/mol))	mp (^{o}C)	Yield(%)	Microanalysis % Calculated (Found)			
				C	H	N	M
L8A	$C_{26}H_{2O}CuN_6O_9$ (633)	>349	54	49.25 (49.79)	4.77 (4.74)	13.25 (13.08)	10.02 (10.85)
L8B	$C_{13}H_{20}ClN_3NiO_7$ (423)	>349	61	36.79 (37.21)	4.75 (4.15)	9.90 (10.07)	13.88 (11.57)
L8C	$C_{13}H_{18}ClCoN_3O_6$ (406)	>349	63	38.39 (38.11)	4.46 (3.71)	10.33 (10.28)	14.49 (14.09)

M.wt. = molecular weight; mp = Melting point

4.5.26 Infrared spectra of *N*-(2-hydroxybenzylidene)isonicotinohydrazide complexes

The Cu(II), Ni(II) and Co(II) complexes of the *N*-(2-hydroxybenzylidene) isonicotinohydrazide were characterized using IR spectroscopy. The results are presented in Table 35. Representative IR spectrum is shown in Figure 60.

Table 35: Characteristic IR bands (cm^{-1}) for the complexes of *N*-(2-hydroxybenzylidene) isonicotinohydrazide

Complex code	Complex	$\nu(H_2O)$	νN-H	νC=O	νC=N	νC-O	ν(M-O)	ν(M-N)
L8A	$[Cu(L8]_2.5H_2O$	-	3000	-	1602	1300	498	466
L8B	$[NiL8.3H_2O].Cl.2H_2O$	3366		-	1595	1277	495	463
L8C	$[CoL8.3H_2O].Cl.H_2O$	-	3013	1738	1598	1285	508	464

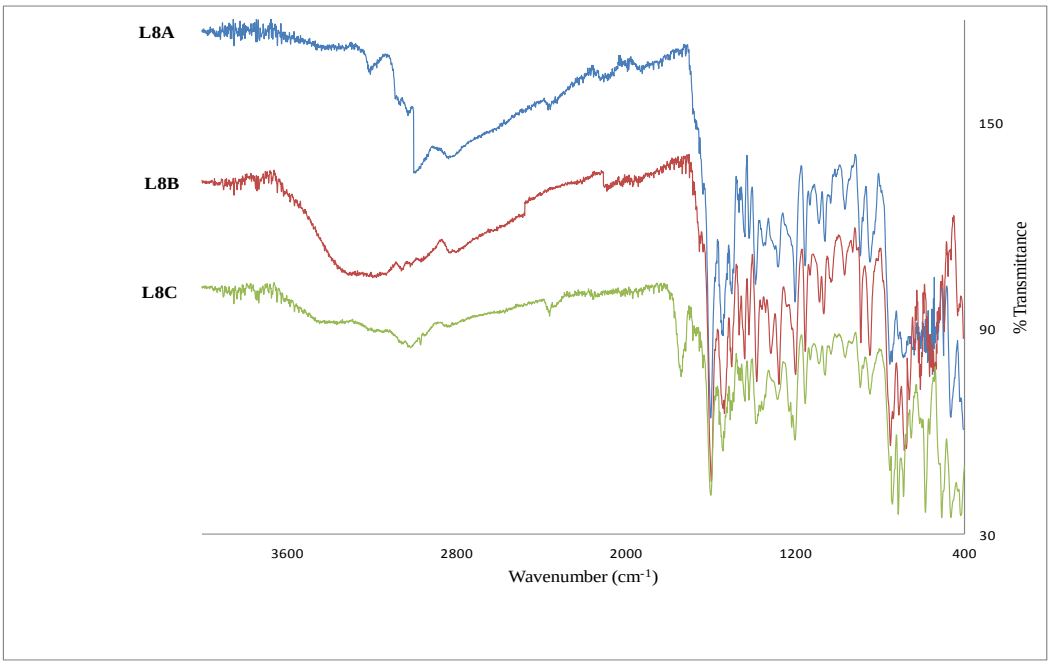

Figure 60: IR spectrum of *N*-(2-hydroxybenzylidene)isonicotinohydrazide complexes

4.5.27 Electronic absorption spectra of *N*-(2-hydroxybenzylidene)isonicotinohydrazide metal complexes

The electronic spectra recorded in 10^{-3} M solution *N*-(2-hydroxybenzylidene)isonicotino hydrazide metal complexes (**L8A-L8C**) in DMF are listed in Table 36. The spectrum is shown in Figure 61.

Table 36: Electronic absorption bands and molar conductance for the complexes of *N*-(2-hydroxybenzylidene)isonicotinohydrazide

Complex code	Complex	λ_{max}(nm)	Assignment	Molar conductance ($ohm^{-1}cm^2mol^{-1}$)	Proposed Geometry
L8A	$[Cu(L8)_2].5H_2O$	361, 425, 466	n-π* d-d d-d	2.64	Octahedral
L8B	$[NiL8.3H_2O].Cl.2H_2O$	300, 330, 420	π-π* n-π* d-d	37.20	Octahedral
L8C	$[CoL8.3H_2O].Cl.H_2O$	324, 397, 447 (sh), 468(sh)	n-π* CT d-d d-d	45.31	Octahedral

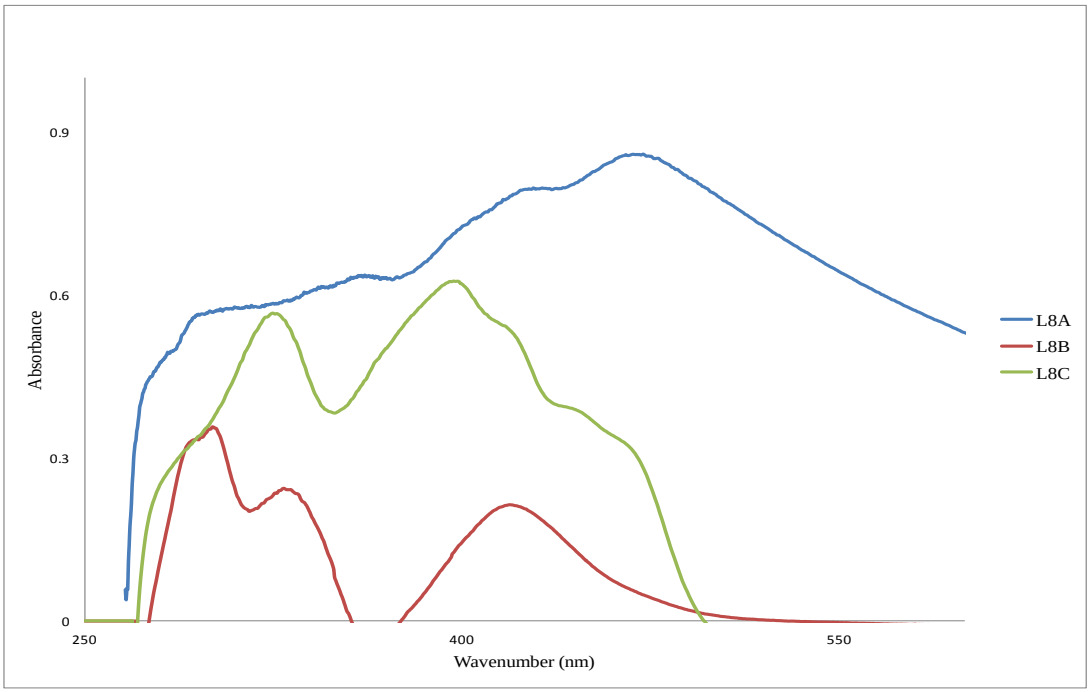

Figure 61: Electronic absorption spectrum of *N*-(2-hydroxybenzylidene)isonicotino hydrazide metal complexes in DMF.

4.5.28 Physical and analytical data of *N*-(5-nitro-2-hydroxybenzylidene)isonicotino hydrazide metal complexes

The physical and analytical data of the metal complexes of *N*-(5-nitro-2-hydroxybenzylidene) isonicotinohydrazide are presented in Table 37. The complexes were all obtained in moderate to good yield in the range 56-66%. The melting points were determined to be >349 ^{o}C. The elemental analysis data is in agreement with the molecular formula suggested for each metal complex.

Table 37: Physical and analytical data for the complexes of *N*-(5-nitro-2-hydroxybenzylidene)isonicotinohydrazide

Complex code	Complex (M.wt. (g/mol))	mp (^{o}C)	Yield (%)	Microanalysis % Calculated (Found)			
				C	H	N	M
L9A	$C_{26}H_{26}CuN_8O_{12}$ (705)	>349	66	44.23 (44.16)	3.70 (2.40)	15.87 (15.23)	9.00 (9.91)
L9B	$C_{13}H_{17}ClN_4NiO_8$ (451)	>349	56	34.59 (34.86)	3.80 (3.40)	12.41 (12.38)	13.00 (12.85)
L9C	$C_{26}H_{24}CoN_8O_{11}$ (683)	>349	65	45.69 (45.70)	3.54 (3.12)	16.40 (16.00)	8.62 (8.72)

M.wt. = molecular weight; mp = Melting point

4.5.29 Infrared spectra of *N*-(5-nitro-2-hydroxybenzylidene)isonicotinohydrazide complexes

The Cu(II), Ni(II) and Co(II) complexes of the *N*-(5-nitro-2-hydroxybenzylidene) isonicotinohydrazide were characterized using IR spectroscopy. The results are presented in Table 38. Representative IR spectrum is shown in Figure 62.

Table 38: Characteristic IR bands (cm^{-1}) for the complexes of *N*-(5-nitro-2-hydroxybenzylidene) isonicotinohydrazide

Complex code	Complex	$\nu(H_2O)$	νN-H	νC=O	νC=N	νC-O	ν(M-O)	ν(M-N)
L9A	$[Cu(L9)_2].4H_2O$	-	3066	-	1602	1321	467	446
L9B	$[NiL9.3H_2O].Cl.H_2O$	3358	3050	-	1595	1269	587	517
L9C	$[Co(L9)_2].3H_2O$	-	3067	-	1595	1296	511	456

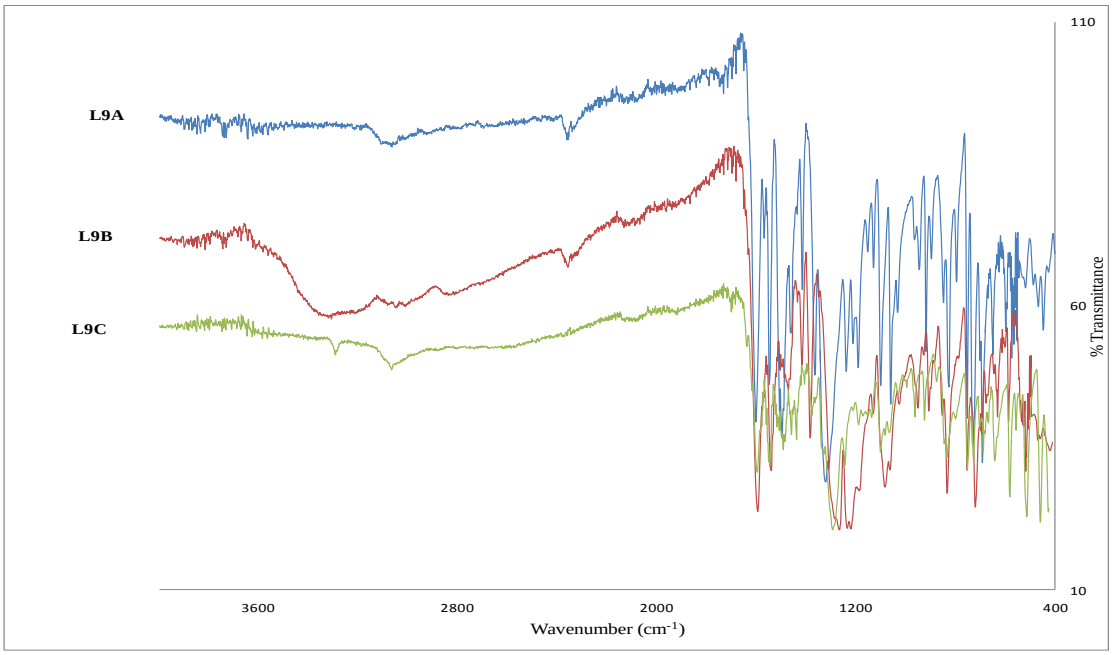

Figure 62: IR spectrum of *N*-(5-nitro-2-hydroxybenzylidene) isonicotinohydrazide Complexes

4.5.30 Electronic absorption spectra of *N*-(2-hydroxybenzylidene)isonicotinohydrazide metal complexes

The electronic spectra recorded in 10^{-3} M solution *N*-(2-hydroxybenzylidene)isonicotino hydrazide metal complexes (**L9A-L9C**) in DMF are listed in Table 39. The spectrum is shown in Figure 63.

Table 39: Electronic absorption bands and molar conductance for the complexes of *N*-(5-nitro-2-hydroxybenzylidene) isonicotinohydrazide

Complex code	Complex	λ_{max}(nm)	Assignment	Molar conductance ($ohm^{-1}cm^2mol^{-1}$)	Proposed Geometry
L9A	$[Cu(L9)_2].4H_2O$	300, 318, 459	π-π* n-π* d-d	3.75	Octahedral
L9B	[NiL9.3H2O].Cl.H_2O	283, 331, 410	π-π* n-π* d-d	48.20	Octahedral
L9C	$[Co(L9)_2].3H_2O$	363(sh), 430	n-π* d-d	2.44	Octahedral

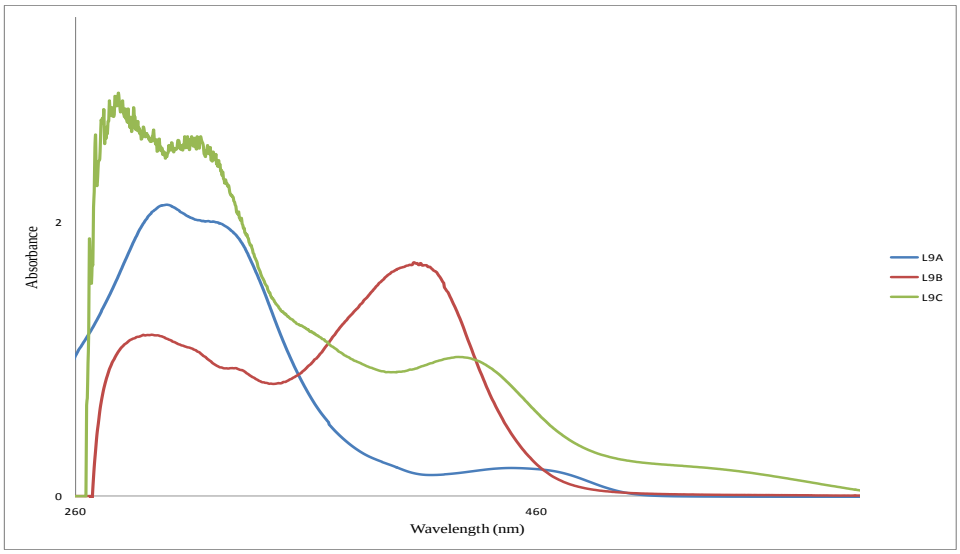

Figure 63: Electronic absorption spectrum of *N*-(5-nitro-2-hydroxybenzylidene) isonicotinohydrazide metal complexes in DMF.

4.5.31 Physical and analytical data of *N*-(5-bromo-2-hydroxybenzylidene)isonicotino hydrazide metal complexes.

The physical and analytical data of the metal complexes of *N*-(5-bromo-2-hydroxybenzylidene)isonicotinohydrazide are presented in Table 40. The complexes were all obtained in moderate to good yield in the range 51-60%. The melting points were determined to be in the range 254-317 ^{o}C. The elemental analysis data is in agreement with the molecular formula suggested for each metal complex.

Table 40: Physical and analytical data for the complexes of *N*-(5-bromo-2-hydroxybenzylidene) isonicotinohydrazide

Complex code	Complex (M.wt (g/mol))	mp(^{o}C)	Yield (%)	Microanalysis % Calculated (Found)			
				C	H	N	M
L10A	$C_{26}H_{26}Br_2CuN_6O_8$ (774)	313-317	58	40.35 (40.00)	3.39 (2.43)	10.86 (10.57)	8.21 (8.81)
L10B	$C_{13}H_{13}BrClN_3NiO_4$ (449)	307-309	51	34.75 (35.95)	2.92 (3.29)	9.35 (9.45)	13.06 (13.27)
L10C	$C_{26}H_{18}Br_2CoN_6O_4$ (697)	254 -257	60	44.79 (45.63)	2.60 (3.57)	12.05 (12.54)	8.45 (8.51)

M.wt = molecular weight; mp = Melting point

4.5.32 Infrared spectra of *N*-(5-bromo-2-hydroxybenzylidene)isonicotinohydrazide complexes

The Cu(II), Ni(II) and Co(II) complexes of the *N*-(5-bromo-2-hydroxybenzylidene) isonicotinohydrazide were characterized using IR spectroscopy. The results are presented in Table 41 and IR spectrum is shown in Figure 64

Table 41: Characteristic IR bands (cm^{-1}) for the complexes of *N*-(5-bromo-2-hydroxybenzylidene) isonicotinohydrazide

Complex code	Complex	$\nu(H_2O)$	νN-H	νC=O	νC=N	νC-O	ν(M-O)	ν(M-N)
L10A	$[Cu(L10)_2].4H_2O$	-	3049	-	1597	1285	541	483
L10B	$[NiL10.Cl.2H_2O]$	3320	-	-	1592	1272	622	495
L10C	$[Co(L10)_2]$	-	3015	-	1598	1288	508	464

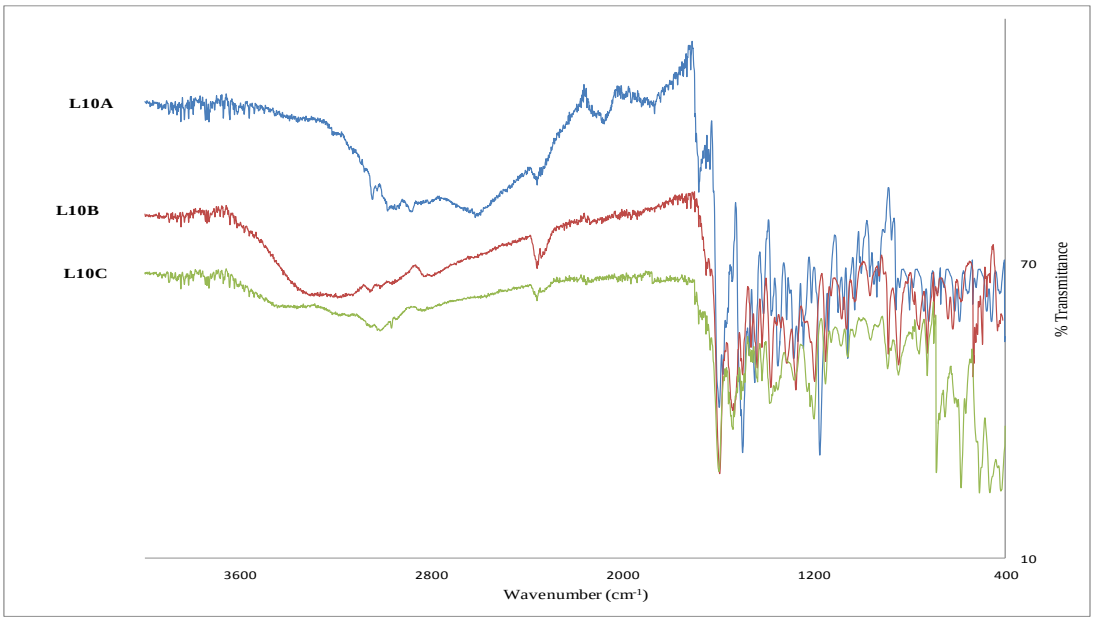

Figure 64: IR spectrum of *N*-(5-bromo-2-hydroxybenzylidene) isonicotinohydrazide complexes

4.5.33 Electronic absorption spectra of *N*-(5-bromo-2-hydroxybenzylidene)isonicotino hydrazide metal complexes

The electronic spectra recorded in 10^{-3} M solution *N*-(5-bromo-2-hydroxy benzylidene)isonicotinohydrazide metal complexes (**L10A-L10C**) in DMF are listed in Table 42. The spectrum is shown in Figure 65.

Table 42: Electronic absorption bands and molar conductance for the complexes of *N*-(5-bromo-2-hydroxybenzylidene)isonicotinohydrazide

Complex code	Complex	λ_{max}(nm)	Assignment	Molar conductance ($ohm^{-1}cm^2mol^{-1}$)	Proposed Geometry
L10A	$[Cu(L10)_2].4H_2O$	282, 336, 427	π-π* n-π* d-d	6.42	Octahedral
L10B	$[NiL10.Cl.2H_2O]$	284, 338, 447	π-π* n-π* d-d	6.17	Octahedral
L10C	$[Co(L10)_2]$	289, 383, 438, 467	π-π* CT d-d d-d	2.80	Octahedral

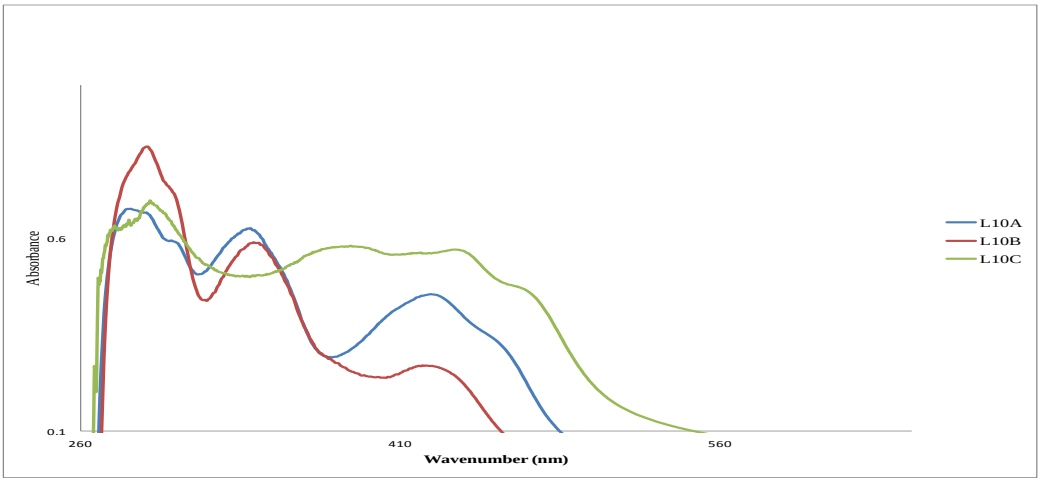

Figure 65: Electronic absorption spectrum of *N*-(5-bromo-2-hydroxybenzylidene) isonicotinohydrazide metal complexes in DMF.

4.5.34 Physical and analytical data of *N*-(5-methoxy-2-hydroxybenzylidene)isonicotino hydrazide metal complexes.

The physical and analytical data of the metal complexes of *N*-(5-methoxy-2-hydroxybenzylidene)isonicotinohydrazide are presented in Table 43. The complexes were all obtained in moderate to good yield in the range 45-68%. The melting points were determined to be in the range >349 ^{o}C. The elemental analysis data is in agreement with the molecular formula suggested for each metal complex.

Table 43: Physical and analytical data for the complexes of *N*-(5-methoxy-2-hydroxybenzylidene) isonicotinohydrazide

Complex code	Complex (M.wt. (g/mol))	mp (^{o}C)	Yield (%)	Microanalysis % Calculated (Found)			
				C	H	N	M
L11A	$C_{28}H_{32}CuN_6O_{10}$ (675)	>349	45	49.74 (49.68)	4.77 (3.96)	12.43 (12.20)	9.40 (8.89)
L11B	$C_{14}H_{22}ClN_3NiO_8$ (453)	>349	63	37.00 (37.79)	4.88 (4.54)	9.25 (9.19)	12.91 (13.40)
L11C	$C_{14}H_{14}ClCoN_3O_4$ (382)	>349	68	43.94 (43.88)	3.69 (3.88)	10.98 (10.91)	15.40 (15.12)

M.wt. = molecular weight; mp = Melting point

4.5.35 Infrared spectra of *N*-(5-methoxy-2-hydroxybenzylidene)isonicotinohydrazide complexes

The Cu(II), Ni(II) and Co(II) complexes of the *N*-(5-methoxy-2-hydroxybenzylidene) isonicotinohydrazide were characterized using IR spectroscopy. The results are presented in Table 44 and IR spectrum is shown in Figure 66.

Table 44: Characteristic IR bands (cm^{-1}) for the complexes of *N*-(5-methoxy-2-hydroxybenzylidene) isonicotinohydrazide

Complex code	Complex	$\nu(H_2O)$	νN-H	νC=O	νC=N	νC-O	ν(M-O)	ν(M-N)
L11A	$[Cu(L11)_2].4H_2O$	3333	3054	1677	1616	1287	601	488
L11B	$[NiL11.3H_2O].Cl.H_2O$	3334	-	-	1601	1272	510	479
L11C	$[Co(L11).Cl].H_2O$	-	3018	1677	1615	1278	597	498

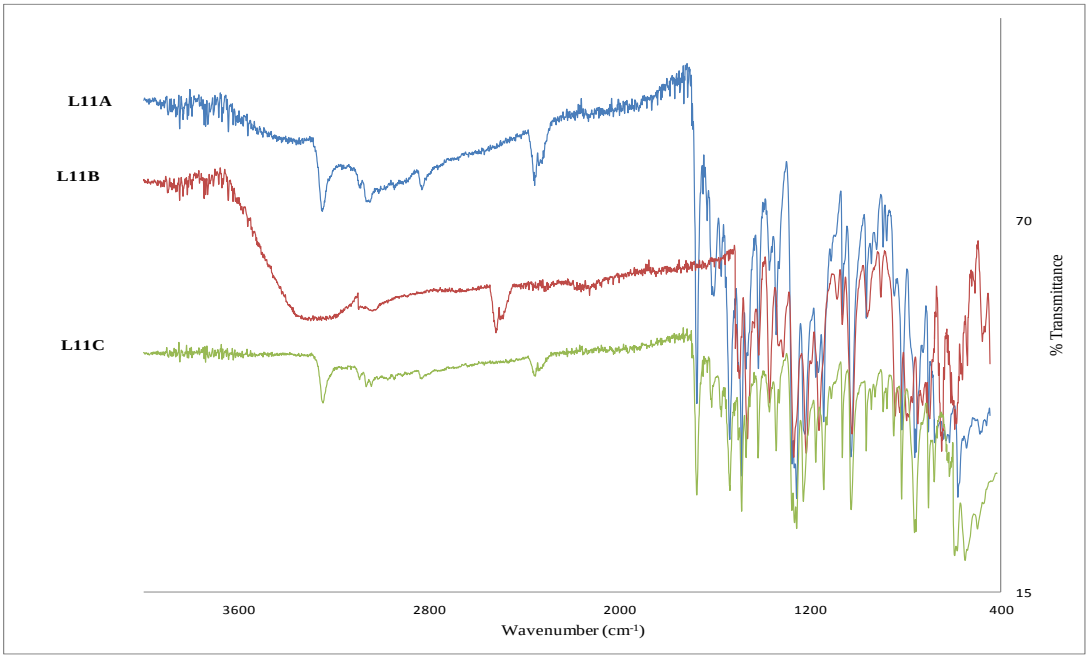

Figure 66: IR spectrum of *N*-(5-methoxy-2-hydroxybenzylidene) isonicotinohydrazide complexes

4.5.36 Electronic absorption spectra of *N*-(5-methoxy-2-hydroxybenzylidene) isonicotinohydrazide metal complexes

The electronic spectra recorded in 10^{-3} M solution *N*-(5-methoxy-2-hydroxy benzylidene)isonicotinohydrazide metal complexes (**L11A-L11C**) in DMF are listed in Table 45. The spectrum is shown in Figures 67.

Table 45: Electronic absorption bands and molar conductance for the complexes of *N*-(5-methoxy-2-hydroxybenzylidene)isonicotinohydrazide

Complex code	Complex	λ_{max}(nm)	Assignment	Molar conductance ($ohm^{-1}cm^2mol^{-1}$)	Proposed Geometry
L11A	$[Cu(L11)_2].4H_2O$	281, 366, 506	π-π* n-π* d-d	3.10	Octahedral
L11B	$[NiL11.3H_2O].Cl.H_2O$	293, 347, 441	π-π* n-π* d-d	35.85	Octahedral
L11C	$[Co(L11).Cl].H_2O$	338, 466	n-π* d-d	2.42	Tetrahedral

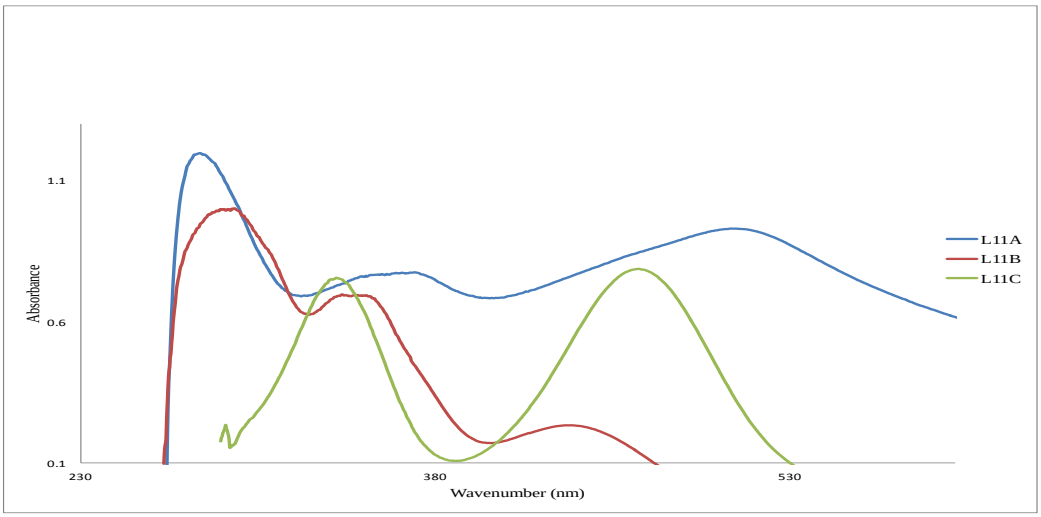

Figure 67: Electronic absorption spectrum of *N*-(5-methoxy-2-hydroxybenzylidene) isonicotinohydrazide metal complexes in DMF.

4.5.37 Physical and analytical data of (E)-N^1 ((1H-pyrrol-2-yl)methylene)isonicotinohydrazide metal complexes

The physical and analytical data of the metal complexes of (E)-N^1 ((1H-pyrrol-2-yl)methylene)isonicotinohydrazide are presented in Table 46. The complexes were all obtained in moderate to excellent yield in the range 49-81%. The melting points were determined to be in the range 265- >349 ^oC. The elemental analysis data is in agreement with the molecular formula suggested for each metal complex.

Table 46: Physical and analytical data for the complexes of (E)-N^1 ((1H-pyrrol-2-yl)methylene)isonicotinohydrazide

Complex code	Complex (M.wt. (g/mol))	mp (^oC)	Yield (%)	Microanalysis % Calculated (Found)			
				C	H	N	M
L12A	$C_{11}H_{12}CuN_4O_{2.5}$ (338)	>349	81	38.95 (39.28)	3.57 (3.32)	16.52 (15.94)	18.73 (18.29)
L12B	$C_{22}H_{19}N_8NiO_{2.5}$ (502)	265 (dec)	49	53.47 (53.22)	3.88 (3.86)	22.68 (22.19)	11.88 (10.97)
L12C	$C_{22}H_{20}CoN_8O_3$ (503)	298-303	54	52.49 (52.48)	4.00 (3.95)	22.26 (21.70)	11.71 (11.32)

M.wt. = molecular weight; mp = Melting point

4.5.38 Infrared spectra of (E)-N^1 ((1H-pyrrol-2-yl)methylene)isonicotinohydrazide complexes

The Cu(II), Ni(II) and Co(II) complexes of the (E)-N^1 ((1H-pyrrol-2-yl) methylene)isonicotinohydrazide were characterized using IR spectroscopy. The results are presented in Table 47 and IR spectrum is shown in Figure 68.

Table 47: Characteristic IR bands (cm^{-1}) for the complexes of (E)-N^1 ((1H-pyrrol-2-yl)methylene)isonicotinohydrazide

Complex code	Complex	*v*C=O	*v*C=N	*v*(>C=N-N=C<)	*v*C=N (py)	*v*(M-O)	*v*(M-N)
L12A	[Cu(L12)].0.5H_2O		1588	1518	1413	689	596
L12B	[Ni(L12)2].0.5H_2O	-	1603	1533	1413	492	428
L12C	[Co(L12)2].H_2O	1740	1602	1528	1412	497	420

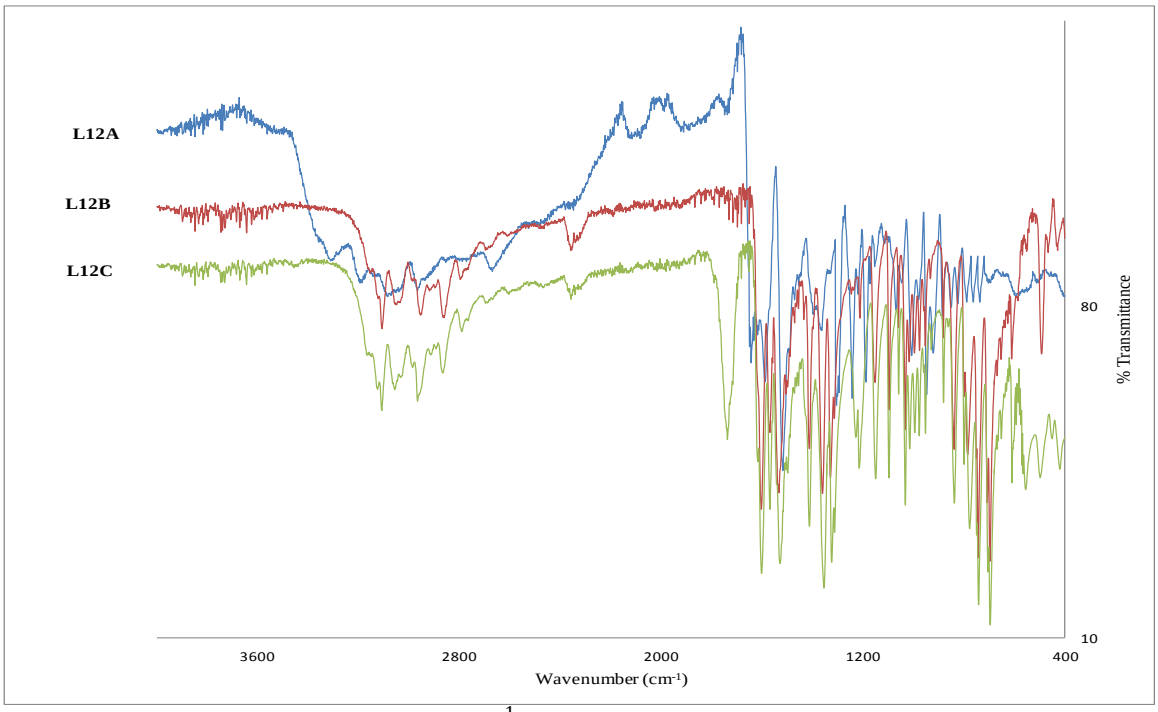

Figure 68: IR spectrum of (E)-N^1 ((1H-pyrrol-2-yl)methylene)isonicotinohydrazide complexes

4.5.39 Electronic absorption spectra of (E)-N^1 ((1H-pyrrol-2-yl)methylene)isonicotinohydrazide metal complexes

The electronic spectra recorded in 10^{-3} M solution (E)-N^1 ((1H-pyrrol-2-yl)methylene)isonicotinohydrazide metal complexes (**L12A-L12C**) in DMF are listed in Table 48. The spectrum is shown in Figure 69.

Table 48: Electronic absorption bands and molar conductance for the complexes of (E)-N^1 ((1H-pyrrol-2-yl)methylene)isonicotinohydrazide

Complex code	Complex	λ_{max}(nm)	Assignment	Molar conductance ($ohm^{-1}cm^2mol^{-1}$)	Proposed Geometry
L12A	$[Cu(L12).Cl.H_2O].0.5H_2O$	265 345 419 505	π-π* n-π* d-d d-d	2.91	Square planar
L12B	$[Ni(L12)_2].H_2O$	264, 310, 375, 479	π-π* n-π* CT d-d	3.14	Square planar
L12C	$[Co(L12)_2].H_2O$	310, 377, 424	n-π* CT d-d	3.76	Square planar

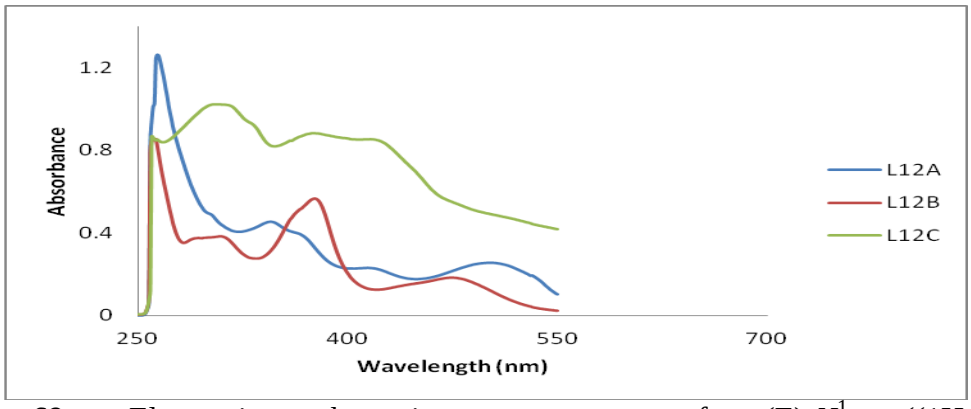

Figure 69: Electronic absorption spectrum of (E)-N^1 ((1H-pyrrol-2-yl)methylene)isonicotinohydrazide metal complexes in DMF.

4.5.40: Physical and analytical data of (E)-N^1 ((thiophen-2-yl)methylene)isonicotinohydrazide metal complexes

The physical and analytical data of the metal complexes of (E)-N^1 ((thiophen-2-yl)methylene)isonicotinohydrazideare pre sented in Table 49. The complexes were all obtained in good yield in the range 59-66%. The melting points were determined to be in the range 300- >349 ^{o}C. The elemental analysis data is in agreement with the molecular formula suggested for each metal complex.

Table 49: Physical and analytical data for the complexes of (E)-N^1 ((thiophen-2-yl)methylene)isonicotinohydrazide

Complex code	Complex (M.wt. (g/mol))	mp (^{o}C)	Yield (%)	Microanalysis % Calculated (Found)			
				C	H	N	M
13A	$C_{11}H_{12}ClCuN_3O_3S$ (364)	>349	59	36.17 (35.95)	3.31 (3.01)	11.50 (11.14)	17.40 (17.01)
13B	$C_{22}H_{22}N_6NiO_5S_2$ (572)	300-305	63	46.09 (46.57)	3.87 (3.57)	14.66 (14.55)	10.24 (10.72)
13C	$C_{22}H_{18}CoN_6O_3S_2$ (537)	>349	66	49.16 (49.37)	3.38 (3.10)	15.64 (15.41)	10.96 (10.38)

M.wt. = molecular weight; mp = Melting point

4.5.41 Infrared spectra of (E)-N^1 ((thiophen-2-yl)methylene)isonicotinohydrazide complexes

The Cu(II), Ni(II) and Co(II) complexes of the (E)-N^1 ((thiophen-2-yl)methylene)isonicotinohydrazide were characterized using IR spectroscopy. The results are presented in Table 50 and IR spectrum is shown in Figure 70.

Table 50: Characteristic IR bands (cm^{-1}) for the complexes of (E)-N^1 ((thiophen-2-yl)methylene)isonicotinohydrazide

Complex code	Complex	*v*C=O	*v*C=N	*v*(>C=N-N=C<)	*v*(M-O)	*v*(M-N)
L13A	$[Cu(L13).Cl.H_2O].H_2O$		1584	1595	548	470
L13B	$[Ni(L13)_2].3H_2O$	-	1584	1516	494	432
L13C	$[Co(L13)2].H_2O$	-	1582	1518	554	516

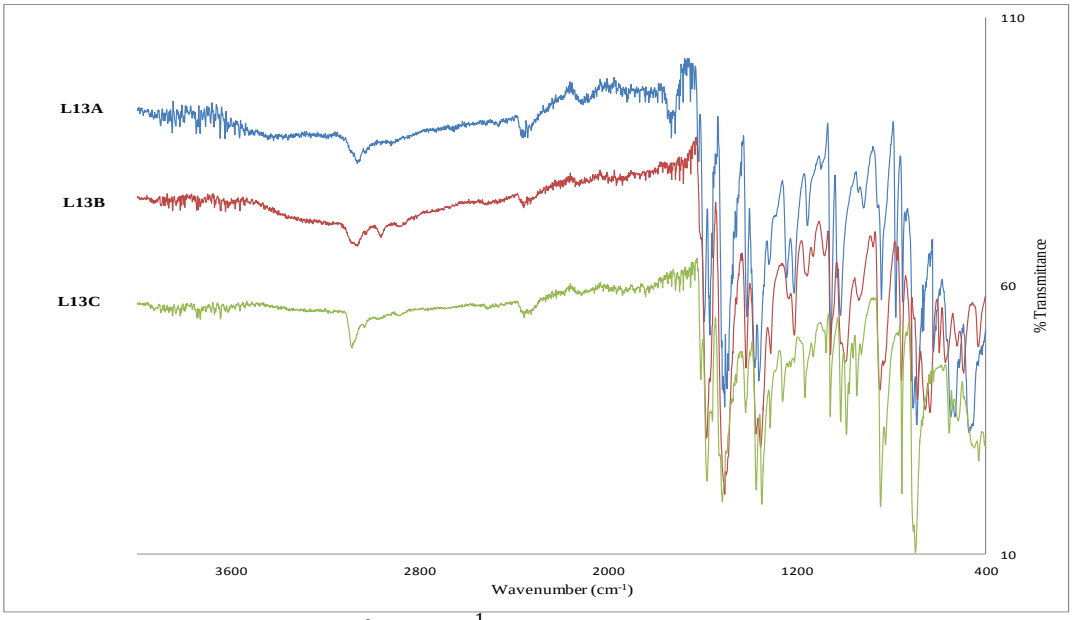

Figure 70: IR spectrum of (E)-N^1 ((thiophen-2-yl)methylene)isonicotinohydrazide complexes.

4.5.42 Electronic absorption spectra of (E)-N^1 ((thiophen-2-yl)methylene)isonicotinohydrazidemetal complexes

The electronic spectra recorded in 10^{-3} M solution (E)-N^1 ((thiophen-2-yl)methylene)isonicotinohydrazide metal complexes (**L13A-L13C**) in DMF are listed in Table 51. The spectrum is shown in Figure 71.

Table 51: Electronic absorption bands and molar conductance for the complexes of (E)-N^1 ((thiophen-2-yl)methylene)isonicotinohydrazide

Complex code	Complexes	λ_{max}(nm)	Assignment	Molar conductance ($ohm^{-1}cm^2mol^{-1}$)	Proposed Geometry
L13A	$[Cu(L13).Cl.H_2O].H_2O$	271, 329, 435	π-π* n-π* d-d	4.22	Square planar
L13B	$[Ni(L13)_2].3H_2O$	347 432 491	n-π* d-d d-d	3.80	Square planar
L13C	$[Co(L13)_2].H_2O$	345 390 429 493	n-π* CT d-d d-d	3.41	Square planar

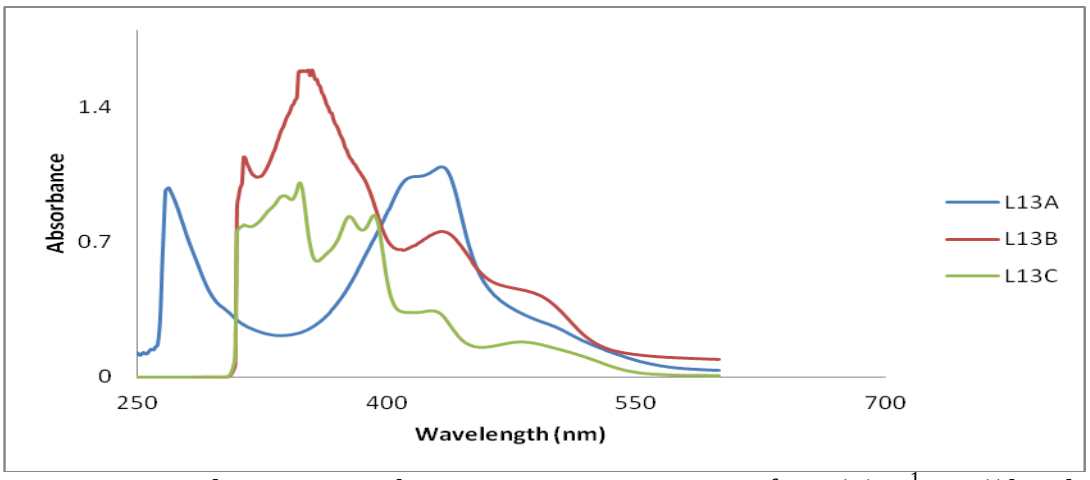

Figure 71: Electronic absorption spectrum of (E)-N^1 ((thiophen-2-yl)methylene)isonicotinohydrazide metal complexes in DMF.

Table 52: List of metal complexes obtained from Schiff bases **(L1-L13)**

Metal complexes of 2-aminopyridine Schiff bases		Metal complexes of 4-aminopyridine Schiff bases		Metal complexes of INH-Schiff bases	
L1A	[CuL1 Cl.H_2O].2H_2O	L5A	[CuL5.Cl.H_2O]	L8A	[Cu$(L8)_2$].5H_2O
L1B	[Ni$(L1)_2$].2H_2O	L5B	[Ni$(L5)_2$.2H2O]	L8B	[NiL8.3H_2O].Cl.2H_2O
L1C	[Co$(L1)_2$ 2H_2O]	L5C	[Co$(L5)_2$.2H2O]	L8C	[CoL8.3H_2O].Cl.H_2O
L2A	[CuL2 Cl H_2O].C_2H_5OH	L6A	[CuL6.Cl.H_2O]	L9A	[Cu$(L9)_2$].4H_2O
L2B	[Ni$(L2)_2$2H_2O].2H_2O	L6B	[Ni$(L6)_2$]	L9B	[NiL9.3H_2O].Cl.H_2O
L2C	[Co$(L2)_2$ 2H_2O].3H_2O	L6C	[Co$(L6)_2$.2H_2O]	L9C	[Co$(L9)_2$].3H_2O
L3A	[CuL3 Cl H_2O]	L7A	[CuL7.Cl.H_2O]	L10A	[Cu$(L10)_2$].4H_2O
L3B	[Ni$(L3)_2$ 2H_2O].2H_2O	L7B	[Ni$(L7)_2$]	L10B	[NiL10.Cl.2H_2O]
L3C	[Co$(L3)_2$ 2H_2O]	L7C	[Co$(L7)_2$ 2H_2O].2H_2O	L10C	[Co$(L10)_2$]
L4A	[CuL4 Cl H_2O].C_2H_5OH			L11A	[Cu$(L11)_2$].4H_2O
L4B	[Ni$(L4)_2$ 2H_2O]			L11B	[NiL11.3H_2O].Cl.2H_2O
L4C	[Co$(L4)_2$ 2H_2O]			L11C	[Co(L11).Cl].H_2O
				L12A	[Cu(L12).Cl.H_2O].0.5H_2O
				L12B	[Ni$(L12)_2$].0.5H_2O
				L12C	[Co$(L12)_2$].H_2O
				L13A	[Cu(L13).Cl.H_2O].H_2O
				L13B	[Ni$(L13)_2$].3H_2O
				L13C	[Co$(L13)_2$].H_2O

4.6 *In-vitro* anti-tuberculosis activity of the Schiff bases and their metal complexes

The *in-vitro* anti-tuberculosis activity of the investigated compounds was evaluated against *M.TB* H37Rv and clinical isolate at a concentration of 0.4-0.1 μg/ml on 10^{-2} and 10^{-4} CFU/ml of the strains. The results are are based on % critical proportion and presented in Tables 53-78.

When

$\%\, critical\ proportion \leq 1$, it signifies an active compound.

When

$\%\, critical\ proportion > 1$, it signifies an inactive compound.

The results of the 2-aminopyridine compounds presented in Tables 53-60 show that the unsubstituted ligand (**L1**) and its copper complex (**L1A**) exhibited no activity at all the concentrations against 10^{-2} and 10^{-4} CFU/ml of *M.TB* strains. However, its nickel (**L1B**) and cobalt(**L1C**) complexes showed activity at 0.2 µg/ml and 0.4 µg/ml on 10^{-4} CFU/ml of *M.TB* $H37R_V$ and clinical isolate. The nitro-containing ligand (**L2**) exhibited activity at all the concentrations used but its activity reduced (0.2 µg/ml) upon coordination to nickel (**L2B**) and cobalt (**L2C**) ions and increased (0.05 µg/ml) in the presence of copper ion (**L2A**) on 10^{-4} CFU/ml of *M.TB* $H37R_V$. Activity increased in the presence of metal ions against 10^{-4} CFU/ml of the clinical isolate at 0.2 µg/ml and 0.4 µg/ml for **L2A**, **L2C** and **L2B** respectively. The bromo substituted ligand (**L3**) and its copper (**L3A**) and cobalt (**L3C**) complexes showed no activity against 10^{-2} CFU/ml of *M.TB* $H37R_V$. However, their activities increased at 0.2 µg/ml and 0.4 µg/ml on 10^{-4} CFU/ml of *M.TB* $H37R_V$ respectively. The nickel complex (**L3B**) showed activity at 0.2 µg/ml and 0.1µg/ml on 10^{-2} and 10^{-4} CFU/ml of *M.TB* $H37R_V$ respectively. In addition, the copper (**L3A**) and cobalt (**L3C**) complexes showed activity against the clinical isolate at 0.4 µg/ml on 10^{-4}CFU/ml. Compound **L4** and its nickel complex exhibited the same level of activity. However, activity increased in the presence of copper (**L4A**) and cobalt (**L4C)** ions at 0.4 µg/ml and 0.1 µg/ml

against 10^{-2} and 10^{-4} CFU/ml of *M.TB* $H37R_V$ respectively. Both ligand L4 and its metal complexes displayed the same level of activity on the clinical isolate.

The 4-aminopyridine Schiff bases and their metal complexes (**L5A-L7C**) showed varying levels of activity as presented in Tables 61-64. The unsubstituted ligand (**L5**) and its nickel complex (**L5B**) showed no activity on both CFU/ml of *M.TB* $H37R_V$ at all the concentrations used. However, its copper (**L5A**) and cobalt (**L5C**) complexes exhibited activity at 0.4 and 0.2 μg/ml on 10^{-4} CFU/ml of *M.TB* $H37R_V$ respectively. None of the compounds showed activity against the clinical isolate at all the concentrations used. The nitro containing compound (**L6**) and its metal complexes showed the same level of activity. on 10^{-2} CFU/ml of *M.TB* $H37R_V$ at 0.2μg/ml. However, the activity enhanced at 0.1 μg/ml on 10^{-2} CFU/ml for copper (**L6A**) and cobalt(**L6C**) complexes. In addition, these complexes (**L6A** and **L6C**) displayed same level of activity as the ligand (**L6**) on the clinical isolate. The metal complexes of the bromo substituted ligand (**L7**) exhibited the same level of activity as the ligand at 0.4 μg/ml on 10^{-2} CFU/ml but the nickel (**L7B**) and cobalt (**L7C**) complexes showed increased activity at 0.2 μg/ml on 10^{-4} CFU/ml of *M.TB* $H37R_V$. None of the compounds showed activity on the clinical isolate.

INH compounds (**L8-L10C**) exhibited varying levels of activity at all the concentrations and strains used. Most of the compounds showed activity at 0.1 μg/ml on both CFU/ml of *M.TB* $H37R_V$. However, the unsubstituted ligand (**L8**), bromo substituted ligand (**L10**) and their nickel complexes (**L8C and L10C**) exhibited activity at 0.2 μg/ml. On the other hand, the copper complex (**L9A**) of the nitro containing ligand (**L9**) showed increased activity at 0.05 μg/ml. The methoxy substituted ligand (**L11**) showed no activity against the standard strain

at all the concentrations used. However, its activity increased in the presence of copper and cobalt ions at 0.4 and 0.2 μg/ml on both CFU/ml of *M.TB* $H37R_V$ respectively. Also, the compounds exhibited varying levels of activity against the clinical isolate. The unsubstituted ligand (**L8**) and its cobalt complex (**L8C**) exhibited activity at 0.4 μg/ml on 10^{-4} CFU/ml *M.TB* $H37R_V$. While its copper (**L8A**) and nickel(**L8B**) complexes showed activity at 0.2 and 0.4 μg/ml on both CFU/ml of *M.TB* $H37R_V$. The nitro containing compound (**L9**) exhibited no activity against the clinical isolate. However, its copper, nickel and cobalt complexes showed activity at 0.2, 0.4 and 0.1 μg/ml on 10^{-4} CFU/ml of clinical isolate respectively. The metal complexes of the bromo containing compounds showed activity at 0.2 μg/ml on both 10^{-2} and 10^{-4} CFU/ml of the clinical isolate. The activity of ligand **L11** remained the same in the presence of copper ion but increased in the presence of nickel and cobalt ion at 0.2 μg/ml against the clinical isolate.

The *in vitro* anti-tuberculosis activity of compound **L12**, the pyrrole containing ligand was observed at 0.2 and 0.4 μg/ml on 10^{-2} and 10^{-4} CFU/ml of *M.TB* $H37R_V$ respectively. The activity reduced to 0.4 μg/ml in the presence of copper ion and increased in the presence of nickel and cobalt ions to 0.05 μg/ml on 10^{-4} CFU/ml of *M.TB* $H37R_V$ respectively. Only the ligand (**L12**), its nickel(**L12B**) and cobalt(**L12C**) complexes showed activity at 0.4 0.2 and 0.2 μg/ml on the clinical isolate. The thiophene containing ligand **L13**, showed activity at 0.4 and 0.2 μg/ml against *M.TB* $H37R_V$. Its copper (**L13A**) and nickel (**L13B**) complexes showed no activity on 10^{-2} CFU/ml but activity was observed at 0.2 and 0.4 μg/ml on 10^{-4} CFU/ml respectively. Increased activity was observed in the presence of cobalt ion (**L13C**) at 0.2 and 0.1 μg/ml on 10^{-2} and 10^{-4} CFU/ml of *M.TB* $H37R_V$. The ligand and its nickel

complex exhibited activity at 0.4 µg/ml on 10^{-4} CFU/ml of the clinical isolate while the copper complex showed activity at 0.4 µg/ml on both CFU/ml. Activity increased in the presence of cobalt ion at 0.2 and 0.1 µg/ml on 10^{-2} and 10^{-4} CFU/ml of the clinical isolate respectively.

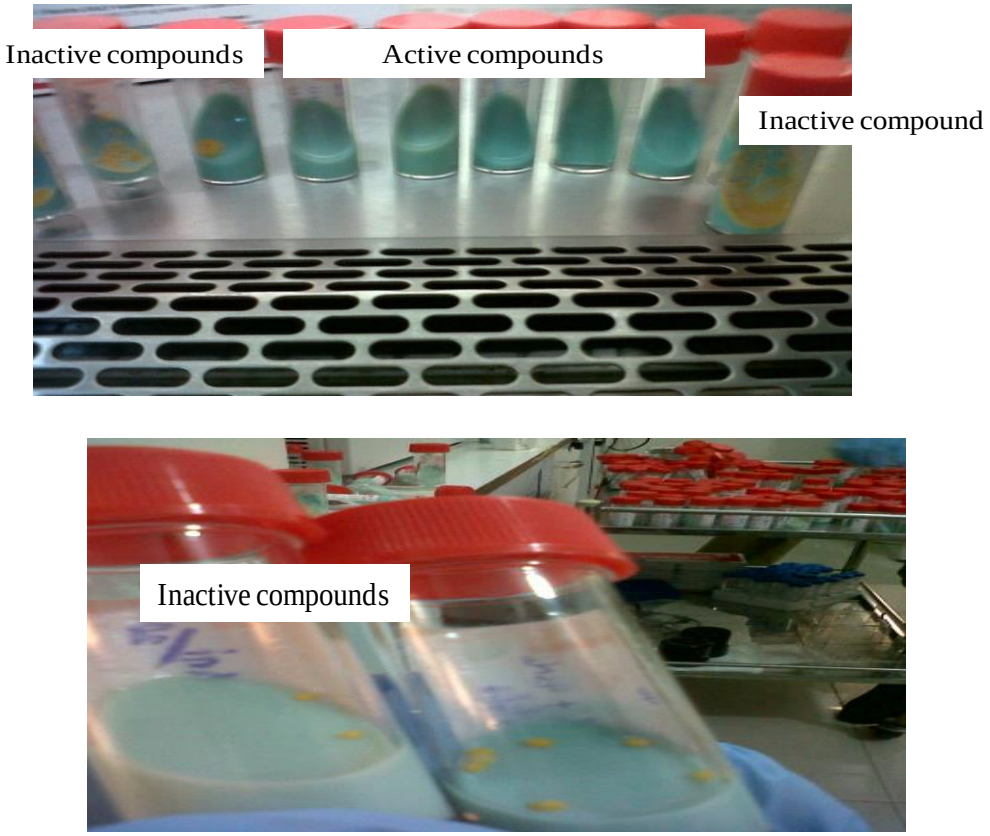

Figure 72: Representative LJ slopes showing the active and inactive compounds.

Table 53: *In vitro* anti-tuberculosis activity of *N*(2-hydroxybenzylidene)pyridin-2-amine and its metalcomplexes on *M.TB* H37Rv

Concentration(µg/ml)	Compound									
	LI		**LIA**		**L1B**		**L1C**		INH	
	10^{-2} y	10^{-4}	10^{-2}	10^{-4}	10^{-2}	10^{-4}	10^{-2}	10^{-4}	10^{-2}	10^{-4}
0.4	20 ± 0.47	2 ± 0.01	16 ± 0.36	2 ± 0.04	7 ± 0.38	0 ± 0.00	0 ± 0.00	0 ± 0.00	0 ± 0.00	0 ± 0.00
0.2	35 ± 0.16	3 ± 0.08	22 ± 0.43	2 ± 0.09	11 ± 0.47	0 ± 0.00	9 ± 0.47	0 ± 0.00	0 ± 0.00	0 ± 0.00
0.1	62 ± 1.53	7 ± 0.42	30 ± 0.49	5 ± 0.07	18 ± 0.67	2 ± 0.01	14± 0.66	0 ± 0.00	12 ± 0.47	8 ± 0.16

y = CFU/ml

Table 54: *In vitro* anti-tuberculosis activity of *N*(2-hydroxybenzylidene)pyridin-2-amine (**L1**) and its metal complexes on clinical isolate

Concentration (µg/ml)	Compound									
	LI		**LIA**		**L1B**		**L1C**		INH	
	10^{-2} y	10^{-4}	10^{-2}	10^{-4}	10^{-2}	10^{-4}	10^{-2}	10^{-4}	10^{-2}	10^{-4}
0.4	35 ± 0.64	33 ± 0.57	30 ± 0.47	14± 0.47	27 ± 0.40	0 ± 0.00	19 ± 0.17	0 ± 0.00	0 ± 0.00	0 ± 0.00
0.2	50 ± 1.21	51 ± 0.87	42 ± 0.79	26± 0.36	41 ± 0.73	12 ± 0.09	22 ± 0.26	10 ± 0.04	0 ± 0.00	0 ± 0.00
0.1	71 ± 1.55	58 ± 1.52	62 ± 2.51	30 ± 0.42	32 ± 0.47	19 ± 0.22	40 ± 0.66	18 ± 0.19	19 ± 0.55	15 ± 0.36

y = CFU/ml

Table 55: *In vitro* anti-tuberculosis activity of *N*(5-nitro-2-hydroxybenzylidene)pyridin-2-amine (**L2**) and its metal complexes on *M.TB* H37Rv

Concentration (µg/ml)	Compound									
	L2		**L2A**		**L2B**		**L2C**		INH	
	10^{-2} y	10^{-4}	10^{-2}	10^{-4}	10^{-2}	10^{-4}	10^{-2}	10^{-4}	10^{-2}	10^{-4}
0.4	0 ± 0.00	0 ± 0.00	0 ± 0.00	0 ± 0.00	0 ± 0.00	0 ± 0.00	0 ± 0.00	0 ± 0.00	0 ± 0.00	0 ± 0.00
0.2	0 ± 0.00	0 ± 0.00	0 ± 0.00	0 ± 0.00	0 ± 0.00	0 ± 0.00	0 ± 0.00	0 ± 0.00	0 ± 0.00	0 ± 0.00
0.1	0 ± 0.00	0 ± 0.00	0 ± 0.00	0 ± 0.00	8 ± 0.56	6 ± 0.33	6 ± 0.32	0 ± 0.00	12 ± 0.47	8 ± 0.16
0.05				0 ± 0.00						

y = CFU/ml

Table 56: *In vitro* anti-tuberculosis activity of *N*(5-nitro-2-hydroxybenzylidene)pyridin-2-amine (**L2**) and its metal complexes on clinical isolate

Concentration (µg/mL)	Compound									
	L2		**L2A**		**L2B**		**L2C**		INH	
	10^{-2} y	10^{-4}	10^{-2}	10^{-4}	10^{-2}	10^{-4}	10^{-2}	10^{-4}	10^{-2}	10^{-4}
0.4	15 ± 0.47	7 ± 0.09	10 ± 0.27	0 ± 0.00	12 ± 0.31	0 ± 0.00	9 ± 0.56	0 ± 0.00	0 ± 0.00	0 ± 0.00
0.2	21 ± 0.87	9 ± 0.55	20 ± 0.79	0 ± 0.00	18 ± 0.67	9 ± 0.55	18 ± 0.68	0 ± 0.00	0 ± 0.00	0 ± 0.00
0.1	32 ± 1.32	25 ± 0.91	17 ± 0.64	11 ± 0.31	24 ± 1.41	15 ± 0.45	23 ± 1.02	13 ± 0.36	19 ± 0.55	15 ± 0.36

y = CFU/ml

Table 57: *In vitro* anti-tuberculosis activity of *N*(5-bromo-2-hydroxybenzylidene)pyridin-2-amine (**L3**) and its metal complexes on *M.TB* H37Rv

Concentration (µg/mL)	Compound									
	L3		**L3A**		**L3B**		**L3C**		INH	
	10^{-2} y	10^{-4}	10^{-2}	10^{-4}	10^{-2}	10^{-4}	10^{-2}	10^{-4}	10^{-2}	10^{-4}
0.4	10 ± 0.28	0 ± 0.00	6 ± 0.16	0 ± 0.00	0 ± 0.00	0 ± 0.00	8 ± 0.17	0 ± 0.00	0 ± 0.00	0 ± 0.00
0.2	12 ± 0.30	0 ± 0.00	10 ± 0.25	0 ± 0.00	0 ± 0.00	0 ± 0.00	19 ± 0.45	2 ± 0.01	0 ± 0.00	0 ± 0.00
0.1	30 ± 0.71	6 ± 0.14	24 ± 0.67	2 ± 0.01	13 ± 0.33	0 ± 0.00	31 ± 0.30	2 ± 0.01	12 ± 0.47	8 ± 0.16

y = CFU/ml

Table 58: *In vitro* anti-tuberculosis activity of *N*(5-bromo-2-hydroxybenzylidene)pyridin-2-amine (**L3**) and its metal complexes on clinical isolate

Concentration (µg/mL)	Compound									
	L3		**L3A**		**L3B**		**L3C**		INH	
	10^{-2} y	10^{-4}	10^{-2}	10^{-4}	10^{-2}	10^{-4}	10^{-2}	10^{-4}	10^{-2}	10^{-4}
0.4	17 ± 0.67	19 ± 0.82	12 ± 0.45	0 ± 0.00	9 ± 0.18	10 ± 0.16	14 ± 0.47	0 ± 0.00	0 ± 0.00	0 ± 0.00
0.2	37 ± 1.52	20 ± 0.87	21 ± 0.96	8± 0.05	13 ± 0.44	17 ± 0.67	20 ± 0.84	12 ± 0.36	0 ± 0.00	0 ± 0.00
0.1	26 ± 1.16	20 ± 0.90	29 ± 1.21	16 ± 0.60	19 ± 0.84	20 ± 0.87	33 ± 1.44	16 ± 0.64	19 ± 0.55	15 ± 0.36

y = CFU/ml

Table 59: *In vitro* anti-tuberculosis activity of *N*(5-methoxy-2-hydroxybenzylidene)pyridin-2-amine (**L4**) and its metal complexes on *M.TB* H37Rv

Concentration (µg/mL)	Compound									
	L4		**L4A**		**L4B**		**L4C**		INH	
	10^{-2} y	10^{-4}	10^{-2}	10^{-4}	10^{-2}	10^{-4}	10^{-2}	10^{-4}	10^{-2}	10^{-4}
0.4	24 ± 0.28	0 ± 0.00	0 ± 0.00	0 ± 0.00	8 ± 0.18	0 ± 0.00	0 ± 0.00	0 ± 0.00	0 ± 0.00	0 ± 0.00
0.2	33 ± 0.47	6 ± 0.07	12 ± 0.18	0 ± 0.00	17 ± 0.22	6 ± 0.06	6 ± 0.09	0 ± 0.00	0 ± 0.00	0 ± 0.00
0.1	41 ± 0.62	10 ± 0.12	26 ± 0.36	4 ± 0.01	26 ± 0.33	8 ± 0.18	15 ± 0.20	8 ± 0.18	12 ± 0.47	8 ± 0.16

y = CFU/ml

Table 60: *In vitro* anti-tuberculosis activity of *N*(5-methoxy-2-hydroxybenzylidene)pyridin-2-amine (**L4**) and its metal complexes on clinical isolate

Concentration (µg/mL)	Compound									
	L4		**L4A**		**L4B**		**L4C**		INH	
	10^{-2} y	10^{-4}	10^{-2}	10^{-4}	10^{-2}	10^{-4}	10^{-2}	10^{-4}	10^{-2}	10^{-4}
0.4	8 ± 0.24	0 ± 0.00	6 ± 0.16	0 ± 0.00	9 ± 0.30	0 ± 0.00	5 ± 0.10	0 ± 0.00	0 ± 0.00	0 ± 0.00
0.2	19 ± 0.67	9 ± 0.28	11 ± 0.36	8 ± 0.20	18 ± 0.66	4 ± 0.08	8 ± 0.22	9 ± 0.28	0 ± 0.00	0 ± 0.00
0.1	25 ± 0.84	28 ± 0.87	14 ± 0.47	19 ± 0.67	30 ± 0.87	7 ± 0.18	19± 0.66	24± 0.80	19 ± 0.55	15 ± 0.36

y = CFU/ml

Table 61: *In vitro* anti-tuberculosis activity of *N*(2-hydroxybenzylidene)pyridin-4-amine (**L5**) and its metal complexes on *M.TB* H37Rv

Concentration (µg/mL)	Compound									
	L5		**L5A**		**L5B**		**L5C**		INH	
	10^{-2} y	10^{-4}	10^{-2}	10^{-4}	10^{-2}	10^{-4}	10^{-2}	10^{-4}	10^{-2}	10^{-4}
0.4	25 ± 0.37	7 ± 0.17	14± 0.28	0 ± 0.00	20 ± 0.36	7± 0.16	0 ± 0.00	0± 0.00	0 ± 0.00	0 ± 0.00
0.2	37± 0.40	13± 0.22	19 ± 0.33	9± 0.19	28 ± 0.37	14± 0.27	12 ± 0.09	0 ± 0.00	0 ± 0.00	0 ± 0.00
0.1	42 ± 0.42	17 ± 0.34	30± 0.39	13± 0.24	29 ± 0.37	19 ± 0.36	17 ± 0.35	11 ± 0.32	12 ± 0.47	8 ± 0.16

y = CFU/ml

Table 62: *In vitro* anti-tuberculosis activity of *N*(2-hydroxybenzylidene)pyridin-4-amine (**L5**) and its metal complexes on clinical isolate

Concentration (µg/mL)	Compound									
	L5		**L5A**		**L5B**		**L5C**		INH	
	10^{-2} y	10^{-4}	10^{-2}	10^{-4}	10^{-2}	10^{-4}	10^{-2}	10^{-4}	10^{-2}	10^{-4}
0.4	58 ± 1.50	50 ± 0.80	47 ± 0.66	35 ± 0.36	38 ± 0.16	41 ± 0.44	41± 0.18	31 ± 0.01	0 ± 0.00	0 ± 0.00
0.2	67 ± 1.55	50 ± 0.82	52 ± 0.88	49 ± 0.76	43 ± 0.51	49 ± 0.79	49 ± 0.79	47 ± 0.67	0 ± 0.00	0 ± 0.00
0.1	75 ± 3.00	56 ± 1.44	61 ± 1.51	52 ± 0.87	54 ± 1.21	54 ± 1.21	58 ± 1.52	49 ± 0.65	19 ± 0.55	15 ± 0.36

y = CFU/ml

Table 63: *In vitro* anti-tuberculosis activity of *N*(5-nitro-2-hydroxybenzylidene)pyridin-4-amine (**L6**) and its metal complexes on *M.TB* H37Rv

Concentration (µg/mL)	Compound									
	L6		**L6A**		**L6B**		**L6C**		INH	
	10^{-2} y	10^{-4}	10^{-2}	10^{-4}	10^{-2}	10^{-4}	10^{-2}	10^{-4}	10^{-2}	10^{-4}
0.4	0 ± 0.00	0 ± 0.00	0 ± 0.00	0 ± 0.00	0 ± 0.00	0 ± 0.00	0 ± 0.00	0 ± 0.00	0 ± 0.00	0 ± 0.00
0.2	20 ± 0.67	0 ± 0.00	14 ± 0.36	0 ± 0.00	20 ± 0.64	0 ± 0.00	18 ± 0.45	0 ± 0.00	0 ± 0.00	0 ± 0.00
0.1	25 ± 0.71	3 ± 0.01	17 ± 0.42	0 ± 0.00	20 ± 0.68	5 ± 0.09	20 ± 0.67	0 ± 0.00	12 ± 0.47	8 ± 0.16

y = CFU/ml

Table 64: *In vitro* anti-tuberculosis activity of *N*(5-nitro-2-hydroxybenzylidene)pyridin-4-amine (**L6**) and its metal complexes on clinical isolate

Concentration (µg/mL)	Compound									
	L6		**L6A**		**L6B**		**L6C**		INH	
	10^{-2} y	10^{-4}	10^{-2}	10^{-4}	10^{-2}	10^{-4}	10^{-2}	10^{-4}	10^{-2}	10^{-4}
0.4	33 ± 0.79	0 ± 0.00	9 ± 0.17	0 ± 0.00	12 ± 0.36	5 ± 0.07	10 ± 0.24	0 ± 0.00	0 ± 0.00	0 ± 0.00
0.2	48 ± 1.55	29 ± 0.66	23 ± 0.60	19 ± 0.47	25 ± 0.64	24 ± 0.58	31 ± 0.67	21 ± 0.48	0 ± 0.00	0 ± 0.00
0.1	50 ± 2.51	38 ± 0.82	44 ± 1.52	27 ± 0.66	40 ± 1.21	32 ± 0.77	38 ± 0.87	33 ± 0.78	19 ± 0.55	15 ± 0.36

y = CFU/ml

Table 65: *In vitro* anti-tuberculosis activity of *N*(5-bromo-2-hydroxybenzylidene)pyridin-4-amine (**L7**) and its metal complexes on *M.TB* H37Rv

Concentration (µg/mL)	Compound									
	L7		**L7A**		**L7B**		**L7C**		INH	
	10^{-2} y	10^{-4}	10^{-2}	10^{-4}	10^{-2}	10^{-4}	10^{-2}	10^{-4}	10^{-2}	10^{-4}
0.4	0 ± 0.00	0 ± 0.00	0 ± 0.00	0 ± 0.00	0 ± 0.00	0 ± 0.00	0 ± 0.00	0 ± 0.00	0 ± 0.00	0 ± 0.00
0.2	37 ± 1.21	4 ± 0.01	29 ± 0.45	20 ± 0.21	30 ± 0.67	0 ± 0.00	26 ± 0.38	0 ± 0.00	0 ± 0.00	0 ± 0.00
0.1	42 ± 1.41	7 0.04	36 ± 1.21	24 ± 0.36	42 ± 1.37	2± 0.01	32 ± 0.98	32 ± 0.87	12 ± 0.47	8 ± 0.16

y = CFU/ml

Table 66: *In vitro* anti-tuberculosis activity of *N*(5-bromo-2-hydroxybenzylidene)pyridin-4-amine (**L7**) and its metal complexes on clinical isolate

Concentration (µg/mL)	Compound									
	L7		**L7A**		**L7B**		**L7C**		INH	
	10^{-2} y	10^{-4}	10^{-2}	10^{-4}	10^{-2}	10^{-4}	10^{-2}	10^{-4}	10^{-2}	10^{-4}
0.4	56 ± 1.44	34 ± 0.36	36 ± 0.47	29 ± 0.28	24 ± 0.26	17 ± 0.18	18 ± 0.20	24 ± 0.27	0 ± 0.00	0 ± 0.00
0.2	66 ± 1.78	50 ± 1.10	41 ± 0.51	42 ± 0.67	33 ± 0.34	26 ± 0.28	57 ± 1.47	38 ± 0.49	0± 0.00	0 ± 0.00
0.1	71 41 ± 2.00	52 ± 1.21	59 ± 1.55	49 ± 0.98	51 ± 0.98	31 ± 0.31	69 ± 1.82	48 ± 0.82	19 ± 0.55	15 ± 0.36

y = CFU/ml

Table 67: *In vitro* anti-tuberculosis activity of *N*-(2-hydroxybenzylidene)isonicotinohydrazide (**L8**) and its metal complexes on *M.TB* H37Rv

Concentration (µg/mL)	Compound									
	L8		**L8A**		**L8B**		**L8C**		INH	
	10^{-2} y	10^{-4}	10^{-2}	10^{-4}	10^{-2}	10^{-4}	10^{-2}	10^{-4}	10^{-2}	10^{-4}
0.4	0 ± 0.00	0 ± 0.00	0 ± 0.00	0 ± 0.00	0 ± 0.00	0 ± 0.00	0± 0.00	0 ± 0.00	0 ± 0.00	0 ± 0.00
0.2	0 ± 0.00	0 ± 0.00	0 ± 0.00	0 ± 0.00	0 ± 0.00	0 ± 0.00	0 ± 0.00	0 ± 0.00	0 ± 0.00	0 ± 0.00
0.1	10± 0.62	3 ± 0.01	8 ± 0.60	0 ± 0.00	0± 0.00	0 ± 0.00	0 ± 0.00	0 ± 0.00	12 ± 0.47	8 ± 0.16

y = CFU/ml

Table 68: *In vitro* anti-tuberculosis activity of *N*-(2-hydroxybenzylidene)isonicotinohydrazide (**L8**) and its metal complexes on clinical isolate

Concentration (µg/mL)	Compound									
	L8		**L8A**		**L8B**		**L8C**		INH	
	10^{-2} y	10^{-4}	10^{-2}	10^{-4}	10^{-2}	10^{-4}	10^{-2}	10^{-4}	10^{-2}	10^{-4}
0.4	27 ± 0.67	0 ± 0.00	0 ± 0.00	0 ± 0.00	0 ± 0.00	0 ± 0.00	19 ± 0.35	0 ± 0.00	0 ± 0.00	0 ± 0.00
0.2	33 ± 0.98	29 ± 0.82	0 ± 0.00	0 ± 0.00	24 ± 0.47	22 ± 0.44	24 ± 0.49	10 ± 0.28	0 ± 0.00	0 ± 0.00
0.1	54 ± 1.53	38 ± 1.21	38 ± 1.24	16 ± 0.32	49 ± 1.44	12 ± 0.32	26 ± 0.58	18 ± 0.37	19 ± 0.55	15 ± 0.36

y = CFU/ml

Table 69: *In vitro* anti-tuberculosis activity of *N*-(5-nitro-2-hydroxybenzylidene)isonicotinohydrazide (**L9**) and its metal complexes on *M.TB* H37Rv

Concentration (µg/mL)	Compound									
	L9		**L9A**		**L9B**		**L9C**		INH	
	10^{-2} y	10^{-4}	10^{-2}	10^{-4}	10^{-2}	10^{-4}	10^{-2}	10^{-4}	10^{-2}	10^{-4}
0.4	0 ± 0.00	0 ± 0.00	0 ± 0.00	0 ± 0.00	0 ± 0.00	0 ± 0.00	0 ± 0.00	0 ± 0.00	0 ± 0.00	0 ± 0.00
0.2	0 ± 0.00	0 ± 0.00	0 ± 0.00	0 ± 0.00	0 ± 0.00	0 ± 0.00	0 ± 0.00	0 ± 0.00	0 ± 0.00	0 ± 0.00
0.1	0 ± 0.00	0 ± 0.00	0 ± 0.00	0 ± 0.00	0 ± 0.00	0 ± 0.00	0 ± 0.00	0 ± 0.00	12 ± 0.47	8 ± 0.16
0.05								0 ± 0.00		

y = CFU/ml

Table 70: *In vitro* anti-tuberculosis activity of *N*-(5-nitro-2-hydroxybenzylidene)isonicotinohydrazide (**L9**) and its metal complexes on clinical isolate

Concentration (µg/mL)	Compound									
	L9		**L9A**		**L9B**		**L9C**		INH	
	10^{-2} y	10^{-4}	10^{-2}	10^{-4}	10^{-2}	10^{-4}	10^{-2}	10^{-4}	10^{-2}	10^{-4}
0.4	10 ± 0.06	7 ± 0.05	0 ± 0.00	0 ± 0.00	27 ± 0.42	0 ± 0.00	19 ± 0.34	0 ± 0.00	0 ± 0.00	0 ± 0.00
0.2	21 ± 0.38	9 ± 0.06	0 ± 0.00	0 ± 0.00	40 ± 0.51	9 ± 0.06	22± 0.38	0 ± 0.00	0 ± 0.00	0 ± 0.00
0.1	32 ± 0.47	25 ± 0.40	26 0.41	11 ± 0.06	59 ± 0.71	15 ± 0.31	40 ± 0.50	0 ± 0.00	19 ± 0.55	15 ± 0.36

y = CFU/ml

Table 71: *In vitro* anti-tuberculosis activity of *N*-(5-bromo-2-hydroxybenzylidene)isonicotinohydrazide (**L10**) and its metal complexes on *M.TB* H37Rv

Concentration (µg/mL)	Compound									
	L10		**L10A**		**L10B**		**L10C**		INH	
	10^{-2} y	10^{-4}	10^{-2}	10^{-4}	10^{-2}	10^{-4}	10^{-2}	10^{-4}	10^{-2}	10^{-4}
0.4	0 ± 0.00	0 ± 0.00	0 ± 0.00	0 ± 0.00	0 ± 0.00	0 ± 0.00	0 ± 0.00	0 ± 0.00	0 ± 0.00	0 ± 0.00
0.2	0 ± 0.00	0 ± 0.00	0 ± 0.00	0 ± 0.00	0 ± 0.00	0 ± 0.00	0 ± 0.00	0 ± 0.00	0 ± 0.00	0 ± 0.00
0.1	6 ± 1.41	6 ± 0.05	0 ± 0.00	0 ± 0.00	6 ± 1.21	4 ± 0.01	0 ± 0.00	0 ± 0.00	12 ± 0.47	8 ± 0.16

y = CFU/ml

Table 72: *In vitro* anti-tuberculosis activity of *N*-(5-bromo-2-hydroxybenzylidene)isonicotinohydrazide (**L10**) and its metal complexes on clinical isolate

Concentration (µg/mL)	Compound									
	L10		**L10A**		**L10B**		**L10C**		INH	
	10^{-2} y	10^{-4}	10^{-2}	10^{-4}	10^{-2}	10^{-4}	10^{-2}	10^{-4}	10^{-2}	10^{-4}
0.4	17 ± 0.35	19 ± 0.26	0 ± 0.00	0 ± 0.00	0 ± 0.00	0 ± 0.00	0 ± 0.00	0 ± 0.00	0 ± 0.00	0 ± 0.00
0.2	26 ± 0.38	20 ± 0.28	0 ± 0.00	8 ± 0.07	0 ± 0.00	0 ± 0.00	0 ± 0.00	0 ± 0.00	0 ± 0.00	0 ± 0.00
0.1	27 ± 0.46	20 ± 0.29	57 ± 0.52	16 ± 0.32	65 ± 0.62	31 ± 0.49	41 ± 0.49	22 ± 0.30	19 ± 0.55	15 ± 0.36

y = CFU/ml

Table 73: *In vitro* anti-tuberculosis activity of *N*-(5-methoxy-2-hydroxybenzylidene)isonicotinohydrazide (**L11**) and its metal complexes on *M.TB* H37Rv

Concentration (µg/mL)	Compound									
	L11		**L11A**		**L11B**		**L11C**		INH	
	10^{-2} y	10^{-4}	10^{-2}	10^{-4}	10^{-2}	10^{-4}	10^{-2}	10^{-4}	10^{-2}	10^{-4}
0.4	24 ± 0.36	3 ± 0.01	0 ± 0.00	0 ± 0.00	8 ± 0.12	0 ± 0.00	0 ± 0.00	0 ± 0.00	0 ± 0.00	0 ± 0.00
0.2	33 ± 0.47	7 ± 0.01	12 ± 0.67	0 ± 0.00	7 ± 0.08	6 ± 0.01	6 ± 0.01	0 ± 0.00	0 ± 0.00	0 ± 0.00
0.1	41 ± 0.56	12 ± 0.64	26 ± 0.35	4 ± 0.01	26 ± 0.54	8 ± 0.22	15 ± 0.66	8 ± 0.19	12 ± 0.47	8 ± 0.16

y = CFU/ml

Table 74: *In vitro* anti-tuberculosis activity of *N*-(5-methoxy-2-hydroxybenzylidene)isonicotinohydrazide (**L11**) and its metal complexes on clinical isolate

Concentration (µg/mL)	Compound									
	L11		**L11A**		**L11B**		**L11C**		INH	
	10^{-2} y	10^{-4}	10^{-2}	10^{-4}	10^{-2}	10^{-4}	10^{-2}	10^{-4}	10^{-2}	10^{-4}
0.4	8 ± 0.07	0 ± 0.00	6 ± 0.14	0 ± 0.00	9 ± 0.08	0 ± 0.00	19 ± 1.12	0 ± 0.00	0 ± 0.00	0 ± 0.00
0.2	19 ± 1.11	9 ± 0.09	11 ± 0.12	8 ± 0.12	15 ± 0.99	0 ± 0.00	24 ± 1.36	0 ± 0.00	0 ± 0.00	0 ± 0.00
0.1	25 ± 1.47	28 ± 1.80	14 ± 0.98	19 ± 0.96	45 ± 2.80	7 ± 0.17	26 ± 1.34	24 ± 0.98	19 ± 0.55	15 ± 0.36

y = CFU/ml

Table 75: *In vitro* anti-tuberculosis activity of (E)-N^1 ((1H-pyrrol-2-yl)methylene)isonicotinohydrazide (**L12**) and its metal complexes on *M.TB* H37Rv

Concentration (µg/mL)	Compound									
	L12		**L12A**		**L12B**		**L12C**		INH	
	10^{-2} y	10^{-4}	10^{-2}	10^{-4}	10^{-2}	10^{-4}	10^{-2}	10^{-4}	10^{-2}	10^{-4}
0.4	0 ± 0.00	0 ± 0.00	23 ± 1.21	0 ± 0.00	0 ± 0.00	0 ± 0.00	0 ± 0.00	0 ± 0.00	0 ± 0.00	0 ± 0.00
0.2	0 ± 0.00	0 ± 0.00	53 ± 1.89	4 ± 0.36	0 ± 0.00	0 ± 0.00	6 ± 0.33	0 ± 0.00	0 ± 0.00	0 ± 0.00
0.1	20 ± 0.79	0 ± 0.00	56 ± 2.51	12 ± 0.45	16 ± 0.89	0 ± 0.00	15 ± 0.67	0 ± 0.00	12 ± 0.47	8 ± 0.16
0.05						0 ± 0.00		0 ± 0.00		

y = CFU/ml

Table 76: *In vitro* anti-tuberculosis activity of (E)-N^1 ((1H-pyrrol-2-yl)methylene)isonicotinohydrazide (**L12**) and its metal complexes on clinical isolate

Concentration (µg/mL)	Compound									
	L12		**L12A**		**L12B**		**L12C**		INH	
	10^{-2} y	10^{-4}	10^{-2}	10^{-4}	10^{-2}	10^{-4}	10^{-2}	10^{-4}	10^{-2}	10^{-4}
0.4	25 ± 0.38	0 ± 0.00	16 ± 0.24	6 ± 0.01	15 ± 0.23	0 ± 0.00	19 ± 0.20	0 ± 0.00	0 ± 0.00	0 ± 0.00
0.2	29 ± 0.44	12 ± 0.21	21 ± 0.30	8 ± 0.05	24 ± 0.34	0 ± 0.00	24 ± 0.31	0 ± 0.00	0 ± 0.00	0 ± 0.00
0.1	55 ± 0.71	27 ± 0.47	29 ± 0.47	19 ± 0.24	45 ± 0.69	18 ± 0.20	26 ± 0.25	24 ± 0.41	19 ± 0.55	15 ± 0.36

y = CFU/ml

Table 77: *In vitro* anti-tuberculosis activity of (E)-N^1 (thiophene-2-yl)methylene)isonicotinohydrazide (**L13**) and its metal complexes on *M.TB* H37Rv

Concentration (µg/mL)	Compound									
	L13		**L13A**		**L13B**		**L13C**		INH	
	10^{-2} y	10^{-4}	10^{-2}	10^{-4}	10^{-2}	10^{-4}	10^{-2}	10^{-4}	10^{-2}	10^{-4}
0.4	0 ± 0.00	0 ± 0.00	9 ± 0.05	0 ± 0.00	35 ± 0.56	0 ± 0.00	0 ± 0.00	0 ± 0.00	0 ± 0.00	0 ± 0.00
0.2	10 ± 0.06	0 ± 0.00	13 ± 0.09	0 ± 0.00	47 ± 0.67	17 ± 0.21	0 ± 0.00	0 ± 0.00	0 ± 0.00	0 ± 0.00
0.1	43 ± 0.65	15 ± 0.16	18 ± 0.19	34 ± 0.45	61 ± 0.84	25 ± 0.22	18 ± 0.21	0 ± 0.00	12 ± 0.47	8 ± 0.16

y = CFU/ml

Table 78: *In vitro* anti-tuberculosis activity of (E)-N^1 ((thiophene-2-yl)methylene)isonicotinohydrazide (**L13**) and its metal complexes on clinical isolate

Concentration (µg/mL)	Compound									
	L13		**L13A**		**L13B**		**L13C**		INH	
	10^{-2} y	10^{-4}	10^{-2}	10^{-4}	10^{-2}	10^{-4}	10^{-2}	10^{-4}	10^{-2}	10^{-4}
0.4	16 ± 0.34	0 ± 0.00	0 ± 0.00	0 ± 0.00	21 ± 0.45	0 ± 0.00	0 ± 0.00	0 ± 0.00	0 ± 0.00	0 ± 0.00
0.2	25 ± 0.45	16 ± 0.06	34 ± 0.98	12 ± 0.32	30 ± 0.66	8 ± 0.00	0 ± 0.00	0 ± 0.00	0 ± 0.00	0 ± 0.00
0.1	51 ± 1.22	43 ± 0.79	66 ± 3.00	22 ± 0.55	33 ± 0.81	19 ± 0.04	11 ± 0.27	0 ± 0.00	19 ± 0.55	15 ± 0.36

y = CFU/ml

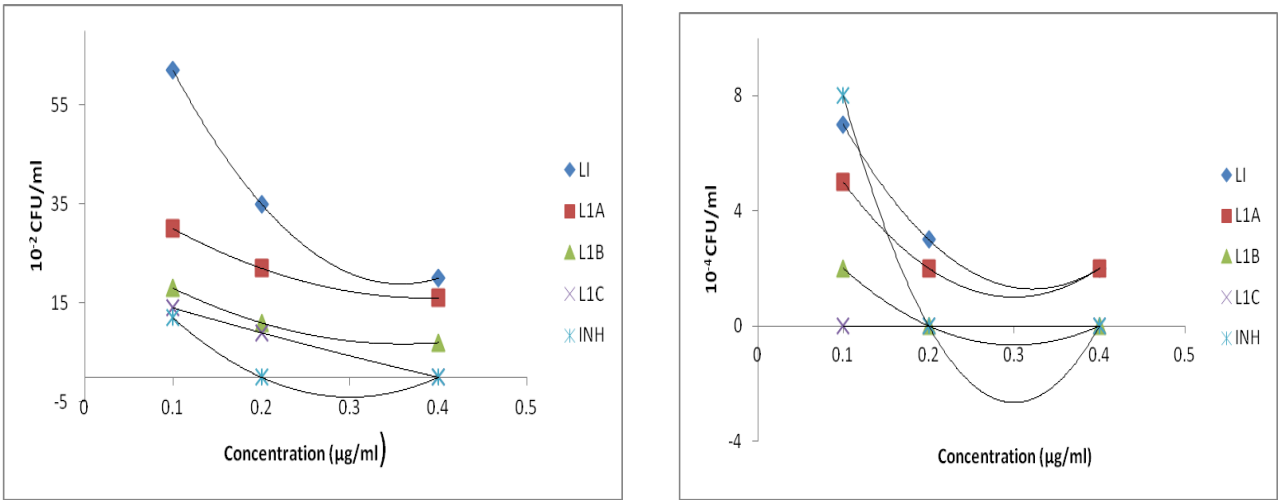

Figure 73: Graphs showing the effect of metal ion on the anti-tuberculosis activity of compound **L1** on *M.TB* H37Rv.

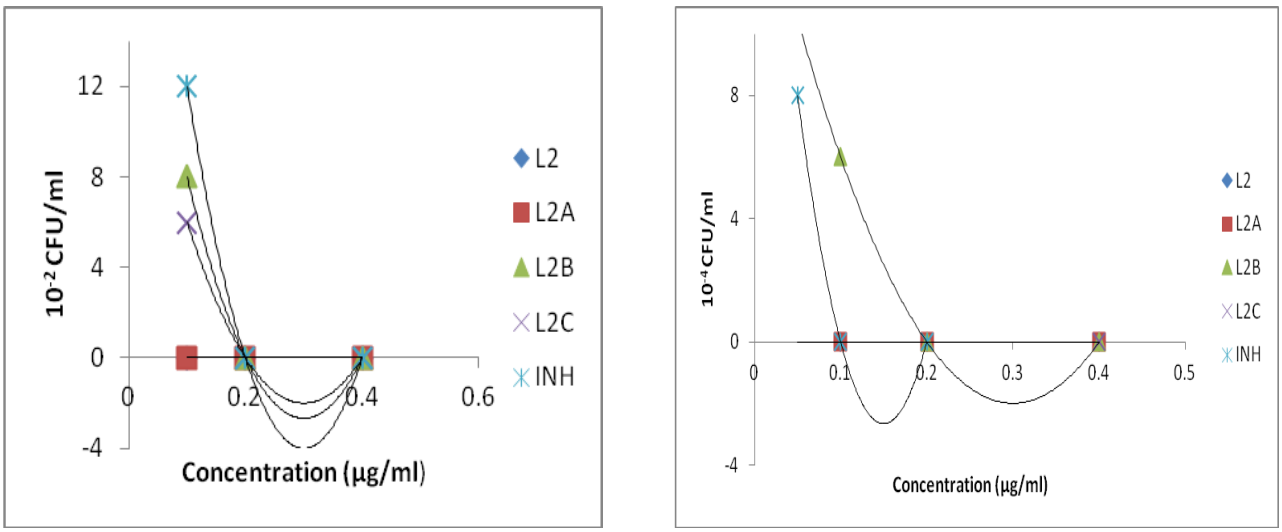

Figure 74: Graphs showing the effect of metal ion on the anti-tuberculosis activity of compound **L2** on *M.TB* H37Rv.

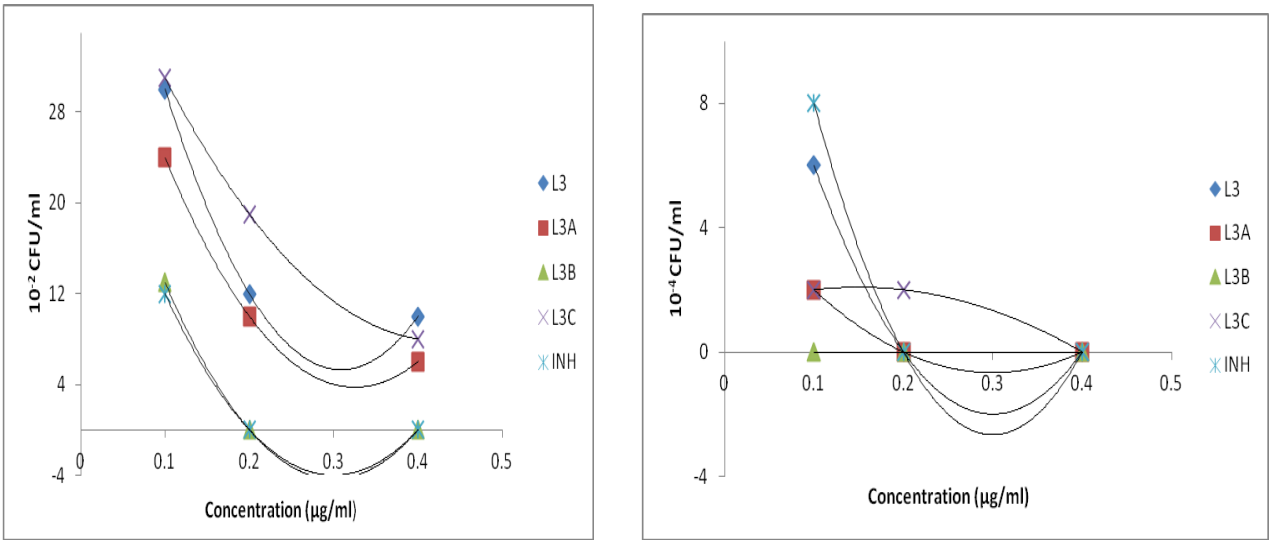

Figure 75: Graphs showing the effect of metal ion on the anti-tuberculosis activity of compound **L3** on *M.TB* H37Rv.

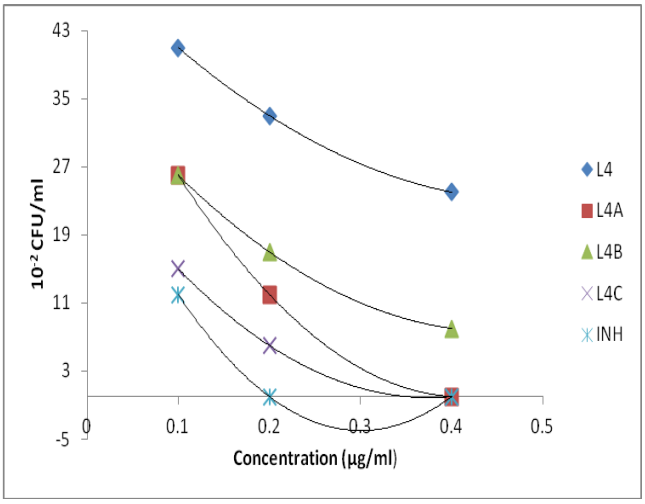

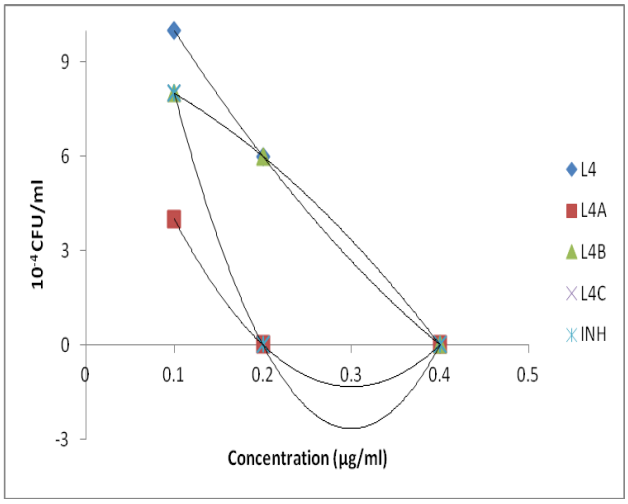

Figure 76: Graphs showing the effect of metal ion on the anti-tuberculosis activity of compound **L4** on *M.TB* H37Rv.

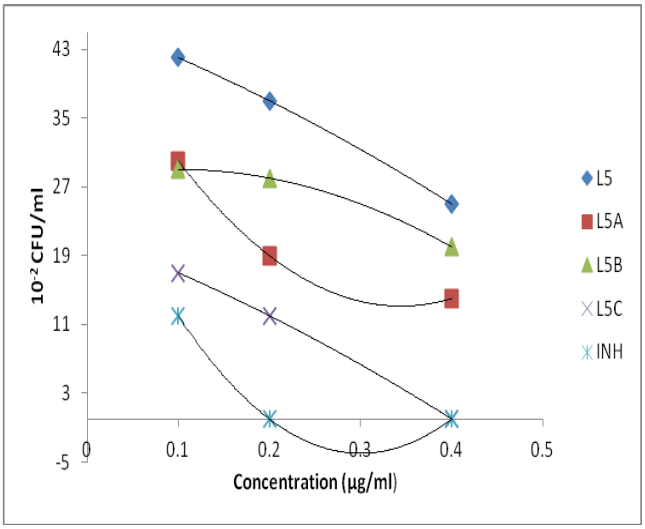

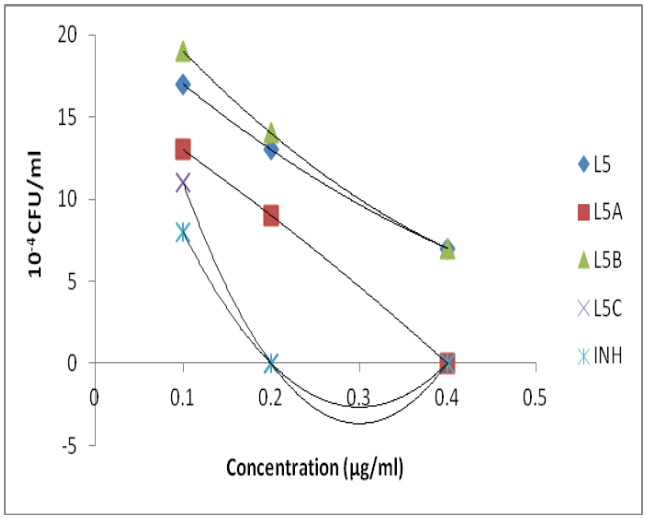

Figure 77: Graphs showing the effect of metal ion on the anti-tuberculosis activity of compound **L5** on *M.TB* H37Rv.

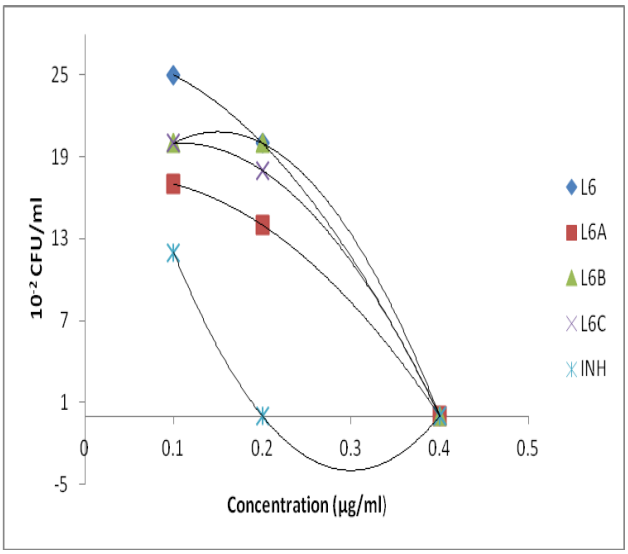

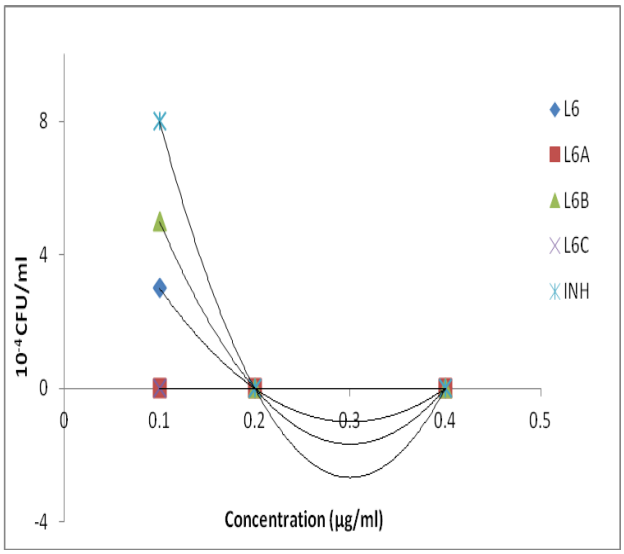

Figure 78: Graphs showing the effect of metal ion on the anti-tuberculosis activity of compound **L6** on *M.TB* H37Rv.

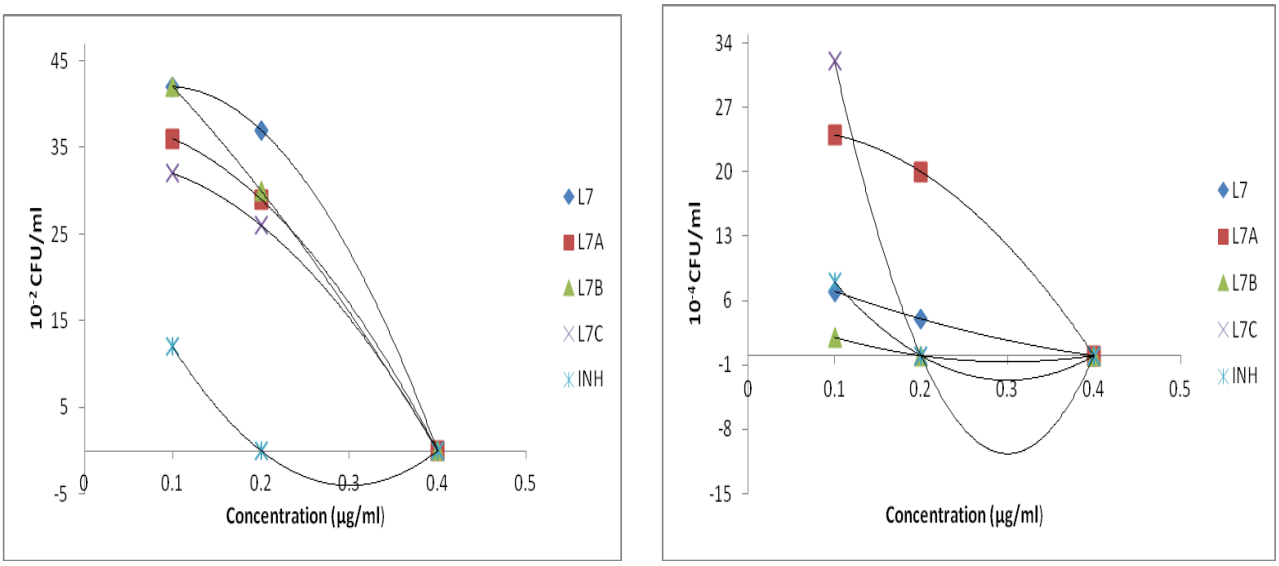

Figure 79: Graphs showing the effect of metal ion on the anti-tuberculosis activity of compound **L7** on *M.TB* H37Rv.

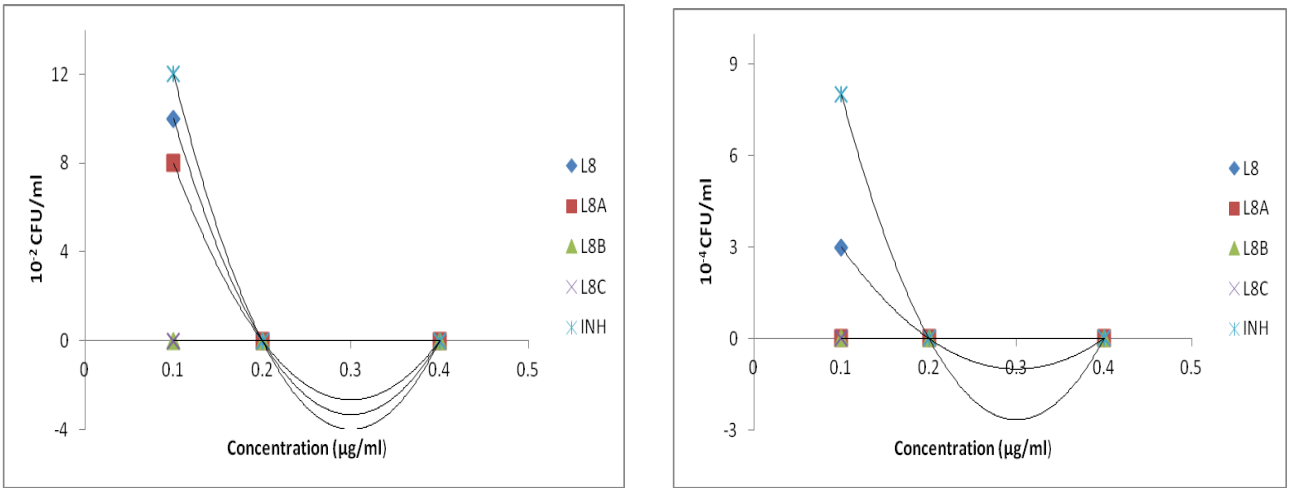

Figure 80: Graphs showing the effect of metal ion on the anti-tuberculosis activity of compound **L8** on *M.TB* H37Rv

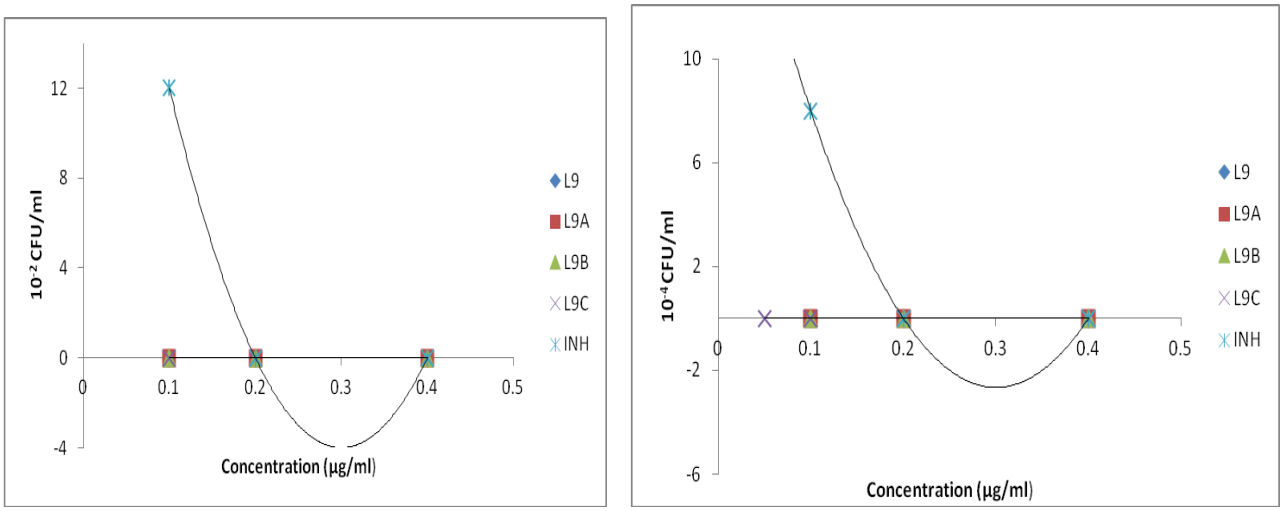

Figure 81: Graphs showing the effect of metal ion on the anti-tuberculosis activity of compound **L9** on *M.TB* H37Rv

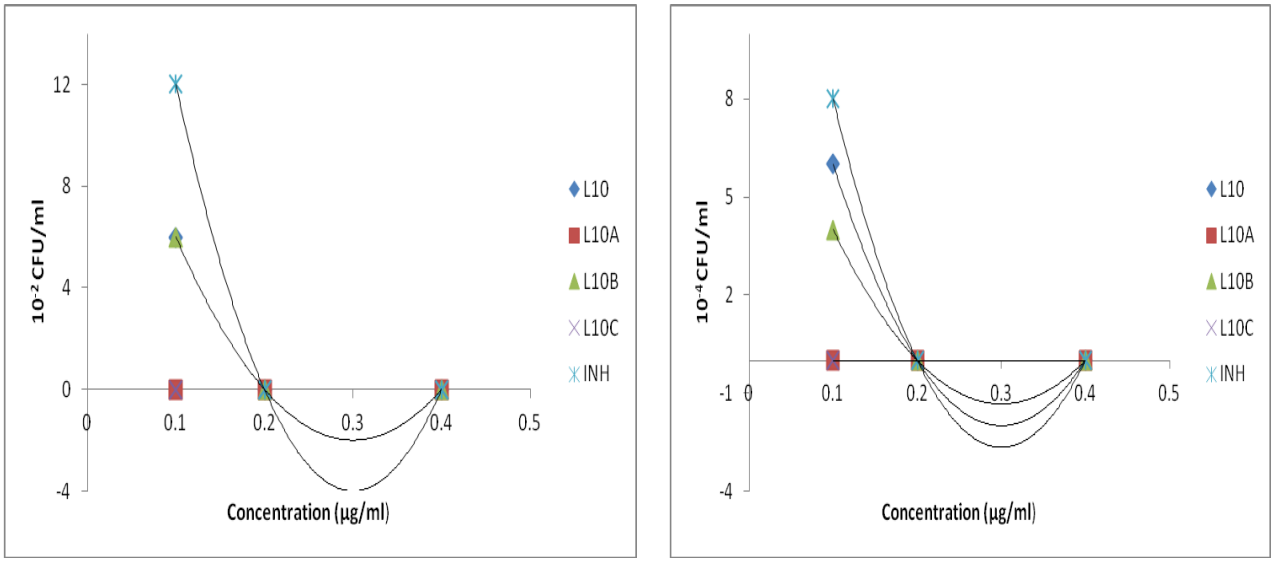

Figure 82: Graphs showing the effect of metal ion on the anti-tuberculosis activity of compound **L10** on *M.TB* H37Rv

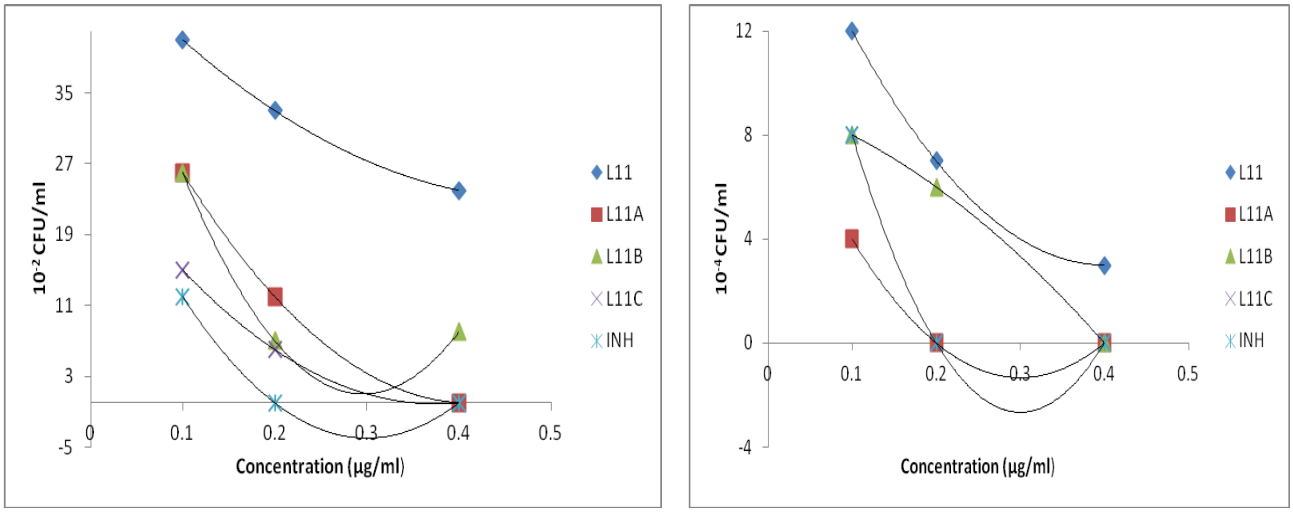

Figure 83: Graphs showing the effect of metal ion on the anti-tuberculosis activity of compound **L11** on *M.TB* H37Rv

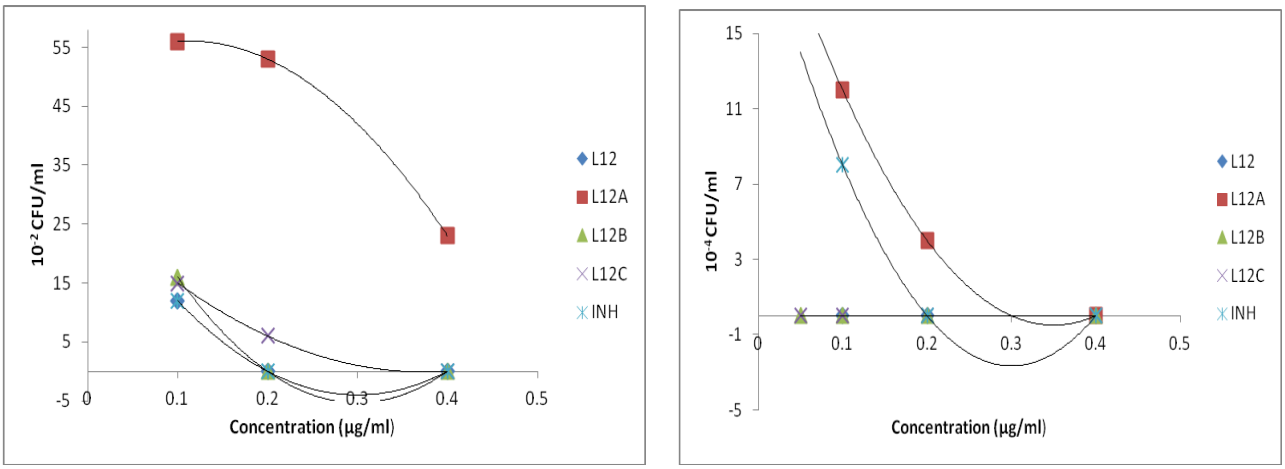

Figure 84: Graphs showing the effect of metal ion on the anti-tuberculosis activity of compound **L12** on *M.TB* H37Rv

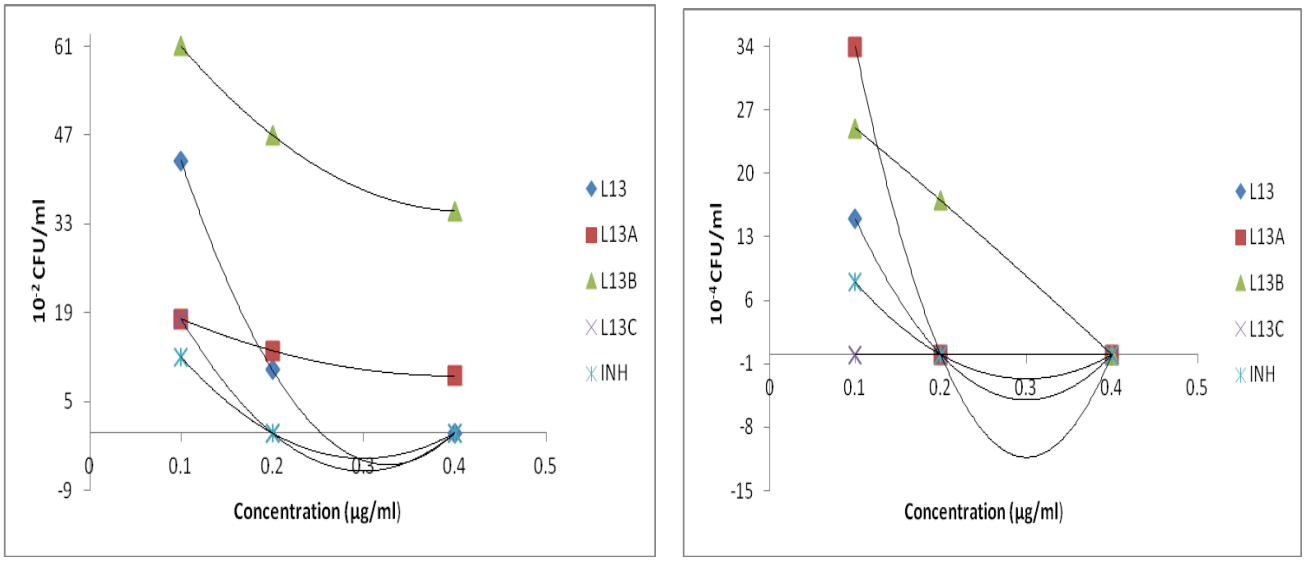

Figure 85: Graphs showing the effect of metal ion on the anti-tuberculosis activity of compound **L13** on *M.TB* H37Rv

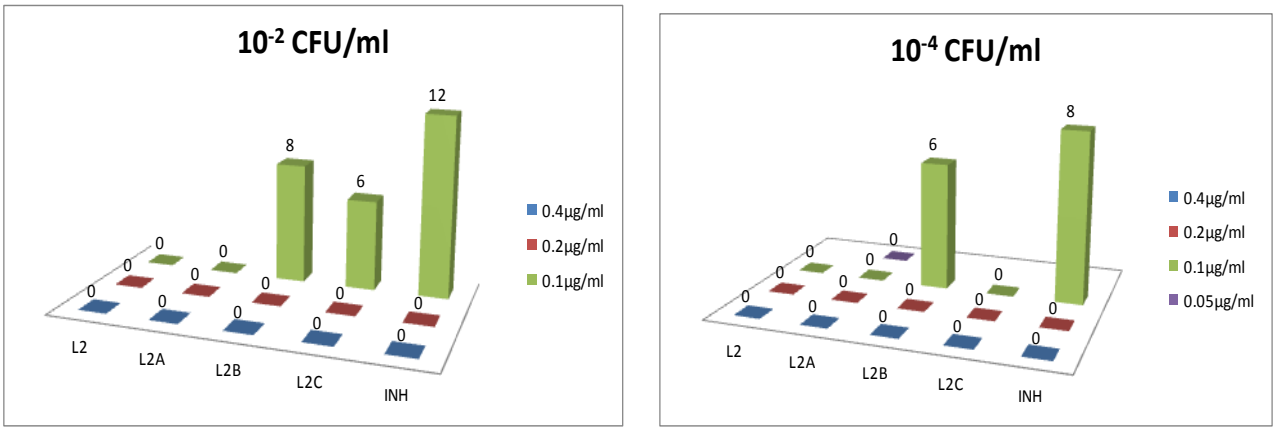

Figure 86: Charts showing the effect of metal ion on the anti-tuberculosis activity of compound **L2**.

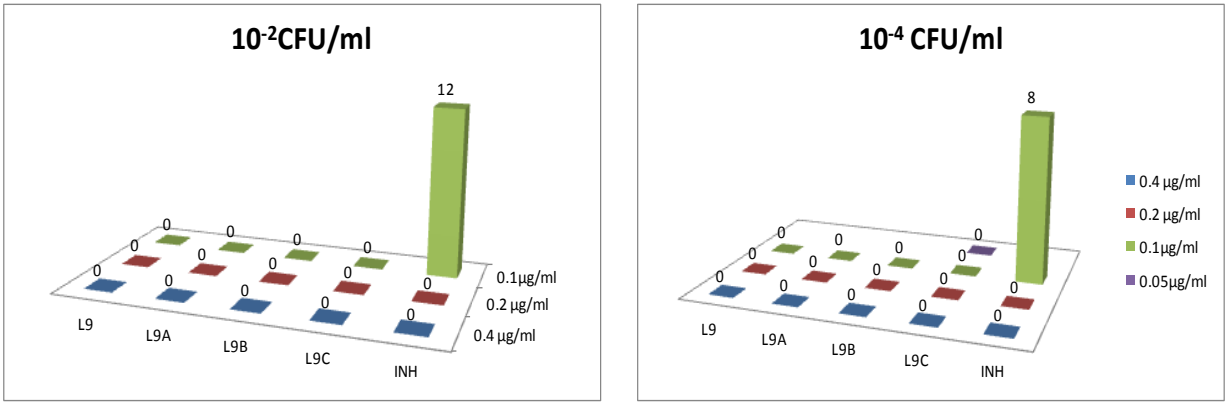

Figure 87: Charts showing the effect of metal ion on the anti-tuberculosis activity of Schiff base **L9**.

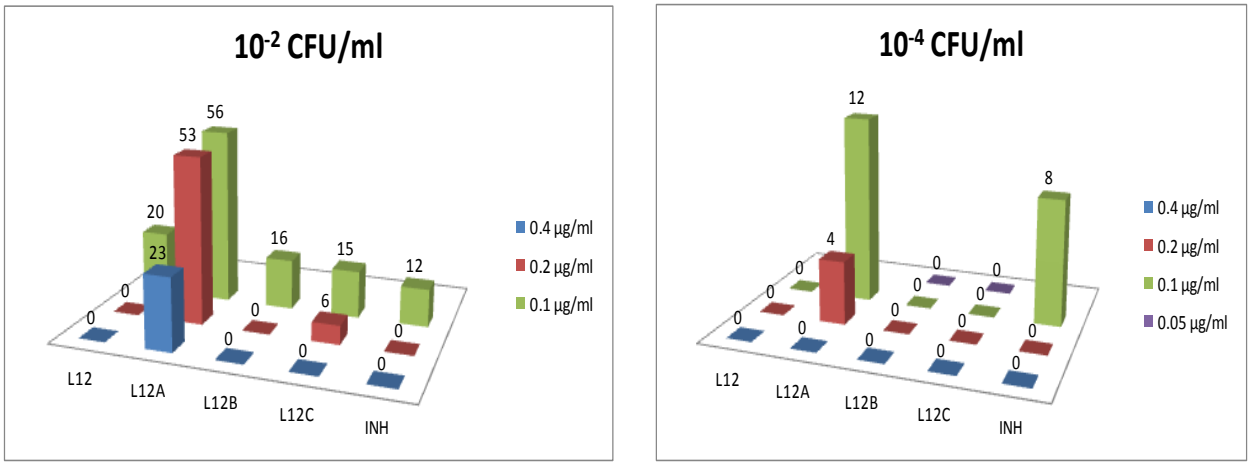

Figure 88: Charts showing the effect of metal ion on the anti-tuberculosis activity of Schiff base **L12**.

CHAPTER FIVE

5.0 DISCUSSION OF RESULTS

5.1 Synthesis and characterization of Schiff bases

Three groups of Schiff bases have been synthesized by the condensation reaction of 2-aminopyridine (**L1-L4**), 4-aminopyridine (**L5-L7**), INH (**L8-L11**) with each of the following aldehydes: 2-hydroxybenzaldehyde, 5-nitro-2-hydroxybenzaldehyde, 5-bromo-2-hydroxybenzaldehyde and 5-methoxy-2-hydroxybenzaldehyde. INH Schiff bases were also synthesized using pyrrole-2-carboxyaldehyde (**L12**) and thiophene-2-carboxyaldehyde (**L13**). Schiff base of 4-aminopyridine with 5-methoxy-2-hydroxybenzaldehyde could not be isolated.

5.1.1 Physical and analytical data of the 2-aminopyridine Schiff bases

Four Schiff bases derived from 2-aminopyridine with 2-hydroxybenzaldehyde (**L1**), 5-nitro-2-hydroxybenzaldehyde (**L2**), 5-bromo-2-hydroxybenzaldehyde (**L3**) and 5-methoxy-2-hydroxybenzaldehyde (**L4**) were obtained in good to excellent yield except the nitro containing ligand **L2** which gave the lowest yield of 46%. The trend is NO_2 <H <OCH_3 <Br. All the compounds had sharp melting points which varied with the nature of substituent on the aldehyde. **L2** had the highest melting point (182-184 ^oC) which may be attributed to the strong electron withdrawing nature of nitro group. The unsubstituted ligand **L1** gave the lowest melting point (62-64 ^oC) in line with previous report of Abdel-Latif *et al*., 2007. The melting point increases with increase in the electron withdrawing effect H< OCH_3< Br< NO_2. The elemental analyses of the Schiff bases support their molecular formulae as the calculated and experimental values do not differ by more than 0.5.

5.1.2 Physical and analytical data of the 4-aminopyridine Schiff bases

Three Schiff bases derived from 4-aminopyridine with 2-hydroxybenzaldehyde (**L5**), 5-nitro-2-hydroxybenzaldehyde (**L6**), and 5-bromo-2-hydroxybenzaldehyde (**L7**) were obtained in excellent yields. The compounds were synthesized in toluene under an inert atmosphere using nitrogen. No reaction was obtained without toluene and nitrogen. Attempts to isolate 5-methoxybenzaldehyde Schiff base were not successful. All the Schiff bases had sharp melting points observed in the range 77-78 ^{o}C, 193-194 ^{o}C and 139-141 ^{o}C for **L5, L6** and **L7** respectively. Again, the highest melting point of **L6** may be attributed to the strong electron withdrawing nature of nitro group. The trend is NO_2>Br>H. The elemental analyses are in good agreement with the molecular formula proposed for the compounds.

The position of the nitrogen atom on the pyridine ring of the aminopyridine Schiff bases slightly affected their physical property. This was observed in the high yield and melting point of the unsubstituted and nitro substituted 4-aminopyridine Schiff bases over their 2-aminopyridine counterparts. However, no significant effect was observed in the physical property of the bromo containing aminopyridine Schiff bases.

5.1.3 Physical and analytical data of the INH Schiff bases

Two classes of INH Schiff bases have been synthesized in excellent yields except **L13** which gave a yield of 40%. The trend for Schiff bases derived using 2-hydroxybenzaldehyde derivatives is Br>H>NO_2>OCH_3 and those derived using heteroaromatic aldehydes is NH>S. The purity of all the compounds was confirmed by their sharp melting points. As observed with the aminopyridine Schiff bases, the nitro containing ligand **L9** gave the highest melting point. The elemental analyses reflected that the compounds have the molecular formula given in Table 9.

The general trend observed in the physical properties of the Schiff bases was that the bromo and nitro containing compounds gave the highest and lowest yield respectively in all cases. Moreso, the nitro containing Schiff bases exhibited the highest melting point due to the strong electron withdrawing nature of this group.

5.2 Infrared spectra of the Schiff bases

The Infrared frequencies of diagnostic bands for the various Schiff bases synthesized are listed in Tables 9-12. Analyses of the Schiff bases are based on previous assignments of similar compounds which are characteristic of typical group frequencies. The stretching frequencies of OH, $C=N_{(imine)}$, C-O, C=N(pyridine) are used as the diagnostic bands while C=O band is included for the INH group. The exact positions of the characteristic bands vary from one Schiff base to another due to substituent on either the aldehyde or amine.

Schiff base synthesis involves formation of an imine group by condensation reaction between a carbonyl and amine functional group. This results in disappearance of the band at 1740 to 1700 cm^{-1} for the carbonyl bond in the aldehyde and 3500 to 3300 cm^{-1} for the amine and appearance of imine band in IR and NMR (Willams and Fleming, 1986). Therefore, the main band of interest in Schiff base is the imine band.

5.2.1 IR spectra of the 2-aminopyridine Schiff bases

The 2-hydroxybenzylidene pyridin-2-amine based Schiff bases (**L1**-**L4**) exhibited broad or medium stretching band in the frequency range 3331-3021 cm^{-1} attributed to the *ν*(OH) stretching frequency. This is observed at 3058 cm^{-1} for **L1** in line with the range expected for similar compound (Nazir *et al*., 2000). The bands displayed in the region 1271-1285 cm^{-1} in all the compounds assigned to *ν*(C-O) stretching frequency support the presence of hydroxyl group. This band observed at 1276 cm^{-1} for

L1 is in line with similar imine compound reported by Tantaru *et al.,* 2012. The characteristic C=N stretching frequency for the compounds are observed in the frequency range 1603 cm^{-1} for **L1,** 1595 cm^{-1} for **L2,** 1608 cm^{-1} for **L3** and 1598 cm^{-1} for **L4** respectively. . It has been reported (Nazir *et al*., 2000, Abdel Latif *et al*., 2007 and Tantaru *et al*., 2012) that similar imine compound of **L1** exhibited this bond at different stretching frequency of 1612, 1647 and 1610 cm^{-1}. The condition to which they reported their work was not be reproduced in this study. This may account for the observed differences. The strong electron withdrawing nitro group may be attributed to lower stretching frequency 1595 cm^{-1} observed for **L2.** The bromo having a halogen can have both inductive and electronic effect which may be responsible for the higher stretching frequency observed at 1608 cm^{-1}.

5.2.2 IR spectra of the 4-aminopyridine Schiff bases

The IR spectra data for the 4-aminopyridine based Schiff bases (**L5**-**L7**) are listed th Table 6. The unsubstituted 2-hydroxybenzylidene pyridin-2-amine (**L5**) showed medium band at 3324 cm^{-1} attributed to the *ν*(OH) stretching frequency. The absence of this band in the other compounds (**L6** and **L7**) is probably due to hydrogen bonding. However, the bands displayed in the region 1271-1295 cm^{-1} in all the compounds assigned to *ν*(OH) stretching frequency support the presence of the hydroxyl group. The characteristic C=N stretching frequency for the compounds observed at 1587 cm^{-1} for **L5,** 1635 cm^{-1} for **L6,** and 1615 cm^{-1} for **L7** confirms the formation of the imine bond. In this case, increase in electron withdrawing effect resulted in higher frequency in the compounds.

The hydroxyl and imine bands of the nitro and bromo substituted 2-hydroxybenzylidenepyridin-4-amine Schiff bases are observed at higher stretching frequency compared to the 2-aminopyridine counterpart. This may be due to stabilization of the bond that is the nitrogen in the fourth position stabilizes the compound hence higher wavenumbers.

5.2.3 IR spectra of the INH Schiff bases

INH based Schiff bases show strong bands in the frequency range of 3188-3308 cm^{-1} assigned to the *v*(OH) stretching frequency. The trend observed is this band shifted to lower wavenumber in all the spectra of the substituted compounds (**L9**-**L11**). The appearance of absorption band at 1286-1299 cm^{-1} due to *v*(C-O) stretching vibration further supports the presence of the hydroxyl group. The presence of the band in the frequency region 1649-1675 cm^{-1} is due to *v*C=O stretching frequency. In this case, the presence of substituent on the aldehyde resulted in a decrease in the stretching frequency which varied with electron donating and electron withdrawing substituent. The characteristic C=N frequency for the compounds are 1611 cm^{-1} for **L8**, 1608 cm^{-1} for **L9**, 1616 cm^{-1} for **L10** and 1613 cm^{-1} for **L11**. The strong electron withdrawing nitro **L9** causes the double bond C=N to become longer and weaker hence lower wavenumber. The inductive and electronic effect of the bromo containing compound **L10** may be responsible for higher value 1616 cm^{-1}. As excepted, the presence of the electron donating OCH_3 is attributed to the high wavenumber value. It has been previously reported by Abou-Melha, 2008 and Nair and Thankamani, 2010 that similar imine compounds of **L8** and **L10** exhibited this band at 1585 cm^{-1} and 1620 cm^{-1}. The difference may be because the condition to which they reported their work was not reproduced in this work. Nevertheless, the frequencies were observed within acceptable range.

The stretching frequency of the INH Schiff bases containing the pyrrole-2-carboxyaldehyde (**L12**) and thiophene-2-carboxyaldehyde (**L13**) show characteristic bands in the frequency 1645 and 1661 cm^{-1} attributed to the *v*C=O stretching frequency. The appearance of *v*C=N stretching frequency at 1593 and 1594 cm^{-1} is an indication of the formation of the Schiff bases.

5.3 NMR spectra of the Schiff bases

The resulting Schiff bases **L1-L14** were fully characterized by NMR analysis. The characteristic feature in each compound is clearly seen in the ^{1}H and ^{13}C NMR. These features support the structure assigned to each compound.

5.3.1 NMR spectra of the 2-aminopyridine Schiff bases

^{1}H-NMR spectrum (Figure 26a) of the ligand **(L1)** shows ten signals. The four protons in the aromatic ring resonate as follows, one proton as a multiplet in the range δ_H 6.91-7.02 ppm, one proton as a doublet in the range 7.16-7.17 ppm, one proton as a doublet in the range 7.18-7.19 ppm and one proton as a triplet in the range 7.25-7.29 ppm. A sharp singlet at δ_H 9.41 and 13.40 ppm were assigned to the imine (HC=N) and hydroxyl protons respectively. Based on literature precedent, these signals were observed at δ_H 9.44 and 13.44 ppm (Nazir *et al*., 2000, Gudasi and Goudar, 2000) and δ_H 9.51 and 13.03 ppm (Ali *et al*., 2009). ^{13}C NMR spectrum (Figure 26b) indicates 12 carbon resonances, out of which δ_C 161.84 and 164.70 are attributed to the imine (C=N) and hydroxyl (C-OH) carbons respectively. The remaining ten carbon signals at δ_C 117.21, 118.93, 119.19, 120.44, 122.54, 133.44, 133.81, 138.45, 148.92 and 157.51 ppm are in agreement with the structure of the ligand. A similar trend has been observed earlier (Ali *et al*., 2009).

The ^{1}H NMR spectrum of ligand **L2** exhibit a singlet at δ_H 9.53 and 14.56 ppm attributed to the imine (HC=N) and hydroxyl (OH) protons respectively. The other seven signals resonate as multiplet in the range δ_H 7.10-8.54 ppm assigned to the aromatic protons. In the corresponding ^{13} C NMR spectrum (Figure 27b), 12 carbons resonate at δ_C 117.79, 118.49, 120.51, 123.60, 128.85, 129.52, 131.63, 138.76, 149.25 and 153.78 ppm out of which δ_C 162.89 and 167.63 ppm are attributed to the imine (C=N) and (C-OH) carbons respectively. The NMR signals are in agreement with the structure of the ligand.

The ^{1}H NMR spectrum (Figure 28a) of ligand **L3** shows nine signals. The imine (HC=N) and hydroxyl (OH) protons resonate as a singlet at δ_H 9.34 and 13.42 ppm respectively. The seven aromatic protons resonate as multiplet in the range δ_H 6.89-8.49 ppm. The ^{13}C NMR spectrum (Figure 28b) shows 12 signals at δ_C 110.60, 119.29, 120.35, 120.62, 122.99, 135.26, 136.36, 138.56, 149.05, 156.98 ppm with imine carbon resonating at δ_C 160.87 and hydroxyl carbon at δ_C 163.40 ppm confirming the structure of the compound.

The ^{1}H NMR spectrum (figure 29a)of ligand **L4** shows twelve signals with three protons resonating at δ_H 3.77, one proton at δ_H 9.37 and δ_H 12.93 ppm assigned to the methoxy (OCH_3), imine (HC=N) and hydroxyl (OH) groups respectively. The seven aromatic protons resonate as multiplet in the range δ_H 6.92-8.48 ppm. The ^{13}C NMR spectrum (Figure 29b) shows 13 signals at δ_C 55.78, 115.79, 118.05, 118.44, 120.46, 121.50, 122.52, 138.42, 148.88, 152.20, 156.16 ppm with imine carbon resonating at δ_C 157.50 and hydroxyl carbon at δ 164.41 ppm. These signals support the structure of the compound.

5.3.2 NMR spectra of the 4-aminopyridine Schiff bases

The ^{1}H NMR spectrum (Figure 32a) of ligand **L5** shows ten signals. The imine (HC=N) and hydroxyl (OH) protons resonate as a singlet at δ_H 8.61 and 12.57 ppm respectively. Two out of the four protons on the pyridine ring resonate as doublet in the range δ_H 8.63-8.64 ppm while the other two resonate in the range δ_H 7.12-7.14 ppm. There are four protons on the aromatic ring with two of the protons resonating as a triplet in the range δ_H 7.40-7.45 ppm and the other two as a doublet in the range δ_H 6.95-7.05 ppm. The ^{13}C NMR spectrum (Figure 32b) shows 10 signals at δ_C 116.10, 117.50, 118.64, 119.45, 132.92, 134.37, 151.15, 155.46 ppm with imine (C=N) hydroxyl(C-OH) carbons resonating at δ_C 161.29 and at δ 165.68 ppm respectively. The NMR signals support the structure of the ligand.

The ^{1}H NMR spectrum of ligand **L6** (Figure 33a) exhibits a singlet at δ_H 8.56 and 10.01 ppm attributed to the imine (HC=N) and hydroxyl (OH) protons respectively. The other seven signals resonate as follows, three protons as multiplet in the range δ_H 7.09-7.22 ppm assigned to the aromatic protons, two protons as multiplet in the ranges δ_H 8.30-8.44 attributed to the pyridine protons and two protons as triplet in the range δ_H 8.69-8.72 ppm also assigned to the pyridine protons In the corresponding ^{13} C NMR spectrum (Figure 33b), 10 carbons resonate at δ_C 115.94, 118.58, 119.04, 128.95, 129.30, 129.67, 131.63 and 151.44 ppm out of which δ 164.14 and 166.39 ppm are attributed to the imine (C=N) and (C-OH) carbons respectively. The NMR signals are in agreement with the structure of the ligand.

^{1}H-NMR spectrum (Figure 34a) of the ligand **L7** shows nine signals, one proton in the aromatic ring resonates as a doublet at δ_H 6.93-6.96 ppm. Two pyridine protons exhibit a doublet at δ_H 7.12-7.13 ppm δ_H. In addition, two other aromatic protons resonate as multiplet in the range 7.48-7.54 ppm. The other two pyridine protons resonate at δ_H 8.66 ppm. A sharp singlet at δ_H 8.54 and 12.57 ppm were assigned to the imine proton (HC=N) and hydroxyl proton (OH). ^{13}C NMR spectrum (Figure 34b) indicates 10 carbon resonances, of which δ_C 160.27 and 164.38 ppm are attributed to the imine (C=N) and hydroxyl (C-OH) carbons respectively. The remaining eight carbon signals at δ_C 110.88, 116.05, 119.53, 119.97, 134.80, 136.93, 151.26 and 154.93 ppm are in agreement with the structure of the ligand.

5.3.3 NMR spectra of the INH Schiff bases

The resulting Schiff bases **L8-L13** were fully characterized by NMR analysis. Eight signals were clearly observed in the ^{1}H NMR spectrum (Figure 38a) of compound **L8**. There are four protons in the aromatic ring, two protons resonate as quadruplet in the range 6.90-6.97 ppm, one proton shows triplet in the range 7.29-7.34 ppm and the other one proton resonates as doublet at 7.59-7.61 ppm. A

singlet at 8.69, 11.11 and 12.31 ppm were assigned to the imine (HC=N), amide (NH) and hydroxyl (OH) protons respectively. The signals corresponding to the four hydrazine protons appeared between 7.85-7.87 ppm and 8.79-8.81 ppm as two protons doublet respectively. The ^{13}C NMR spectrum (Figure 38b) show 11 carbons signals excepted with the imine, hydroxyl and carbonyl-amide carbons at 149.46, 158.01 and 161.87 ppm. The remaining 8 carbons signals at δ_C 116.97, 119.22, 119.96, 122.05, 129.73, 132.28, 140.49 and 150.92 ppm are in agreement with the structure of the compound.

Compound **L9**, showed signals corresponding to three aromatic protons which appeared as one proton each resonating as doublet in the range 7.10-7.13 ppm, 8.17-8.20 ppm and 8.60-8.61 ppm respectively in the ^{1}H NMR spectrum (Figure 39a). A sharp singlet at 8.76, 12.20 and 12.43 ppm were assigned to the imine (HC=N), hydroxyl (OH) and amide (NH) protons respectively. The signals corresponding to the four hydrazine protons appeared as two protons doublet resonating at 7.840-7.860 ppm and 8.80-8.81 ppm respectively. The ^{13}C NMR spectrum (Figure 39b) show 10 carbons signals with the imine, carbonyl-amide and hydroxyl carbons at 145.41, 162.17 and 163.22 ppm. The remaining carbons signals at δ_C 117.68, 120.59, 122.07, 123.84, 127.44, 140.40 and 150.94 ppm support the structure of the compound.

^{1}H-NMR spectrum (Figure 40a) of the ligand **L10** shows seven signals. The three protons in the aromatic ring resonate as follow, one proton as a doublet at δ_H 6.90-6.93 ppm, one proton as a quadruplet at 7.43-7.47 ppm. In addition, the signal observed in the range 7.83-7.85 ppm comprise of one aromatic proton (1H, Ar-H) and two hydrazine proton (2H, nict-H). The other two hydrazine protons resonate at δ_H 8.79-8.81 ppm. A sharp singlet at δ_H 8.65, 11.14 and 12.36 ppm were assigned to the imine (HC=N) hydroxyl proton (OH) and amide (NH) protons. The ^{13}C NMR spectrum (Figure 40b) indicates 11 carbons signals, of which δ_C 146.81, 156.98 and 162.02 ppm were attributed to the imine (C=N) hydroxyl (C-OH) and carbonyl-amide carbons respectively. The remaining eight

carbons signals at δ_C 111.09, 119.23, 121.84, 122.07, 130.60, 134.44, 140.41 and 150.91 ppm support the structure of the ligand.

Seven signals were clearly seen in the ^{1}H NMR spectrum (Figure 41a) of compound **L11**. The methoxy protons resonate as a singlet at 3.72 ppm. Out of the three aromatic protons, two protons resonate as multiplet in the range 6.86-6.95 ppm, one proton shows doublet in the range 7.17-7.18 ppm. A sharp singlet at 8.68, 10.53 and 12.29 ppm were assigned to the imine (HC=N), hydroxyl (OH) and amide (NH) protons respectively. The signals corresponding to the four hydrazine protons appeared between 7.84-7.86 ppm and 8.79-8.80 ppm as two protons doublet respectively. The ^{13}C NMR spectrum (Figure 41b) show 12 carbons signals expected with the methoxy, imine, hydroxyl and carbonyl-amide carbons at 56.00, 148.77, 152.71 and 161.92 ppm. The remaining 8 carbons signals at δ_C 112.22, 117.89, 119.21, 119.50, 122.08, 140.59, 150.91 and 152.09 ppm are in agreement with the structure of the compound.

^{1}H-NMR spectrum (Figure 42a) of the ligand **L12** shows seven signals. The three protons in the pyrrole ring resonate as follow, one proton as a quadruplet at δ_H 6.14-6.19 ppm, one proton as a singlet at 6.53 ppm and one proton as a doublet at 6.93-6.94 ppm. Two protons each which resonate as a doublet in the range 7.80-7.82 ppm and as triplet in the range 8.76-8.78 ppm were assigned to the four hydrazine protons. A sharp singlet at δ_H 8.29, 11.60 and 11.73 ppm were assigned to the imine (HC=N) NH-pyrrole and amide (NH) protons respectively. The ^{13}C NMR spectrum (Figure 42b) indicates 9 carbons signals, of which δ_C 142.63 and 161.66 ppm were attributed to the imine (C=N) and carbonyl-amide carbons respectively. The remaining seven carbons signals at δ_C 110.10, 114.60, 122.18, 123.65, 127.44, 141.48 and 150.95 ppm support the structure of the ligand.

Seven signals were clearly seen in the ^{1}H NMR spectrum (Figure 43a) of compound **L13**. The three aromatic protons resonate as follow, one proton as a quadruplet in the range 7.14-7.17 ppm, one proton as a doublet at 7.51-7.52 ppm and one proton as a doublet at 7.79-7.81 ppm respectively. Two protons each which resonate as a doublet in the range 7.71-7.70 ppm and as triplet in the range 8.77-8.79 ppm were assigned to the four hydrazine protons. A sharp singlet at 8.68 and 12.03 ppm were assigned to the imine (HC=N) and amide (NH) protons respectively. The ^{13}C NMR spectrum (Figure 43b) show 9 carbons signals as expected with the imine and carbonyl-amide carbons a 139.27 and 161.96 ppm. The remaining 7 carbons signals at δ_C 122.01, 128.49, 130.00 132.13, 140.94, 144.58 and 150.86 ppm are in agreement with the structure of the compound.

5.4 Electronic absorption spectra of the Schiff bases

Electronic spectra provides information on the molecular structure of compounds. The electronic absorption spectra of the Schiff bases within 260-500 nm was performed in 10^{-5} M solution of the compound in DMF. The spectra of the compounds comprise of electronic transition bands ascribed to $\pi-\pi^*$, n- π^* and intramolecular charge tranfer (CT).

The first band (A) appearing within 260-290 nm region can be assigned to $\pi-\pi^*$ transition of the aromatic rings. These bands are sensitive to substitution on the aromatic ring (Hammud *et al*., 2006). The electronic absorption spectra consist of bands in the 200-500 nm region. Band B observed within the wavelength range 295-330 nm is due to transition between the π -orbital localized on the central azomethine (CH=N) bond (Soliman, 1997). The third band located within the 340-400 nm region can be ascribed to charge transfer within the entire Schiff base molecule. This band is commonly observed in *o*-hydroxyl Schiff bases (Gahr, 1990) and is based on strong intramolecular hydrogen bonding between the hydroxyl group of the salicylidene and the azomethine nitrogen (Sovilj *et al*., 1998).

5.4.1 Electronic absorption spectra of the 2-aminopyridine Schiff bases

The use of freshly prepared solution allows a study of the substituent effect on the shift in absorption maxima for the enol-imine tautomer with minium interference from the keto-amine tautomer. The 2-aminopyridine Schiff bases (**L1**-**L4**) exhibited a reduced tendency to tautomeric interconversion as aresult of decreased basicity of the imino nitrogen group due to electron delocalization (Nazir, *et al*., 2000, Tezer and Karakus, 2009). However, the acidity of the 2-hydroxybenzylidene OH increases in the presence of the electron withdrawing nitro group **L2.** This favours the existence of keto-amine tautomer (431 nm).

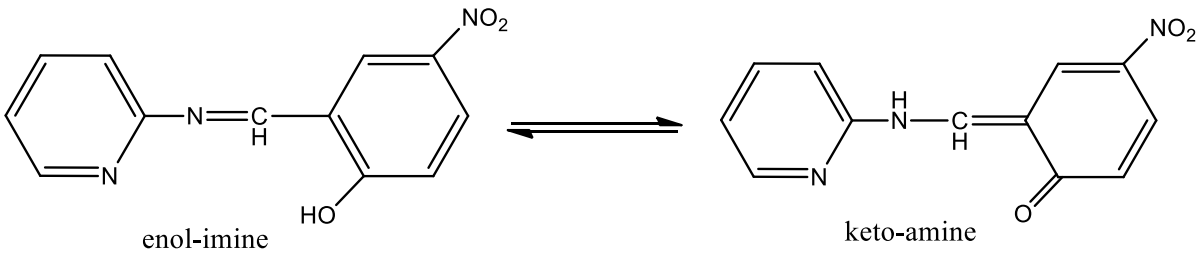

Figure 89: Keto-enol tautomer in N(5-nitro-2-hydroxybenzylidene)pyridin-2-amine (**L2**)

The charge transfer band (Band C) was observed in all compounds within 358-373 nm. In this case, the presence of the substituent resulted in a shift to longer wavelength in the order $H<Br<OCH_3<NO_2$. This parallels the electronwithdrawing nature of the substituent. varied shifts to longer wavelength with a change. The band due to $\pi-\pi*$ is insensitive to the nature of the substituent and apperaed only in the unsubstituited and nitro substitutented compounds. The high extinction coefficient observed in all the bands for the electro withdrawing nitro group suggest that these compound have better interactions with the solvent leading to the high intensity of absorbance (Nazir, *et al*., 2000).

5.4.2 Electronic absorption spectra of the 4-aminopyridine based Schiff bases

The electronic absorption spectra of the 4-aminopyridine Schiff bases reveal that the compounds exhibited a reduced tendency to tautomeric interconversion. This is as a result of to decreased basicity of the imino nitrogen group due to electron delocalization (Nazir, *et al*., 2000, Tezer and Karakus, 2009). On the other hand, the electronwithdrawing nitro group **L6** increases the acidity of the 2-hydroxybenzaldehyde OH thereby favouring keto-amine tautomeric formation like the 2-aminopyridine counterpart. This is reflected in the band observed at 430 nm in the spectrum of **L6**.

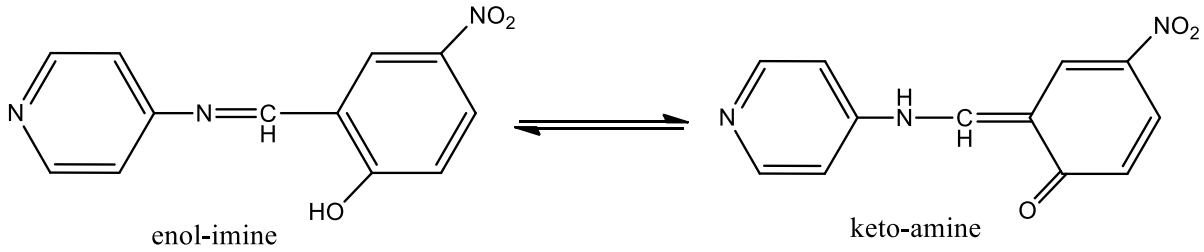

Figure 90: Keto-enol tautomer in N(5-nitro-2-hydroxybenzylidene)pyridin-4-amine (**L6**)

The charge transfer band observed in all the compounds is more porounced in **L6**, strong electro withdrawing nitro group substituent. This makes it behave as a good charge transfer acceptor center with the non-bonding orbital of the azomethine group as the main participant of the electron donor group. The charge transfer band shifts to longer wavelength in the order H<Br<NO_2. The band due to $\pi-\pi*$ observed in all the compounds is insensitive to the nature of the substituent.

The position of the nitrogen atom in the pyridine ring contributed to some differences observed in the spectra of the 2- and 4-aminopyridine Schiff bases. The band due to transition between the $\pi-$orbital largely localized on the central C=N bond observed in the spectra of the 2-aminopyridine Schiff bases was absent in the spectra of the 4-aminopyridine Schiff bases counterparts. Also, the charge transfer transition was observed at lower wavelength with higher extinction coefficient in the spectra of the 4-aminopyridine Schiff bases than the 2-aminopyridine counterparts. This indicates that there is more

interaction between the 4-aminopyridine Schiff bases and the solvent which lead to the decrease in the π–electron of the aromatic ring.

5.4.3 Electronic absorption spectra of the INH-based Schiff bases

The electronic absorption spectra of the INH based Schiff bases were also recorded in DMF in the region 260-500 nm. The results show that there is no interference from the keto-amine tautomer. All the compounds exist predominantly in the enol-imine tautomer The charge transfer band shifts to longer wavelength with increase in the electrowithdrawing nature of the substituent in the order H<OCH_3<Br<NO2. This indicates a decrease in HOMO-LUMO energy gap probably as aresult of stabilization of the HOMO by the electro withdrawing groups on the aldehyde. There is no observable substituent effect as on the π–π∗ transition band.

5.5 Synthesis and characterization of Schiff base metal complexes

Each synthesized Schiff base was reacted with $CuCl_2.2H_2O$, $NiCl_2.6H_2O$ and $CoCl_2.6H_2O$ to obtain Cu(II), Ni(II) and Co(II) complexes. The complexes were characterized using melting point, elemental analyses, atomic absorption, infrared (IR) and electronic absorption spectroscopy.

5.5.1 Physical and analytical data of 2-aminopyridine Schiff base metal complexes

The physical and analytical data of the 2-aminopyridine Schiff base metal complexes presented in Tables 13, 16, 19 and 22 show that the melting points of all the complexes are different from those of their corresponding ligands suggesting the formation of the metal complexes. The complexes were obtained in relatively good yields except compounds **L2B** (46%) and **L4B** (49%). The elemental analysis of each of the metal complexes agreed with the molecular formula suggested.

5.5.2 Physical and analytical data of 4-aminopyridine Schiff base metal complexes

The physical and analytical data of the 4-aminopyridine Schiff base metal complexes are presented in Tables 25, 28 and 31. Their melting points are different from those of their corresponding ligands suggesting the formation of the metal complexes. The complexes were obtained in good yields. The elemental analysis of each of the metal complexes agreed with the molecular formula suggested.

5.5.3 Physical and analytical data of INH Schiff base metal complexes

The physical and analytical data of the INH Schiff base metal complexes are presented in Tables 34, 37, 40, 43 and 46. The melting points reveal the formation of the metal complexes due to difference from those of their corresponding ligands. The complexes were obtained in good yields. The elemental analysis of each of the metal complexes agreed with the molecular formula suggested.

5.6 Infrared spectra of the Schiff bases metal complexes

Ligand vibrations occur in the high frequency (wavenumber) region while the low frequency region originates from both ligand vibrations and metal-ligand (M-L) coordinate bonds. The high frequency vibrations are generally expected to be predominantly ligand sensitive while low frequency vibrations are likely metal sensitive. However, the nature of the ligand is also extended to the behavior of the metal-ligand vibrations (Housecroft and Sharpe, 2008). The ligand substituent can sometimes affect the behavior of the M-L vibration but this depends on how well it can coordinate to the metal ion. Based on this, the infrared spectra of the free ligands were compared with those of their corresponding isolated complexes in order to ascertain the binding mode of the Schiff bases to the metal ion.

5.6.1 Infrared spectroscopy of the 2-aminopyridine Schiff bases metal complexes

A study and comparison of the IR spectra of the 2-aminopyridine Schiff base and their metal complexes suggest that the Schiff bases (**L1-L4**) act as bidentate ligands in nature with the

azomethine nitrogen and phenolic oxygen as the two coordination sites. It is well known that the ligand bands are shifted to either lower or higher frequency with simultaneous variation in the intensity when a metal complex is formed (Housecroft and Sharpe, 2008). The general trend observed is that the band due to phenolic OH group disappeared in the spectra of the complexes indicating the involvement of the phenolic oxygen group in coordination. In addition, a considerable shift (v±6-20) was observed in the v(C-O) frequency as a consequence of coordination of the phenolic oxygen of the ligands to the metal ion. This result corroborates the findings of Tantaru *et al*., 2012. The $C=N_{(imine)}$ stretching frequency increased to higher wavenumber in the spectra of most complexes except the **L1A** and **L1B** complexes of the unsubstituted ligand and the **L3C** complex of the bromo substituted ligands which have their stretching frequencies shifted to a lower wavenumber. This result suggests that coordination to most of the metal ions increased the electron density of the $C=N_{(imine)}$ bond which resulted in increased double bond character. The implication is that there is no metal-ligand backbonding. In contrast, the corresponding **L1A**, **L1B** and **L3C** differs with the lowering of the $v(C=N)_{(imine)}$ suggesting significant backbonding from the metal into the antibonding orbital of the $C=N_{(imine)}$ bond. The presence of coordinated water in the spectra of the metal complexes was confirmed by the appearance of bands at 842-888 cm^{-1} (Abdel-Latif *et al*., 2007). In the spectra of all the metal complexes, new bands appeared at 482-521 cm^{-1} and 444-477 cm^{-1} assigned to v(M-O) and v(M-N) vibrations respectively (Naeimi and Moradian, 2012). This strongly supports coordination through the phenolic oxygen and imine nitrogen respectively. It is also interesting to note that these bands are absent in the spectra of the ligands.

5.6.2 Infrared spectroscopy of the 4-aminopyridine Schiff bases metal complexes

The spectra data of the 4-aminopyridine Schiff base complexes given in Tables 26, 29 and 32-30 show that the coordination sites are the azomethine nitrogen (C=N) and the phenolic oxygen atoms.

Unlike the 2-aminopyridne complexes, these complexes exhibited opposite shift in the C=N stretching frequencies. Most of the spectra shifted to lower wavenumber except **L5B**, **L5C** and **L6B**.

The shift to lower wavenumber suggests metal-ligand backbonding while compounds **L5B**, **L5C** and **L6B** experienced no backbonding from the metal into the antibonding orbital of the $C=N_{(imine)}$. The C-O stretching frequencies for all the 4-aminopyridine complexes increased to higher wavenumbers when compared to the spectra of the corresponding ligands suggesting that the phenolic oxygen atom is involved in coordination. This result corroborates the findings of Abdel-Latif *et al*., 2007 and Abd El-Halim, *et al*., 2011. The orientation of the pyridine nitrogen does not favour its use as coordination site. The analytical data suggest presence of water molecule in all the complexes except **L5B** and **L6B**. Weak absorption in the region 850-874 cm^{-1} substantiate this evidence. . New bands which are absent in the spectra of the ligands appeared at 453-529 cm^{-1} and 414-489 cm^{-1} in the spectra of all the complexes. These bands are assigned to *v*(M-O) and *v*(M-N) vibrations respectively (Abdel-Latif *et al*., 2007; Abd El-halim *et al*., 2011).

The slight differences observed in the spectra of the 2-and 4-aminopyridine Schiff base complexes is evidence that the position of nitrogen atom in the pyridine moiety insignificantly affected the IR character. Consequently, nitrogen is not involved in the coordination.

5.6.3 Infrared spectroscopy of the INH Schiff bases metal complexes

A comparison of the IR spectra of the INH- Schiff base and their metal complexes suggest that the Schiff bases (**L8-L11**) act as tridentate ligands in nature with the phenolic oxygen, carbonyl oxygen and azomethine nitrogen as the three coordination sites as shown in Tables 35, 38, 41 and 44. This is inconsistent with the reports of Abou-Melha, 2008, Singh and Gupta, 2008, Mishra and Sharma, 2009, Kriza *et al*., 2010, Nair and Thankanami, 2010 and Patel *et al*., 2011. The *v*OH stretching vibration disappeared in the spectra of the metal complexes confirming coordination of the ligands to

the metal ions through the phenolic oxygen. This is also supported by a shift to either a lower or higher wavenumber observed in the *v*C-O stretching frequency. Broad band suitable as coordinated water *v*(H_2O)appeared in the spectra of the nickel complexes (**L8B**, **L9B** and **L10B**) within the region

3320-3366 cm^{-1}. There was noticeable changes in the C=O stretching frequency in the spectra of all the metal complexes (**L8A**-**L11C**). This band disappeared in the spectra of most of the complexes and shifted to higher wavenumber in the spectra of **L8C** and **L11A,** thus suggesting involvement of the carbonyl oxygen in coordination to the metal (Abou-Melha, 2008, Mishra and Sharma, 2009; Joseph *et al*., 2012). The $C=N_{(imine)}$ stretching frequency shifted to lower wavenumber in the spectra of all the metal complexes. This result suggests significant backbonding from the metal into the antibonding orbital of the $C=N_{(imine)}$ bond and support coordination through the imine nitrogen atom (Kriza *et al*., 2010, Nair and Thankanami, 2010 and Patel *et al*., 2011). New bands absent in the spectra of the ligands were observed in the spectra of the metal complexes within the region 467-622 and 446-548 cm^{-1} assigned to the *v*(M-O) and *v*(M-N) vibrations respectively. The general trend observed in the spectra of complexes **L8A**-**L11C** is that there is no significant substituent effect observed in the IR character and the ligands coordinated through the oxygen and nitrogen atoms.

The bonding mode of the INH ligands containing the hetero atoms was elucidated by the comparison of IR spectra of the ligands **L12–L13** with those of the corresponding metal complexes **L12A-L13C**. The absorption bands observed at 1644–1661 cm^{-1} for *v*(C=O) of the ligands disappeared in most of the complexes but shifted by a frequency +96 cm^{-1} upon coordination of **L12** with the cobalt ion **L12C**, thus suggesting involvement of the carbonyl oxygen in coordination to the metal (Aboul-Fadi *et al*., 2003; Mishra and Sharma, 2009; Joseph *et al*., 2012). The bands in the region *v*(NH) 3007–3198 cm^{-1}, which were observed in the IR spectra of the free ligands were absent in the spectra of all

the complexes. This observation in our view suggest coordination of the potentially tautomeric ligands (Figure.78) to the metal through the imidol oxygen in analogy with the literature precedents

(Deepa and Dravindakshan, 2004, Singh and Kumar, 2006; Wu *et al*., 2007, Sharma *et al*., 2010). This is further supported by the appearance of a new band in the region 1516–1533 cm^{-1} of the spectra of the complexes attributed to the azine group > C=N-N=C< (Sharma *et al*., 2010).

The bands due to the azomethine group of the ligands shifted by lower frequency of about 11–14 cm^{-1} in the complexes confirming metal–ligand bond formation through the azomethine nitrogen. New bands appearing in the region 494–702 and 432–596 cm^{-1}, which are assigned to *v*(M–O) and *v*(M–N) respectively (Usharani *et al*., 2012) further confirming the bidentate nature of the ligands with carbonyl-oxygen (C=O) and azomethine nitrogen (C=N-) as coordination sites.

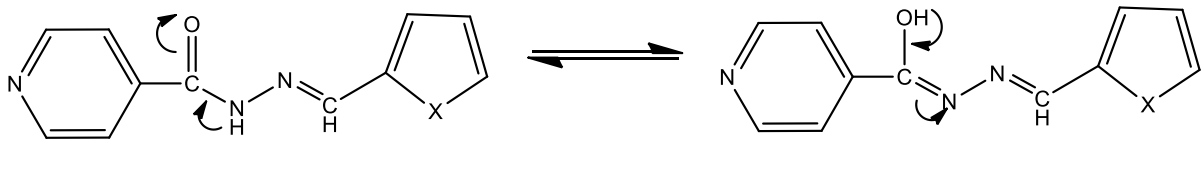

X
NH = L12
S = L13

Figure 91: Tautomeric form of INH-Schiff bases containing hetero-atom.

5.7 Electronic absorption spectra data of the Schiff bases metal complexes

The absorption bands of the metal complexes in 10^{-3} M DMF solutions were recorded at room temperature. The spectra provide information on all the complexes as bands in the region above 400 nm is indicative of the coordination of the ligands to the metal ion in most cases.

5.7.1 Electronic absorption spectra the 2-aminopyridine Schiff bases metal complexes

The electronic absorption data of the isolated complexes of the 2-aminopyridine Schiff bases are listed in Tables 15, 18, 21 and 24 while the spectra are shown in Figures 47, 49, 51 and 53. The spectra of the copper complexes of this series **(L1A-L4C)** exhibited absorption band at 410-430 nm. This could be attributed to the d-d transition characteristics of a square planar geometry for a d^9 complex. This is in analogy with the literature precedent **(**Abdel-Latif *et al*., 2007**).** However, the d-d

transition is not easy to discern in the spectra of the nitro containing complex **(L2A)** because no band was observed above 400 nm. Based on available data, a square planar geometry has been proposed

for the complex. The nickel complexes of the unsubstituted **(L1B)** and methoxy substituted **(L4B)** ligands displayed bands at 496 and 454 nm respectively. These bands are assigned to the d-d transition of a square planar geometry for a d8 complex. This corroborates the finding of Naeimi and Moradian, 2012. In addition, the nickel complexes of the nitro (L2B) and bromo(L3B) substituted ligands show bands distinctive of an octahedral geometry for a d^8 complex. Chohan *et al*., 2001 and Aliyu and Mohammed, 2009, also assigned an octahedral geometry to a Schiff base nickel complex. All the cobalt complexes of this series displayed bands characteristic of an octahedral geometry and were assigned accordingly.

5.7.2 Electronic absorption spectra the 4-aminopyridine Schiff bases metal complexes

The 4-aminopyridine Schiff base complexes exhibited similar spectral behaviour as the 2-aminopyridine counterpart. All the copper complexes displayed bands characteristic of a square planar geometry within the region 401-424 nm. While this is true, the nickel complexes exhibited varied geometries. The nickel complex of the unsubstituted ligand (**L5B**) exhibited bands at 561 and 677 nm. These bands are typically characteristic for octahedral configuration (Abd-Elzaher, 2004, Raja, *et al*., 2009). On the other hand, there is a high energy shift of the band positions as the

substituent on the ligand becomes better electron withdrawing.Such shifts have been observed for the nickel complexes containing the nitro (**L6B**) and the bromo (**L7B**) substituted ligands. These complexes consist of bands at 402 and 424 nm which are characteristic for square planar geometry. As observed for the 2-aminopyridine-based cobalt complexes, all the 4-aminopyridne based cobalt complexes displayed bands typical of octahedral configuration.

5.7.3 Electronic absorption spectra of the INH Schiff bases metal complexes

The electronic spectra data of the copper, nickel and cobalt complexes of the INH based Schiff bases (**L8A-L13C**) are presented in Tables 36, 39, 42, 45, 48, 51 and spectra shown in Figures 61, 63, 65, 67, 69 and 71. The first series of this group (**L8A-L11C**) displayed similar electronic transition. The copper complex of the unsubstituted ligand (**L8A**) showed a band at 466 nm which is characteristic for octahedral geometry. There was a high energy shift of the band position as the substituent on the ligand became electron withdrawing. The shift was observed for the nitro (**L9A** = 459 nm) and bromo (**L10A** = 427nm) containing complexes. On the other hand, low energy shift was observed for the methoxy (**L11A**) containing complex. In this case as in previous report (Shebi *et al*., 2010) octahedral geometry was proposed for all the copper complexes. All the nickel complexes of this series displayed bands at 410-447 nm. It is important to consider a combination of factors other in assigning geometries to simple transition metal complexes.

On the basis of the physical and spectral data of the nickel complexes, octahedral geometry was proposed to all the nickel complexes. On the other hand, the electronic spectra of the cobalt complexes showed significant bands in the range 430-468 nm which may be assigned to the transition in an octahedral geometry (Shebi *et al*., 2010). While this is true for the cobalt complexes of the unsubstituted (**L8C**), the nitro(**L9C**) and bromo (**L10C**) substituted ligands, the methoxy containing

complex (**L11C**) displayed a well structured bands at 338 and 466 nm. The band at 466 nm is characteristic band for a tetrahedral geometry.

The electronic absorption spectra data of the complexes of INH ligands containing the hetero atoms (**L12A-L13C**) are presented in Tables 48-49 and the spectra shown in Figures 53-54.

The general trend is that the complexes have the same tentative geometries. The electronic spectra data of ligands **L12** and **L13** copper complexes displayed a band at 419, 505 nm and 435 nm which may be attributed to square planar geometry. The nickel and cobalt complexes of ligand **L13** exhibited bands at a higher wavelength compared to the **L12** counter parts. The shift in the electronic bands of **L13B** and **L13C** in 10^{-3} M DMF implies that the d-d bands are affected to some extent by the complex dissociation in DMF.

On the basis of the information from the electronic spectra of most of the complexes discussed above, proposed geometries are assigned to the complexes. The microanalysis and IR data also support these geometries.

5.8 Molar conductance for the Schiff bases metal complexes

The molar conductance of the isolated complexes (**L1A-L14C**) were measured in 10^{-3} M DMF solutions. The molar conductance measurement of the 2-aminopyridine Schiff base complexes ranged from 2.16–8.40 $ohm^{-1}cm^2mol^{-1}$. This shows they are non-electrolytes. Also, the 4-aminopyridine Schiff base complexes had values in the range 2.10-4.24 $ohm^{-1}cm^2mol^{-1}$ indicating their non-electrolytic nature. There is a high compliance with the general formula $[MLX.nH_2O].nH_2O$ for the aminopyridine Schiff base complexes (**L1A-L7C**). The INH-based metal complexes had values 2.42-6.42 $ohm^{-1}cm^2mol^{-1}$ except compounds **L8B**, **L8C**, **L9B** and **L11B** which had values in the range 35.85-48.20 $ohm^{-1}cm^2mol^{-1}$. This corresponds to a proposed formula of $[ML.nH_2O].X.nH_2O$ which reveal they are 1:1 electrolytes (Aboul-Melha, 2008).

5.9 Proposed structures of some of the Schiff bases metal complexes

The structures of the Schiff base metal complexes were proposed based on the spectroscopic and analytical data.

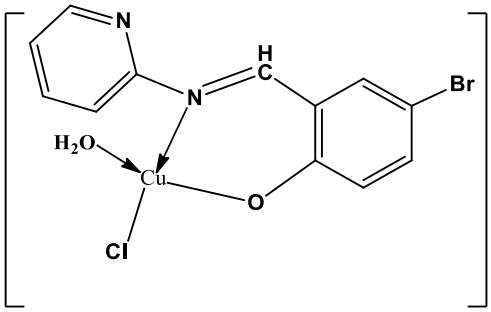

L3A

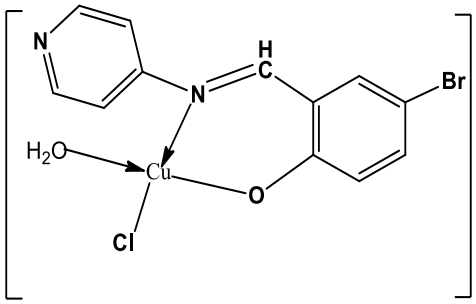

L7A

Figure 92: Proposed structures for some copper(II) complexes of aminopyridine Schiff bases

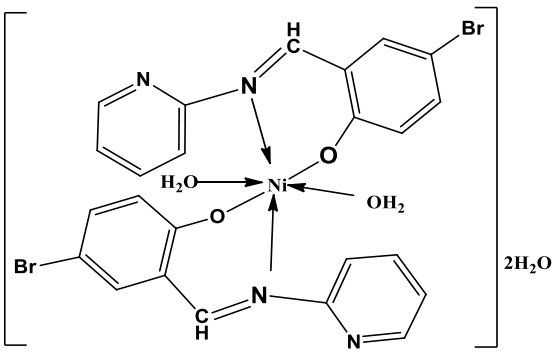

L3B

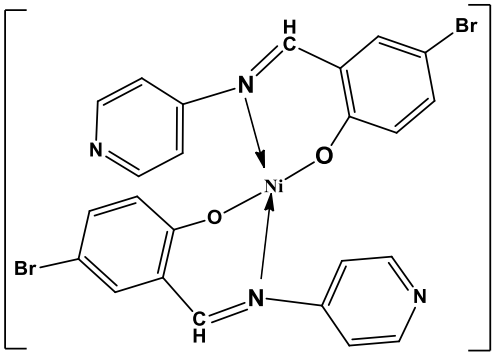

L7B

Figure 93: Proposed structures for some nickel(II) complexes of aminopyridine Schiff bases

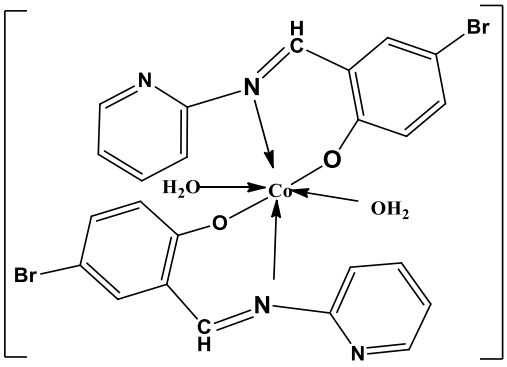

L3C

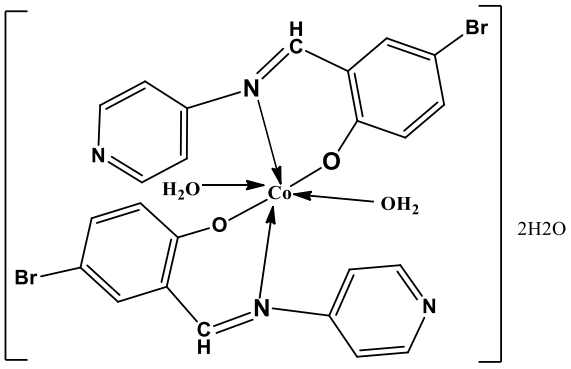

L7C

Figure 94: Proposed structures for some cobalt(II) complexes of aminopyridine Schiff bases

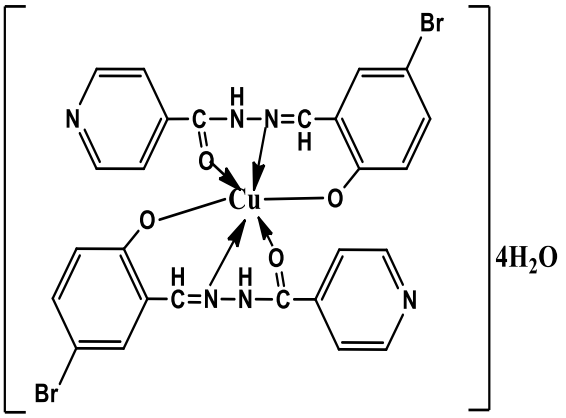

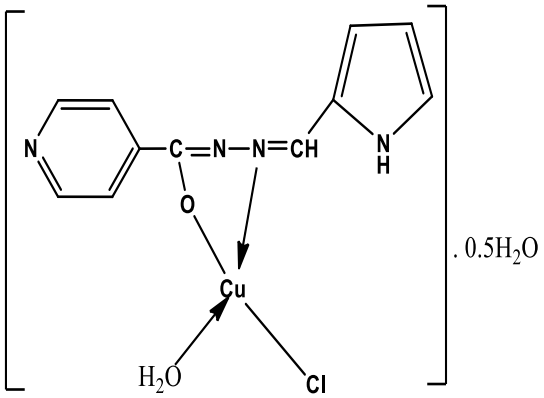

L9A **L12A**

Figure 95: Proposed structures for some copper(II) complexes of INH Schiff bases

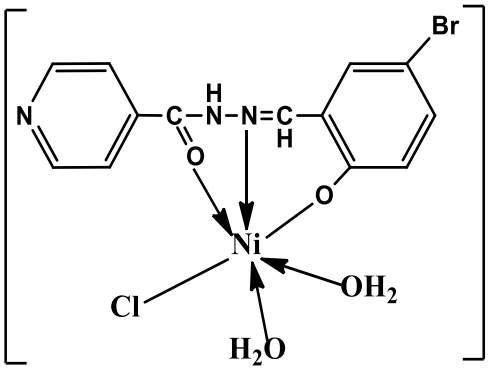

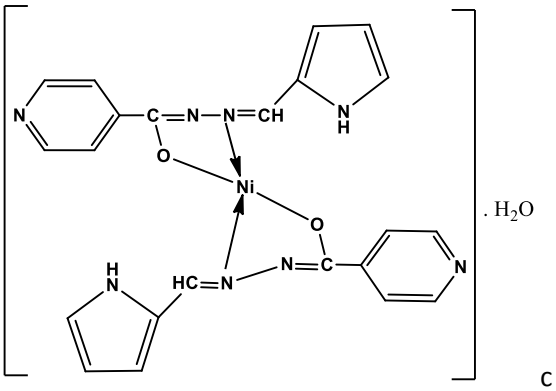

L9B **L12B**

Figure 96: Proposed structures for some nickel(II) complexes of INH Schiff bases

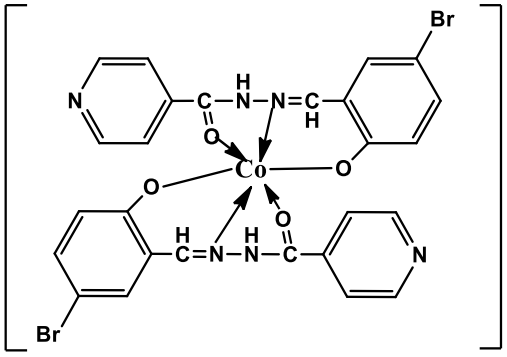

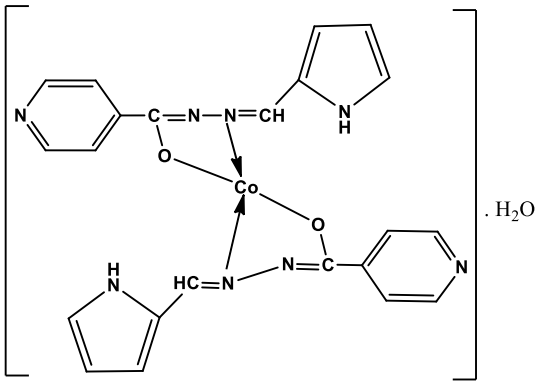

L9C **L12C**

Figure 97: Proposed structures for some cobalt(II) complexes of INH Schiff bases

5.10 Antituberculosis study

Results of the *in-vitro* anti-tuberculosis activity showed that not all the compounds are active against *Mycobacterium tuberculosis* $H37R_V$ and the clinical isolate. However, comparative study of the Schiff bases and their metal complexes showed that some of the complexes exhibited enhanced anti-tuberculosis activity over the free ligands and the reference compound used (INH). The increased anti-tuberculosis activity of the metal complexes over the ligands and the reference compound (INH) in line with previous reports arises due to increase in cell permeability (Tarallo *et al*., 2010; Joseph *et al*., 2012) and can be explained on the basis of overtone concept and chelation theory. According to

overtone concept, metal complexes are expected to exhibit better activity over their corresponding ligands as the lipid membrane that surrounds the *M.TB* cell favours passage of lipid soluble materials. Metal complexes according to chelation theory have high lipid character over the ligands. This is because chelation reduces the polarity of the metal ion by the partial sharing of its positive charge with the donor group. This interaction, in turn increases the delocalization of the pi-electrons over the whole chelate ring and hence enhances the lipophilicity of the complexes. This increased lipophilicity enhances the penetration of the complexes into the lipid membrane (Siddappa and Sunilkumar, 2013).

5.10.1 The anti-tuberculosis activity of the 2-aminopyrdine Schiff bases

The activity of this group reveals the significant effect of substituent on anti-tuberculosis activity. It was evident that **L1**, the unsubstituted ligand did not show activity against all the strains and concentrations of bacteria used but on addition of nitro (**L2**), bromo (**L3**) or methoxy (**L4**) group, activity was observed. This may be attributed to the increased weight (bulkiness) which may have contributive effect on the activity. The increased activity of **L2** when compared to the reference compound (INH) supports the findings of Solak and Rollas (2006) and Pandey *et al*. (2011) that the presence of a nitro group is responsible for the increased antimycobacterial activity of the Schiff base compounds. In addition, many compounds containing nitro group are known to be toxic. The activity

of **L4**, the methoxy containing ligand on the clinical isolate qualifies it as a very potential anti-tuberculosis agent.

5.10.2 The anti-tuberculosis activity of the complexes of 2-aminopyrdine Schiff bases

The introduction of copper, nickel or cobalt ion into the 2-aminopyridine Schiff base scaffold either increased or reduced the anti-tuberculosis activity of the corresponding ligand. This is in analogy with the literature precedents (Chohan *et al*., 2001, Deepa and Aravindakshan, 2004). The coordination of **L2** to copper ion (**L2A**) resulted in significant increased toxicity when compared with other complexes in this group and reference compound (INH). Activity was observed at 0.05 μg/mL.

The general trend observed was that the 2-aminopyridine Schiff bases and their corresponding complexes showed enhanced activity on the standard strain than the clinical isolate. As expected, activity increased with increase in the concentration of the compound and decrease in the colony forming unit per milliliters (CFU/ml) of the bacteria strain.

5.10.3 The anti-tuberculosis activity of the 4-aminopyrdine Schiff bases

The results of the *in vitro* anti-tuberculosis activity of the 4-aminopyridine Schiff bases presented in Tables 61-66 showed that the ligands from this group were poorly active compared with the 2-aminopyridine analogue. The reason for this poor activity may be due to the 4-position of the nitrogen atom in the pyridine moiety. This group also exhibited significant substituent effect on their activity. The nitro containing compound (**L6**) showed activity comparable to the reference compound (**INH**).

5.10.4 The anti-tuberculosis activity of the complexes of 4-aminopyrdine Schiff bases

The 4-aminopyridine Schiff bases exhibited remarkable increase anti-tuberculosis activity upon complexation to copper, nickel and cobalt ions. This may be due to the high lipid character of the metal complexes over the ligand which enhanced penetration of the metal complexes into the

Mycobacterium tuberculosis cell membrane. When compared with the reference compound used in the study, the complexes showed comparable activity with it (INH). However, the copper and cobalt complexes of the nitro (**L6A and L6C**) containing ligands displayed enhanced activity over the reference compound. In addition, **L6A** exhibited activity against the clinical isolate at 0.4 μg/mL.

Based on the *in vitro* anti-tuberculosis activity results of the 2-and 4-aminopyridine based compounds, the 2-aminopyridine compounds exhibited increased activity over the 4-aminopyridine analogue in all cases. It may be that the presence of the nitrogen atom in 2-position is important for the increased activity. The aminopyridine based Schiff based showed reduced activity against the clinical isolate. This poor activity may be attributed to differences in the morphology of this organism as a result of mutation.

5.10.5 The anti-tuberculosis activity of the INH Schiff bases

The evaluation of the *in vitro* anti-tuberculosis activity of the INH-based Schiff bases reveal that most of the synthesized ligands exhibited comparable activity with the reference compound against the standard strain. However, the nitro containing compound (**L9**) showed increased activity over the reference compound. Most of the ligands exhibited activity against the clinical isolate at 0.4 μg/mL except the nitro and bromo containing ligands. This shows that the presence of electronwithdrawing group decreases activity against the clinical isolate. Surprisingly, ligand **L14** showed the highest activity on 10^{-4} CFU/ml of the clinical isolate which is comparable with the reference compound. This implies that having a sulphur group in addition to INH may lead to an increased anti-tuberculosis activity. In general, activity was slightly influenced by the type of substituent. The poor activity against the clinical isolate in all the cases may be attributed to differences in the morphology of this organism as a result of mutation.

5.10.6 The anti-tuberculosis activity of the complexes of INH Schiff bases

The activity of the INH-based Schiff bases increased upon complexation. This implies that formation of complexes reduces polarity and hence improves toxicity. The result shows that the complexes exhibited enhanced activity over the reference compound (INH) in most cases. Of significance is the nickel complexes of **L12** and cobalt complexes of **L9** and **L12** which exhibited striking activity on 10^{-4} CFU/ml of the standard strain at 0.05 μg/mL compared with the reference compound with highest activity at 0.2 μg/mL. With the exception of **L12A** all the complexes in this group exhibited varied activity. It is interesting to know that the presence of nickel and cobalt ion enhanced the activity of the sulphur containing ligand L14. These complexes (**L14B** and **L14C**) showed increased activity on the clinical isolate at 0.1 μg/mL compared with the reference compound with highest activity at 0.2 μg/mL.

In general, the presence of the metal ion enhanced the in vitro anti-tuberculosis activity of Schiff bases on both strains of *M.TB* used. Although, some of the complexes exhibited either comparable or more activity relative to the reference compound, it is envisaged that their modes of action may be different from that of the reference compound. which may make it difficult for the bacterium to develop resistance.

CHAPTER SIX

6.0 SUMMARY OF FINDINGS AND CONCLUSION

This research was set out to identify new potential metal-based anti-tuberculosis agents. The study design involved synthesis, characterization and evaluation of the *in vitro* anti-tuberculosis activity of new pyridine and INH based metal complexes against *M.TB* strains.

Seven pyridine-based Schiff base ligands were obtained from the reaction of 2- (**L1-L4**) and 4-(**L5-L7**) aminopyridine with 2-hydroxybenzaldehyde, 5-nitro-2-hydroxybenzaldehyde , 5-bromo-2-hydroxybenzaldehyde and 5-methoxy- 2-hydroxybenzaldehyde. However, all efforts to obtain the Schiff base with 4-aminopyridine and 5-methoxy-2-hydroxybenzaldehyd e using different methods did not give the excepted products rather multiple products which were difficult to separate were obtained.

Six INH based Schiff base ligands (**L8-L13**) were also synthesized from INH and 2-hydroxybenzaldehyde, 5-nitro-2-hydroxybenzaldehyde, 5-bromo-2-hydroxybenzaldehyde, 5-methoxy-2-hydroxybenzaldehyde, pyrrole-2-carboxaldehyde and thiophene-2-carboxaldehy
de.

The synthesized compounds (**L1-L13**) were fully characterized using melting point, elemental analysis, infrared, NMR and electronic absorption spectroscopy. Metal complexes were obtained by reacting the ligands with Cu, Ni and Co chlorides. The metal content was obtained using atomic absorption spectroscopy.

Four Schiff bases which to the best of my knowledge are being reported for the first time include *N*-(5-nitro-2-hydroxybenzylidene)pyridine-2-amine (**L2**), *N*-(5-nitro-2-hydroxybenz

ylidene)pyridine-4-amine (**L6**), *N*-(5-bromo-2-hydroxybenzylidene)pyridine-4-amine.(**L7**) and *N*-(5-nitro-2-hydroxybenzylidene)isonicotinohydrazide (**L9**).

Reaction of the Schiff bases (**L1-L13**) with $CuCl_2.2H_2O$, $NiCl_2.6H_2O$ and $CoCl_2.6H_2O$ afforded thirty nine (39) metal complexes of which twelve (12) metal complexes comprising of the copper, nickel and cobalt complexes of *N*-(5-nitro-2-hydroxybenzylidene)pyridin-2-amine, *N*-(5-nitro-2-hydroxybenzylidene)pyridin-4-amine, *N*-(5-bromo-2-hydroxybenzylide ne)pyridin-4-amineand*N*-(5-nitro hydroxybenzylidene)isonicotinohydrazide are reported for the first time to the best of my knowledge.

The *in-vitro* anti-tuberculosis activity of the Schiff bases and their metal complexes was investigated on *Mycobacterium tuberculosis* $H_{37}R_V$ and clinical isolate using the proportion method. The 2-aminopyridine compounds exhibited higher activity than the 4-aminopyridine compounds in all cases. The nitro and bromo substituted Schiff bases showed increased activity over the unsubstituted compounds.

Compounds with INH moiety were more active than the reference compound (INH) in most cases with the nitro and bromo substituted Schiff bases exhibiting increased activity than the unsubstituted.

In most cases, the presence of the metal ion increased the anti-tuberculosis activity of the Schiff bases. Of significance is the copper and cobalt complexes of the nitro containing compounds (**L2A** and **L9C**) and the nickel complex of the pyrrole containing compound (**L12B**) which showed increased activity at 0.05 μg/mL when compared to the reference compound (INH) with highest activity at 0.2 μg/mL. In addition, the cobalt complexes with pyrrole and thiophene moiety have shown the heteroaromatic as desirable compounds in the development of new antituberculosis agent.

Some of the investigated compounds represent a novel strategy to prepare new anti-tuberculosis agents considering the present results especially those obtained for ligands **L2**, **L9** and complexes **L2A**, **L9C**, **L12B**, **L12C** and **L13C** which were found to be comparable to approved compound with anti-tuberculosis effects even at a lower concentrations.

Future research in this area to complement the findings reported here include,

- *In vivo* anti-tuberculosis study of *N*-(5-nitro-2-hydroxylbenzylidene)pyridine-2-amine, *N*-(5-nitro-2-hydroxylbenzylidene)pyridine-4-amine, INH-derivatives and their metal complexes against several clinical strains of *M.TB* using water as solvent. This will actually demonstrate the effectiveness of the compounds in anti-tuberculosis drug development.

- Anti-tuberculosis activity of more Schiff base metal complexes containing heteroaromatic atom needs to be investigated.

- Investigation of the mechanism of action of the potential antituberculosis compounds reported.

- The x-ray structural studies (crystal or powder) of the synthesized metal complexes needs to be carried out.

- Also the screening for anticancer activity of the synthesized compounds.

CHAPTER SEVEN

7.0 CONTRIBUTIONS TO KNOWLEDGE

1. This study has established a reproducible synthetic route to 4-aminopyridine Schiff bases which have been previously difficult to isolate. The following Schiff bases were isolated: *N*-(5-nitro-2-hydroxybenzylidene)pyridin-4-amine and *N*-(5-bromo-2-hydroxybenzylidene) pyridin-4-amine. It also reports for the first time the synthesis of *N*-(5-nitro-2-hydroxybenzaldehyde) pyridin-2-amine and *N*-(5-nitro-2-hydroxybenzaldehyde)isonicotinohydrazide.

2. This research has also provided additional baseline data on the synthesis of **12** novel Cu(II), Ni(II) and Co(II) complexes of the newly synthesized Schiff bases.

3. The study represents the first probe of the *in-vitro* anti-tuberculosis activity of all the Cu(II), Ni(II) and Co(II) complexes synthesized. Some of these may be useful in guiding future efforts to discover new compounds with increased anti-tuberculosis activity

REFERENCES

Ababei, L. V., Kriza, A., Andronescu, C. and Musuc, A. M. (2011). Synthesis and characterization of new complexes of some divalent transition metals with isonicotinamido-4-chlorobenzaladimine, *J. Serb. Chem*., **76**(8), 1103-1115.

Abdel-Latif, S. A., Hassib, H. B. and Issa, Y. M. (2007). Studies on some salicylaldehyde Schiff base derivatives and their complexes with Cr(III), Mn(II), Fe(III), Ni(II) and Cu(II). *Spectrochim. Acta Part A*, **67**, 950-957.

Abd El-Halim, H. F., Omar, M. M.; Mohamed, G. G and El-Ela Sayed, M. (2011). Spectroscopic and biological activity studies on tridentate Schiff base ligands and their transition metal complexes. *Eur. J. Chem*., **2**(2), 178-188.

Abd-Elzaher, M. M. (2004). Synthesis and spectroscopic characterization of some ferrocenyl Schiff bases containing pyridine moiety and their complexation with cobalt, nickel, copper and zinc. *J. Chinese Chem. Soc.,* **51**, 499-504.

Aboul-Fadi, T., Abdel-Hamid, M. and Hassan, E. (2003). Synthesis, antitubercular activity and pharmacokinetic studies of some Schiff bases derived from 1-alkylisatin and isonicotinic acid hydrazide (INH). *Arch. Pharm. Res*., **26**, 778-784.S

Abou-Melha, K. S. (2008). Transition metal complexes of isonicotinic acid (2-hydroxybenzylidene)hydrazide. *Spectrochim. Acta Part A*, **70**, 162-170.

Abu-Surrah, A.S. and Kettunen, M. (2006). Platinum Group Antitumor Chemistry: Design and development of New Anticancer Drugs Complementary to Cisplatin. *Curr. Med. Chem*., **13**, 1337-1357.

Adeleye, A. I., Ayolabi, C. I., Onubogu, C. C., Isawumi, A. O. and Nshiogu, M. E. (2004). Antimicrobial activity of crude extracts of twelve medicinal plants and Epa-ijebu (a wonder cure concoction) used in the South-West Nigeria on five common bacterial pathogens. *Handard Medicus,* **51**, 1-8.

Agilent Technologies Inc. (2012). Flame Atomic Absorption Spectrometry Analytical Methods, Manual Part Number: 8510000900, 10th Edition.

Aggarwal, N., Kumar, R., Dureja, P. and Rawat, D. S. (2009). Schiff bases as potential fungicides and nitrification inhibitors. *J. Agric. Food Chem*., **57**, 8520-8525.

Agrawal, S., Thomas,N. S., Dhanikula, A. B., Kaul, C. L. and Panchagnula, R. (2001). Antituberculosis drugs and new drug development. *Curr. Opin. in Pulmonary Med*., **7,** 142–147.

Agotegaray, M. A., Boeris, M. A. and Quinzani, O. V. (2010). Significant Anti-Inflammatory properties of a copper(II) Fenoprofenate complex compared withb its parent drug. Physical and chemical characterization of the complex. *J. Braz. Chem. Soc*., **21**, 2294-2301.

Al-Douh, M. H., Al-Fatlawy, A.A. and Abid, O. H. (2003). Synthesis and characterization of some 2-(N-benzoyl-N-pyrid-4-yl aminobenzyl)-aminobarbituric acids via Schiff bases. *Hadhramout for studies and Res*., **4**, 1-15.

Ali, S A., Youssef, T A. and Abdel-Rahman, L H.(2009). Structural studies of new group 6 complexes of salicylidene-2-aminopyridine. *J. Coord. Chem*., **62**(4), 577—582.

Alias, M., Kassum, H. and Shakir, C. (2014).Synthesis, physical characterization and biological evaluation of Schiff base M(II) complexes. *J. Assoc. Arab Uni. Basic Appl. Sci*., **15**, 28-34.

Aliyu, H. N. and Mohammed, A. S.(2009). Synthesis and characterization of iron (II) and nickel (II) Schiff base complexes. *Bayero J.Pure and Appli. Sci*., **2**(1), 132-134.

An, C., Feng, X., Zhao, N., Liu, P., Wang, T. and Lian, Z. (2014). Synthesis, structures, and third-order nonlinear optical properties of three new copper complexes based on salicylaldehyde phenoxyacetohydrazide ligand. *J. Coord. Chem*., **67**(22), 3621-3632.

Ananthi, N., Balakrishnan, U., Velmathi1, S., Manjunath,K. B. and Umesh, G. (2012). Synthesis, characterization and third order non linear optical properties of metallo organic chromophores. *Optics and Photonics J*., **2**, 40-45.

Anitha, C., Sumathi, S., Tharmaraj, P. and Sheela, C.D. (2011). Synthesis, characterization, and biological activity of some transition metal complexes derived from novel hydrazone azo Schiff base ligand. *Int. J. Inorg. Chem*., 1-8.

Arshi, N., Shahnawaaz, M., Rao, A. V., Seth, D. S. and Sharma, N.K. (2009).Synthesis of Schiff bases *via* environmentally benign and energy-efficient greener methodologies. *E-J. Chem.*, **6**(S1), S75-S78.

Arulmurugan, S., Kavitha, H. P. and Venkatraman, B. R. (2010). Biological activities of Schiff base and its complexes: A Review. *Rasayan J. Chem*., **3**(3), 385-410.

Asiri, A. M. and Badahdah, K. O.(2007), Synthesis of Some New Anils: Part 1. Reaction of 2-Hydroxy-benzaldehyde and 2-Hydroxynaphthaldehyde with 2-Aminopyridene and 2-Aminopyrazine, *Molecules*, **12**, 1796-1804

Azzouz, A. S. P. (2010). Synthesis of Schiff bases derived from benzaldehyde and salicylaldehyde with some amino acids by a new develop method. *Nat. J. Chem.*, **37**, 158-168.

Baricordi, N., Benetti, S., Biondini, G., De Risi, C.and. Pollini, G. P.(2004). A new one-pot synthesis of 2-substituted 3-nitropyrrolidines through a multicomponent domino reaction, *Tetrahedron Lett*., **45** (7), 1373–1375.

Banerjee, A., Dubnau, E. and Quemard, A. (1994). InhA, a gene encoding a target for isoniazid and ethionamide in Mycobacterium tuberculosis. *Sci*., **263**, 227-230.

Barris E. (2000). Tuberculosis in times of health sector reform. *Int. Tuberc. Lung Dis.*, **4**, 595–596.

Barceloux, D. G.and Barceloux, D. (1999). Nickel. *Clinical Toxicology*, **37**(2), 239-258.

Bayrak, H., Demirbas, A., Karaoglu, S. A.and Demirbas, N. (2009).Synthesis of some new 1,2,4-triazoles, their Mannich and Schiff bases and evaluation of their antimicrobial activities *Eur. J. Med. Chem*., **44** (3), 1057–1066.

Behpour, M., Ghoreishi, S. M., Mohammadi, N., Soltani, N. Salavati-Niasari, M. (2010). Investigation of some Schiff base compounds containing disulfide bond as HCl corrosion inhibitors for mild steel. *Corrosion Sci.*, **52**, 4046–4057.

Berkowitz, B. A and Katzung, B. G. (2004). Basic and clinical pharmacology. Lange Medical, McGraw–Hill, New York, 9th edition, 67–74.

Bernstein, J., Lott, W. A., Steinberg, B. A. and Yale, H. L. (1952). Chemotherapy of experimental tuberculosis in isinicotinic acid hydrazide (nydrazid) and related compounds. *Am. Rev. Tuber*., **65**, 357-364.

Bhagat, S., Sharma, N. and Chundawat, T. S. (2013). Synthesis of Some Salicylaldehyde-Based Schiff Bases in Aqueous Media. *J. Chem.*, **2013**, 1-4.

Blumberg, G., Koitzsch, A., Gozar, A., Dennis, B. S., Kendziorac, A., Fournier, P. and Greene, R.L. (2003) American thoracic society/centers for disease control and prevention/infectious diseases societyof America: treatment of tuberculosis. *Am. J. Respir*. *Crit. Care Med*., **167**, 603-662.

Budhani, P., Igbal, S. A., Bhattacharya, S. M. M. and Mitu, L. (2010). Synthesis, characterization and spectroscopic studies of pyrazinamide metal complexes. *J Saudi Chem. Soc*., **14**, 281-285.

Chakraborty, H., Paul, N. and Rahman, M. L. (1994). Catalytic activities of Schiff base aquo complexes of copper(II) towards hydrolysis of amino acid. *Trans. Metal Chem*., **19**, 524-526.

Chakraborty, M., Baweja, S., Bhagat, S. and Chundawat, T.(2012). Microwave assisted synthesis of Schiff bases: A Green Approach. *Int. J. Chem. Reactor Engr*., **10**(1), 1542-6580.

Chen, P., Gearhart, J., Protopopova, M., Einck, L. and Nacy, C. A. (2006). Synergistic interactions of SQ109, a new ethylene diamine, with front-line antitubercular drugs *in vitro*. *J. Antimicro. Chemother.*, **58**, 332–337.

Chohan, Z. H., Arif, M., Shafiq, Z., Yaqub, M. and Supuran, C. T. (2006). *In vitro* antibacterial, antifungal and cytotoxic activity of some isonicotinoylhydrazide Schiff bases and their cobalt (II), copper (II), nickel (II) and Zn(II) complexes. *J. Enzyme. Inhibit. Med. Chem*., **21**(1), 95-103.

Chohan, Z. H., Munawar, A. and Supuran, C.T. (2001). Transition metal ion complexes of Schiff bases. Synthesis, characterization and antibacterial properties, *Metal-Based Drugs*, **8**(3), 137-143.

Chohan, Z. H. and Kausar, S. (2000). Synthesis, characterization and biological properties of tridentate NNO, NNS and NNN donor thiazole derived furanyl, thiophenyl and pyrrolyl Schiff bases and their Co(II), Ni(II), Cu(II) and Zn(II) metal chelates. *Metal-Based Drugs*, **7**(1), 17-22.

Cimerman, Z., Miljanić, S. and Galić, N. (2000). Schiff bases derived from aminopyridines as spectroflourimetric analytical reagents. *Croatica Chem. Acta,* **73**, 81-95.

Cocco, M. T., Congiu, C., Onnis, V., Pusceddu, M. C., Shivo, M. L. and Logu, A. (1999). synthesis and antimycobacterial activity of some isonicotinohydrazones. *Eur. J. Med. Chem*., **34**, 1071-1076.

Corbett, E. L., Steketee, R. W., ter Kuile, F. O., Latif, A. S., Kamali, A. and Hayes, R. J. (2002). HIV-1/AIDS and the control of other infectious diseases in Africa. *The Lancet*, **359**(24), 2177-2187.

Costi, R., Artico, M. and Di-Santo, R. (1999). Pyridinylpyrroly analogs of isoniazid: Synthesis and antimycobacterial activities. *Med. Chem. Res*., **9**, 408-423.

Crouch, P. J., Hung, L. W., Adlard, P. A., Cortes, M. and Lal, V. (2009). Increasing Cu bioavailability inhibits Abeta oligomers and tau phosphorylation. *Proc. Natl. Acad. Sci.*, **106**, 381–386.

Dabrowiak, J. C. (2009). Nanomedicine, in Metals in Medicine, John Wiley and Sons, Ltd, Chichester, 4th edition. pp, 322.

Da Silva, C. M., Da Silva, D. L., Modolo, L. V., Alves, R. B., De Resende, M. A., Martins, C. V. B. and De Fatima, A. (2011). Schiff bases: A short review of their antimicrobial activities. *J. Adv. Res*., **2**, 1-8.

Dearling, J. L. J., Lewis, J. S., Muller, G. E. D., Welch, M. J. and Blower, P. J. (2002). Copper bis(thiosemicarbazone) complexes as hypoxia imaging agents: structure-activity relationships. *J. Bio. Inorg. Chem*., **7**, 249-259.

Deepa, K. P. and Aravindakshan, K. K. (2004). Synthesis, characterization and antifungal studies of transition metal complexes of ω–bromoacetoacetanilide isonicotinylhydrazone. *Appl. Biochem. and Biotech*., **118**, 283-291.

De Souza, M.V.N. (2006). Current status and future prospects for new therapies for pulmonary tuberculosis. *Curr. Opin. Pulm. Med*., **12**, 167–171.

Dholariya, H. R., Patel, K.S., Patel, J. C., Patel, A. K.and Patel, K. D. (2013). Thermal, kinetic, spectroscopic studies and anti-microbial, anti-tuberculosis, anti-oxidant properties of clioquinol and benzo-coumarin derivatives mixed complexes with copper ion. *Med. Chem. Res*., **22**(12), 5848-5860.

Di Bella, S., Fragala, I., Guerri, A., Dapporto, P. and Nakatani, K. (2004). Second-order non-linear optical properties of transition metal complexes. *Inorg. Chim. Acta*, **357**, 1161-1167.

Dimiza, F., Papadopoulos, A.N., Tangoulis, V., Psycharis, V., Raptopoulou, C P., Dimitris P. Kessissoglou, D. P.and Psomas, G.(2012). Biological evaluation of cobalt(II) complexes with non-steroidal anti-inflammatory drug naproxen. *J. Inorg. Biochem*., **107**(1)**,** 55-64.

Donnelly, P. S., Liddel, J. R., Lim, S. C., Paterson, B. M., Cater, M. A., Sawa, M. S. and Mot, A. L. (2008). Selective intracellular release of copper and zinc ion from bis(thiosemicarbazonato)

complexes reduces levels of Alzheimer disease amyloid-beta peptide, *J. Biol. Chem*., **283**, 4568-4577.

Eicher, T., Hauptmann, S., and Speicher, A. (2013). The Chemistry of Heterocycles: Structures, Reactions, Synthesis, and Applications. Wiley-VCH., New York, 3rd edition, pp, 632.

Falzari, K., Zhu, Z., Pan, D., Liu, H., Hongmanee, P. and Franzblau, S. G. (2005). *In vitro* and *in vivo* activities of macrolide derivatives against *Mycobacterium tuberculosis. Antimicrob. Agents Chemother*., **49**, 1447-1454.

Fasina, T. M. and Dada, R. O. (2013). Substituent effect on electronic absorption and biological properties of Schiff bases derived from aniline. *J. Chem. Pharma. Res*., **5**(10), 177-181.

Fasina, T. M., Ogundele, O.O., Ejiah, F. N. and Dueke-Eze, C. U. (2012). Biological activity of copper(II), cobalt(II) and nickel(II) complexes of Schiff base derived from o-phenylenediamine and 5-bromosalicayaldehyde. *Int. J. Bio. Chem*., **6**, 30 -37.

Ferreira, M. De L., Thatyana, R.A., Vasconcelos, T. R. A., De Carvalho, E. M., Lourenço, M. C. S., Wardell, S. M. S. V., Wardell, J. L., Ferreira, V. F. and De Souza, M. V. N. (2009)**.** Synthesis and antitubercular activity of novel Schiff bases derived from D mannitol.*Carbohydrate Res*., **344**(15), 2042-2047.

Ferreira, M. De L., Gonçalves, R. S. B., De F. Cardoso, L. N., Kaiser, C. R., Candéa1, A. L. P.,Maria das Graças M. de O. Henriques , Lourenço, M. C. S., Bezerra, F. A. M. and Marcus De Souza, M. V. N. (2010). Synthesis and antitubercular activity of heteroaromatic isonicotinoyl and 7-Chloro4-quinolinyl hydrazone derivatives. *Sci. World J*., **10**, 1347–1355.

Fessenden, R. J. and Fessenden, J. S. (1998). Organic Chemistry, Brooks/Cole Publishing company, California. 6th edition, pp, 587.

Figgs, B. N. (1966). An introduction to Ligand Field. Wiley. New York, 2nd edition.

Firn, R. (2010). Nature's Chemicals. Oxford University Press, Oxford. p 74-75.

Fox W., Ellard, G. A. and Mitchison, D. A. (1999). Studies on the treatment of tuberculosis undertaken by the British Medical Research Council Tuberculosis Units, 1946–1986, with relevant subsequent publications.. *Int. J. Tuberc. Lung Dis*., **3**, 231-279.

Fugu, M. B., Ndahi, N. P., Paul, B. B. and Mustapha, A. N. (2013). Synthesis, characterization, and antimicrobial studies of some vanillin schiff base metal (II) complexes. *J.Chem. Pharm. Res*., **5**(4), 22-28.

Fujimori, T., Yasui, H., Hiromura, M. and Sakurai, H. (2007). Suppressive effect of orally administered copper(II)-aspirinate (Cu-2(asp)(4)) complex on the generation of reactive oxygen species in the skin of animals subjected to UV exposure. *Exp. Dermatol*.,**16**, 746-752.

Gahr, A. A. (1990). Spectrophotometric studies on some Schiff bases derived from benzidine. *Spectrochim. Acta*, **46A**, 1751-1757.

Ganjali, M. R., Norouzi, P., Alizade, H. and Salavati-Niasari, M. (2007). Synthesis of a new hexadentate Schiff base and its application in the fabrication of a highly selective mercury(II) sensor. *Bull. Korean Chem. Soc*., **28**(10), 68-72.

Gemma, S., Kukreja, G., Fattorusso, C., Persico, M., Romano, M., Altarelli, M., Savini, L., Xu, S-L., Lu, R-C., Shi, L. and Zhu, H-L. (2010). Design, synthesis and pharmacological investigation of iodine salicylimine, new prototype of antimalarial drug candidate. *Arch. Pharm. Chem*., **343**, 382-390.

Gibaud, S. and Metzler-Nolte, N. (2010). Arsenic-Based drugs: From fowler's solution to modern anticancer chemotherapy. *Organomet. Chem*., **32**, 1-20.

Gluster, J. R. (1991). Structural aspects of metal liganding to functional groups in protein. *Adv. Protein Chem*., **42**, 1-73.

Golpalakrishnan, M., Sureshkumar, P., Kanagarajan, V and Thanusu, J. (2007). New environmentally friendly, solvent free synthesis of imines ssing calcium oxide under microwave irradiation. *Res. Chem. Intermed*., **33**(6), 541-548.

Grange, J. M and Zumla, A. (2002). The global emergency of tuberculosis: what is the cause? *J. Royal Soc. Promotion of Health*, **122** (2), 78–81.

Gudasi, K. B. and Goudar, T. R. (2000). Synthesis and characterization of lanthanide(III) complexes with salicylidene 2-aminopyridine. *Synth. React. Inorg. Met-org. Chem*., **30**(10), 1859-1869.

Gul, N. Y., Topal, A., Cangul, T. and Yanik, K. (2008). The effects of topical tripeptide copper complex and helium-neon laser on wound healing in rabbits. *Veterinary Dermatol*., **19**, 7-14.

Guo, Z., Xing, R., Liu, S., Zhong, Z., Ji, X. and Wang, L.(2007). Antifungal properties of Schiff bases of chitosan, *N* -substituted chitosan and quaternized chitosan. *Carbohydrate Res.*, **342** (10), 1329–1332.

Guo, Z. and Sadler, P. J. (1999). Metals in Medicine : Reviews, *Angew Chem. Int. Ed*., **38**, 1512-1531.

Guzen,K.P., Guarezemini, A.S., Órfão, A. T. G., Cella, R., Pereira, C. M. P.and Stefani, H. A. (2007). Eco-friendly synthesis of imines by ultrasound irradiation. *Tetrahedron Lett*., **48** (10), 1845–1848.

Gwaram, N. S., Ali, H. M., Saharin, S. M., Abdulla, M. A., Hassandarvish, P., Lin, T. K., Ching, C. L. and Cher Lin Ooi, C. L. (2012). Synthesis, characterization and biological applications of some acetyl pyridine and acetophenone derivatives. *J. Appli. Pharmac. Sci.,* **2** (12), 027-038.

Haas, K. L. and Franz, K. J. (2009). Application of metal coordination chemistry to explore and manipulate cell biology. *Chem Rev*., **109**, 4921-4960.

Halli, M. B., Patil, V. B. and Bevinamarada, S. R. (2011). Synthesis, characterization, and biological activity studies of (E)-N-((thiophen-2-yl)methylene)benzofuran-2-carbohydrazide and its metal(II) complexes. *Turk. J. Chem*., **35**, 393 – 404.

Hambley, T. W. (2007). Developing Metal-based therapeutics: challenges and opportunities. *J. Chem. Soc*. *Dalton Trans*., **10**(43), 4929-4937.

Hammud, H. H., Ghannoum, A. and Masoud, M. S. (2006). Spectral regression and correlation coefficients of some benzadimines and salicylaldimines in different solvents. *Spectrochim. Acta* A, **63**, 255-265.

Hamza, M. S., Dücker-Benfer, C.and Van Eldik, R. (2000). Ligand substitution behavior of a simple model for Coenzyme B_{12}. *Inorg. Chem.*, **39**(17), 3777-3783.

Harish, R. and Kumar, G. A. (2009). Synthesis and antitubercular activity of some novel Schiff bases of 2-amino-5-aryl-1,3,4-oxadiazoles. *Res. J. Chem and Environ*., **13**(4), 55-58.

Hearn, M. J. and Cynamon, M. H. (2004). Design and synthesis of antituberculosis: Preparationand evaluation against *Mycobacterium tuberculosis* of an isoniazid Schiff base. *J. Antimicrob. Chemother*., **53**, 185-191.

Hearn, M. J., Cyanamon, M. H., Chen, M. F., Coppins, R., Davis,J., Kang, H. J-O., Noble, A., Tu-Sekine, B., Terrot, M. S., Trombino, D., Minh, T., Webster, E. S. and R. Wilson, R. (2009). Preparation and antitubercular activities of *in vitro* and *in vivo* of novel Schiff bases of Isoniazid. *Eur. J. Med. Chem*., **44**, 4169-4178.

Heffern, M. C.,Yamamoto, N., Holbrook, R. J., Eckermann, A L. and Thomas J Meade (2013). Cobalt derivatives as promising therapeutic agents. *Curr. Opin. Chem. Bio*, **17**, 189–196.

Hernandes, M. M., Mckee, M. L., Keizer, T. S., Yeaswood, B. C. and Atwood, D. A. (2002). Six-coordinate aluminium cations: characterization, catalysis, and theory. *J. Chem. Soc., Dalton Trans*, , 410-415.

Hine, J. and Yeh, C.Y. (1967). Equilibrium information and conformational isomerisation of imines derived from isobutyraldehyde and saturated aliphatic primary amines. *J. Am. Chem. Soc.,* **89**, 2669-2693.

Holm, R. H. and Solomon, E. I. (1966). Bioinorganic enzymology. *Chem. Rev*., **96**(7), 15-18.

Housecroft, C.E. and Sharpe, A. G. (2008). Inorganic Chemistry, Pearson and Education Ltd., Prentice Hall, 3rd edition, p, 638-640.

Hunoor, R.S.; Patil, B. R.; Badiger, D. S.; Vadavi, R. S.; Gudasi, K. B.; Chandrashekhar, V. M. and I.S. Muchchandi, I. S. (2010). Spectroscopic, magnetic and thermal studies of Co(II), Ni(II), Cu(II) and Zn(II) complexes of 3-acetylcoumarin–isonicotinoylhydrazone and their antimicrobial and anti-tubercular activity. *Spectrochim. Acta Part A: Mol and Biomol. Spect*., **77**, 838–844.

Ibrahim, M. N. and Sharif, S. A. (2007). Synthesis, characterization and use of Schiff bases as fluorimetric analytical reagents. *E-J. Chem*., **4**, 531-535.

Imramovsky, A., Polanc, S., Vinsova, J., Kocevar, M., Jampilex, J., Reckova, Zand. Kaustova, J.(2007). A new modification of antitubercular active molecules. *Bioorg. Med. Chem*., **15**, 2551-2559.

Jain, R. K. and Mishra, A. P. (2012). Microwave synthesis, spectral, thermal and antimicrobial activities of some transition metal complexes involving 5-bromosalicylaldehyde moiety. *Curr. Chem. Lett*., **1**, 163-174.

Jameison, E. R. and Lippard, S. J. (1999). Structure, recognition and processing of cisplatin-DNA adducts. *Chem. Rev*., **99**, 2467-2498.

Jammi, S., Saha, P., Sanyashi, S., Sakthivel, S. and Punniyamurthy, T. (2008). Chiral Binuclear Copper(II) catalysed Nitroaldol Reaction: Scope and mechanism. *Tetrahedron*, **64**, 11724-11731.

Joule, J. A. and Mills, K. (2013). Heterocyclic Chemistry at a glance. John Wiley, New York,. 2nd edition, pp 2.

Joule, J. A., Mills, K. and Smith, G. F. (1995). Heterocyclic Chemistry. Chapman and Hall, London. 3rd edition; pp 516.

Joseph, J., Nagashri, K. and Janaki, G.B. (2012). Novel metal based antituberculosis agent: Synthesis, characterization, catalytic and pharmacological activities of Copper complexes. *Eur. J. Med. Chem*., **49**, 151-163.

Kabak, M., Elmali, A and Elerman, Y. (1999). Keto–enol tautomerism, conformations and structure of N-(2-hydroxy-5-methylphenyl), 2-hydroxybenzaldehydeimine. *J. Mol. Struct.,* **477**, 151-159.

Kanwar, S. S., Lumba, K., Gupta, S. K., Katoch, V. M., Singh, P., Mishra, A. K., Kalia, S. B. (2008). Synthesis and mycobactericidal properties of metal complexes of isonicotinoyldithiocarbazic acid. *Biotech. Lett.,* **30**, 677-688.

Karbouj, R., El-Dissouky, A., Jeragh, B. and Al-Saleh, E. (2010). Synthesis, characterization and biological activity studies on (E)-N-[2-hydroxy-1,2-di(pyridine-2-yl)ethylidine] aroylhydrazides and their copper(II) complexes. *J. Coord. Chem*., **63**(5), 868-883.

Karmaker, S., Saha, T. K. and Sakurai, H. (2007). Investigation of a Cu-II-poly(gamma-glutamic acid) complex in aqueous solution and its insulin-mimetic activity. *Macromol. Biosci*., **7**, 456-466.

Karthikeyan, M. S., Prasad, D., J., Poojary, B., Bhat, K. S., Holla, B. S.,Kumari, N. S. (2006). Synthesis and biological activity of Schiff and Mannich bases bearing 2,4-dichloro-5-fluorophenyl moiety. *Bioorg. Med. Chem*., **14**(22), 7482–7489.

Keshavjee S. and Farmer, P. E.(2012). Tuberculosis, drug resistance, and the history of modern medicine. *N. Engl. J. Med.,* **367**, 931–936.

Khadsan, R. E., Tambatkar, G. D. and Meshram, Y. K. (2010). Synthesis of Schiff bases via eco-friendly and energy efficient greener methodologies. *Oriental J. Chem*., **26**(2), 681-683.

Kriza, A., Ignat, I., Oprea, O. and Stanica, N. (2010). Synthesis, characterization and thermal behavior of complexes compounds derived from Cu(II), Co(II), Ni(II) and Zn(II) and isonicotinoylhydrazone-2-indoline. *Rev. Chim*., **61**, 733-739.

Kulkarni, A., Patil, S. A.and Badami, P.S. (2009). Synthesis, characterization, DNA cleavage and *in vitro* antimicrobial studies of La(III), Th(IV) and VO(IV) complexes with Schiff bases of coumarin derivatives. *Eur. J. Med. Chem.,* **44** (7), 2904–2912.

Kuntz, I. D.(1992). Structure-based strategies for drug development and discovery. *Sci.*, **257**, 1078-1082.

Kuzniarska-Biernacka, I,, Bartecki, A and Kurzak, K. (2003). UV-Vis-NIR spectroscopy and colour of bis(N-phenylsalicylaldiminato)cobalt(II) in a variety of solvents. *Polyhedron*, **22**, 997-1007.

Kwan, C. K. and Ernst, J. D. (2011). HIV and tuberculosis: a deadly human syndemic. *Clin. Microbio. Rev*., **24**(2), 351-376.

Lee, A. S., Teo, A. S. and Wong, S. Y. (2001). Novel mutations in isoniazid resistant *Mycobacterium tuberculosis* isolates. *Antimicrob. Agents Chemother*., **45**, 2157-2159.

Lee, S., Hille, A., Frias, C., Kater, B., Bonitzki, B., Wolf, S., Scheffler, H., Prokop, A.and Gust, R. (2010). [Ni(II)(3-OMe-salophene)]: A Potent Agent with Antitumor Activity, *J .Med. Chem.*, **53**(16), 6064–6070.

Li, S., Chen, S., Ma, H., Yu, R. and Liu, D. (1999). Investigation on some Schiff bases as HCl corrosion inhibitors for copper" *Corros. Sci*., **41**, 1273-1279.

Li, G-Y., Du, K-J., Wang, Y., Liang, J-W., Kou, J-F., Hou, X-J., Ji, L-N. and Chao. H. (2013). Synthesis, crystal interaction and structure, DNA anticancer activity of tridentate copper(II) complexes. *J. Inorg. Biochem*., **119**, 43-53.

Liang, J-W., Wang, Y., Du, K-J., Li, G-Y., Guan ,R-L., Ji, L-N. and Chao. H. (2014). Synthesis, DNA interaction and anticancer activity of copper(II) complexes with 4'-phenyl-2,2':6',2″-terpyridine derivatives. *J. Inorg. Biochem*., **141**, 17-27.

Liu, Z-C., Yang, Z-Y., Li, T-R., Wang, B-D, Li, Y. and Wang, M-F. (2011). DNA-binding, antioxidant activity and solid state fluorescence studies of copper(II), zinc(II) and nickel(II) complexes with a Schiff base derived from 2-oxo-quinoline-3-carbaldehyde. *Trans. Met. Chem.*, **36**, 489-489.

Lourenco, M.C.S., Souza, M.V.N., Pinheiro, A.C., Ferreira, M. L., Goncalves, R.S.B., Nogueira, T.C.M. and Peralta, M. A. (2007). Evaluation of antitubercular activity of nicotinic and isoniazid analogues. *Arkivoc*, **15**, 181-187.

Lourenço, M. C, Ferreira, M. L., De Souza, M. V, Peralta, M. A, Vasconcelos, T. R, Henriques, M. D. (2008). Synthesis and antimycobacterial activity of (E) N'(monosubstitutedbenzylidene)isonicotinohydrazide derivatives. *Eur. J. Med. Chem*., **43**(6), 1344-1347.

Maccari, R., Ottana, R.and Vigorita, M. G. (2005). *In vitro* advanced antimycobacterial screening of isoniazid-related hydrazones, hydrazides and cyanoboranes: Part 14. *Bioorg. Med. Chem. Lett*., **15**, 2509–2513.

Marwani, H. M., Asiri, A. M. and Khan, S. A. (2012). Green-synthesis, characterization, photostability and polarity studies of novel Schiff base dyes using spectroscopic methods. *Bioorg. Chem*., **38**(5), 604-609.

Mashaly, M. M., Abd-Elwahab, Z. H. and Faheim, A. A. (2004). Preparation, spectral characterization and antimicrobial activities of Schiff base complexes derived from 4-aminoantipyrine. Mixed ligand complexes with 2-aminopyridine, 8-hydroxyquinoline and oxalic acid and their pyrolytical products. *J. Chinese Chem*., **51**(5A), 901-915.

McCord, J. M. and Fridovic, I. (2003). Superoxide dismutase an enzymic function for erythrocuprein (hemocuprein). *J. Biol. Chem*., **244**, 6049-6052.

Mehta, D. K., Martin, J., Jordan, B., Macfarlane, C. R., Ryan, R. S. M., Wagle, S.M. S., Hashmi, F. T., Kakar, S., Kouimtzi, M., Masieh, D., Radia, H.C. G., Sharm, V.K., Shing, T., Gallagher, G. P. (2003). Antituberculous drugs. *British National Formulary*, 283–287.

Mendham, J., Denney, R. C., Barnes, J. D. and Thomas, M. (2004). Vogel's textbook of quantitative chemical analysis. 6th edition, Pearson Education Ltd., Singapore. pp, 605.

Ming, L. J. (2003). Structure and Function of Metalloantibiotics. *Med. Res. Rev*., **23** (6), 697 –762.

Mishra, A.P. and Sharma, N. (2009). Synthesis, characterization, X-ray and thermal studies of some Schiff base metal complexes. *J. Ind. Council Chem*., **26**, 125-129.

Mittal, P., Joshi , S., Panwar, V. and Uma, V. (2009). Biologically active Co (II), Ni (II), Cu (II) and Mn(II) Complexes of Schiff Bases derived from Vinyl aniline and Heterocyclic Aldehydes. *Int. J. ChemTech. Res.,* **1**(2), 225-232.

Moffett, R. B. and Rabjohn, N. (1963). Organic Synthesis. John Wiley and Sons. Inc., New York, 4th edition, pp, 605.

Mohamed, M., Hapipah, M. A., Mahmood, A. A. and Robinson, T.W. (2009).Synthesis, structural characterization, and anti-ulcerogenic activity of Schiff base ligands derived from tryptamine and 5-chloro, 5-nitro, 3,5-ditertiarybutyl salicylaldehyde and their nickel(II), copper(II), and zinc(II) complexes. *Polyhedron*. **28**, 3993–3998.

Moulton, B. D. and Ma, Z. (2007). Neutral Pharmaceuticals. U.S. Patent Application 12/227,471.

Morrison, R. T. and Boyd, R. N. (2007). Organic Chemistry, sixth edition, Pearson Prentice Hall, New York, pp, 486.

Naeimi, H., Salimi, F. and Rabiei, K. (2006). Mild and convenient one pot synthesis of Schiff bases in the presence of P_2O_5/Al_2O_3 as new catalyst under solvent-free conditions. *J. Mol. Catal. A Chem*., **260** (1–2), 100–104.

Naeimi, H. and Moradian, M. (2012). Efficient synthesis and characterization of some novel nitro-Schiff bases and their complexes of nickel(II) and copper(II). *J. Chem*., **2013**, 1-8.

Nair, M. L. H. and Thankamani, D. (2010). Synthesis, physicochemical, antimicrobial and 3D molecular modeling studies of oxomolybdenum(V) and dioxomolybdenum(VI) complexes with a Schiff base isonicotinoyl(5-bromo-2-hydroxybenzylidene)hydrazide. *Russian J. Coord. Chem*., **36**(4), 259-268.

Nandi, J. and Sankar, V. K. (2012). Synthesis and Docking of the Schiff base derived from 4- aminopyridine, *J. Pharm. Sci. Inno.*, **1**(5), 9-12.

Navarro, M., Cisneros-Fajardo, E.; Lehmann, T.; Sánchez-Delgado, R. A.; Atencio, R.; Silva, P.; Lira, R. and Urbina, J. A. (2001). Toward a Novel Metal-Based Chemotherapy against Tropical Diseases: Synthesis and Characterization of New Cu(II) and Au(I) Clotrimazole and Ketoconazole Complexes and Evaluation of their Activity against *Trypanosoma Cruzi*. *Inorg. Chem.*, **40,** 6879-6884.

Nazir, F., Bukhari, I. H., Arif, M., Riaz, M., Naqvi, S. A R., Bokhari, T. H. and Jamal, M. A. (2013). Antibacterial Studies And Schiff Base Metal Complexes With Some Novel Antibiotics. *Int. J. Curr. Pharm. Res.*, **5(**3), .

Nazir, H., Yildiz, M., Yilmaz, H., Tahir, M. N. and Ulku, D. (2000). Intramolecular hydrogen bonding and tautomerismn in Schiff bases. Structure of N-(2-pyridil)-2-oxo-1-naphthylidenemethylamine. *J. Mol. Struct.*, **524**, 241-250.

Nestle, F. O., Speidel, H. and Speidel, M. O.(2002). Metallurgy: High nickel release from 1- and 2-euro coins. *Nature*, **419,** 132.

North Central Agricultural Experiment Stations. (1998). Recommended Chemical Soil Test Procedures for the North Central Region, Research Publication No. 221.

Olie, G. H. and Olive, S. (1984). The Chemistry of dye, Springer publishing press, Berlin, pp. 152.

Osowole, A.A.; Kolawole, G.A. and Fagade, O.E. (2005), Synthesis, physicochemical and biological properties of nickel(II), copper(II) and zinc(II) complexes of unsymmetrical tetradentate Schiff base and their Adducts. *Synth. React. Inorg. Met-Org. Chem.*, **35**, 829-834.

Osowole, A. A. and Balogun, S. A. (2012). Spectral, magnetic, thermal and antibacterial properties of some metal(II) complexes of aminodanyl Schiff base, *Eur. J. Appl. Sci*., **4**(1), 6-13.

Ott, I., Kircher, B., Bagowski, C.P., Vlecken, D.H.W., Ott, E.B., Will, J., Bensdorf, K., Sheldrick, W.S.and Gust, R. (2009). Modulation of the Biological Properties of Aspirin by Formation of a Bioorganometallic Derivative. *Angewandte Chemie*, **48**(6), 1160–1163.

Orvig, C. and Abrams, M. J. (1999). Medicinal Inorganic Chemistry: Introduction. *Chem. Rev*., **99**(9), 2201-2204.

Pandey, A., Dewangan, D., Verma, S., Mishra, A. and Dubey, R. D. (2011). Synthesis of Schiff bases of 2-amino-5-aryl-1,3,4-thiodiazole and its analgesic, anti-inflammatory, antibacterial and antituberculosis activity. *Int. J. ChemTech. Res*., **3**(1), 178-184.

Pandey, S and Srivastava, R. S. (2009). Anticonvulsant activity of some Schiff bases synthesized from 2- aminopyridine. *Pharmacology*, **2**, 1048-1074.

Patel, R. N., Singh, A., Shukla, K. K.,. Patel, D. K. and Sondhiya, V. P (2011). Synthesis, characterization and biological activity studies of octahedral nickel(II) complexes. *Trans. Met. Chem*., **36**, 179–187.

Patel, P. R., Thaker, B. T. and Zele, S. (1999). Preparation and characterisation of some lanthanide complexes involving a heterocyclic β-Diketon. *Indian J. Chem*., **38**A, 563-567.

Paterson, B. M. and Donnelly, P. S. (2011). Copper complexes of bis(thiosemicarbazones): from chemotherapeutics to diagnostic and therapeutic radiopharmaceuticals. *Chem. Soc. Rev*., **40**, 3005-3018.

Patil, S., Jadhav, S. D. and Patil, U. P. (2012). Natural Acid Catalyzed Synthesis of Schiff Base under Solvent-free Condition: As a Green Approach. *Archives of Appl. Sci. Res*., **4** (2), 1074-1078.

Patil, R. D. and Adimurthy, S. (2013). Catalytic methods for imine synthesis: Focus Review. *Asian J. Org. Chem.,* **2**, 726 – 744.

Patole, J., Shingnapurkar, D., Padhye, S. and Ratledge, C. (2006). Schiff base conjugates of p-aminosalicylic acid as antimycobacterial agents. *Bioorg. Med. Chem. Lett*., **16**, 1514-1517.

Pillay, V., Du Toit, L. C. and Danckwerts, M. P. (2006). Tuberculosis chemotherapy: current drug delivery approaches. A Review. *Respiratory Res*., **7**, 118-125.

Pourjavid, M. R., Sehat, A. A., Rezaee, M., Hosseini, M. H. and Razavi, T. (2012). Design and construction of high-sensitive and selective Dysprosium(III) electrochemical membrane sensor based on a thiourea derivatives. *Int. J. Electrochem. Sci*., **7**, 5133-5146.

Prakash, A. and Adhikari, D. (2011). Application of Schiff bases and their metal complexes-A Review. *Int. J. ChemTech. Res.*, **3**(4), 1891-1896.

Prasad, K. S., Kumar, L. S., Shekar, S. C., Prasad, M. and Revanasiddappa, H. D. (2011). Oxovanadium complexes with bidentate N, O ligands: Synthesis, characterization, DNA binding, nuclease activity and antimicrobial studies. *Chem. Sci. J*., **12**, 1-10.

Protopopova, M., Hanrahan, C. and Nikonenko, B. (2005). Identification of a new antitubercular drug candidate, SQ109, from a combinatorial library of 1,2-ethylenediamines. .*J. Antimicrob.*. *Chemother*., **56**, 968–974.

Ragavendran, J., Sriram, D., Patel, S., Reddy, I., Bharathwajan, N., Stables, J.and Yogeeswari , P. (2007). Design and synthesis of anticonvulsants from a combined phthalimide-GABA-anilide and hydrazone pharmacophore. *Eur. J. Med. Chem.*, **42**, 146-151.

Ragno, R., Marshall, G. R., Di Santo, R., Costi, R., Massa, S., Pompei, R. and Artico, M. (2000). Antimycobacterial pyrroles: Synthesis, antimycobacterium tuberculosis activity and QSAR studies. *Bioorg. Med. Chem*., **8**, 1423-1432.

Raja, K. K., Easwaramoorthy, D., Rani, S. K., Rajesh, J., Jorapur, Y., Thambidurai, S., Athappan, P. R. and Rajagopal, G. (2009). Synthesis, spectral, electrochemical and catalytic properties of Cu(II), Ni(II) and Co(II) complexes containing N, O donors. *J. Mol. Cataly*., **303,** 52-59.

Rakesh, Sun, D., Lee, R. B., Tangallapally, R. P.and Lee, R. E. (2009). Synthesis, optimization and structure activity relationships of 3,5-disubstituted isoxazolines as new anti-tuberculosis agents. *Eur. Med. Chem*., **44**, 460–472.

Raman, N., Ravichandran, S. And Thangaraja, C. (2004). Copper(II), cobalt(II),nickel(II) and zinc(II) complexes of Schiff base derived from benzil-2,4-dinitrophenylhydrazone with aniline. *J. Chem. Sci.,* **116**, 215-220.

Rao, S. N., Kathale, N., Rao, N. N. and Munshi, K. N. (2007). Catalytic air oxidation of olefins using molybdenumdioxo complexes with dissymmetric tridentate O, N, S-donor Schiff base ligands derived from o-hydroxyacetopheneone and S-benzyldithiocarbazate or S-methyldithiocarbazate. *Inorg. Chim. Acta*, **360**(14), 4010-4016.

Rathelot, P., Vanelle, P., Gasquet, M., Delmas, F., Crozet, M. P. and Timon-David, P. (1995). Synthesis of novel functionalized 5-nitroisoquinolines and evaluation of *in vitro* antimalarial activity. *Eur. J. Med. Chem*., **30**(6), 503–508.

Raval, J. P., Patel, N. H., Patel, H. V. and Patel, P.S. (2010). *In vitro* antimycobacterial activity of novel N-(4-(substituted phenyl amino)-6-(pyridine-2-yl amino)1,3,5-trizin-2-yl)isonicotinohydrazide. *Med. Chem. Res*., **20**(3), 274-279.

Ravishankar, L., Patwe, S. A., Gosarani, N. and Roy, A. (2010). Cerium(III)-catalyzed synthesis of schiff bases: a green approach. *Synthetic Communi.*, **40**(21), 3177–3180.

Rigamonti, L., Cinti, A., Forni, A., Pasini, A. and Piovesana, O. (2008). Copper(II) complexes of tridentate Schiff bases of 5-substituted salicylaldehydes and diamines: The role of the substituent and the diamine in the formation of mono-, di-and trinuclear Species, crystal structures and magnetic properties. *Eur. J. Inorg. Chem*., 3633–3647.

Rollas, S. and Kuckkguzel, S. G. (2007). Biological activities of hydrazones derivatives. *Molecules*, **12**, 1910-1939.

Rosenberg, B. (1971). Some biological effects of platinum compounds. *Platinum Metal Review*, 15, 42-47.

Rosu, T., Pahontu, E., Maxim, C., Georgescu, R., Stanica, N. and Gulea, A. (2011). Some new Cu(II) complexes containing an ON donor Schiff base: Synthesis, characterization and antibacterial activity. *Polyhedron*, **30**, 154-162.

Rujt, S. H. V. and Sadler, P. J. (2009). *Drug Discov. Today*, **14**, 23-24.

Sakthilatha, D. and Rajavel, R. (2013). The template synthesis, spectral and antibacterial investigation of new N_2O_2 donor Schiff base Cu(II), Ni(II), Co(II), Mn(II) and VO(IV) complexes derived from 2-hydroxyacetophenone with 4-chloro-2,6-diaminepyrimidine. *J. Chem. Pharm. Res*., **5**(1), 57-63.

Sandbor, U., Padhye, S., Billington, D., Rathbone, D., Franzblau, S., Anson, C. E. and Powell, A. K. (2002). Metal complexes of carboxamidrazone analogs as antitubercular agents 1. Synthesis, X-ray crystal-structures, spectroscopic properties and antimycobacterial activity against *Mycobactetrium tuberculosis* $H_{37}RV$. *J. Inorg. Biochem*., **90**, 127-136.

Sangamesh, A. P., Manjumatha, M., Udaykumar, V. K. and Prema, S. B. (2011). Synthesis, spectral, characterization and biological evaluation of Co(II), Ni(II), Cu(II), and Mn(II) metal complexes of novel isatin Schiff base ligand. *Der. Pharma. Chem*., **3**(3), 97-108.

Savchenko, V. I., Dorokhov, V. G., Yakushchenko, I. K., Zyuzin, I. N. and Aldoshin,, S. M. (2010). Developing state-of-the-art antiseptic based on pyridine derivatives. *Herald Russ. Acad. Sci*., **80**(2), 149-154.

Sawant, S., Yagmar, R. and Nivid, Y. (2013). Synthesis , Characterisation and anti- tuberculosis activity of novel transition metal complexes of heterocyclic Schiff bases. *Int. J. Adv. Res*., **1**(9), 1-21.

Schiff, H.(1864). Mittheilungen aus dem universitaslaboratorium in Pisa: Eine neue organischer basen. *Justus Liebigs Ann. Chem*., **131**(1), 118-119.

Shamspur, T., Sheikhshoaie, M., Mashhadizadeh, M. H.and Saeednia, S. (2012). A PVC Membrane Electrode for Zirconium Based on 4-Nitrophenylazo-n-(2-hydroxypropylamine) Salicylidine. *Gazi University J. Sci*., **25**(3), 609-616.

Sharma, S. K., Mohan, A. and Kadhiravan, T. (2005). HIV-TB co-infection: epidemiology, diagnosis and management. *Indian J. Med. Res.*, **121**(4), 550-567.

Sharma, K. K., Singh, R., Fahmi, N. and Singh, R. V. (2010). Synthesis, coordination behavior and investigation of pharmacological effects of some transition metal complexes with isoniazid Schiff bases. *J. Coord. Chem*., **63**(17), 3071-3082.

Shaw, C. F. III, (1999). Gold-based therapeutic agents. *Chem. Rev*., **99**, 2589-2600.

Shebi, M., Khalil, S. M. E.and Al-Gohani, F. S. (2010). Preparation, spectral characterization and antimicrobial activity of binary and ternary Fe(III), Co(II), Ni(II), Cu(II), Zn(II), Ce(III) and UO_2(VI) complexes of a thiocarbohydrazone ligand. *J. Mol. Struct*., **980**, 78-87.

Sheeja-Lovely, K. L. P. and Christudhas, M. (2013). Synthesis, characterization and biological activities of Schiff base complexes of Cu(II), Ni(II), and Co(II) with 4-pyridine carboxaldehyde and 3-aminopyridine. *J. Chem. Pharma. Res*., **15**(2), 184-191.

Siddappa, K. and Sunilkumar, B. M. (2013). Pharmacological activity of (E) 3-2-(1-(1-hydroxynaphthalen-2-yl)methyleneamino)phenyl)-2-methylquinazole-4(3H)-one Schiff base and its transition metal complexes. *Int. J. Pharm. Pharmaceut. Sci*., **5**(3), 725-732.

Simeon, A., Maquart, F. X., Chastang, F., Birembaut, P., Gillery, P. and Wegrowski, Y. (1999). Expression and activation of matrix metallo-proteinases in wounds: modulation by the tripeptide –coppercomplex glycyl-L-histidyl-L-lysine-Cu^{2+} *J. Invest. Dermatol*., **112**(6), 957-964.

Singh, V. P.(2008). Synthesis, electronic and ESR spectral studies on copper(II) nitrate complexes with some acylhydrazines and hydrazones. *Spectrochim. Acta Part A*, **71**, 17–22.

Singh, V. P. and Gupta, P. (2008). Synthesis, physic-chemical characterization and antimicrobial activity of cobalt(II), copper(II), zinc(II) and cadmium(II) complexes with some acyldihydrazones. *J. enzyme inhibit. Med. Chem*., **23**(6), 797-805.

Singh, P. K. and Kumar, D. N. (2006). Spectral studies on cobalt(II), nickel(II) and copper(II) complexes of naphthaldehyde substituted aroylhydrazones. *Spectrochim. Acta Part A***, 64**, 853-858.

Singh, P. and Dhakarey, R. K. S. (2009). Synthesis, characterization and antimicrobial studies of metal complexes with Schiff bases derived from 2-thienyl glyoxal. *Rasayan J. Chem*., **2**(4), 869-874.

Singh, J., Jain, P. and Tyagi, M. (2014). Synthesis, IR, EPR, Uv-visible characterization and *in vitro* antimicrobial activity of macrocyclic Schiff's base and its metal complexes of Mn(II) and Co(II). *World J. Pharmacy Pharma. Sci*., **3**(10), 953-964.

Sitasawad, S., Deshpande, M., Katdare, M., Tirth, S. and Parab, P. (2001). Beneficial effect of supplementation with copper sulfate on STZ-diabetic mice. *Diabetes Res. Clin. Pract*., **52**, 77-84.

Solak, N. and Rollas, S. (2006). Synthesis and antituberculosis activity of 2-(aryl/alkyl amino)-5-(4-aminophenyl)-1,3,4-thiadiazoles and their Schiff bases. *Arkivoc*, **XII**, 173-181.

Soliman, A. A. (1997). Effect of solvents on the electronic absorption spectra of some salicylidene thio Schiff bases. *Specrochim. Acta A*., **53**, 509-515.

Sousa-Pedrares, A., Camiña, N., Romero, J., Durán, M. L., García-Vázquez, J. A. and Sousa, A. (2008). Electrochemical synthesis and crystal structure of cobalt (II), nickel (II), copper (II), zinc (II) and cadmium (II) complexes with 2-pyridinecarbaldehyde-(2′-aminosulfonylbenzoyl) hydrazone. *Polyhedron*, **27**(16), 3391-3397.

Sovilj, S P., Vasic, V. M., Stojic, D. L., Stojceva-Radovanovi, B. and Petkovska, L. T. (1998). Spectrophotometric Studies of the influence of organic solvents and substitutents on some Schiff bases. *Spect. Lett.*, **31**, 1107-1122.

Spinu, C., Pleniceanu, M. and Tigae, C. (2008). Biologically active transition metal chelates with a 2-thiophenecarboxyaldehyde-derived Schiff base: Synthesis, characterization and antibacterial properties. *Turk. J. Chem*., **32**, 487-493.

Sriram, D., Yogeeswari, P. and Madhu, K. (2005). Synthesis and *in vitro* and *in vivo* antimycobacterial activity of isonico-tinoyl hydrazones. *Bioorg. Med. Chem. Lett*., **15**, 4502–4505.

Sriram, D., Yogeeswari, P., Myneedu, N. S. and Saraswat, V. (2006). Abacavir prodrugs: Microwave-assisted synthesis and their evaluation of anti-HIV activities. *Bioorg Med Chem Lett*., **16** (8), 2127–2129.

Sriram, D., Senthikumar, P., Dinakaran, M., Yogeeswari, P., China, A. and Nagaraja, V. (2009). Antimycobacterial activities of novel fluoro quinolones. *Biomed. Pharmacother*., **63**(1), 27-35.

Srivastava, K. P., Vidyarthi, S. N. and Singh, R. (2011). Environmentally benign studies of bivalent transition metal complexes of tridentate (NNO donor) Schiff base ligands. *Der Chemica Sinica*, **2**(2), 66-76

Storr, T., Thompson, K. H. and Orvig, C. (2006). Design of targeting ligands in medicinal inorganic Chemistry. *Chem. Soc. Rev*., **35**, 534-544.

Sun, R. W-Y., Ma, D-L., Wong, E. L-M. and Che, C-M. (2007). Some uses of transition metal complexes as anti-cancer and anti-HIV agents. *J. Chem. Soc*. *Dalton Trans*., **10**(43), 4884-4892.

Surati, K. R. (2011). Synthesis, spectroscopy and biological investigations of manganese (III) Schiff base complexes derived from heterocyclic diketone with various primary amine and 2, 2′-bipyridyl. *Spectrochimica Acta Part A: Mol. and Biomol. Spectro.*, **79**(1), 272-277.

Swamy, B. N., Suma, T. K., Rao, G. V. and Reddy, G. C. (2007). Synthesis of isonicotinoylhydrazones from anacardic acid and their *in vitro* activity against *Mycobacterium smegmatis*. *Eur. J. Med. Chem*., **42**, 420–424.

Szekely, R., Waczek, F., Szabadkai, I., Nemeth, G., Hegymegi-Barakonyi, B., Eros, D., Szokol, B., Pato, J., Hafenbradl, D., Satchell, J., Saint-Joanis, B., Cole, S. T., Orfi, L., Klebl, B. M. and Keri, G. (2008). A novel drug discovery concept for tuberculosis: inhibition of bacterial and host cell signaling. *Immun. Lett*., **116**, 225–231.

Takayama, K., Wang, L. and David, H. L. (1972). Effect of isoniazid on the *in vivo* mycolic acid synthesis, cell growth and viability of *Mycobacterium tuberculosis*. *Antimicro. Agents. Chemother*., **2**, 29-35.

Talati, J. D., Desai, M. N. and Shah, N. K. (2005). Ortho-, meta-, and para-aminophenol-N-salicylidenes as corrosion inhibitors of zinc in sulfuric acid. *Anti-Corr. Methods and Mater.*, **52**(2), 108–117.

Tantaru, G., Vieriu, M. and Poiata, A. (2011). Synthesis and antimicrobial evaluation of different Schiff bases and their metal complexes. *Natura Montenegrina, Podgorila*, **9**(3), 889-895.

Tarallo, M. B., Urquiola, C., Monge, A., Costa,B. P., Ribeiro, R. R., Costa-Filho, A.J., Mercader, R. C., Pavan, F. R., Leite, C.Q-F., Torre, M. H. and Gambino, D. (2010). Design of novel Iron compounds as potential therapeutic agents against tuberculosis. *J. Inorg. Biochem*., **104**, 1164-1170.

Temel, H and Iihan, S. (2008). Prepared and characterization of new macrocyclic Schiff bases and theior binuclear copper complexes. *Spectrochim. Acta Part A*, **69**, 896-903.

Tezer, N. and Karakus, N. (2009). Theoretical study on the ground state intramolecular proton transfer (IPT) and salvation effect in two Schiff bases formed by 2-aminopyridine with 2-hydroxy-1-naphthaldehyde and 2-hydroxy salicylaldehyde. *J. Mol. Model*, **15**, 223-232.

Thompson, K. H. and Orvig, C. (2003). Boon and bane of metal ions in medicine. *Sci.*, **300**, 936-939.

Thompson, K. H. and Orvig, C. (2006). Metal complexes in medicinal Chemistry: New vistas and challenges in drug design. *J. Chem. Soc. Dalton Trans*., **6**, 761-764.

Timmns, G. S. and Deretic, V. (2006). Mechanisms of action of isoniazid. *Mol Microbiol*., **62**, 1220–1227.

Trujillo, A., Fuentealba, M., Carrillo, D., Manzur, C., Ledoux-Rak, I., Hamon, J-R. and Saillard, J-Y. (2010). Synthesis, spectral, structural, second-order non-linear optical properties and theoretical studies on new organometallic Donor-Acceptor Substituted nickel(II)and copper(II) unsymmetrical Schiff base complexes. *Inorg. Chem*., **49**, 2750-2764.

Ulucam, G. and Beynek, N. (2007). Template synthesis of new Schiff base complexes and determination of the structure of these complexes. *Scientific papers*. **35**(5), 65-70.

Utku, S., Gokce, M., Aslan, G., M Bayram, G., Ulger, M., Emekdas, G. and Fethisahin, M. (2011). Synthesis and in vitro antimycobacterial activities of novel 6-substituted-3(2H)-pyridazinone-2-acetyl-2-(substituted/non substituted acetophenone)hydrazone. *Tubitak,* **35**, 331-339.

Usharani, M., Akila, E. and Rajavel, R. (2012). Mixed ligand Schiff base complexes: synthesis, spectral characterization and antimicrobial activity. *J. Chem. Pharm. Res*., **4**(1), 726-731

Vedanayaki, S., Sandhanamalar, D., Jayaseelan, P. and Rajavel, R. (2010). Synthesis, structural characterization, thermal and antimicrobial evaluation of binuclear Cu(II), Ni(II) and VO(IV) Schiff base complexes. *Int. J. Pharm. and Tech*., **2**, 1118-1123.

Vibhute,A.Y., Mokle,S. S., Nalwar,Y. S., Vibhute, Y. B., Vasant M. and Gurav, V. M. (2009). An efficient and operationally simple synthesis of some new Schiff bases using grinding technique. *Bull. Catal. Soc. India*, **8**, 164-168.

Vicini, P., Incerti, M., Doytchinova, I., La Colla, P., Busonera, B.and Loddo, R. (2006). Synthesis and antiproliferative activity of benzo[d]isothiazole hydrazones. *Eur. J. Med. Chem*., **41**, 624-632.

Vilcheze, C., Morbidoni, H. R. and Weisbrod, T. R. (2000). Inactivation of the *inh*A-encoded fatty acid synthase II (FASII) enoyl-acyl carrier protein reductase induces accumulation of the FASI end products and cell lysis of *Mycobacterium Smegmatis. J. Bacteriol*., **182**, 4059-4067.

Vilcheze, C., Wang, F. and Arai, M. (2006) Transfer of a point mutation in *Mycobacterium tuberculosis* inhA resolves the target of isoniazid. *Nat Med*., **12**, 1027–1029.

Wang, J. Y., Burger, R. M. and Drlica, K. (1998). Role of superoxide in catalase–peroxidase-mediated isoniazid action against Mycobacteria. *Antimicrob Agents Chemother*., **42**, 709–711.

Williams, D. H. and Fleming, I. (1989). Spectroscopic Methods in Organic Chemistry, Mc-Graw Hill, New York, 4th edition, 40-52.

World Health Organization. (1994). TB: A Global Emergency. WHO Report No. 14977. WHO, Geneva, Switzerland.

World Health Organization. (2012). A Global Tuberculosis Report 2012., Geneva, Switzerland.

Wu, L-M., Teng, H-B., Ke, X-B., Xu, J-T., Liang, S-C. and .Hu, X-M. (2007). Copper(II) complexes of salicylaldehyde hydrazone: synthesis, structure and DNA interactions. *Chem. and Biodiver*., **4**, 2198-2209.

Yamgar, R. S., Y.Nivid, Y. and Sawant, S. S. (2013).Synthesis,characterisation and anti tuberculosis activity of novel transition metal complexes of heterocyclic Schiff bases. *Int. J. Adv. Res.,* **1**(9), 1-21.

Yang, H. J., Sun, W. H., Li, Z. I. and Ma, Z. (2002). The rapid synthesis of Schiff-base without solvent under microwave irradiation. *Chinese Chem. Lett*., **13**(1), 3–6.

Yang, Z. and Sun, P. (2006). Compare of three ways of synthesis of simple Schiff base, *Molbank,* **6**, 1-3.

Zhang, Y., Post-Martens, K. M. and Denkin, S. (2005). The magic bullets and tuberculosis drug targets: New drugs candidates and therapeutic targets for tuberculosis therapy. *Annual Rev. Pharmacol. Toxicol*., **45**, 529-564.

Zheng, Y., Ma, K., Li, H., Li, J., He, J. and Sun, X. (2009). One pot synthesis of imines from aromatic nitro compounds with novel Ni/SiO_2 magnetic catalyst. *Catal. Lett*., **128**(3-4), 465-474.

APPENDIX

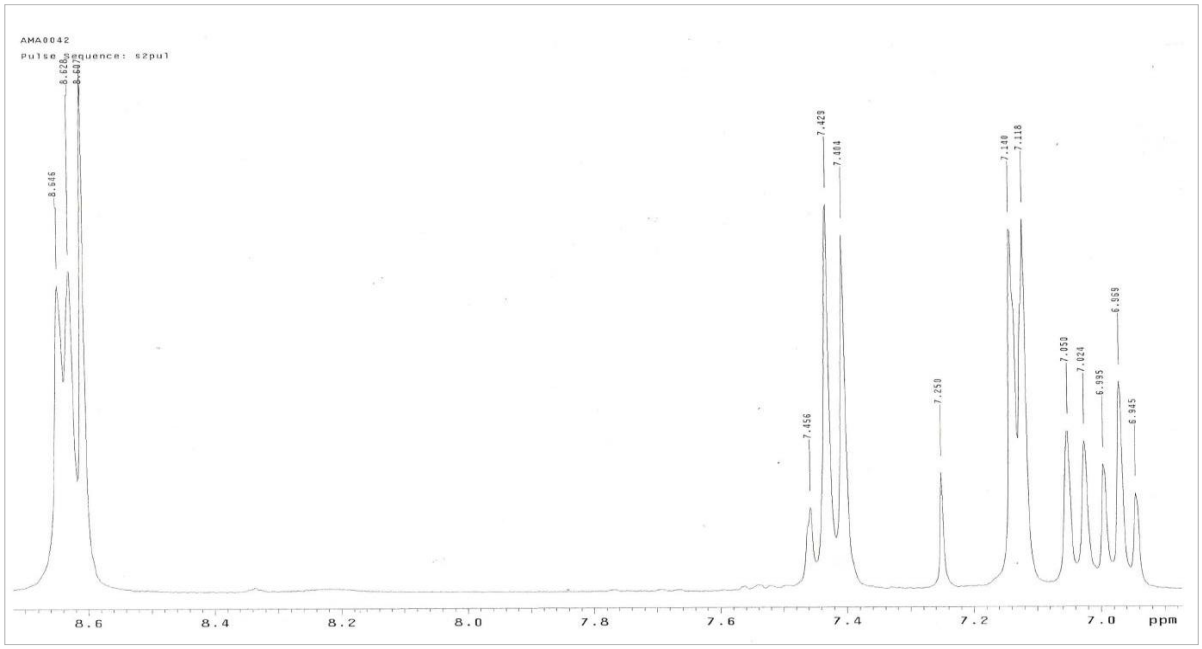

Appendix 1: ^{1}H NMR spectrum of *N*-(2-hydroxybenzylidene)pyridine-4-amine **L5** in $CDCl_3$

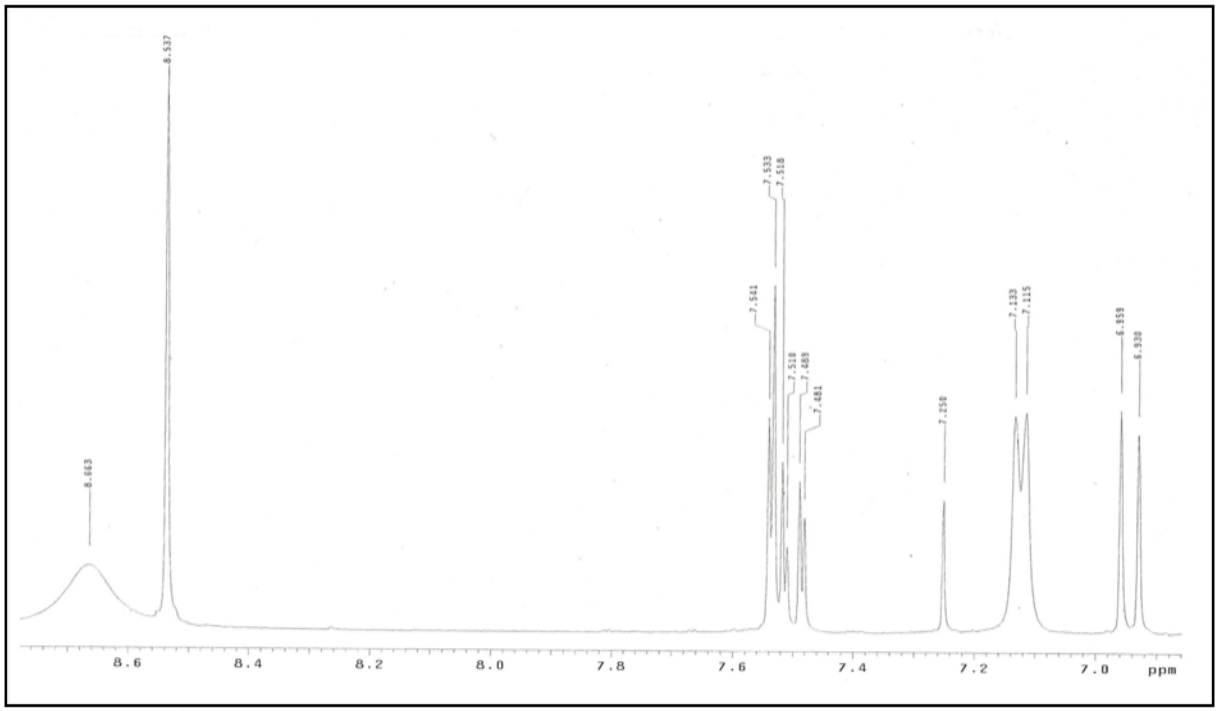

Appendix 2: ^{1}H NMR spectrum of *N*-(5-bromo-2-hydroxybenzylidene)pyridine-4-amine **L7** in $CDCl_3$

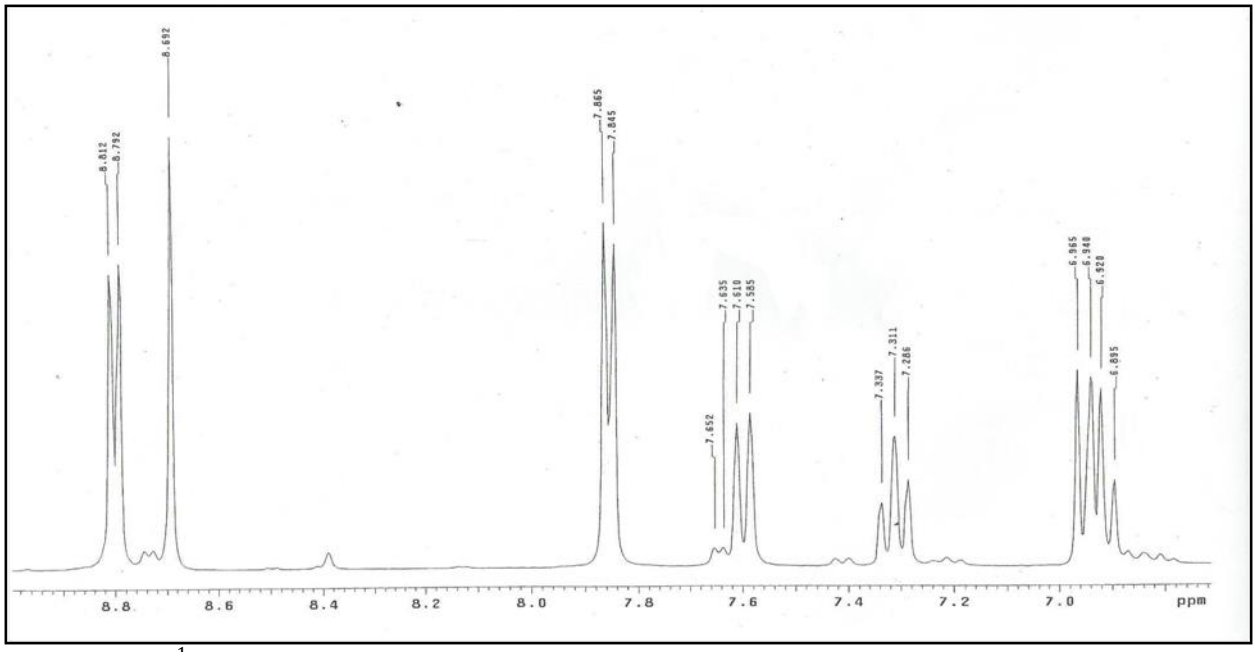

Appendix 3: ^{1}H NMR spectrum of *N*-(2-hydroxybenzylidene)isonicotino hydrazide **L8** in DMSO-d_6

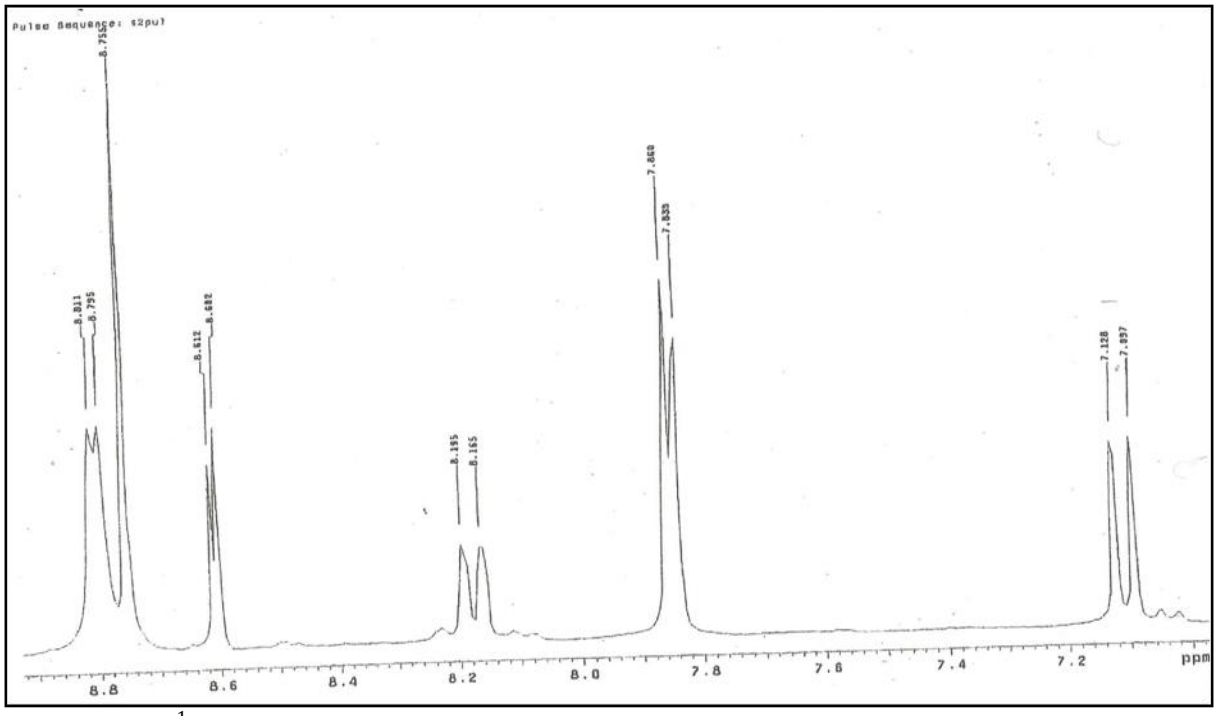

Appendix 4: ^{1}H NMR spectrum of *N*-(5-nitro-2-hydroxybenzylidene)isonicotino hydrazide **L9** in DMSO-d_6